



University of
Salford
MANCHESTER

Managing the restoration of membranes in reverse osmosis desalination using a digital twin

By:

Fredericus Ignatius Maria van Rooij

Thesis submitted to the University of Salford for the degree of
Doctor of Philosophy (PhD)

The University of Salford
Salford Business School

February 2022

Table of Contents

| | |
|--|-------|
| List of Tables..... | vii |
| List of Figures | viii |
| List of Equations | xv |
| Declaration | xviii |
| Acknowledgements | xix |
| List of Abbreviations..... | xxi |
| Publications and presentations | xxv |
| Abstract | xxvi |
| 1 Introduction..... | 1 |
| 1.1 Research aim and objectives..... | 2 |
| 1.1.1 Position of this work within the related literature..... | 3 |
| 1.2 Maintenance theory..... | 4 |
| 1.2.1 A framework of maintenance principles | 4 |
| 1.2.2 Positioning of the DSS in regard to the CMMS..... | 9 |
| 1.3 Methodology..... | 11 |
| 1.3.1 Case study | 11 |
| 1.3.2 Research Design..... | 12 |
| 1.4 How the thesis is organised | 13 |
| 2 Setting the baseline of the research..... | 15 |
| 2.1 Maintenance, one of the pillars of business strategy | 15 |
| 2.2 Establishing the baseline..... | 16 |
| 2.3 Calculation of the performance indicators..... | 20 |
| 2.4 Calculation of the baseline..... | 23 |
| 2.5 Improving maintenance performance | 23 |
| 2.6 Summary | 26 |
| 3 Research Methodology..... | 28 |

| | | |
|-------|--|----|
| 3.1 | Research problem statement | 28 |
| 3.1.1 | Observations prior to the research..... | 28 |
| 3.2 | Research design | 30 |
| 3.2.1 | Role of Modelling and Simulation in Scientific Discovery | 33 |
| 3.2.2 | Positivist research..... | 34 |
| 3.2.3 | Deductive and inductive inference..... | 36 |
| 3.2.4 | Objective and subjective inference | 38 |
| 3.2.5 | Testing and validation | 40 |
| 3.2.6 | Research onion by Sanders et al. | 42 |
| 3.3 | Techniques and procedures..... | 44 |
| 3.3.1 | Data Collection..... | 46 |
| 3.3.2 | RO performance data normalisation | 50 |
| 3.3.3 | MATLAB | 52 |
| 3.4 | Research ethics | 53 |
| 3.5 | Summary..... | 54 |
| 4 | Reverse Osmosis seawater desalination..... | 55 |
| 4.1 | Desalination to combat water shortage..... | 55 |
| 4.1.1 | What is Reverse Osmosis..... | 57 |
| 4.1.2 | RO Desalination in practice | 58 |
| 4.2 | Biofouling the Achilles' heel of desalination plants..... | 60 |
| 4.2.1 | Lack of research in RO maintenance management..... | 61 |
| 4.2.2 | Membrane degeneration due to fouling | 62 |
| 4.2.3 | Biofouling | 63 |
| 4.3 | Monitoring membrane fouling..... | 66 |
| 4.3.1 | Membrane Autopsy to determine the fouling type | 68 |
| 4.3.2 | Seasonal algal blooms | 69 |
| 4.4 | Mitigation of Membrane degeneration | 74 |

| | | |
|-------|---|-----|
| 4.4.1 | Prevention | 74 |
| 4.4.2 | Restoration | 75 |
| 4.5 | Summary | 77 |
| 5 | A RO vessel as a multi-component system..... | 80 |
| 5.1 | Multi-component systems in maintenance theory | 80 |
| 5.2 | Dependencies affecting degeneration | 82 |
| 5.2.1 | Extrinsic and intrinsic wear..... | 84 |
| 5.2.2 | A multi-component system with non-identical components..... | 88 |
| 5.2.3 | Rate-state interactions | 90 |
| 5.2.4 | Degradation models | 91 |
| 5.2.5 | Economic dependence from operational performance..... | 93 |
| 5.3 | Management of restoration | 94 |
| 5.3.1 | Structural dependence | 95 |
| 5.3.2 | Economic dependence..... | 96 |
| 5.3.3 | Block replacement..... | 97 |
| 5.4 | Summary | 98 |
| 6 | Modelling degeneration and restoration of an RO vessel | 101 |
| 6.1 | Mathematical model | 101 |
| 6.1.1 | Modelling pressure distribution | 102 |
| 6.1.2 | Modelling wear increase | 104 |
| 6.1.3 | Modelling membrane restoration | 105 |
| 6.2 | Parameter estimation..... | 106 |
| 6.2.1 | Results wear parameters α | 107 |
| 6.2.2 | Results wear parameters β and γ | 112 |
| 6.2.3 | The (non)-Gaussian character of wear parameter κ | 118 |
| 6.2.4 | Bootstrap sampling | 121 |
| 6.2.5 | Results wear parameter κ utilizing Weibull distribution..... | 123 |

| | | |
|-------|--|-----|
| 6.2.6 | Results restoration parameter δ for C1 and C2 | 128 |
| 6.3 | Summary | 128 |
| 7 | The Digital Twin | 131 |
| 7.1 | Industry 4.0 and smart maintenance | 131 |
| 7.2 | A different approach towards a digital twin | 133 |
| 7.3 | The architecture of the DSS | 136 |
| 7.3.1 | Data sources | 140 |
| 7.4 | Modelling Historical State-Space | 141 |
| 7.5 | Modelling Projections | 143 |
| 7.6 | Modules of the DSS | 146 |
| 7.6.1 | Data analysis module | 146 |
| 7.6.2 | Planning module | 149 |
| 7.6.3 | Projection | 151 |
| 7.7 | Summary | 154 |
| 8 | Exploring restoration policies | 157 |
| 8.1 | Current policies of the O&M company and alternatives | 157 |
| 8.2 | Analysis | 165 |
| 8.2.1 | Projections utilizing bootstrap sampling | 166 |
| 8.2.2 | Projections utilizing Weibull distribution | 169 |
| 8.3 | Risk assessment | 172 |
| 8.4 | Summary | 177 |
| 9 | Measuring the results compared to the baseline | 179 |
| 9.1 | Forecasting demand | 180 |
| 9.1.1 | Regression models | 184 |
| 9.1.2 | Exponential smoothing and moving average | 190 |
| 9.1.3 | Autoregressive moving average | 192 |
| 9.1.4 | Summary forecasting. | 193 |

| | | |
|------------|---|-----|
| 9.2 | Condition-based maintenance of centrifugal pumps | 193 |
| 9.2.1 | Vibration monitoring and analysis of centrifugal pumps..... | 194 |
| 9.2.2 | Pump performance monitoring | 199 |
| 9.2.3 | Implementation. | 207 |
| 9.3 | Summary results compared to baseline | 209 |
| 10 | Discussion | 212 |
| 10.1 | A DT-driven DSS for maintenance planning | 213 |
| 10.1.1 | Understanding the drivers of degradation of the specific EO | 214 |
| 10.1.2 | The EO, from a maintenance engineering perspective | 215 |
| 10.1.3 | Degradation model | 216 |
| 10.1.4 | Evaluating the performance of different policies..... | 217 |
| 10.1.5 | Sensitivity analysis..... | 217 |
| 10.2 | Research contributions..... | 218 |
| 10.2.1 | The novelty of this research | 219 |
| 10.2.2 | Research contribution to the current discussion on Industry 4.0 | 219 |
| 10.2.3 | Achievement of this research | 221 |
| 10.3 | Conclusions..... | 222 |
| 10.4 | Limitations | 223 |
| 10.5 | Further research | 224 |
| | References | 226 |
| Appendix A | Instructions for MATLAB application of the RO train digital twin..... | a |
| Appendix B | CMMS work order examples..... | h |
| B.1 | membrane replacement..... | h |
| B.1.1 | Attachment 1: Standard Operating Procedure (SOP)..... | j |
| B.1.2 | Attachment 2: Plan of elements permutations..... | r |
| B.1.3 | Attachment 3: Serial numbers of elements | s |
| B.2 | CMMS work order example CIP SBS socking..... | t |

B.3 CMMS work order example High and Low CIP.....u

Appendix C Additional projections with Bootstrappingw

C.1 Projection with bootstrap sampling with smoothing -1,+4.....w

C.2 Projection with bootstrap sampling with smoothing -2,+8.....z

Appendix D MATLAB source code for Functions Model historical state-space and
Projections dd

D.1 Function: Model historical state-spacedd

D.2 Function: Projectionsgg

About the author.....pp

List of Tables

| | |
|--|-----|
| Table 2-1. Impact of availability of the production resources on plant-designed capacity. | 20 |
| Table 2-2. Performance Indicator 1: adjusted shortfall in production in 2016, 2017, and 2018. | 21 |
| Table 3-1. Data collection of SWRO performance data from the MIS operational database.. | 48 |
| Table 3-2. Data collection of primary equipment status from the MIS operational database . | 49 |
| Table 4-1. Dates of algal blooms (week number of operation of the plant in brackets)..... | 69 |
| Table 4-2. Average RO feed source water condition during algae bloom and non-algae bloom conditions between 2017 and 2020 (ND = non detect). In those cases, SDI > 5 or Turbidity > 0.35 NTU, RO feed water supply is interrupted..... | 72 |
| Table 4-3. Procedure high and low pH CIP (C1)..... | 75 |
| Table 6-1. Limitations parameters for the PF. | 113 |
| Table 6-2: Estimates of parameters..... | 126 |
| Table 8-1. Membrane maintenance history of the first five years of operation..... | 157 |
| Table 8-2. Considered policies with element replacement rate per year, total cleaning frequency per year and cost (\$000s) for each year over the five-year planning horizon..... | 160 |
| Table 9-1. Forecasting methods and determining variables of daily demand forecast models (source: Donkor et al., 2014)..... | 182 |
| Table 9-2. Population, home value and household income per town in San Diego County.. | 183 |
| Table 9-3. Water utilities supplying to SDCWA (source sdcwa.org (2016) | 184 |
| Table 9-4. Coefficients regression models with an R-squared of above 0.4..... | 186 |
| Table 9-5. Demand for days above 51 MGD per dry and wet season | 188 |
| Table 9-6: Coefficients of the polynomials for flow calculation | 203 |
| Table 9-7: Coefficients of the polynomials for pump shaft efficiency calculation | 204 |
| Table 9-8: Coefficients of the polynomials for the efficiency calculation of the drive | 205 |

List of Figures

| | |
|---|----|
| Figure 1-1. Maintenance theory framework..... | 5 |
| Figure 1-2. Positioning of the DSS in the maintenance management system | 10 |
| Figure 2-1. Simplified process diagram of the plant involving the main equipment..... | 18 |
| Figure 2-2. Availability and delivery relative to the demand for each month of operation..... | 21 |
| Figure 2-3. Performance Indicator 2: Percentage of maintenance activity by type and by unit for 2018. “Overall” involves all the plant equipment (primary and secondary sub- systems together). | 22 |
| Figure 2-4. Average normalized RO PD..... | 22 |
| Figure 2-5. Total number of failures per unit vs median downtime per failure for production- critical failures. | 24 |
| Figure 2-6. Total number of failures per unit vs median downtime per failure including production-noncritical failures | 24 |
| Figure 2-7. Total annual equipment downtime in hours. | 25 |
| Figure 3-1: Philosophical direction of the research, defined by Saunders et al. (2009) as a table of research philosophies in management research and translated into a flowchart by the thesis author..... | 32 |
| Figure 3-2: Cross-section research onion of Saunders et al. (2017). applied to this research . | 43 |
| Figure 3-3. Experiment setup | 45 |
| Figure 3-4: Operational data retrieval from Historian database..... | 47 |
| Figure 3-5. Surface plot of the difference between inspected biomass and modelled wear distribution at parameter α values 0.4 to 0.8 for the 14 RO trains | 52 |
| Figure 4-1 a) Seven water resource regions Southwestern region of the United States. Map data ©OpenStreetMap contributors, available under the Open Database License (http://www.openstreetmap.org/copyright), accessed through Stamen OpenSource Tools (https://stamen.com/open-source/). b) Drainage basin of the Colorado River in the Southwestern United States and Mexico (Public domain image from USGS). | 56 |
| Figure 4-2. Principle of reverse osmosis..... | 57 |
| Figure 4-3. Spiral-wound element construction (courtesy Wiles and Peirtsegaele, 2018) | 58 |
| Figure 4-4. A single first pass RO vessel with eight membrane elements..... | 59 |
| Figure 4-5. A view of the 14 RO trains of the case study..... | 60 |

Figure 4-6. Lifecycle of the biofilm (Modification of work by American Society for Microbiology).....64

Figure 4-7. Normalized DP (pressure) for each train from the start of operation of the plant.67

Figure 4-8. Membrane surface of the front element and feed spacer during the autopsy.....68

Figure 4-9. Membrane surface of the tail element and feed spacer during the autopsy.69

Figure 4-10. Map of the Southern California Bight. Courtesy Smith et al. (2018).70

Figure 4-11. Intake Lagoon condition during Red Tide in Spring 2020.....72

Figure 4-12. Net Tow sample seawater.....72

Figure 4-13. Observed dead fish at the Intake Lagoon associated with the Red Tide in Spring 202072

Figure 4-14. Protoperidinium and Ceratium species (left), Pseudo-nitzschia species (middle) and Dinophysis, Lingulodinium polyedra and Cochlodinium species (right)....72

Figure 4-15. Feedwater CDP, magnification 10x Left 5 May, Middle 8 Nov., Right 18 Nov. 202173

Figure 4-16. Membrane replacement77

Figure 5-1. Multiple stacks (trains) of vessels in parallel with multiple membrane elements in series.81

Figure 5-2. Train 8: Observation of limited restoration following an interruption of operation due to low salinity flushing after stopping the train.85

Figure 5-3. (a) Three-dimensional Optical Coherence Tomography image with biomass (brown colour), feed spacer, membrane. (b) Three-dimensional simulation of particle deposition on top (red) and bottom (black) membranes in a spacer-filled feed channel. Source Bucs et al. (2018).86

Figure 5-4. Biofouling at a 15.5 thousand m³/h submersible Brine dilution pump at CDP after one year of operation. Left: Pump body covered by mussels and barnacles. Middle: Pump discharge covered with barnacles. Right: Close-up of attached barnacles.88

Figure 5-5. Pressure vessels connected in parallel in CDP. Courtesy WaterWorld 2018.89

Figure 5-6. Average NPD vs the SPC (intake and product pumps excluded).93

Figure 5-7. Membrane permutation. The first element is discharged, and the new element is inserted at socket 4. Elements 2, 3 and 4 need to be removed before the new element can be inserted.....95

Figure 5-8. Components of a RO vessel. Source: Wilf (2015)96

Figure 6-1: Hydraulic representation of an RO vessel with eight membrane elements. The stronger the shade of green, the stronger the salinity.102

Figure 6-2. Inspection of biomass accumulation at the elements by weighting.107

Figure 6-3, (a) and (b) Deviation from the measured distribution with α from 0.4 to 0.8 for all 14 trains. The surface plot is shown at different angles.110

Figure 6-4: Relative element weights (\blacksquare) and relative modelled wear-states (---) for all trains (train number and time of weighing indicated with α at the best value for the specific train).111

Figure 6-5. Principle of PF for parameter estimation113

Figure 6-6. PF collapse114

Figure 6-7. Illustration of the S-G filter for the NPD of Train 8. The polynomial degree of the filter is 4, and the approximation interval by a moving window of 150115

Figure 6-8: Histogram using ten bins for 200k particles of γ , β , κ_1 and κ_2 and fits a normal density function. The result per parameter is the sum of the particles times the weight. Plots train 1 and 2.115

Figure 6-9: Histogram using ten bins for 200k particles of γ , β , κ_1 and κ_2 and fits a normal density function. The result per parameter is the sum of the particles times the weight. Plots train 3 to 8.116

Figure 6-10: Histogram using ten bins for 200k particles of γ , β , κ_1 and κ_2 and fits a normal density function. The result per parameter is the sum of the particles times the weight. Plots train 9 to 14.117

Figure 6-11. State-space values of κ (grey dots) and daily mean of κ ($\mu\kappa$ –blue dots) ordered according to the year's day. Top left (a): unsmoothed, top right (b): smoothing of -1,4, bottom left (c): -2,8, and bottom right (d): -4, 16.118

Figure 6-12. CDF and PDF with top smoothing of -1,4, (a) κ and (b) $\mu\kappa$. Middle smoothing of -2,8 (c) κ and (d) $\mu\kappa$. Bottom smoothing of -4, 16 (e) κ and (f) $\mu\kappa$119

Figure 6-13. Histogram and PDF of daily κ (a) MLE for parameters with normal distribution, (b) MLE for parameters with Weibull distribution120

Figure 6-14. Random duration algae bloom by Normal Distribution with a mean of 23.5 and σ of 33.7121

Figure 6-15. Histogram of the population on a random day 55 of κ smoothen -1,4 dataset, bootstrap sample and Bootstrap at the mean.122

Figure 6-16: Outputs of the change-point analysis of RO trains 1 to 4124

Figure 6-17: Outputs of the change-point analysis of RO trains 5 to 12125

Figure 6-18: Outputs of the change-point analysis of RO trains 13 and 14.....126

Figure 6-19. Histogram of κ with scaled PDF from the Weibull fit, (a) κ_{low} and (b) κ_{high}127

Figure 6-20. Histogram of (a) day of year start algae bloom and (b) duration in days with scaled PDF from the Weibull fit.....127

Figure 6-21: Histograms with scaled PDF from the Weibull fit of the observed effects for cleaning-in-place for cleaning modes C1 (a) and C2 (b).....128

Figure 7-1. The architecture of DSS. (1) Data analyse module, (2) Planning module, and 3) DT.....136

Figure 7-2. Interface (GUI) of the decision support system (DSS).137

Figure 7-3. Flowchart App Design DSS139

Figure 7-4. Flow chart diagram function ‘Model Historical State-Space.’141

Figure 7-5. Flow chart diagram function ‘Projection’.145

Figure 7-6. Data analysis module of the decision support system (DSS).....146

Figure 7-7. Model – biomass fit plots for train 11 at the Data analysis module. For α left 0.4, middle 0.6 and right 0.8.....148

Figure 7-8. Model – biomass fit plots for train 11 at the Data analysis module with $\alpha=0.6$ and γ left 0.4, middle 0.8 and right 1.2.....148

Figure 7-9. The output of the DT of the modelled state-space. Top in a table, bottom a plot.149

Figure 7-10. Data analysis tool and planning module of the decision support system (DSS).150

Figure 7-11. Projection control box152

Figure 7-12: NPD projection output from the DT for one of the trains.....152

Figure 7-13: Projection interface of the DT.....153

Figure 7-14: Ensemble projection progress bar.154

Figure 8-1. left: Notation of a vessel with all new elements, right: element age colour code.158

Figure 8-2. Membrane permutations 2017 to 2020.....158

Figure 8-3. Current membrane replacement policies (1 & 10) of the O&M company.....159

Figure 8-4. Permutations of policies 2 and 3.162

Figure 8-5. Permutations policy 4.....162

Figure 8-6. Permutations policies 5, 6 and 11.....163

Figure 8-7. Permutations policy 7.....163

Figure 8-8. Aging of membrane elements after five years (Policy 8).....163

Figure 8-9. Permutations policy 9 and 12164

Figure 8-10: DT output of NPD projection based on bootstrap sampling for train 11, policy 1
(top) to policy 4 (bottom).166

Figure 8-11: DT output of NPD projection based on bootstrap sampling for train 11, policy 5
(top) to policy 8 (bottom).167

Figure 8-12: DT output of NPD projection based on bootstrap sampling for train 11, policy 9
(top) to policy 12 (bottom).168

Figure 8-13: DT output of NPD projection based on Weibull distribution for train 11, policy 1
(top) to policy 4 (bottom).169

Figure 8-14: DT output of NPD projection based on Weibull distribution for train 11, policy 5
(top) to policy 8 (bottom).170

Figure 8-15: DT output of NPD projection based on Weibull distribution for train 11, policy 9
(top) to policy 12 (bottom).171

Figure 8-16. DT output with risk thresholds172

Figure 8-17. Matrix of different risk analyses173

Figure 8-18. Risk analysis of the Policies ranked by the total cost (\$000s) over five years and
showing downtime per train (%), number of stops per train per year, and boxplots
of risk.174

Figure 8-19. Policy ranking based on risk assessment of all eight risk assessments175

Figure 8-20. Ageing of membranes in 2030 following policies 2 and 3.....175

Figure 8-21. Modelled wear on $\tau-1$, where τ is when permutations occur involving the
replacement of three elements. Left: surface plot of all 14 trains, right: plot of the
mean modelled wear distribution.176

Figure 9-1. Regressions models with an R-squared > 0.4 . Data from January 2016 to April
2019186

Figure 9-2. Trend charts of regression models with an R-squared of above 0.4. The Y-axes
show the daily water demand in MGD, and the X-axes show the days.187

Figure 9-3. Daily demand requests from 2016 to 2019. The Y-axes show the daily water
demand in MGD, and the X-axes show the days arranged per month.189

Figure 9-4. Trend charts of regression models applied to the data from January to March
2019. The Y-axes show the daily water demand in MGD, and the X-axes show
the days. The blue pen is the actual, Red pen is the forecast.....190

Figure 9-5. Left, a scatterplot of the predicted (*Y-axes*) vs the actual demand (*X-axes*) of
exponential smoothing. Right, a trend chart of the time-series data. The blue pen

is the actual, Red pen is the forecast. The Y-axes show the daily water demand in MGD, and the X-axes show the days.191

Figure 9-6. Left, a scatterplot of the predicted (*Y-axes*) vs the actual demand (*X-axes*) of by moving average. Right, a trend chart of the time-series data. The Y-axes show the daily water demand in MGD, and the X-axes show the days. The blue pen is the actual, Red pen is the forecast.191

Figure 9-7. Left a trend chart of the time-series data by moving average. The blue pen is the actual, Red pen is the forecast. The Y-axes show the daily water demand in MGD, and the X-axes show the days. Right, a scatterplot of the predicted (*Y-axes*) vs the actual demand (*X-axes*).....192

Figure 9-8: Scatterplot of vibrations vs frequency for DE and non-drive-end (NDE) of HPB pump 2 (Data 2016). Y-axes vibrations, X-axes motor frequency.....196

Figure 9-9. Scatter plot of the maximum vibration data vs the Frequency of HPB pump 2. Y-axes vibrations, X-axes motor frequency.197

Figure 9-10: normalized vibration data HPB pump 2 (left) and for HPB pump 3 (right). Y-axes vibrations, X-axes date.198

Figure 9-11: Left, Grooves inner raceway ring NDE bearing; Middle: expanded detail Grooves; Right, Denting roller surface.....198

Figure 9-12. Digitalizing of pump curves.201

Figure 9-13: Pump TDH against pump flow for both operating points. Left shaft speed of 859 rpm, right shaft speed of 1197 rpm.....201

Figure 9-14: Pump shaft efficiency against pump flow for both operating points. Left shaft speed of 859 rpm, right shaft speed of 1197 rpm.202

Figure 9-15: Scatterplot of empirically estimated drive efficiency and polynomial trendline205

Figure 9-16: Scatterplots of measured power vs expected calculated power for HPB pumps 1 and 2 (Data 2019).206

Figure 9-17. Incorporation of an anomalies detection module into the OT MIS.....208

Figure 9-18. Availability, demand, and delivery from Jan 2019 to November 2021210

Figure 9-19. Performance indicators for water shortfall, ratio failure-based to all maintenance activities, and annual percentage of membrane changes. All expressed in days of lost production. Grey needle is the performance at the baseline of the year 2018, black needle is the performance in 2021.210

Figure A-1: MATLAB Toolstrip showing the installed RO train DT application a

Figure A-2: Decision Support System (DSS) dashboard after the start-up of the application. .b
Figure A-3: Selection of preferable pressure units, Bar or PSI.....b
Figure A-4: Method of determining historical κc
Figure A-5: the selection of trainc
Figure A-6: retrieval of historical data of train 1 over a period of five years.c
Figure A-7: DT of modelled wear (X), P and daily κd
Figure A-8: Maintenance planning moduled
Figure A-9: Projection setupe
Figure A-10. Progress indicator during computation of the projection.f
Figure A-11. Decision Support System (DSS) dashboard after finalizing a projection.g
Figure C-1: Bootstrap with smoothening -1,+4, Train 11 for policy 1, (top) to policy 3
(bottom).w
Figure C-2: Bootstrap with smoothening -1,+4, Train 11 for policy 4, (top) to policy 7
(bottom).x
Figure C-3: Bootstrap with smoothening -1,+4, Train 11 for policy 8, (top) to policy 11
(bottom).y
Figure C-4: Bootstrap with smoothening -1,+4, Train 11 for policy 12.z
Figure C-5: Bootstrap with smoothening -2,+8, Train 11 for policy 1, (top) to policy 3
(bottom).z
Figure C-6: Bootstrap with smoothening -2,+8, Train 11 for policy 4, (top) to policy 7
(bottom).aa
Figure C-7: Bootstrap with smoothening -2,+8, Train 11 for policy 8, (top) to policy 11
(bottom).bb
Figure C-8: Bootstrap with smoothening -2,+8, Train 11 for policy 12.cc

List of Equations

- Element-specific version of NPD calculation $PD = C \times Flow^B$ (1).....50
- Viscosity equation (μ) $\mu = \frac{e^{-3.7188 + \frac{578.919}{-137.546 + Tw + 273.15}}}{1000}$ (2).....51
- Normalised Pressure Differential (NPD) $NPD_i = PD_i \times \left(\frac{Q_{f,ref} + Q_{r,ref}}{Q_{f,t} + Q_{r,t}} \right)^{1.4} \times \left(\frac{\mu_{ref}}{\mu_t} \right)^{0.6}$ (3).....51
- Pressure-differential across the vessel: $P_t = \sum_{i=1}^n P_{i,t}$. (4).....101
- Pressure-differential across a socket: $P_{i,t} = \omega_i P_0 X_{i,t}$, $i = 1, \dots, n$, (5).....102
- Net Driving Pressure: element 1 $P_{feed} - \frac{P_1}{2} - \Pi_1 - P_{permeate}$ and element i ($i = 2, \dots, n$)
- $P_{feed} - \sum_{j=1}^{i-1} P_j - \frac{P_i}{2} - \Pi_i - P_{permeate}$, (6)102
- Recovery: $R_i = \bar{Q}_i / Q_i$. (7).....103
- Recovery trailing sockets from R1: $R_i = R_1 / \{1 + (i-1)sR_1\}$, $i = 2, \dots, n$. (8).....103
- Vessel recovery R from R1: $R = R_1 + \sum_{i=2}^n \left\{ \frac{R_1}{1 + (i-1)sR_1} \prod_{j=2}^i \frac{1 - (1 - (j-2)s)R_1}{1 + (j-2)sR_1} \right\}$ (9).....103
- Socket pressure coefficient $\omega_i = R_i / \sum_{i=1}^n R_i$, $i = 1, \dots, n$, $\sum_{i=1}^n \omega_i = 1$ (10).....103
- Wear differential: $\Delta X_{i,t} = X_{i,t} - X_{i,t-1}$. (11).....104
- Wear increase: $\Delta X_{i,t} = \kappa_t \alpha^{i-1} \{ \sum_{j=i+1}^n X_{j,t-1} / (n-i) \}^{R\gamma}$, (12).....104
- Wear increase when vessel offline: $\Delta X_{n,t} = \kappa_t \alpha^{n-1}$. (13).....104
- Following the end of an algae bloom, the decay of $\kappa_t = (\kappa_2 - \kappa_1)e^{-\beta\tau}$ (14).....105
- Wear following swapping: $X_{i,t^+} = X_{j,t^-}$, $X_{j,t^+} = X_{i,t^-}$ (15).....105
- State of the cleaned element in socket i $X_{i,t^+} = (1 - \delta)X_{i,t^-} + \delta$, (16).....106
- Restoration due to cleaning: $P_{t^+} = (1 - \delta)P_{t^-} + \delta P_0$ (17).....106
- The estimated biomass distribution $w_i = \frac{W_i - \min\{W_1, W_2, \dots, W_n\}}{\min\{W_1, W_2, \dots, W_n\}}$ (18).....108

Extrinsic component: $\kappa_t = \frac{P_t - P_{t-1}}{P_0 \sum_{i=1}^n \alpha^{i-1} f(x, i)^{R\gamma} \omega_i}$, (19).....108

Smallest deviation of the measured biomass distribution from the modelled wear

$$\sum_{i=1}^n \left(\frac{\Delta X_i}{\Delta X} - \frac{w_i}{\bar{w}} \right)^2 \quad (20).....109$$

The equation for the ARMA(p,q) model is $Y_t = c + \sum_{i=1}^p \phi Y_{t-i} + \sum_{i=1}^q \theta_i \varepsilon_{t-i}$ (21)192

Pump Affinity Laws

Pump TDH (H) $H = \frac{100,000 \times \Delta P}{\rho \times g}$ (22)201

Polynomial 4th order flow against TDH $Q_o = \alpha + \beta_1 H_o + \beta_2 H_o^2 + \beta_3 H_o^3 + \beta_4 H_o^4$ (23)201

Ratio Pump actual speed and flow vs nominal $\frac{Q_1}{Q_2} \approx \frac{N_1}{N_2}$ (24)201

Ratio Pump actual speed and Head vs nominal $\frac{H_1}{H_2} \approx \left(\frac{N_1}{N_2} \right)^2$ (25)202

Pump Head form OEM $H_o = H_a \left(\frac{N_o}{N_a} \right)^2$ (26)202

Ratio pump speed vs nominal $y = \frac{N_a}{N_o}$ (27)202

Deduction: (Eq. 25) and (Eq. 25) follows: $H_o = \frac{H_a}{y^2}$ (28)202

Deduction: (Eq. 27) into (Eq. 21): $Q_o = \alpha + \beta_1 \frac{H_a}{y^2} + \beta_2 \frac{H_a^2}{y^4} + \beta_3 \frac{H_a^3}{y^6} + \beta_4 \frac{H_a^4}{y^8}$ (29)202

Derived from (Eq. 23) follows: $Q_o = Q_a \frac{N_o}{N_a} = Q_a \frac{1}{y}$ (30)202

Putting (Eq. 29) into (Eq. 27): $\frac{Q_a}{y} = \alpha + \beta_1 \frac{H_a}{y^2} + \beta_2 \frac{H_a^2}{y^4} + \beta_3 \frac{H_a^3}{y^6} + \beta_4 \frac{H_a^4}{y^8}$ (31)202

Expected flow vs speed: $Q_a = \alpha y + \beta_1 \frac{H_a}{y} + \beta_2 \frac{H_a^2}{y^3} + \beta_3 \frac{H_a^3}{y^5} + \beta_4 \frac{H_a^4}{y^7}$ (32)202

Pump Power and efficiency calculations

Required hydraulic power (P_h) in kW: $P_h = \frac{Q\rho gH}{3.6 \times 10^6}$ (33)203

Pump shaft power (P_s): $P_s = \frac{P_h}{\eta_p}$ (34)203

Shaft efficiency (η_s): $\eta_s = \gamma + \delta_1 Q + \delta_2 Q^2 + \delta_3 Q^3$ (35)203

Drive efficiency: $\eta_d = \iota + \kappa_1 N + \delta \kappa_2 N^2 + \kappa_3 N^3$ (36)203

Total expected input power (P_t): $P_t = \frac{P_s}{\eta_d}$ (37)204

Overall expected efficiency (η_t): $\eta_t = \eta_s \times \eta_d$ (38)204

Deviation of efficiency (σ_η): $\frac{\frac{P_h}{P_m} - \eta_t}{\eta_t}$ (39)204

Deviation in power (σ_p): $\sigma_p = \frac{P_m - P_t}{P_t}$ (40)205

Deviation in Flow (σ_Q): $\sigma_Q = \frac{Q_m - Q}{Q}$ (41)205

Declaration

I hereby certify that this work is that of the author, except for those areas where acknowledgements are duly made.

Acknowledgements

This research focuses on modelling degeneration and restoration of reverse osmosis (RO) membrane elements in a pressure vessel. As a lead system integrator, the author of this thesis had the honour to meet Dr Sidney Loeb when the RO membranes pioneer in 2003 visited Israel's first major desalination plant in Ashkelon under commissioning.

The author owes a lot to Prof Phil Scarf in his PhD research journey. Prof Phil Scarf was instrumental in initiating the PhD study. After being accepted as a PGR student at the Salford Business school, Prof Phil guided me as a supervisor until his departure in March 2020. Prof Phil supervised the research up to the end of the Interim Assessment, where leading up to this milestone, the focus of the research and the fundamentals have been moulded. After Prof Phil's departure, we stayed in close contact and collaborated on several papers involving this research. This process has forced me to continuously re-evaluate the mathematical foundation of the model, the shaping of the Digital Twin (DT) and the statistical methods underlying it. Prof Phil's guidance was instrumental to my development as a researcher and academic author. Further, Prof Phil provided me with an indispensable soundboard for testing my ideas.

Prof Phil brought me in contact with Dr Phuc Do, Professor (Associate) in reliability and maintenance engineering at the University of Lorraine, Nancy, in France. We met at the 29th European Safety and Reliability Conference (ESREL) in September 2019 in Hannover, Germany. Dr Phuc collaborated with us in the publishing of papers. Further, Dr Phuc stimulated my desire to familiarise myself with MATLAB, which gave me a whole new perspective on applying statistical methods to the research.

Dr Christos Papanagnou took over the supervision of my PhD journey after the departure of Prof Phil, with Dr Yiannis Polychronakis as the second supervisor. Dr Christos became involved in the research at the end of the second academic year of the research. As the author mentioned, the shape of the research and the mathematical model underlying it had been relatively completed at this stage. It is a significant challenge to take over the supervision after the research has matured to such a degree. For most of the third academic year, Dr Christos was non-active due to health reasons to complicate matters further. Since this is a part-time study conducted parallel to a full-time professional career, the study duration is five years. The research and the internal evaluation were completed at the end of the third academic year. So the fourth academic year was oriented toward writing the thesis. Dr Christos has shown tremendous patience and provided me with valuable advice and support, especially in preparation for the viva.

Further, I would like to thank Dr Marie Griffiths for providing support and assistance, especially during the internal evaluation run-up. In addition, I am deeply thankful to take part in the bi-weekly Salford Business School (SBS) seminars organised by Dr Marie, which were conducted online. As an overseas postgraduate student, participation in academic activities and life is minimal. In these seminars, researchers, staff and PhD students present their research. The seminars have a semi-formal character, are diverse, refreshing, and help build a social network. I always looked forward to these seminars.

I also would like to acknowledge the support of the management of IDE Technologies Ltd, which provided me with access to data, a workplace to test my research and financial support. My colleagues who showed interest in the research allowed me to present to the team locally and overseas at the headquarters, which resulted in the practical application.

Finally, I would like to thank my family, my wife, Ria and my children, who patiently endured the limited time I had to offer them during this journey. Without their support and understanding, it would have been challenging to bring this journey to success. I hope that my five children, of which two already have their Master's or are in the process of getting them, will follow my example one day.

List of Abbreviations

| | |
|--|---------|
| Algal Organic Matter | (AOM) |
| American Society for Testing Materials | (ASTM) |
| Autoregressive integrated moving average | (ARIMA) |
| Artificial Neural Networks | (ANN) |
| Artificial Inteligence | (AI) |
| Autoregressive moving average | (ARMA) |
| AutoRegressive Integrated Moving Average | (ARIMA) |
| Brackish Water Reverse Osmosis | (BWRO) |
| Carlsbad Desalination Plant | (CDP) |
| Central limit theorem | (CLT) |
| Central Processor Unit | (CPU) |
| Clean-in-place | (CIP) |
| Computerized Maintenance Management System | (CMMS) |
| Condition-based Maintenance | (CBM) |
| Continuous Function Charts | (CFC) |
| Contribution Ratio | (CR) |
| Cumulative distribution function | (CDF) |
| Cyber-Physical System | (CPS) |
| Decentralized Control Systems | (DCS) |
| Decision Support System | (DSS) |
| Design out Maintenance | (DOM) |
| Digital Twin | (DT) |
| Dissolved Air Flotation | (DAF) |
| Dissolved Air Flotation Filtration | (DAFF) |
| Drive-end | (DE) |
| Energy Recovery System | (ERS) |
| Engineered Object | (EO) |
| Environmental Protection Agency | (EPA) |
| Enterprise Resource Planning | (ERP) |
| Fast Fourier Transformation | (FFT) |
| Gallons per Minute | (GPM) |

| | |
|---|--------|
| Graphical User Interface | (GUI) |
| Harmful Algae Blooms | (HOB) |
| Hidden Markov Models | (HMM) |
| High-Pressure Booster | (HPB) |
| High-Pressure pumps | (HPP) |
| Human-Machine-Interface | (HMI) |
| Least-squares estimation | (LSE) |
| Industrial Control Systems | (ICS) |
| Intake Pumps | (IP) |
| Internet of Things | (IoT) |
| Industrial Internet of Things | (IoT) |
| Life Cycle Costing | (LCC) |
| Low Salinity | (LS) |
| Low-Pressure Booster | (LPB) |
| Management Information System | (MIS) |
| Maximum likelihood estimation | (MLE) |
| Micro-filtration | (MF) |
| Million US Gallons | (MG) |
| Million Gallons a Day | (MGD) |
| Nano-Filtration | (NF) |
| National Oceanic and Atmospheric Administration | (NOAA) |
| National Science Foundation | (NSF) |
| Natural Organic Matter | (NOM) |
| Net Driving Pressure | (NDP) |
| Non-drive-end | (NDE) |
| Normalized Pressure Differential | (NPD) |
| Null Hypothesis | (H0) |
| Occupational Safety and Health Administration | (OSHA) |
| Open Platform Communications | (OPC) |
| Operate to Fail | (OTF) |
| Operational Expenses | (OPEX) |
| Operational Technology | (OT) |
| Operations and Maintenance | (O&M) |

| | |
|--|---------|
| Original Equipment Manufacturers | (OEM) |
| Particle filtering | (PF) |
| Performance Indicators | (PI) |
| Pounds per Square Inch | (PSI) |
| Pressure Differentials | (PD) |
| Product Water Pumps | (PWP) |
| Programmable Logic Controllers | (PLC) |
| Probability density function | (PDF) |
| Proportional, Integral, and Derivative | (PID) |
| Reliability-Centred Maintenance | (RCM) |
| Remaining Useful Life | (RUL) |
| Remote Input/Output | (RIO) |
| Research Questions | (RQ) |
| Reverse Osmosis | (RO) |
| Savitzky-Golay filter | (S-G) |
| San Diego County Water Authorities | (SDCWA) |
| Seawater Reverse Osmosis | (SWRO) |
| Short-time Fourier transform | (STFT) |
| Silt Density Index | (SDI) |
| Skill Level Upgrade | (SLU) |
| Sodium Bisulfite | (SBS) |
| Southern California Bight | (SCB) |
| Specific Conductance | (SC) |
| Specific Power Consumption | (SPC) |
| Standard Operating Procedure | (SOP) |
| Structured Text | (ST) |
| Supervisory Control and Data Acquisition | (SCADA) |
| Sustainable Supply Chain Management | (SSCM) |
| System Dynamics | (SD) |
| System Integrator | (SI) |
| Time-based Maintenance | (TBM) |
| Total Dynamic Head | (TDH) |
| Total Productive Maintenance | (TPM) |

| | |
|---------------------------------------|--------|
| Transparent Exopolymer Particles | (TEP) |
| Ultra-Filtration | (UF) |
| University of California, Los Angeles | (UCLA) |
| University of Salford | (UoS) |
| User interface | (UI) |
| Variable Frequency Drives | (VFD) |
| Work Orders | (WO) |

Publications and presentations

ORCID: [0000-0002-0222-1726](https://orcid.org/0000-0002-0222-1726)

1. van Rooij, F. and Scarf, P., 2019. Towards a maintenance requirements analysis for maximizing production¹. Hannover, Germany, European Safety and Reliability Association. Doi: 10.3850/978-981-11-2724-3_0127-cd.
2. A Digital Twin of a Reverse-Osmosis Desalination Train. Presented at the SBS online seminar on 1 July 2020
3. van Rooij, F. and Scarf, P., 2021. Modelling maintenance of a multi-component system with wear rate-state dependence: the case of a seawater reverse-osmosis desalination train. Presented at the 11th IMA International Conference on Modelling in Industrial Maintenance and Reliability (MIMAR).
4. Modelling deterioration and restoration of membrane elements in a reverse osmosis pressure vessel. A digital twin of an RO Train. Presented online at the corporate process engineering department of IDE Technologies on 23 Aug 2021.
5. van Rooij, F; Scarf, P. and Do, P., 2021. Modelling the Maintenance of Membranes in Reverse-Osmosis Desalination. Angers, France, 31st European Safety and Reliability Conference. Paper presented on 19-23 September 2021. Doi: 10.3850/978-981-18-2016-8_117-cd
6. van Rooij, F; Scarf, P. and Do, P., 2021. Modelling degradation and restoration of membrane elements in a reverse osmosis pressure vessel². In the journal *Desalination*, volume 519, December September 2021. Doi. 10.1016/j.desal.2021.115214.
7. Modelling deterioration and restoration of membrane elements in a reverse osmosis pressure vessel. A digital twin of an RO Train. Presented at the SBS online seminar on 14 Oct 2021

¹ Cited by 1

² Cited by 3

Abstract

This thesis studies degradation and restoration policies for a pressure vessel in a reverse osmosis (RO) desalination plant. In the study context, biofouling is the primary cause of the degradation of the RO membrane elements, amplified by seasonal algal blooms. This research developed a decision support system (DSS) for evaluating membrane restoration strategy. The engine of the DSS is a digital twin (DT), a virtual representation of wear (degradation) and restoration of membrane elements in a RO pressure vessel. The basis of the DT is a mathematical model that describes an RO pressure vessel as a novel multi-component system in which the hidden wear-states of individual elements (components) are quantified, and elements can be swapped or replaced. This contrasts with the contemporary presentation of a membrane system as a single system in the literature. The parameters of the model are estimated using statistical methods. The research approach is described in the context of a case study on the Carlsbad Desalination Plant in California. Results show a good fit between the observed and the modelled wear-states. Competing policies are compared based on risk, cost, downtime, and the number of stoppages. Projections indicate that a significant cost-saving can be achieved while not compromising the integrity of the plant. Alternative policies 11 and 12 showed better wear management than the current policy 10 of the maintenance company while reducing costs between \$0.7 to \$1.7 million for the next five years.

The research in the thesis contributes toward maintenance modelling. New models of multivariate degradation and imperfect repair are presented. The research makes an important contribution to desalination and water treatment engineering, providing a unique membrane maintenance management approach currently absent from the literature. The thesis also contributes to the maintenance theory. It proposes a general approach for applying a decision support system (DSS) for maintenance requirements analysis, involving a digital twin (DT) for wear and repair projections when wear is stochastic, and repair effects are not immediately apparent. The essential elements of a DSS are discussed. This research encourages a dialogue between researchers of maintenance theory and modelling and practitioners of maintenance planning about decision support systems and digital twins that not only project the *when* but also evaluate the *what* in maintenance strategy. The presented concept of a DSS driven by a DT for maintenance requirement analysis has valuable practical implications, and the thesis, in discussing this concept, makes an essential contribution to the discussion about Industry 4.0, digital twins, and maintenance.

1 Introduction

Maintenance is part of daily life. Anybody who owns or takes care of a house or car knows that it needs continuous maintenance, or they fall apart or break down. We usually do not wait until the latter occurs. Cars undergo an oil change at regular intervals instead of waiting until the low oil warning comes up on the dashboard. Production facilities are no different. Equipment deteriorates and malfunctions, resulting in poor quality performance, production instabilities or even a complete halt. Malfunction of equipment can further impact operational safety. Maintenance practitioners do not wait until equipment fails in today's competitive markets but undertake planned actions to keep the equipment in an acceptable state. Maintenance planning involves when and what interventions to undertake to warrant the reliability of the equipment.

Risk management is undertaken to determine what maintenance planning is required. This risk assessment can be based on previous equipment history, accelerated life testing or maintenance modelling. The latter involves the probability and intensity of equipment deterioration, establishing the lifecycle and simulation of different repair strategies to determine the restoration of the state of the equipment to establish the most efficient and cost-effective maintenance policies.

This research is about maintenance modelling. Managing a system's long-term reliability in stochastic wear conditions involving imperfect maintenance, whereby the long-term results are uncertain. This research is motivated by an actual maintenance topic. The following approach is adopted. A solution to a practical maintenance problem is demonstrated. The proposed answer is a decision support system (DSS). Subsequently, the thesis proposes general requirements for a DSS towards the research community and that of practitioners of maintenance planning.

The thesis then focuses on the details of the development and implementation of the DSS in a novel case study, a niche branch in the process industry: The Carlsbad Desalination Plant in California, which suffers from biofouling due to seasonal algae blooms. A mathematical model is developed that provides the concept of a digital replica of the wear and the repair of the cascaded membrane elements in an RO vessel. This thesis will use repair and restoration interchangeably.

The mathematical model is then implemented as a simulation application, a Seawater Reverse Osmosis (SWRO) vessel's Digital Twin (DT). The DT is embedded in a DSS where

various maintenance policies can be evaluated on risk, cost, downtime, and the number of stoppages. The DT provides long-term projections of the state of a stack of Reverse Osmosis (RO) vessels, also referred to as a RO train, in the presence of uncertain extrinsic wear conditions. Specifically, the uncertainty in occurrence, length, and intensity of algal blooms in this case.

The solution presented has the potential to reduce the costs of operations and maintenance (O&M) companies by optimising membrane maintenance management and eliminating ad hoc decision-making. The DSS aims to provide the maintenance practitioner with a tool to establish the most cost-effective maintenance plan. The research further offers a unique example of maintenance requirement analysis for stochastic degradation processes involving uncertain imperfect repairs by designing and implementing a DSS driven by a DT. This research, therefore, provides a unique contribution to the body of knowledge of maintenance theory and modelling.

1.1 Research aim and objectives

This research aims to establish a maintenance planning methodology for an engineered object (EO). Of interest is the long-term reliability of the EO in the presence of stochastic wear conditions. Consider that a multitude of possible maintenance policies can be applied, but maintenance involves imperfect repair, and the long-term effectiveness of the policies is unknown. Without a degree of knowledge about the probability of the level of repair the policies will provide, in consideration of the cost, any decision is ad hoc and could not be the right strategy. The objective is a Decision Support System (DSS) to forecast the effectiveness before implementing the policies.

This thesis starts with presenting principles for designing a DSS for maintenance requirements. These principles are outlined in Figure 1.1. Subsequently, general requirements for a DSS towards the research community and practitioners of maintenance planning are proposed. With this thesis, the author seeks to demonstrate how such DSS can be implemented using a novel case study. The thesis, therefore, addresses the following research questions (RQ):

RQ1: *What are the general requirements of a DSS for restoration so that the DSS is fit for purpose?*

Next, a case study is demonstrated using a DSS to solve an actual maintenance problem. A DSS is used for the long-term maintenance planning of reverse osmosis (RO) membranes in

seawater desalination, affected by biofouling due to seasonal algae blooms. A second RQ is, therefore:

RQ2: *How should the restoration of membrane elements in RO desalination in the presence of seasonal algal blooms be managed?*

This research contributes in two ways to the body of existing work of maintenance modelling and the simulation literature. Firstly, the thesis discusses an essential issue in maintenance theory. It proposes an answer to RQ1 that requires further debate (see section 1.2 Maintenance theory), which the thesis author encourages by a dialogue between researchers of maintenance theory and practitioners of maintenance planning.

Secondly, this thesis addresses in detail RQ2. The study is publicised in brief in the journal *Desalination* (van Rooij et al., 2021). See page xxiv for a list of publications and presentations. The article in *Desalination* has to date been cited by three papers. Sun et al. (2022) referred to the article to illustrate an example of a DT for modeling real systems: *the introduction of DTs to monitoring systems in industrial facilities and and the relevant issues... are actively used to solve the problems of building systems for modeling the behavior of real objects.*

The novelty of this research is first that a general framework for the design of a DT for maintenance planning has been introduced. To date, this has been absent from the literature and will provide important guidance for academics and practitioners pursuing a DT for maintenance management support.

Following a real practical example is presented for the desalination industry. Jamieson et al. (2021) expressed the desire for future research to focus on the fouling timeline, especially regarding the fouling of all the RO membranes within a vessel. This research fulfils this gap for membranes subjected to biofouling. The journal editor and reviewers appraised the contribution in *Desalination* as *an interesting and novel approach to [the] maintenance of RO systems. The idea of creating a digital twin of the SWRO membrane trains in terms of simulation of their fouling process is very important, interesting and innovative.*

The presented novel model of degradation of a multi-component system and its DT simulation application are further unique contributions to the body of existing work of maintenance modelling and the simulation literature.

1.1.1 Position of this work within the related literature

Within the body of existing work, the presented research contributes towards maintenance theory and modelling. The presented work is related to multivariate degradation processes

and imperfect repair models. A mathematical model is developed of the degeneration and restoration of the RO train. From this model, a simulator is built, a digital twin of an RO train.

This research is also situated generally in desalination and water treatment engineering. The presented work is situated in the body of the existing works that identify biofouling due to algal blooms as a dominant source of membrane degeneration. The research reviews publications about membrane maintenance strategies. Despite the potential severity of biofouling and the costly consequences, little attention has been given so far in the literature to the management of membrane maintenance. To this thesis author's knowledge, only Koutsakos and Moxey (2007) describe a maintenance protocol for membranes. However, while their system records the position of every element in an RO vessel, it quantifies neither the states of elements nor the long-run costs of interventions. This research intends to fill this gap in knowledge, both theoretically and practically.

The research is relevant to managers, practitioners and applications. The study demonstrates a solution to a real maintenance planning problem, demonstrating an advance toward maintenance 4.0 (Jasiulewicz-Kaczmarek and Gola, 2019) and Industry 4.0 (Silvestri et al., 2020).

1.2 Maintenance theory

Maintenance has been defined by many (e.g. Gits, 1992; Ben-Daya et al., 2000; Waeyenbergh and Pintelon, 2002; Ben-Daya et al., 2016; Brundage et al., 2019). Broadly, it is the planning, execution, and review of actions for the care of engineered objects. Maintenance is one activity within the four phases of asset management: acquisition; deployment; operation and maintenance; and disposal (El-Akruti et al., 2018). Maintenance theory is the body of knowledge about maintenance that can be summarised in a framework of maintenance principles and sub-principles. This thesis uses the definition of *EO* by Ben-Daya et al. (2016) to denote human-made systems. Note that an *EO* can be a sub-unit composition, and the maintenance intervention is being directed to the sub-unit. In this thesis, maintenance is referred to as the activities that retain or restore the function of an *EO* (Gits, 1992; Murthy, 2000; Ben-Daya et al., 2016).

1.2.1 A framework of maintenance principles

The thesis author proposes a framework of maintenance principles and sub-principles shown in Figure 1-1. The latter does not yet exist in the literature. The framework's purpose is to provide guidelines for designing a maintenance decision support system driven by a DT.

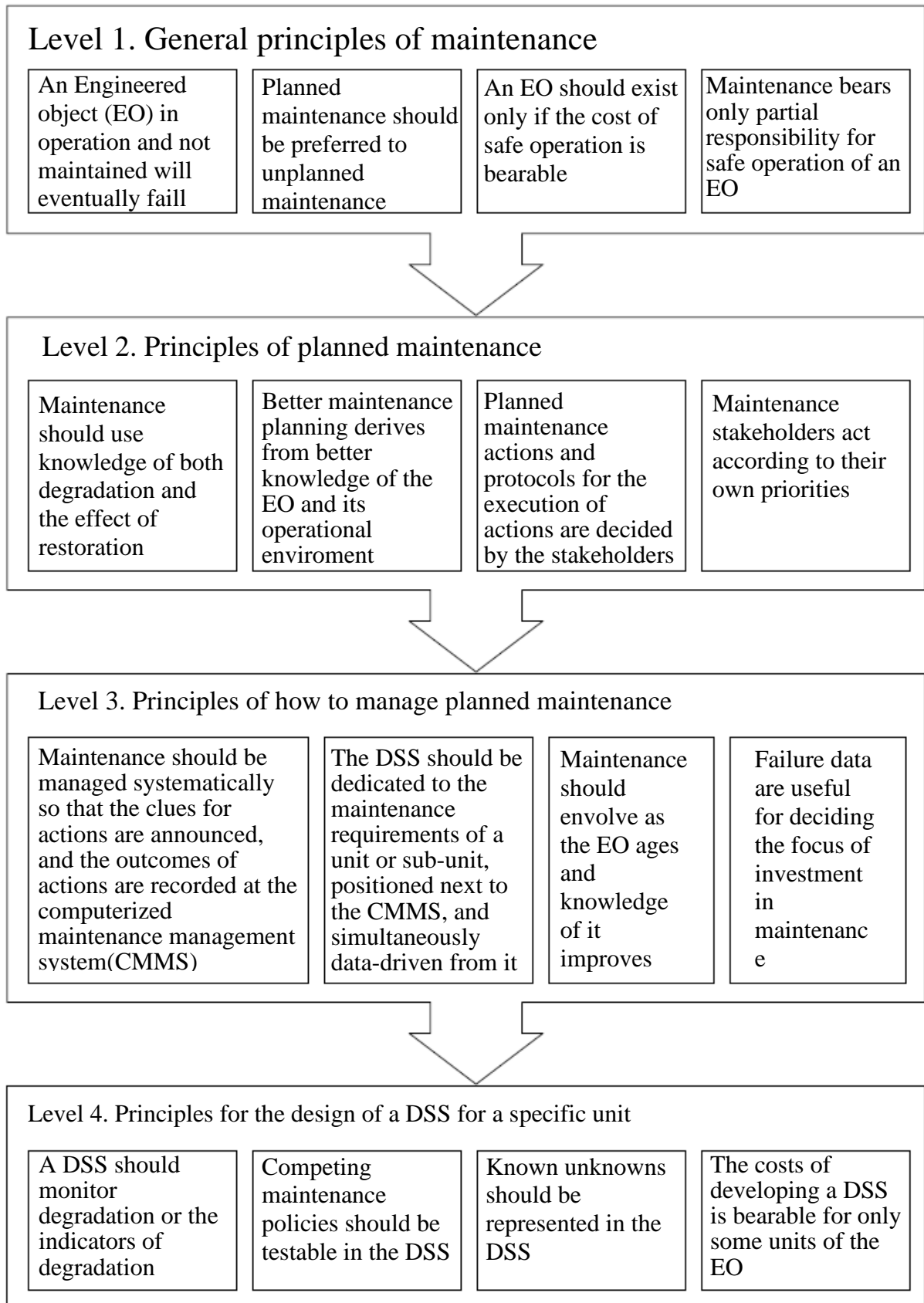


Figure 1-1. Maintenance theory framework.

The maintenance principles have been classified into several layers to derive the requirements for designing a DSS for the maintenance concept of a specific unit. The maintenance principles and sub-principles are classified into levels.

Each successive level of sub-principles is derived from the previous level. The first level is the general principles of maintenance. Level 2 principles of planned maintenance follow them. From principles of planned maintenance, we obtain a new level, principles of how to manage planned maintenance. Finally, we obtain the last level, level 4, Principles for designing a DSS for a specific unit. Level 4 proposes that the DSS is dedicated to a particular unit of the EO. The objective of the DSS is to test competing maintenance policies, also referred to as the maintenance concept (Pintelon and Parodi-Herz, 2008; Ben-Daya et al., 2016) and defined by Gits (1992) as a set of rules that recommend what maintenance is required for a unit of the EO and when.

Testing maintenance policies at a physical unit are costly and potentially will sacrifice the unit. Therefore, testing the maintenance policies for a unit requires a simulator. This testing cannot be seen separately from the degradation process.

However, the degradation process or some of the drivers of the degeneration can be stochastic. Therefore, these known unknowns need to be represented in the DSS. Thus, level 4, *principles for the design of a DSS for a specific unit*, implies that those policies can be tested using a simulator that encodes a stochastic model of degradation and restoration.

1.2.1.1 Level 1. General principles of maintenance

This thesis proposes the first layer as the primary maintenance principle in these contents. Gits (1992) and Ben-Daya et al. (2016) state that an EO in operation and not maintained will eventually fail; therefore, maintenance is inherent, or the EO is disposed of. Research has shown that planned maintenance, in general, is preferred to unplanned maintenance, although there are cases where to operate to fail (OTF) should be considered as an informed decision (Gits, 1992; Waeyenbergh and Pintelon, 2002; Labib, 2008; Ben-Daya et al., 2016; Brundage et al., 2019). Maintenance should take into consideration the cost. Imperfect repair could cost-wise be more effective than perfect repair. Although an EO should only exist if the cost of safe operation is bearable (Gits, 1992; Waeyenbergh and Pintelon, 2002; Riane et al., 2009), maintenance bears only partial responsibility for the safe operation of an EO. Thus, uncontrollable risks can be inherent to the architecture of the EO (Hansson, 2013; Verhulst, 2014).

1.2.1.2 Level 2. Principles of planned maintenance

Following the first layer of primary principles, we can derive the following sub-class that deals with the principles of planned maintenance. Maintenance should use knowledge of both degradation and the effect of restoration (Ben-Daya and Duffuaa, 2000). Consequently, better maintenance planning derives from a better understanding of the EO and its operational environment (Riane et al., 2009; Liyanage et al., 2009; Dwight et al., 2012; Ben-Daya et al., 2016). The stakeholders decide planned maintenance actions and protocols for the execution of activities. Stakeholders are:

- Original Equipment Manufacturers (OEM)
- Operators and maintenance (O&M) providers
- Asset owners
- Clients
- Extended Warranty providers
- Consultants
- Regulators

Maintenance stakeholders act according to their own priorities (Dwight, 1999; Murthy, 2000; Waeyenbergh and Pintelon, 2002; Murthy and Jack, 2008; Pintelon and Parodi-Herz, 2008; Labib, 2008; Diallo et al., 2009; Duffuaa and Ben-Daya, 2009; Raouf, 2009; Waeyenbergh and Pintelon, 2009; Duffuaa and Raouf, 2015; Lai et al., 2019).

Asset owners and extended warranty providers often engage consultants as auditors. Auditors usually base their assessment on common assumed standards of what is good maintenance. Practically this means that the maintenance concept is based on the time-based maintenance schedule of OEM manuals. Consultants barge the time-based method out of lack of a deep understanding of the organisation's business (Dwight, 1999).

Another group of stakeholders are, e.g., Occupational Safety and Health Administration (OSHA) and Environmental Protection Agency (EPA) in the US (Mobley, 2002; Duffuaa and Raouf, 2015). These governmental regulators for public safety (Murthy and Jack 2008) have no interest in maintenance cost-saving and, as a result, intend to address maintenance in the same perspective as consultants of owners and warranty providers.

O&M providers can also approach consultants. These consultants are often professional reliability engineers. Their services are offered as short-term consultants rather than become long-term employees. These consultants do not necessarily have the basic knowledge required for the specific organisation (Mobley, 2002). Other consultants are pushing distinct

business philosophies concerning maintenance motivated by their own profit gains. Typical examples of business philosophies are Total Productive Maintenance (TPM), Reliability-Centered Maintenance (RCM) and Life Cycle Costing (LCC) approaches. Obviously, these concepts have both advantages and shortcomings (Pintelon and Muchiri, 2009; Pintelon and Parodi-Herz, 2008; Waeyenbergh and Pintelon, 2002). Others promote their "off-the-shelf" maintenance concept for the same own profit gains (Waeyenbergh and Pintelon, 2009).

Companies are often locked into the OEM to buy spare parts (Murthy, 2000; Murthy and Jack, 2008). Frequently, maintenance policies are directly copied from the O&M manual of the OEM. The recommended Time-based maintenance schedules at these O&M manuals can be biased by commercial interests (Diallo et al., 2009).

1.2.1.3 Level 3. Principles of how to manage planned maintenance

From the second layer of principles of planned maintenance, another sub-class can be derived dealing with principles of how to manage planned maintenance. Triggers for maintenance action, the action itself and the results need to be documented to enable tangible metrics of the effectiveness of these maintenance policies (Dwight et al., 2012). Therefore, maintenance should be systematically managed so that the cues for actions are announced, and the outcomes of actions are recorded at a computerised maintenance management system (CMMS) (Labib, 2008; Raouf, 2009; Duffuaa and Haroun, 2009; Ben-Daya et al., 2016; Bakri and Januddi, 2020; Catt, 2020). The DSS to design the maintenance concept should be dedicated to a unit or sub-unit (Labib, 2008; Liyanage et al., 2009; Burhanuddin et al., 2011; Sharma and Govindaraju, 2020), positioned next to the CMMS and simultaneously data-driven from it. However, Labib (2008), referring to CMMS implementation, stated that there is a black hole when it comes to the DSS. Further, maintenance should evolve as the EO ages and knowledge improves, and failure data are useful for deciding the focus of investment in maintenance (Dwight et al., 2012; Ruiz et al., 2014).

1.2.1.4 Level 4. Principles for the design of a DSS for a specific unit

Last, from the third layer of principles of how to manage planned maintenance, we derive the final sub-class that deals with principles for the design of a DSS for a specific unit (RQ1). The objective of the DSS is to optimise the maintenance concept of a particular unit of the EO. The latter requires an analysis of the degradation process and its severity to understand the level of degradation, i.e., the state of wear at a given time. Data for analysis can be gathered by monitoring the degradation or the degradation indicators in case we cannot observe the degradation directly. Monitoring can be an inspection or continuous real-time

sensor data. So, a DSS should monitor degradation or the indicators of degradation. Degradation is often stochastic to a degree due to the severity and occurrence of extrinsic factors. (Dohi et al., 2000; Ben-Daya et al., 2016).

The state of wear imposes the need for maintenance intervention. Maintenance is often partial restoration, even if components are being replaced with new ones. EO units are often complex multi-component systems, and frequently only some of the components are reworked or replaced. The maintenance practitioner has various options resulting in different stochastic levels of restoration. The unit's state can vary even more when multiple different maintenance actions are undertaken during the unit's lifespan. Therefore, by assessing maintenance policies, the impact of the policies must be known to a certain degree. If the maintenance policies can be tested at the DSS without undergoing the physical lifecycle process, this will reduce the decision time, cost and improve effectiveness (Dohi et al., 2000; Nakagawa, 2000; Ben-Daya et al., 2016). Therefore, competing maintenance policies should be testable in the DSS (Labib, 2008; Liyanage et al., 2009; Burhanuddin et al., 2011).

So, both degradation and restoration are to a degree stochastic. These are the known unknowns in projections. These known uncertainties in projections due to uncertainties of factors that drive condition deterioration (Duffuaa and Ben-Daya, 2009; Duffuaa and Raouf, 2015) should be represented in the DSS. Finally, time, knowledge, skills, and high implementation costs are often significant barriers (Noor et al., 2021). Therefore, the cost of developing a DSS is bearable for only some units of the EO.

1.2.2 Positioning of the DSS in regard to the CMMS

This thesis proposes that the DSS be positioned alongside the CMMS. The DSS should be dedicated to specific units of EO. This is instead of an integrated module of the CMMS dedicated to the overall EO. We can illustrate the reasoning of this architecture with an analogy of the evolution of the computerised Industrial Control Systems (ICS) since the 1960s. The ICS evolved in two different philosophies. Decentralised Control Systems (DCS), which is the standard in the Oil-and-Gas and power generation sectors and Programmable Logic Controllers (PLC) with a Human-Machine-Interface (HMI) what is the standard in the discrete manufacturing industry. The HMI was added in the later years. Nowadays, both architectures can do technically the same thing. However, the philosophy between the two is different. PLC/HMI is the lean architecture, where the System Integrator (SI) must program everything from scratch and involves a significant amount of engineering hours. The DCS has the philosophy that engineering by the SI should be minimised, and the role of the SI

should focus on configuration instead of programming. Therefore, the DCS comes with a library of standard control blocks for each EO, e.g., an automated valve actuator or motor drive (Mazur et al., 2021).

However, each customer has different demands, so the DCS vendors responded to this by adding more and more options. In the end, the control blocks are so giant, with so many whistles and bells, that it becomes heavy in resources and quite confusing for the SI. The latter must go through a handbook of the specific control block to understand the various options, most of which the SI will not use. Worst of all, the particular functionality the SI is looking for is often not fully supported, so the integrator must build ways around it.

Like the ICS, this would be the same for a DSS as part of a CMMS intended to cover all the units of the EO. Most organisations today have some CMMS (Duffuaa and Raouf, 2015). The particulars of an EO at a specific environment and operational conditions are so diverse that an "out of the box" would be inefficient. A DSS will have to be tailored to the particular category of EO to perform effectively. Integrating a tailored DSS at an existing CMMS requires significant customisation of the CMMS software, and implementation often fails this alignment (Catt, 2020).

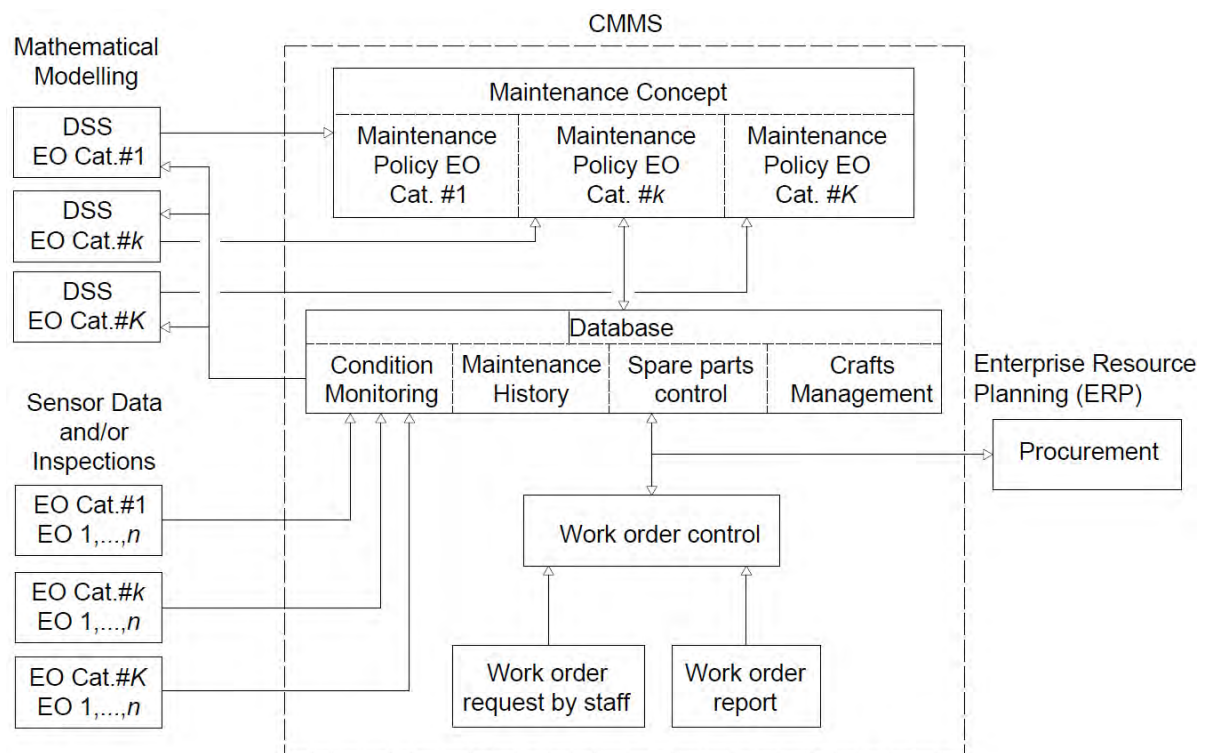


Figure 1-2. Positioning of the DSS in the maintenance management system

Therefore, the researcher's proposal is for a practical reason. Position the DSS next to the CMMS and dedicate a DSS to a particular maintenance requirements analysis of a category

of EOs. Thus, not as a module on top of the CMMS serving the overall EO. Consequently, in this architecture, several DSS can exist. A production facility has numerous of EOs with their sub-units. The Carlsbad Desalination Plant (CDP), as an example, has approximately 23,500 assets registered in the CMMS, including tools. Developing a DSS for even a fraction of these units will be unendurable.

Further, the thesis author proposes that the DSS is data-driven by the CMMS's maintenance history and operational data. If the ICS and CMMS are not directly integrated, the DSS must further be data-driven by the Operational Technology (OT) historian. This data-driven linkage will enable the DT-driven DSS to monitor degradation or the degradation indicators and maintenance effects. A block diagram of the concept is shown in Figure1-2.

A DSS designed for a specific category of EO further simplifies the DSS design process since specific maintenance requirements can be picked out one at a time. So the concept is divided into manageable segments. A DSS for a particular category of EO will be demonstrated further in this thesis.

1.3 Methodology

The research applies the following methodology to address the RQs. The methodology to address RQ1 is inference. This thesis opens a debate to establish the required characteristics of a good DSS for a maintenance concept by proposing a group of principles (Figure 1-1) and from contributions of others in the literature. The debate on the requirements of a good DSS for maintenance is addressed in the previous section, 1.2 Maintenance theory. Then, this methodology of DSS for maintenance requirements is demonstrated by a real example from the practice (RQ2).

1.3.1 Case study

The case study involves the Carlsbad Desalination Plant in California, suffering from biofouling due to seasonal algae blooms. First, the theoretical background of the specific degeneration characteristics is reviewed, followed by standard mitigation methods. The events of the plant are thereby evaluated against the literature. After that, data is collected on the degeneration and restoration of the case study and analysed. Then, the literature is reviewed about publications regarding maintenance strategies to deal with this specific degeneration process. The thesis further places the case study against the maintenance theory literature. From the previous steps, we then derive a mathematical model of degeneration and restoration of this particular case study and use this mathematical model as the engine of a virtual representation, a digital twin, that enables us to project long-term behaviour of

degeneration and restoration. The digital twin is embedded in a DSS that allows for evaluating different maintenance policies. Before evaluating competing policies, the model parameters are first established using statistical methods. Finally, competing policies are compared based on risk, cost, downtime, and the number of stoppages. In more detail, the research is conducted as follow:

- Evaluate the theoretical background of SWRO membrane degeneration, particularly biofouling due to algae blooms, and what has been published on membrane maintenance strategies.
- Evaluate membrane degeneration and restoration from the perspective of maintenance modelling theory.
- Develop a mathematical model of wear and restoration of an RO vessel.
- Estimate the model parameters using statistical methods.
- Build a simulator in MATLAB that enables the analyses of the history of the RO train and provides a mid-to-long-term projection.
- Evaluate different policies to conduct the most efficient membrane maintenance strategy.

Sensitivity analysis is conducted on several fronts. First, the data analysis module of the DSS is utilised for the sensitivity analysis of the parameters of the model (see section 7.6.1). Further, the robustness of the model is tested by running the same projections multiple times at different sampling methods from a distribution for the stochastic extrinsic wear dependency and imperfect repair factor. In addition, various data smoothing regimes are applied when bootstrap sampling is utilized for the stochastic extrinsic wear dependency (see chapters 6.2 and 7.6.1). The results of the projections utilizing different sampling methods and smoothing regimes are then compared against each other for robustness (see chapter 8.2).

The thesis author has chosen not to develop a DT-based DSS that would generate an optimum maintenance policy, but for a DT-based DSS where various policies drawn up by the practitioner can be tested on long-term wear management and cost. The researcher believes that the latter would be less likely to be met with scepticism from the practitioner.

1.3.2 Research Design

The primary data of this research is retrieved from the Historical Database of the OT system and the Computerized Maintenance Management System (CMMS). Further, reports from the O&M company to the stakeholders are consulted. Although this is primary data directly retrieved for the purpose of this research, the data storage is an integral aspect of the

O&M. From a research methodological perspective, the retrieval of the data can be considered as secondary data collected through a case study. The plant started commercial operation in December 2015, and data is available from that date onwards. This research used the data of the RO trains from November 2015 to October 2020, so approximately five years. Although the secondary data is collected from the SWRO desalination plant in California, the research is not limited to this plant. The plant is merely used as a test case for a global problem of the desalination industry.

The research design, conducted as described in section 1.3.1, is a positivist, quantitative deductive research in character (Jonker and Pennink, 2010). More details on the research design are given in chapter 3, Research methodology.

1.4 How the thesis is organised

The structure of this thesis is comparable to that used in physical sciences, described by Dunleavy (2003) as the *opening out model*. The *opening out model* contrasts the classic *focus down model*, often used in social sciences and humanities. The former directly informs the reader of the contributions to the academic community. It builds the literature review, research set up, and analyses around it. The classic focus down model involves the introduction, literature review, and methodology before the thesis addresses the research contributions. The reader often must go through a significant part of the already established knowledge to acquaint the reader with what is new in the presented research. The thesis author is of the opinion that the chosen style provides a better flow in presenting the research.

The thesis is structured as follows. Chapter 2 establish the baseline of the research. Performance indicators are defined and calculated. This chapter was presented as a paper at the 29th European Safety and Reliability Conference (ESREL) in Hannover, Germany (van Rooij and Scarf, 2019).

Following the *opening out model* thesis structure, the research methodology is often discussed in an appendix, as Dunleavy (2003) proposed. Since this research is conducted at a business school, a combination is made between the *opening out model* and to classic *focus down model* thesis structure. Thus, the research methodology is discussed in chapter 3.

Then, Chapter 4 concentrates on the main aspect of RO membrane degradation, biofouling, from a process engineering approach. The phenomena of algae blooms and how this affects the biofouling of the RO membranes. Further, the mitigation of membrane degeneration is reviewed. Chapter 5 describes an RO train from the perspective of maintenance modelling theory as a unique multi-component system. The degeneration

processes are compared with that of other multi-component systems specified in the literature.

Following Chapter 6, the mathematical model is set out, followed by the parameter estimation of the model. Chapter 7 describes the implementation of the model into the DT, which in turn is embedded into the DSS applied to this case study. In Chapter 8, the research applies the DSS of the case study to evaluate the maintenance requirement. Various maintenance policies are described for testing, and the results and analysis of the projections are provided.

Before concluding this research, the thesis returns to the baseline of the research in chapter 9. The outcome of the study is compared against the performance indicators of the baseline. Finally, the conclusions, limitations, and recommendations for further research are drawn up.

The thesis has not a single literature chapter, but the literature is consulted throughout the thesis. Here are some examples. The thesis describes the case study first from a water engineering perspective and embedded a literature review of membrane fouling, particularly biofouling and preventative, corrective actions. Then, the reverse osmosis vessel is approached from the perspective of maintenance theory. This chapter, a literature review of maintenance theory, is embedded specifically towards a reverse osmosis pressure vessel. After that, the thesis concentrates on the mathematical model of degeneration and restoration of the membrane elements in the vessel. This chapter again involves existing literature on maintenance modelling. The parameters of the model are established using statistical methods. These methods are established knowledge, and the literature about these methods is consulted. Following a DSS incorporating a DT of an RO vessel is developed. Here the literature around DTs is consulted.

The next chapter, setting the baseline of the research, is an initial evaluation of where the plant in this case study stands after the first three years of operation. The purpose of the baseline was to establish metrics that would allow tangible measurements of O&M performance improvement. The chapter further presents the initial maintenance requirements analyses, which led to this thesis topic.

2 Setting the baseline of the research³

This chapter describes preliminary work on the case study. The chapter was presented at the 29th European Safety and Reliability Conference (ESREL) in Hannover, Germany. The study identified three categories of possible improvement: shortfall of delivery; the share of failure based unplanned maintenance activity; and the rate of membrane replacement. Performance indicators were set for all three categories. Further, to measure operations and maintenance planning effectiveness, a baseline for maintenance performance must be set. It provides the metrics by which the effectiveness of future maintenance policies can be measured.

The analysis of the plant data indicates that the shortfall of the first three years of operation, especially that in the second year of operation, is characteristic of a 'break-in' period. This phenomenon is referred to as the bathtub curve, which identifies a higher failure rate at the beginning and the end of the equipment lifespan (Mobley, 2002; Duffuaa & Raouf, 2015). However, the latter does not apply to the membrane replacement requirements, with an annual element replacement rate higher than initially projected. Improvement of the membrane lifespan is not expected due to passing the 'break-in' period; therefore, improvement of this particular EO directly results from improvement of maintenance planning. Thus, following this study, the research concentrates mainly on membrane maintenance performance analysis. Membrane maintenance management is a niche speciality under maintenance practitioners and academics in the maintenance research disciplines. More details on membrane maintenance management are provided, starting with chapter 4.

2.1 Maintenance, one of the pillars of business strategy

Industries are under constant pressure to reduce production costs and improve performance simultaneously (Wang et al., 2007). Maintenance has an important role in this. In the early post-World War period, business strategy neglected maintenance. This changed in the 1970s. For example, in the 1980s, a prominent US car manufacturer increased the production output of one of its production lines from 70% to 99%, thereby increasing its annual profit by approx. \$30M. This was achieved principally by adopting preventive maintenance in place of corrective maintenance (Gallimore and Penlesky, 1988). By the

³ This chapter is a slightly modified version of *Towards a maintenance requirements analysis for maximizing production* presented at the 29th European Safety and Reliability Conference (ESREL) in Hannover, Germany. Published by Research Publishing Services and has been reproduced here with the permission of the copyright holder.

1990s, maintenance was recognized as a potential “profit contributor” (Pintelon and Parodi-Herz, 2008). Today, maintenance is recognized as one of the pillars of business strategy.

Nevertheless, maintenance is frequently still driven by short-term issues such as costs and resources, and often maintenance strategy is not sufficiently focused on competitiveness and sustainability (Carnero Moya, 2004). Furthermore, maintenance policies are often not directly associated with the production itself. It is then difficult to relate maintenance spending to production targets (Scarf, 1997). The absence of a long-term vision and the roadmap towards it means that management cannot see the short-term benefits of maintenance. Consequently, confidence is easily lost, and the essential resources for establishing effective maintenance policies are not made available (Carnero Moya, 2004).

This is especially the case for the introduction of predictive maintenance. In the early stage of design and implementation, data and expertise on the condition of critical equipment must be gathered before predictive maintenance policies can be turned into practice. Often, small O&M teams do not have the resources to implement successfully predictive maintenance policies (Carnero Moya 2004, Önel et al. 2009). Only 10% of those surveyed around the change of the millennium indicated that condition-based maintenance added value to plant performance; 50% indicated that it did not provide a return on investment. Often an important reason for this was that no baseline was established before introducing the new maintenance policies, and therefore no metrics were available to measure success (Mobley, 2002). A baseline must be more than an isolated summary of maintenance and operations records; it must provide data on the effectiveness of the current maintenance policies (VanHorenbeek and Pintelon, 2013). We address these issues in the case study of this research.

The structure of the chapter is as follows. We first discuss briefly maintenance performance measurement. Then we describe the context, define the performance indicators and the baseline derived from these performance indicators. The baseline is then calculated based on the initial plant data. Finally, we analyze how maintenance performance can be improved.

2.2 Establishing the baseline

Maintenance can be defined as “the total of activities required to retain the systems in or restore them to the state necessary for the fulfilment of the production function” (Gits, 1992, p. 217). The maintenance concept, or maintenance requirements analysis, can be defined as a set of rules that recommend what maintenance is required and when (Gits, 1992). Ben-Daya,

Kumar, and Murthy (2016) defined the maintenance concept, based on terminology proposed by Pintelon and Parodi-Herz (2008), as “a set of maintenance policies and actions of various types and the general decision structure in which these are planned and supported”.

A key part of the maintenance requirements analysis is a maintenance performance measurement system, with performance indicators that are determined from corporate goals (Parida and Kumar 2006, Van Horenbeek and Pintelon 2013). Arts et al. (1998) define performance indicators as “a numeric value for an aspect of a (sub) process that is not influenced by related processes and is representative as a measure for the effectiveness and, or efficiency of that aspect of the (sub) processes”. These performance indicators will form the baseline. The effectiveness of a change in the maintenance requirements analysis can then be evaluated based on tangible metrics (Parida 2007, Åhrén and Aditya 2009). The resources required for improvements in maintenance to close the gap between potential performance and actual performance can then be justified (Van Horenbeek and Pintelon, 2013), and reviews of maintenance policies can be driven by asset requirements rather than financial contingency (Dwight et al., 2012).

This research involves a case study of a Seawater Reverse Osmosis (SWRO) Desalination Plant. The plant processes seawater into high-quality potable water. The plant, currently the largest of its kind in the Western Hemisphere, is owned by a project development company. The company that is contracted to operate and maintain the plant we shall call the O&M company. This company, highly specialized in desalination, also designed the plant. The plant was commissioned in 2015, and delivery of product began in December of 2015. Figure 2-1 shows a simplified process diagram of the plant. The primary sub-systems are as follow:

- Intake pumps (IP)
- Low-Pressure Booster (LPB) Pumps
- High-Pressure Booster (HPB) pumps
- High-Pressure pumps (HPP)
- Energy Recovery System (ERS) units
- Reverse Osmosis Trains (RO)
- Product Water Pumps (PWP).

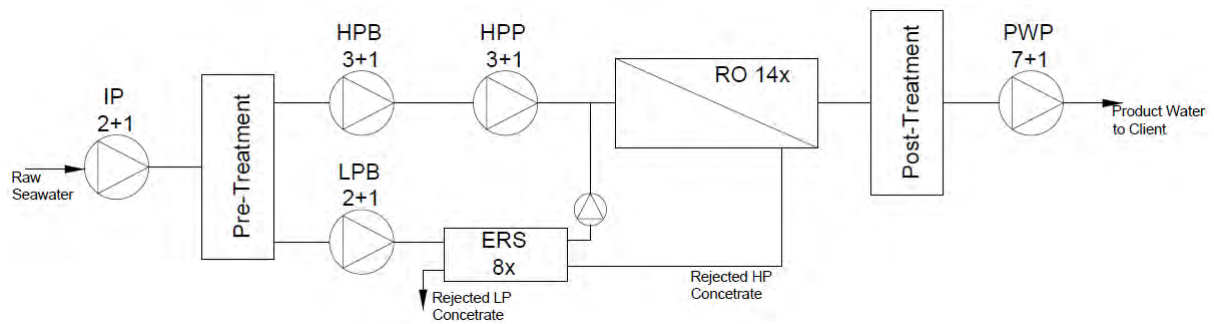


Figure 2-1. Simplified process diagram of the plant involving the main equipment.

The O&M contract stipulates that the plant should deliver a daily-specified volume of potable water, the demand, to the end client, the regional water authority. The O&M company is penalized if the cumulative amount of potable water supplied in a month, which we shall call the delivery, does not meet the demand for that month. When supply has not met demand, the daily delivery is allowed to exceed the daily demand by at most five percent in order to make up this deficit. The accumulated deficit over a month, which we shall call the shortfall, is evaluated. Notice then that production capacity can exceed the delivery. We call the total production capacity in a month the availability for that month.

Thus, operation and maintenance aim to minimize shortfall rather than maximize (plant or product) availability. This case study focuses on one aspect of an overall objective to explore the improvement of system performance through the joint planning of production and maintenance. This joint planning aims to manage production output so that maintenance pit-stops and planned maintenance shutdowns can be postponed when demand is high and executed when demand is low. Such policies require continuous monitoring of equipment conditions, demand, and environmental conditions. Equipment condition needs to be monitored to prevent more costly faults and longer downtime due to the postponement of maintenance. The Carlsbad Desalination Plant (CDP) is rich in continuous field measurements. It has approximately 990 analogue sensors, of which 31% measure temperature, 17% pressure, 16% flow, 14% water analytics, 9% vibrations, 8% levels, and 5% power. Thus a broad spectrum of environmental and operational data that is logged in the Operational Technology (OT) historical database.

Demand needs to be monitored and forecasted to anticipate suitable maintenance and shutdown periods and prepare resources for these. It is important that maintenance activities are not dominated by surprise failure-based reactive repairs to plan maintenance but by scheduled preventive maintenance. According to Emerson process management (2003), the target of failure-based maintenance should be less than 25% of overall maintenance.

An important part of condition-based maintenance of SWRO plants is the reversal of membrane deterioration due to fouling. Pre-treatment should mitigate fouling but will not prevent this. Clean-in-place (CIP) is a condition-based maintenance activity to reverse the deterioration of the membranes due to fouling. CIP should be undertaken when the normalized Pressure Differential (PD) or salt passage has increased by 10 to 15% or when the permeate flow decreased by 10 to 15% (Kim et al., 2017). See section 3.3.2 for RO data normalization.

The knowledge of how to deal with the environmental conditions resulting in fouling and more sophisticated cleaning procedures to reverse the degeneration has shortcomings. A successful CIP program in one part of the world might be unsuitable in other regions due to different environmental conditions leading to the fouling (Ruiz-García et al., 2017). If CIP is not effective or performed too late, degeneration will be irreversible. Those membranes where the degeneration cannot be reversed with CIP need to be replaced. An 11.5% replacement of membranes annually is acceptable.

The objectives expressed by the CEO of the O&M company are to reduce shortfall and reduce costs. Membrane replacement is a substantial part of the costs. Based on the above objectives, we identify performance indicators that relate to:

- the shortfall;
- failure-based maintenance activity of the main equipment (see Figure 2-1);
- membrane replacement.

The derived performance indicators are considered annually by the O&M company, they are expressed in a common unit, days of lost production, and defined in the following way.

- P1: The ratio of shortfall (volume of potable water) to designed capacity (volume of potable water per day).
- P2: Ratio of failure-based to all maintenance activity, expressed in days of lost production.
- P3: Annual percentage of membrane replacement, expressed in days of lost production.

To convert the ratio of failure-based to all maintenance activity to days of lost production, we estimate the marginal cost of an increase in this ratio (due to the additional cost of equipment failure and emergency orders for spare parts). We then convert this cost to days of lost production using the known penalty cost of the shortfall. We find that the cost of a one percent increase in this ratio is equivalent to half a day of lost production. The known cost of membrane replacement is treated in a similar manner so that the cost of replacement of one percent of membranes is equal to the penalty cost of 5.4 days of lost production.

The overall performance is the sum of these performance indicators, expressed in days of lost production. The baseline is then the value of this overall performance indicator. Although, following the maintenance performance analysis in section 2.5, the research will concentrate on just one of the three performance indicators, setting the baseline for all three indicators identified will prevent pulling away resources from other fields. Thus giving a one-sided improvement at the expense of other aspects of O&M. For instance, excessive downtime of RO trains for maintenance could negatively affect the shortfall.

2.3 Calculation of the performance indicators

The data to calculate the performance indicators are retrieved from a historical database and the Computerized Maintenance Management System (CMMS). The historical database is used to retrieve information on demand, delivery, shortfall, and availability. The CMMS provides information on maintenance activity and the labour hours used. The number of membranes replaced annually is also retrieved from the CMMS.

To define availability, we consider operational technology, according to Kranendonk (2016), as the hardware and software controlling all physical processes on production sites. We classify the pumps, RO Trains, and ERS units as complete units, including valves and other auxiliary equipment. For example, a fault on auxiliary equipment, e.g., a suction or discharge valve of an intake pump, results in a master fault of the specific pump. The same applies if there is a fault from the motor drive of a pump.

Each pump sub-system (IP, LPB, HPB, HPP, and PWP) has one standby unit (redundancy). Introduction of standby equipment is a maintenance policy applied when either the costs or risk of breakdown is extremely high (Gallimore and Penlesky, 1988). The ERS and RO trains do not have standby units. Failure of systems with redundancy can still impact on production (Table 2-1).

Table 2-1. Impact of availability of the production resources on plant-designed capacity.

| Sub-System | Units | Units required (R) for nominal production | Availability reduction when units up is R-1 |
|------------|-------|---|---|
| IP | 3 | 2 | 46% |
| LPB | 3 | 2 | 46% |
| HPB | 4 | 3 | 26% |
| HPP | 4 | 3 | 26% |
| ERS | 8 | 8 | 3% |
| RO | 14 | 14 | 7% |
| PWP | 8 | 7 | 5% |

Availability must be looked at in relation to the demand since equipment can be taken offline for preventive maintenance when the demand is low. Thus, a unit is idle since it is not required for the demand at the time, and the maintenance team uses the opportunity to conduct preventive maintenance.

Further, shortcomings in delivery are not always due to (un-)availability. Figure 2-2 below shows the availability and delivery in relation to the demand, whereby the demand for water delivery is taken as a baseline (100%).

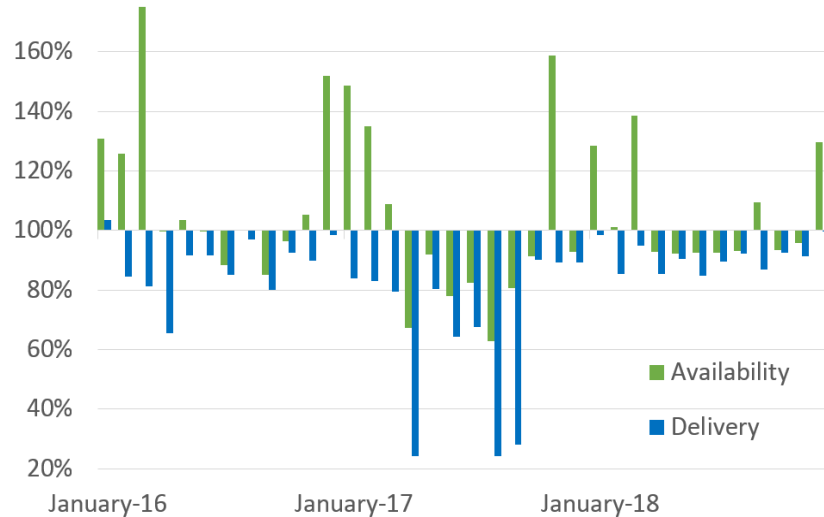


Figure 2-2. Availability and delivery relative to the demand for each month of operation.

Thus, although availability in several cases is higher than the demand, there is still a shortfall. Shortfall in these cases is caused by operational or external factors. The annual demand over the first three years of operation varies, and due to this, we cannot compare directly the shortfalls. We, therefore, introduced a correction factor that equals the designed availability divided by the demand. Table 2-2 below shows the adjusted shortfall in million US Gallons (MG) over the first three years of operation. The shortfall is further expressed in days of lost production.

Table 2-2. Performance Indicator 1: adjusted shortfall in production in 2016, 2017, and 2018.

| Year | Correction factor Availability/Demand | Shortfall (MG) | Lost days of production |
|------|--|-------------------|----------------------------|
| 2016 | 1.18 | 447 | 8 |
| 2017 | 1.15 | 3,116 | 59 |
| 2018 | 1.12 | 672 | 13 |

In addition to the availability, we retrieved the manhours spent on the various maintenance activities. Figure 2-3 shows the percentage of maintenance hours spent on failure-based, preventive maintenance, and inspections per each primary subsystem, the combined primary subsystems and further for the plant overall. At the level of the primary subsystems, failure-based maintenance accounts for 45% of maintenance manhours in 2018. The CMMS does not make a distinction between time-based and condition-based maintenance. Both are classified as preventive maintenance.

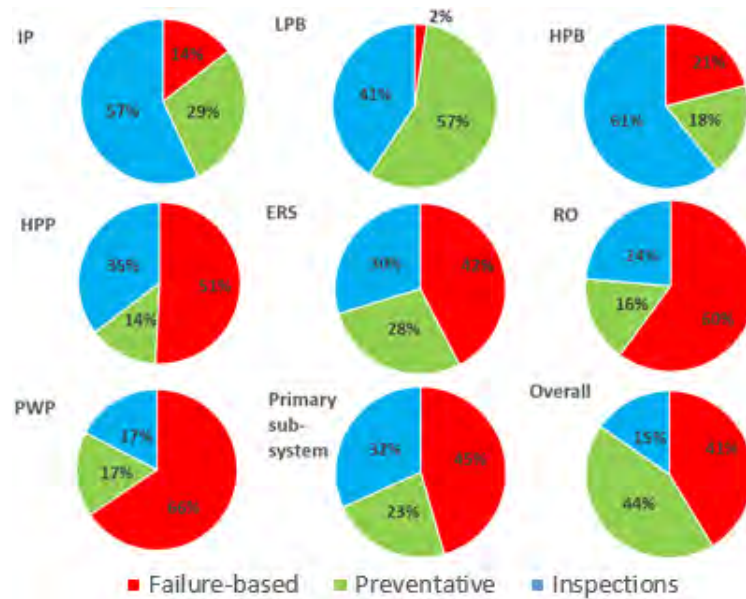


Figure 2-3. Performance Indicator 2: Percentage of maintenance activity by type and by unit for 2018. “Overall” involves all the plant equipment (primary and secondary sub-systems together).



Figure 2-4. Average normalized RO PD.

An important issue for condition-based maintenance of SWRO desalination plants is the fouling of the membranes. Figure 2-4 shows the average normalized PD of all RO trains combined over the years 2017 and 2018. The increase of differential pressure, starting in March/April 2017, is the effect of fouling. This phenomenon occurs with the annual season of an algae bloom. The rate of increase in PD was so severe that the O&M team was unable to catch up with the required frequency of CIP. As a result, 25% of the membranes were replaced during the summer of 2017. 2018 shows a repetition of 2017.

2.4 Calculation of the baseline

We defined earlier three performance indicators derived from the O&M company objectives. These performance indicators provide the metrics to establish the baseline by which future improvements of the maintenance policies can be verified. The first two performance indicators are directly measured annually. Membrane replacement varies greatly from year to year. Therefore, we use a two-year moving average so that, for example, P3 in 2018 is the mean of the percentage of membrane replacements in 2017 and 2018.

P1 is given in Table 2-2. The corrected shortfall in 2018 was 672 MG or 13 days of lost production. For P2, the hours spent on failure-based maintenance for the primary subsystems was 45% in 2018. The target for P2 is 25%. Using the percentage-days conversion (1% above 25% is equivalent to half a day of lost production) described in chapter 4, we have that P2 in 2018 is ten days of lost production. The two-year moving average of membrane replacement over the years 2017 and 2018 was 12.5% annually. The target is 11.5%. The difference is equivalent to 5 days of lost production. We use 2018 to define the baseline since we can assume that by 2018 the plant had passed the 'break-in' period. So, summing the PIs for 2018, we have that the baseline is $13+10+5=28$ days of lost production.

2.5 Improving maintenance performance

Labib (2004) proposed to use multi-dimensional Pareto diagrams as a guide for maintenance planning. The inputs of these analyses are typically the average downtime per failure and the number of failures per unit. These charts can be used to identify those sub-systems whose failure most impacts upon plant performance. They can also give an indication of the stage of the maintenance lifecycle of the plant, in this case, whether the plant is in or has passed the period of 'break-in' or start-up period, wherein reliability and availability can be low due to installation and design problems (Mobley, 2002; Ben-Daya et al., 2016).

Careful presentation of these data is required, particularly where there is redundancy. Therefore, we present the data in two ways. Firstly, we count only those failures that are production-critical. That is, they affect availability (Figure 2-5). For example, for intake pump failure, production capacity is affected only if the number of available pumps is less than two. We count the frequency of these failures. We then calculate the median downtime of these failures for the sub-system. Thus, demand does not impact upon the calculation here, so it is possible that such a failure does not contribute to the shortfall. Using the mean instead of the median downtime can give a distorted impression in the case when a sub-system is unavailable for an unusually long time. Secondly, we repeat this calculation for all failures regardless of whether plant-production capacity is affected (Figure 2-6). E.g., the failures and downtime of the HPB in 2017 are substantial in Figure 2-6. However, Figure 2-5 indicates that the RO trains and PWP had a much greater impact on the production.

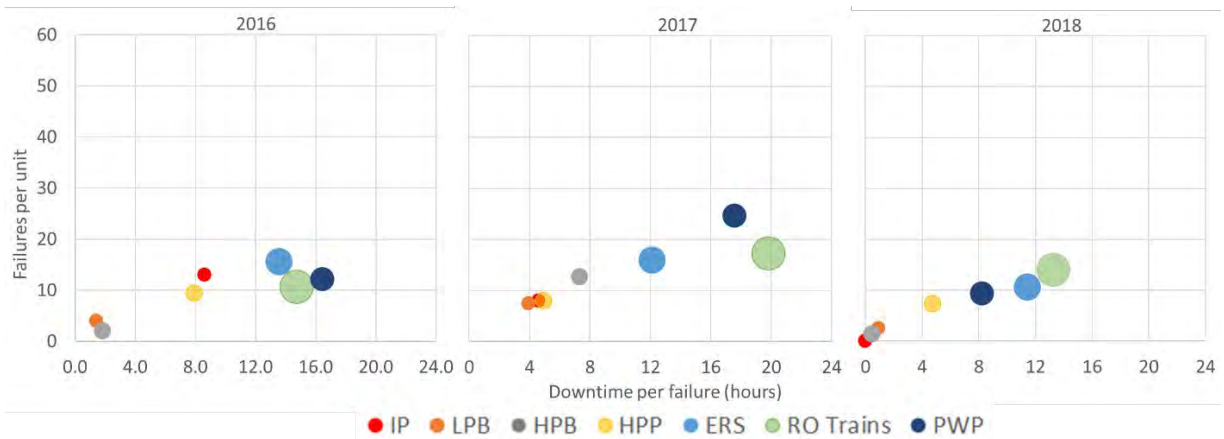


Figure 2-5. Total number of failures per unit vs median downtime per failure for production-critical failures.

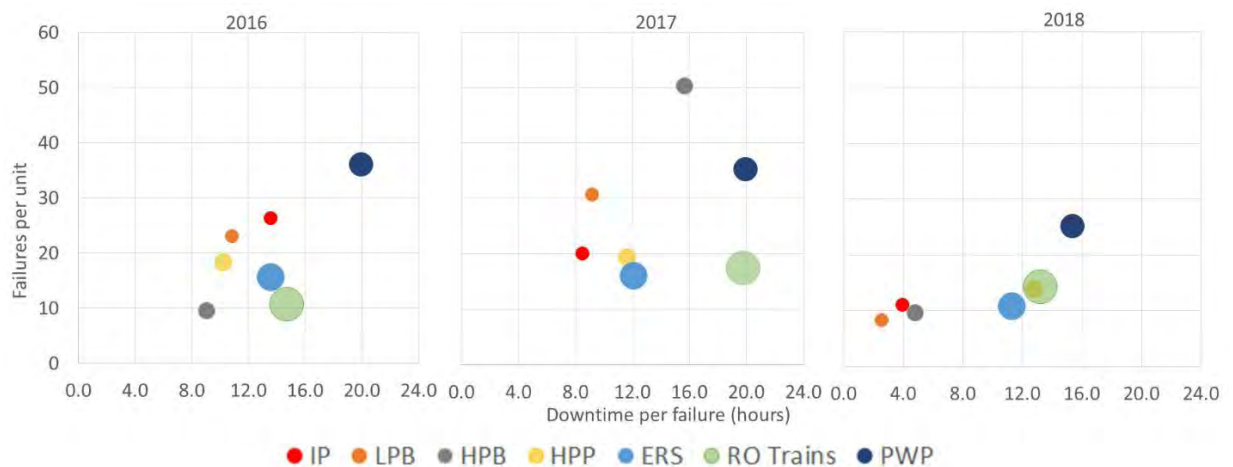


Figure 2-6. Total number of failures per unit vs median downtime per failure including production-noncritical failures

Planned plant shutdowns are disregarded since the equipment is taken out of service during these periods of routine, preventive maintenance. In both charts, the size of the plotted symbols is representative of the number of individual units in the subsystem.

These charts can then inform maintenance planning in the manner described by Labib (2014). Thus, maintenance policies for sub-systems with low frequency of failure and low downtime can be considered as operate to fail (OTF). Those systems with high in frequency of failure and low downtime require skill level upgrade (SLU), i.e., operator training. Systems with failures resulting in high downtime but are less frequent would be the best addresses with condition-based maintenance (CBM). Failures high in frequency and high in downtime are design shortcomings and require design out maintenance (DOM). Those failures that cannot be classified by any of the above groups are best addressed by time-based maintenance (TBM).

Interpreting the data of Figures 2-5 and 2-6, we see that in both 2016 and 2017, the first and second years of operation, the frequency and downtime duration are slightly higher than in 2018. 2017 is the worst year, and suggesting to the O&M team that there were design-related failures and lack of experience by the contractor at the construction phase, e.g., the loading of the membranes. We can identify the following circumstances as design-related failures (DOM) and training related (SLU):

- Failed o-rings at RO membrane inter-connectors during 2017 indicates improper shimming between the membranes and the endcap in vessels (SLU)
- The use of pump packing instead of mechanical seals at the product water pumps (DOM)
- Incorrect material selection for suction valves of Booster and HP pumps to withstand corrosive seawater (DOM)



Figure 2-7. Total annual equipment downtime in hours.

The overall annual downtime of the equipment (Figure 2-7) shows a starker contrast between the first two years and the third year. The data of 2018 suggests that the plant has

started to leave the 'break-in' period behind. However, it is still too early to ratify this conclusion.

Implementation of predictive maintenance should mitigate unforeseen equipment breakdowns. Health-deterioration indicators will be established for critical equipment based on a combination of real-time field measurements and modelling of deterioration rates to overcome the constrained resources of the relatively small team in the O&M company.

Our analysis of the multi-dimensional Pareto diagrams indicates that sub-systems with a redundant unit mitigate production-critical failures. The analysis further indicates that the plant underwent a 'break-in' period during the first two years of operation. Some sub-systems were subject to DOM, others to SLU. Finally, the analysis suggests an OTF policies for the IPS, LPB and HPB systems and a CBM policies for HPP, ERS, RO and PWP systems.

2.6 Summary

A baseline has been established using three performance indicators: shortfall in delivery, the ratio of hours spent on failure-based maintenance to overall maintenance activities, and the percentage of annual replacement of membranes. The performance indicators are expressed in a common unit, days of lost production. 2018 is used as the baseline year, and the baseline is 37 days of lost production per annum. The performance indicators are derived from the corporate objectives: reduction of shortfall of delivery and reduction of O&M costs.

Analysis of failure data by means of multi-dimensional Pareto diagrams indicates that the plant went through its 'break-in' period during 2016 and 2017, the first two years of operation. There are indications that the operation and maintenance of the plant are now more mature. This, to an extent, justifies using 2018 as the baseline year.

Our analysis of the multidimensional Pareto diagrams suggests an operate to failure (OTF) policies for the IPS, LPB and HPB systems. However, this may be rather short-sighted, given the cost and the long lead-time for these pumps. OTF is further unacceptable if it affects safety (Ben-Daya, Kumar, and Murthy, 2016). Therefore, following this research, it is recommended that condition-based maintenance (CBM) be considered for these systems. The analysis further suggests CBM for HPP, ERS, RO and PWP. Predictive maintenance is therefore recommended for all the analysed subsystems.

Predictive maintenance programs have a high chance of failure if the organization is not adequately prepared. This applies more so to industries with a small O&M team with constrained resources. We assume that automation of predictive maintenance within the Operational Technology (OT) system can mitigate the lack of resources. The predictive

maintenance system can be established by modelling health-deterioration indicators. By integrating predictive maintenance within the OT system, the plant operators can strengthen the expert team.

Further research should also focus on improving system performance by the joint planning of production and maintenance. This improvement entails three approaches. The demand must be forecasted. An attempt to forecast demand is presented in chapter 9.1. Production planning further requires the collaboration of all stakeholders, especially the client, to project medium-term demand. Secondly, degradation must be modelled and forecasted. Finally, reducing the time spent on failure-based maintenance will reduce unpredictability so that planned maintenance can be carried out more effectively. Some simple tools for condition-based maintenance for centrifugal pumps are presented in Chapter 9.2.

Membrane deterioration contributes to O&M costs. Particular attention should be given to the predictive maintenance of the RO membranes. The latter requires a membrane condition-based monitoring system. In this way, continuous improvements in RO operating conditions can slow down the deterioration. Further, improvements of the clean-in-place (CIP) procedure and schedule, which can reverse membrane deterioration to acceptable levels, is vital for the maintenance policy. In chapter 9, we return to the results of all three performance indicators following three years of operation since the baseline was set. The performance indicators at the end of the research are compared to the baseline.

In contrast to condition-based maintenance of centrifugal pumps and demand forecasting, RO membrane maintenance received little attention in the literature. This research, therefore, further concentrates on managing the restoration of RO membranes. The next chapter first outlines the research methodology so that the research is founded on a solid base.

3 Research Methodology

The study in this thesis is positivist, quantitative deductive research. This chapter outlines the philosophical framework of the research. The chapter is organised as follows. First, the research problem statement is outlined in section 3.1. The chapter then concentrates on the researcher's philosophical choices, the approach to theory development, and methodological choice in section 3.2 Research Design. Then section 3.3 concentrates on the practical methods applied in this research. Section 3.4 deals with ethics.

3.1 Research problem statement

This research considers maintenance modelling. Managing the long-term reliability of a system in the presence of stochastic wear conditions involving imperfect maintenance, with uncertain long-term effectiveness of the interventions. This research is motivated by a real practical maintenance problem: a seawater desalination plant, where the wear of the Reverse Osmosis (RO) membranes was higher than initially expected. The wear is accelerated due to a physical-biochemical reaction, known as biofouling (Stoodley et al., 2002), driven by seasonal algae blooms (Chiou et al., 2010; Villacorte et al., 2015; Li et al., 2015; Villacorte et al., 2017).

The corporate CEO of the operations and maintenance (O&M) company expressed his concern about the projection of long-term maintenance costs. The latter was due to the high rate of annual membrane replacements during the first several years of operation. The strategic aim of the O&M company is to bring the long-term membrane replacement ratio more in line with the initial projection. The above objective is outlined further in Chapter 2 of the thesis.

3.1.1 Observations prior to the research

The reason for the rapid degeneration of the membranes was identified before the launch of the research. Elevated pressure differentials (PD) were noted over the RO trains after the first half-year (see chapter 4.3.2. RO Desalination in practice). The Carlsbad Desalination Plant (CDP) has been in commercial operation since December 2015 (for system configuration, see chapter 4.3.2. RO Desalination in practice for system configuration). An increase of 10 to 15 per cent of the normalised pressure differential (NPD) over an RO train (see section 3.3.2. Monitoring membrane fouling and RO performance data normalization) indicates RO membrane fouling (Li et al., 2015; Jiang et al., 2017; Kim et al., 2017; Villacorte et al., 2017).

To determine the fouling type, the O&M team of CDP removed the lead and the tail membrane element from a random vessel. The membranes were sent for membrane autopsy (see chapter 4.4.2. Membrane Autopsy to determine the fouling type). The autopsy concluded that the degeneration of the membranes resulted from biofouling. Following this, the O&M team undertook a clean-in-place (CIP) of a few RO trains with the highest PD, with limited success (see chapter 4.5.2. Restoration). Another ad-hoc action applied at one of the trains was to swap the lead and the tail element. The lead membrane element now positioned at the tail was thereby turned around, so the feed side became the rejected side. This action provided some improvement.

The deterioration of the RO membranes during the first year of operation followed a period of deteriorating pre-treatment. However, the two events were not put in context. The declining runtime of the pre-treatment multimedia gravity filters was assumed to result from operational inexperience and the need for operational optimisation. The following year, the O&M team struggled again with the pre-treatment around the start of spring. This time, however, an algae bloom was identified as the cause. Simultaneously, the PD over the RO trains accelerated. In a matter of weeks, the degeneration of the RO membranes was so severe that immediate action was required.

In the following months, the first significant membrane replacement took place. Per train, every membrane was weighted to observe the elements with the highest biomass. In practice, the first two elements had significantly higher weights. Consequently, per train, two elements were replaced. The reconfiguration of the position of the elements was further arbitrary.

Although the knowledge of the preceding observations can be deduced from theories presented in the engineering literature, conclusions by the O&M team was often a result of perceptual assumptions. The swapping of the lead and the tail element, undertaken at one of the trains, illustrate this. The action was in response to the critical state of the train. Although the action improved the train's condition slightly (See chapter 6.1.1. for an explanation of this phenomenon), the intervention was driven by trial and error.

Science provides a considerably more nuanced approach to reasoning than the layperson. Pruzan (2016) illustrates the difference in reasoning using an example from Hempel (1948) to explain the observation of a mercury thermometer that is rapidly immersed in hot water. First, the thermometer drops in the mercury column, then a swift temperature rise follows. The layperson could reason that the temperature first is dropping, followed by a rapid increase. However, from a scientific inference, the glass tube holding the mercury is first heated, whereby the tube expands and thus provides a larger volume for the mercury. Following the

heath, conduction raises the temperature of the mercury, and its coefficient of expansion is considerably higher than that of glass.

The scientific inference, in this case, is deducted from general laws of physics, i.e., the thermic expansion of mercury and glass and the thermic conductivity of glass. Thus, although the cause of the business challenge was known, the thesis author does not take the latter assumptions for granted. Therefore, this research re-examines previous observations.

3.2 Research design

As the response of the O&M company for restoration was initially merely based on ad-hoc decisions, the researcher intends to develop a scientific solution for a cost-effective long-term membrane maintenance plan. The research aims to provide the tools to implement the corporate strategy as stated in the introduction: to bring the long-term membrane maintenance cost more in line with the initial projection.

Chapter 1 of this thesis outlines the research problem and approach. For research methodology design, here follows an interpretation:

- The researcher must resolve a strategic business issue.
- The nature of the business issue is increased long-term maintenance cost due to unforeseen stochastic wear of a vital part of a technical system. The maintenance practitioner can apply a multitude of imperfect maintenance actions. However, the long-term results are uncertain.
- The researcher presents a decision support system (DSS) to evaluate the longterm-maintenance requirements as the solution.
- Following the researcher translate the requirements of the DSS for general-purpose. So, the presented method of a DSS for maintenance requirements can benefit researchers and practitioners of maintenance in general.

To conduct scientific research, we first need to define the approach of the research. It is crucial to identify the nature of the study. The methodology provides a framework for solid research, independently of unacquainted bias due to the researcher's perception (Growther and Lancaster, 2005; Paltridge and Starfield, 2007; Jonker and Pennink, 2010; Pruzan, 2016). The latter is particularly prominent in qualitative research, where the data is descriptive. Qualitative research not founded on a solid methodology has insignificant scientific value. Perception is less likely to influence positivist quantitative research, where data is based on measurable numbers. Thus, in natural science research, typically, a reference is made to the methods used and rarely emphasises methodology (Gauch Jr, 2003; Pruzan, 2016). The

methodological approach needs to be adopted accordingly to the research problem we want to resolve. Saunders et al. (2009), referencing Johnson and Clark (2006), maintain that it is not essential whether the research should be philosophically-informed, rather than how correctly we can reflect on the philosophical choices and defend these choices. So, we must undertake the research methodology design departing from the research problem and the path we intend to resolve it.

The knowledge of what is known and what is unknown at the onset of the research is vital for the research direction. The preceding section, 3.1.1, outlined the conclusions of the observations made prior to the research. From the outset of the study, the cause of the business challenge was presumed to be known. The researcher might be influenced by his engineering background in taking a clear decision that the research direction should be oriented towards predictive analytics. However, besides that, there is no other alternative. To optimise the maintenance of an engineered object, we have to deal with the specifics of this engineered object.

Predictive analytics inherent involves maintenance modelling. A management study dealing with maintenance modelling concentrates predominantly on engineering and statistical inference, i.e., applied natural and applied formal science. The research philosophy becomes that of positivism. Saunders et al. (2009) have outlined the research philosophies in management research in a convenient table. The thesis author has applied this table to a flowchart to define the philosophical direction of the research (see Figure 3-1). According to this flowchart, we can summarise the philosophical choices made in this research as an external objective without social actors. Quantitative data provide only observable phenomena, whereby the researcher can not influence the interpretation of the data. So, the research is positivist using quantitative data. The researcher's epistemologist view of what constitutes proper knowledge is further of minor importance in case we deal with pure deductive inferences. However, if the approach to theory development involves inductive inference, this is another matter.

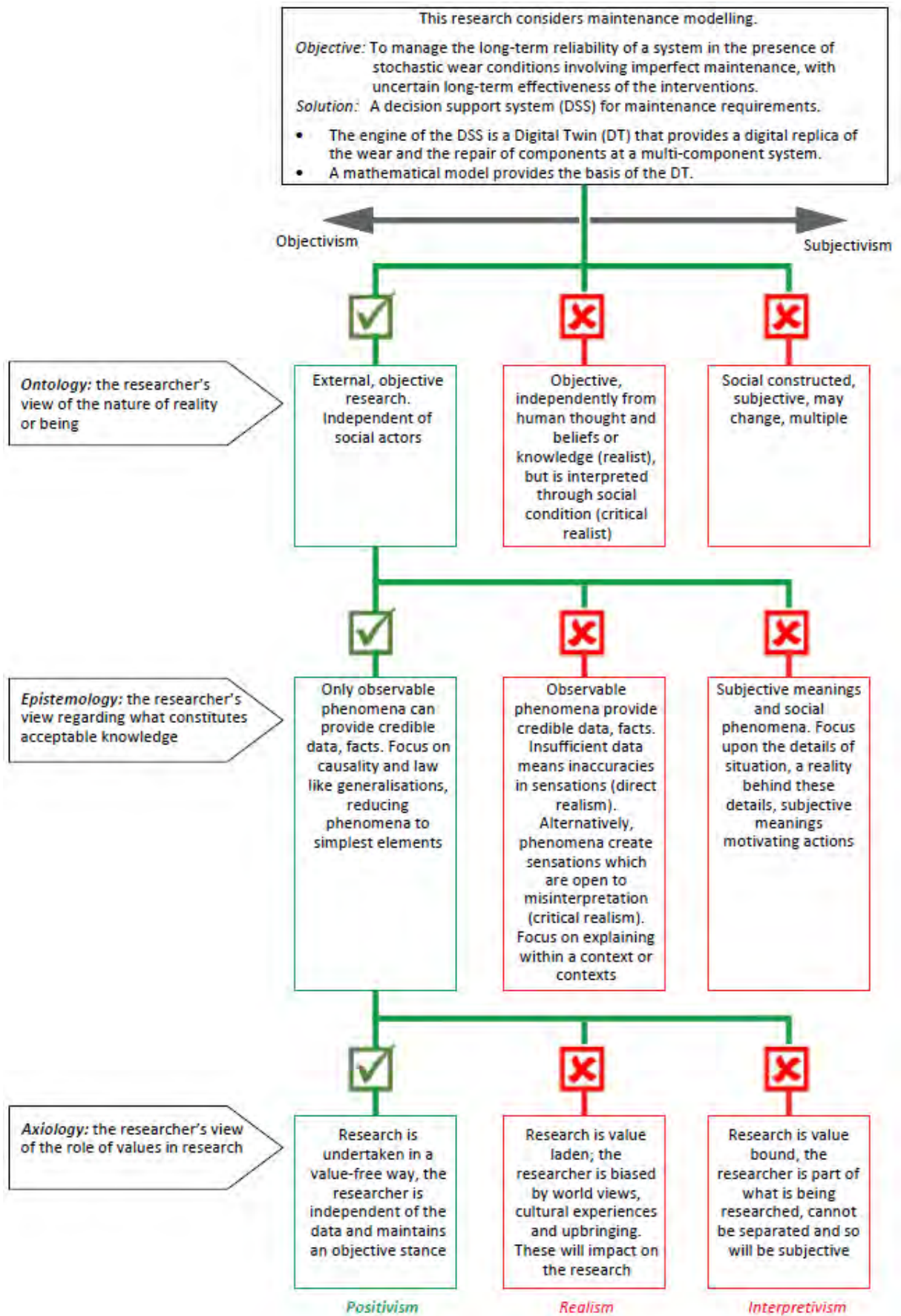


Figure 3-1: Philosophical direction of the research, defined by Saunders et al. (2009) as a table of research philosophies in management research and translated into a flowchart by the thesis author.

3.2.1 Role of Modelling and Simulation in Scientific Discovery

Management scientists frequently utilise modelling and computer simulations to deal with feasibility options in a decision problem. In management science, it is the most commonly used method (Pidd, 2004). Several review papers have been published on the subject of modelling in manufacturing and supply chain management. Jahangirian et al. (2010) presented a literature review on the role of simulation techniques within manufacturing and business between 1997 and 2006; (Mourtzis et al. (2014) gave a review of significant milestones in simulation technologies in industrial and research between 1970 and 2014 and future recommendations; Negahban and Smith (2014) reviewed discrete event simulation, published between 2002 and 2013; Xu et al. (2015) reviewed, and classified simulation optimization techniques in health care, logistics and manufacturing; Utomo et al. (2018) presented a literature review on agri-food supply chains based on agent-based modelling.

More recent literature reviews are conducted involving simulation and modelling in the context of Industry 4.0. Negri et al. (2017) reviewed the conception of the Digital Twin (DT) from the aerospace field to the manufacturing domain in Industry 4.0 and smart manufacturing research; Zhong et al. (2017) and Alcácer and Cruz-Machado (2019) reviewed topics such as intelligent manufacturing, Internet of Things (IoT)-enabled manufacturing, and cloud manufacturing and other enabling technologies and systems of the manufacturing environment in the context of Industry 4.0; Kritzinger et al. (2018) presented a literature review on the guidelines for DTs in manufacturing; Tao et al. (2019) reviewed the differences between cyber-physical systems and DTs; Silvestri et al. (2020) presented a literature review on changing management strategies in the context of Industry 4.0, involving simulations and digital representations; Jasiulewicz-Kaczmarek and Gola (2019) presented a literature review on Maintenance 4.0 involving big data; Cui et al. (2020) reviewed the state-of-the-art of big data in manufacturing; Mourtzis (2020) reviewed the major milestones of manufacturing simulation technologies and recent industrial and research approaches in key fields of manufacturing; Zhang et al. (2019) presented a review of research and application of modeling and simulation technology involving intelligent manufacturing; van der Zee (2019) reviewed manufacturing simulation and proposed model simplification; Finally, Machado et al. (2020) gave a review on the identification and recommendations of sustainable manufacturing in the development of Industry 4.0.

In placing supply chain management in the context of Industry 4.0, Panetto et al. (2019) presented a review paper on the integration of Cyber-Physical Manufacturing with Cyber Supply Chain, and Rebs et al. (2019) presented a Literature review on sustainable supply chain management (SSCM) simulation. Rebs et al. propose system dynamics (SD) modelling guidelines in SSCM research.

The office of Nuclear Energy in the US (NEAC, 2013) defines the process of the scientific method as the scientific discovery, or knowledge, that entails three aspects:

- Formulation of theory to explain observed phenomena.
- Design and execution of experiments to test a theory
- Feedback of experimental results to advance theory.

Modelling and simulation are positioned at the crossroad between theory and experiment. The model itself is an expression of theory. At the same time, the simulation tool or a DT, founded on the model, is, when executed, in essence, a virtual experiment (NEAC, 2013). The researcher applied this methodology in the research.

Maintenance modelling involves mathematical equations, whereby the output and input of the model are quantitative numerical data. Mathematics is not natural science but is defined as formal science and is deductive in nature. Nevertheless, mathematics is essential in natural sciences. The laws of nature are expressed in mathematical equations (Pruzan, 2016). Thus, according to Jonker and Pennink (2010), quantitative research based on an empirical cycle is, in nature, deductive.

3.2.2 Positivist research

The natural sciences, as taught and understood by most scientists, are bound to realism. Natural science is footed on rational methods that provide objective facts about an independent physical reality. The realistic epistemological method aims at ontological knowledge. Ontological realism considers that objective scientific statements can represent the physical world, even those parts of nature that are not available to our senses, like black holes in the universe (Pruzan, 2016).

At the same time, natural sciences are considered to be positivists. Realism is an apparent contradiction to positivism. In the positivist epistemological view, reality does not claim to present a true picture of the universe but only enables us to interpret its laws (Pruzan, 2016). Stephen Hawking takes a clear positivist position that absolute truth is meaningless: *I don't demand that a theory corresponds to reality because I don't know what it is. Reality is not a quality you can test with litmus paper. All I'm concerned with is that the theory should*

predict the results of measurement (Hawking and Penrose, 1996, p. 121). Positivism rejects metaphysics and theism. Reasonings like that as *God exists or not* is entirely unscientific in this view since we cannot prove God exists, nor can we prove that God does not exist (Dawkins, 2008).

Positivism should not be confused by philosophical Realism. Realism is the philosophy that claims that the world exists independent of the mind. Positivism does not claim that. The researcher does not take a realist position, rather that of positivism. The positivist perspective is that scientific investigation should not be *influenced by human perception* by utilizing only well-founded data and free from philosophical speculation. Hypotheses must be scientifically verified by logical or mathematical proof.

On the other hand, realism is metaphysical and allows non-scientific sources of knowledge based on the assumption that they are independent of the mind. Science is not based on realism but rationalism (Kuhn, 1996), i.e., reason and knowledge rather than religious belief or emotional response. Positivism, also referred to as logical empiricism or logical positivism, holds the perspective that scientific statements have no place for metaphysics or presuppositions. What is real is measurable.

Further, a single, understandable, measurable physical reality reducible to elements can be studied independently. In principle, this external reality can be exhaustively scientifically described, where true propositions are in a one-to-one relation to facts about reality, including facts that are not observable. Independent observers can study reality since the knower is autonomous of the known. Observations can be made independent of existing theory and an observer's values. There are real causes that temporally precede or are simultaneous with their effects. Generalizations can be made time- and context-free (Pruzan, 2016).

As stated in section 3.1, Research problem statement, this research is motivated by a practical maintenance problem. Does this research, therefore, incorporate pragmatism philosophically? The thesis author thinks it does not. Pragmatism has much in common with positivism. Both pragmatism and positivism see philosophy as a method rather than a theory. However, there is a distinct difference. Pragmatism does not reject metaphysics. The pragmatist circle originally included several theologians (Nekrašas, 2001). The thesis author agrees with Dawkins (2008) that religion and other metaphysics have no place in the scientific method. We do not require pragmatism in a philosophical sense to resolve a practical problem. The positive mind is itself already only interested in what is useful and practical (Nekrašas, 2001).

3.2.3 Deductive and inductive inference

In deductive inference, the conclusions are deduced logically from known presuppositions, whether proven (theory) or not (hypothesis). In a simplified definition, deductive reasoning is an inference from generalization top-down towards specific instances, while inductive reasoning is an inference from specific instances bottom up towards generalization (Pruzan, 2016).

Deductive reasoning starts with general premises and then looks at a specific situation. This research starts with the general physical, biochemical premises of biofouling of RO membranes. The research further starts with the general maintenance theory that identifies an engineered object (EO) consisting of several parts as a multi-component system. Following, we look at an RO vessel as a specific novel multi-component system. A mathematical model is deduced on how biofouling unequally spreads among the cascaded components in the vessel. Therefore, we deduct from the general to the particular (see chapters 4 and 5). This deductive approach is very specific and therefore objective. The presented mathematical model of degradation and restoration of an RO vessel is thereby a simplification of reality.

Having established the mathematical foundation based on deductive inference, the researcher must apply the latter to build an RO train's DT. A DT is not just a simulator. It must include forecasting capabilities (Julien and Martin, 2021). In this research, the DT provides a long-term projection of several years under uncertain stochastic degradation and imperfect restoration.

Projection, in this case, involves predicting extrinsic wear conditions and imperfect repair. Such predictions are a crucial concept in the scientific method to test a hypothesis. Predictions are generated from deductive inference from a hypothesis or, in the case of this research, the mathematical equations of deterioration and restoration of RO membrane elements (see chapter 6). Then the analysis from the observations or experiments is evaluated against the predictions. The results will confirm whether the hypothesis is confirmed or rejected. Therefore, predictions are the application of logical, mathematical inference of a dynamic physical system. This mathematical system is entirely indifferent from time. Note that predictions do not always can or need to be evaluated by experiment to be scientific. (Pruzan, 2016).

Presuming that our physical-biological degradation and imperfect maintenance assumptions and theories are valid implies that the deductive inference leading to the mathematical model is truth-preserving. Gómez and Fontaine (2017), citing Gabbay and

Woods, claim that deduction is truth-preserving and induction is probability-ampliative.

Deductive reasoning leads to certainty, inductive reasoning towards probability.

One can argue that these projections involve inductive generalisation (Oh, 2012; McMullin, 2013; Beirlaen, 2017). According to King et al. (1994), deductive and inductive inference applied together in research is not a contradiction. Although it is possible to formulate universal rules for deductive inference, this is not the case for inductive inference. In natural sciences, the inductive hypothesis is applied to reason from the particular to the universal. In the latter case, the relationship between observations and evidence is always influenced by perception (Salmon, 2017). Inductive generalisation is common in natural science. Beirlaen (2017) illustrates how the physics research community inferred from the particular to the universal involving the electrical charge of an electron using an inductive generalisation. So far, the charge of only a few electrons has been measured. The result was 1.6×10^{-19} Coulombs. So, we assume that this value is the case for all electrons.

Can one presume the same inductive generalisation is valid when projecting future extrinsic wear severity? We do not know when annually algae blooms occur, nor the length and the severity. However, we have five years of data for 14 trains of the daily extrinsic wear coefficient κ (See chapter 6.2 Parameter estimation). So this gives us 70 data points per day. Applying random sampling with replacement, we can extend the quantity to any value. The research uses 100 data points per day. We denote this data set as

$$K = \begin{bmatrix} \kappa_{11} & \kappa_{12} & \cdots & \kappa_{1d} \\ \kappa_{21} & \kappa_{22} & \cdots & \kappa_{2d} \\ \vdots & \vdots & \ddots & \vdots \\ \kappa_{i1} & \kappa_{i2} & \cdots & \kappa_{id} \end{bmatrix} : \begin{cases} 0 < d \leq 365 : d \in \mathbb{N}^+ \\ 0 < i \leq 100 : i \in \mathbb{N}^+ \end{cases}$$

So, for each projected day of the 365 days a year (leap year disregarded for convenience), any daily future κ_d is a group element of K_d $\therefore \forall \kappa_d \in K_d$.

The above reasoning is not truth-preserving, but that is not the aim. Crucially, we do not reason from the particular to the universal nor develop a hypothesis: *I see only white swans, so all swans are white*. The latter would be a hypothesis through inductive generalisation. A weak hypothesis, according to Salmon (2017).

Deterministic prediction is not achievable, neither in principle nor in practice (Pruzan, 2016). Pruzan, citing Hawking and Mlodinow (2010; 72), states that *the outcomes of physical processes cannot be predicted with certainty because they are not determined with certainty*.

Instead, given the initial state of a system, nature determines its future state through a process that is fundamentally uncertain.

Nevertheless, the method to predict uncertain stochastic wear and imperfect repair is not a generalisation. Yes, the DT might not give an absolute true representative of the actual degeneration and restoration process. However, we use probability theory for the known unknowns. We are not seeking truth but evaluating the probability using statistical logic inference: *probably the next swan I see is white*. Nevertheless, although probability is inductive reasoning (Salmon, 2017), probability theory can be subjective or objective, depending on the statisticians' school of thought being followed.

According to Adams and Levine (1975), probability theorems are mathematically deduced. Pruzan (2016) refers to Hempel (1945) reasons that formal analysis applies to scientific prediction. Say we have statements of initial conditions C_1, C_2, \dots, C_k and scientific laws L_1, L_2, \dots, L_r , the logic deduction based on these statements and laws leads to E. We speak of reason if the phenomenon has already occurred. However, if we derive E before the actual phenomenon has occurred, then we speak of prediction. An example of criticism of Hempel's reasoning is illustrated by game theory. Theoretical knowledge of why a roulette wheel stops at a specific number has no basis for predicting the number beforehand.

3.2.4 Objective and subjective inference

Adams and Levine (1975) reason that probability theorems are deductive, Salmon (2017) claim that probability theory is not deductive but inductive inference. The seeming contradiction arises from the divide in the thought of the statisticians' community, which often confuses. Gelman (2011) divides the schools into Frequentist and Bayesian thought, whereby the Frequentist school orient towards the objective, deductive inference and the Bayesian school towards subjective, inductive inference. Bayesian hypothesis testing permits assigning strong assumptions to probabilities (Lehmann, 1993).

The researcher approaches the philosophy from the Frequentist school of thought. A direct reference is a method for long-term projections, which the researcher applied in this study. Martin (2015) proposes bootstrap for frequentist plausibility function-based tests and confidence regions. This research uses two sampling methods for ensemble forecasts, Bootstrap and Weibull distribution, from a sample of the previous five years of operation.

The main division in the scientific community concentrated around the inference of statistical significance between Fisher's ideas on significance testing and inductive inference and Neyman-Pearson's views on hypothesis testing and inductive behaviour (Lehmann,

1993; Hubbard et al., 2003). Fisher, Neyman and Pearson are the main contributors to frequentists classical methods. All three scientists were hostile to the Bayesian interpretation of probability theory. The formulation and philosophy of hypothesis testing in a Fisherian or Neyman-Pearsonian mode have become the most used quantitative methodologies. Although Fisher uses the term significance testing, both doctrines are concerned with the testing of hypotheses. Fisher's significance test is based on the deviation from the null hypothesis (H_0), e.g. P -value. Rather than relying on approximations, the P -value can be precisely calculated. Neyman and Pearson introduced a competing hypothesis allowing investigating two types of errors (Lehmann, 1993). Fisher objected to the type II hypothesis of Neyman and Pearson. Indebt review of the difference between Fisher, Neyman and Pearson is further irrelevant for this research.

Bayesian probability considers that only subjective probabilities exist instead of objective probabilities based on the prior distribution frequency. Probabilities arise from a person degree of belief of an event at a given moment and with a given set of knowledge. The irrationality of Bayesian subjective probabilities was illustrated during the investigation of the Challenger space shuttle disaster of 1986. The Rogers Commission that investigated the cause of the catastrophe learned that NASA officially estimated the probability of failure 1 in 100,000. However, historically the failure rate of solid rocket boosters was about 1 in 25 (Salmon, 2017).

According to Bayesian reasoning, a theory cannot be falsified following an outcome of an experiment. Experiments disapproving of the theory can fail due to other reasons or are not essential. Further, other angles of the theory can yet not be explored. Theories can neither be approved nor disapproved. The degree of belief in a hypothesis will only change when more evidence occur (De Finetti, 2017).

The Bayesian reasoning that hypothesis can neither be approved nor disapproved has resulted in a tendency under Bayesian statisticians to neglect predictive model checking. In some cases, these statisticians are uninterested in checking the fit of their models and even consider such checks illegitimate. This sloppiness has taken hold under quantitative researchers in social sciences who also regularly ignore to stress test their models (Gelman, 2011). The scientific inference is not inductive but deductive, according to Popper objectivism. We infer from the particular to the general through models, and this inference is deductive (Gelman, 2011).

3.2.5 Testing and validation

One of the 20th century's most influential philosophers of science, Karl Popper (Thornton, 2015), developed his reasoning of the scientific method in response to influential scholars at his time, Einstein's theory of relativity, Marx's theory of history, Freud's psychoanalysis and Adler's so-called *individual psychology*. Popper questioned the scientific validity of the last three scholars. These scholars' theories could be interpreted so that they would always be correct, no matter the path of future evidence. In Poppers' view, this resembles weakness, and he branded these theories as pseudo-science. In contrast, Einstein's theory of relativity involved reasoning that could be tested by observations and thereby confirmed or refuted. The British astronomer, mathematician and physicist Arthur Eddington just did that. He performed observations that confirmed that light bends under the influence of heavy bodies, like our sun. If his observation had shown that light did not bend, then that had refuted Einstein's gravitational theory (Pruzan, 2016).

It is the fallibility, according to Popper (1959), that distinguishes science from pseudoscience. If a theory can not be confirmed or unconfirmed empirically, there is no evidence of the theory's truth. So, the scientific method requires that theories are falsifiable, or refutable or testable. In more detail, this means the following (Pruzan, 2016):

- It is easy to confirm or verify nearly every theory if we look for them.
- Confirmations are only valid if the results are risky predictions.
- Good scientific theory forbids certain things to happen. The more, the better.
- Theory not refutable by any plausible event is non-science.
- An honest test of a theory attempts to refute it.
- Some theories are more testable than others, i.e., they forbid certain things to happen.
- Evidence should be based on serious but unsuccessful attempts to falsify it.
- If testable theories, when found to be false, are still upheld by their followers, this is at the price of lowering their scientific status.

A more recent example of the inability of falsification is the 'string theory' advocated by a small group of theorists. String theorists claim their hypothesis is sufficiently elegant and explanatory; therefore, it does not need to be verified experimentally. Since the hypothesis is unprovable, there is no method to prove that the theory is true or false. Therefore it cannot be scientifically (Ellis and Silk, 2014).

The same applies to an experiment that cannot be replicated. In 1989, two scientists, Pons and Fleischmann, claimed that they succeeded in a simple experiment to generate a cold fusion reaction. They presented their research not in a respected peer-reviewed journal but in a press release. So far, the experiment has not been replicated successfully (Pruzan, 2016). The experiment's outcome has little value if it cannot be confirmed by replication by other scientists. Therefore, the cold fusion experiment by Pons and Fleischmann did not find recognition in the scientific community.

As hypotheses need to be tested to be verified to compare the compatibility with the physical world or real world, so do need models in maintenance science. To enable us to compare the model with the real world, we need to understand what the real world is. A model is an interpretation by the creator, while the real world is an observation by the latter. Pidd (2004), referring to Popper, defines scientific theory as the inference of the real world. Experimentation may support the theory or refute the theory. As we have reasoned earlier, a model, when executed, is a virtual experiment (NEAC, 2013). Ideally, a simulation model is directly compared against the real world. However, since the real world is subjective, the modeller can be satisfied that the observation of the model displays identical characteristics to the observations of the real world (Pidd, 2004).

Pidd refers to the experimental framework of Zeigler (1976) in computer modelling. In this *experimental frame*, the *real system* as the source of observable data is replicated in a *base model* that defines a hypothetical model. The hypothetical model accounts for all of the input and output behaviour of the former. Then a *lumped model* is defined as an explicit and simplified version of the base model. The lumped model is then deployed as a *computer program*. The purpose is to simplify the model to the intention of the modelling.

Common mistakes in simulation modelling are over-elaboration and over-simplification. In the case of the former, this is an attempt to capture as much realism as possible. The model becomes too heavy, whereby the running of the simulations becomes slow, and the wrong issues are addressed. In the case of over-simplification, the danger arises that essential details are overseen, and the model does not handle the full complexity of the simulated system (Pidd, 2004). The right balance of model simplification requires an in-depth understanding of the drivers of the process being simulated (see chapters 4 and 5).

In this research, the base model of an RO pressure vessel includes, among other characteristics, the observed pressure differential (PD), salt rejection, and ageing of membranes. The lumped model of the RO vessel is reduced to the PD characteristics. We are interested in the latter in this research and not the other characteristics.

Verification is then the process by which we assure ourselves that the lumped model is deployed correctly in the computer program. Besides verification that the lumped model is correctly implemented, a model needs credibility. Credibility is the willingness of the manager to base decisions on the output of the model. Finally, acceptability includes the whole scope, i.e., the definition of the lumped model to capture the research, the verification and credibility (Pidd, 2004).

3.2.6 Research onion by Sanders et al.

Academics at business schools often emphasise a research methodology structured according to the *research onion* proposed by Sanders et al. (2017). The researcher is of the opinion that this works well for social studies and studies in humanities, but not always for applied natural sciences. Researchers of social studies and studies in humanities can decide to conduct qualitative or quantitative research based on philosophical choices. The researcher is driven in this choice by their epistemological views, i.e., the researcher's view about the development and nature of knowledge.

However, we cannot always characterise studies at a business school as social studies. For instance, today, maintenance is recognised as one of the pillars of business strategy (See chapter 2, Setting the baseline of the research). Therefore, maintenance theory and maintenance modelling have a rightful place in the business school. Especially maintenance modelling studies can be classified as applied natural sciences research involving quantitative data.

In the case of (applied) natural sciences, philosophical choices are limited, and the methodology design does not follow the structure of the research ring. Quantitative research is the offset of the research in the case of the latter. The approach to theory development is of interest only if the model includes probability theory. If probability is involved, the researcher needs to clarify if his view orients towards the frequentists or the Bayesian school of thought. The research is positivist, deductive or subjective inductive based on the researcher's view towards the statistical school of thought. The thesis author's epistemology follows the first school of thought.

Referring to Saunders et al. research onion, the strategy choice is an experiment since maintenance modelling and DTs are virtual experiments (NEAC, 2013). At the same time, this research uses a case study. According to Blatter and Haverland (2012), case studies are conducted to explain and compare the value of opposing or matching theories. Often, many complex causes of a specific phenomenon must be explored, or a particular niche case makes

a difference. The degradation (in the presence of biofouling) and imperfect restoration of RO membrane elements is a niche case of maintenance modelling. The research infers the DSS of this novel case study from the particular to the universal requirements of a decision support system (DSS) for restoration so that the DSS is fit for purpose.

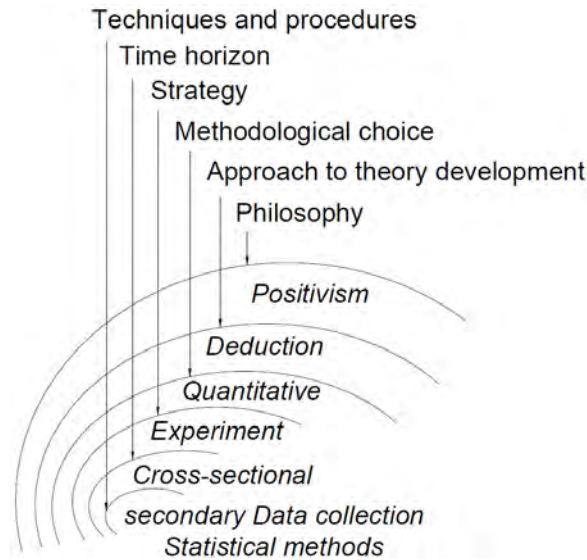


Figure 3-2: Cross-section research onion of Saunders et al. (2017). applied to this research

Although primary data is retrieved for the purpose of this research, data storage is an integral aspect of the O&M. From a research methodological perspective, the retrieval of the data can be considered secondary data. The most extensive dataset is retrieved from the historical database of Operational Technology (OT). This data involves daily PD, the status, recoveries and other operational data of the trains. Saunders et al. (2009) refer to this type of data retrieval as data collection over a *longitudinal time horizon*. Large time-series quantities of a small selection of data are retrieved. However, since this data involves quantitative data retrieved at discrete time intervals, we do not refer to time-series data as Longitudinal Data. The latter, also called panel data, is data collected through a series of repeated observations widely used in the social sciences. It can be compared towards a repetition of cross-sectional data but observing the same objects, e.g., individuals. Cross-sectional data, in contrast to Time series data, captures a point-in-time.

Further data containing the maintenance interventions are retrieved from the Computerised Maintenance Management System (CMMS). In addition, an aspect of archival research is conducted. Reports from the O&M company towards stakeholders are consulted to retrieve recorded periods of algae blooms, annual demand versus supplied water and records of membrane autopsies.

Finally, we can summarise the research methodology. This research methodology is positivist deductive research using quantitative secondary data. The strategic approach is that of a virtual experiment, i.e., DT, involving objective statistical logic. The researcher believes whether the DT makes an exact copy of the reality is of minor importance, as long as the results provide enough confidence for the best maintenance strategy. In his book, *The Universe in a Nutshell*, Steven Hawking, defending the theory of time, made a similar judgement.

[any] sound scientific theory, whether of time or of any other concept, should in my opinion be based on the most workable philosophy of science ... [A] scientific theory is a mathematical model that describes and codifies the observations we make. A good theory will describe a large range of phenomena on the basis of a few simple postulates and will make definite predictions that can be tested. If the predictions agree with the observations, the theory survives that test, though it can never be proved to be correct. On the other hand, if the observations disagree with the predictions, one has to discard or modify the theory. If one takes the positivist position, as I do, one cannot say what time actually is. All one can do is describe what has been found to be a very good mathematical model for time and say what predictions it makes (Hawking, 2001, p. 31).

We can summarize the research philosophy of this research. This research is a positivist, quantitative deductive research in character involving only quantitative secondary data. The research follows a logical and rational driven approach and is objective, focusing on facts. In line with the positivist method, the research involves testing and verification. Finally, the research is outcome-oriented, presenting a practical solution for a real problem in the industry.

3.3 Techniques and procedures

Having outlined the philosophical choices the researcher has taken in this research, we can further outline the methods applied in this research experiment. The methods involved can be ordered as follows:

- Data collection.
- RO performance normalization.
- Data analysis and identification of the effects of maintenance.
- Model development and Coding of the DSS and DT.

- Statistical procedures for parameter estimation.
- Simulation of NPD and comparison against the observed NPD.
- Statistical probabilities for stochastic parameters projection.
- Run projections involving different maintenance policies
- Analyses involving statistical procedures for risk assessment
- Conclusions and preferred maintenance policies

Figure 3-3 gives a more detailed diagram of the experiment setup of this research. The numbering shows the flow sequence of the research setup. The literature review is not assigned as a fixed step since the literature is consulted throughout the research.

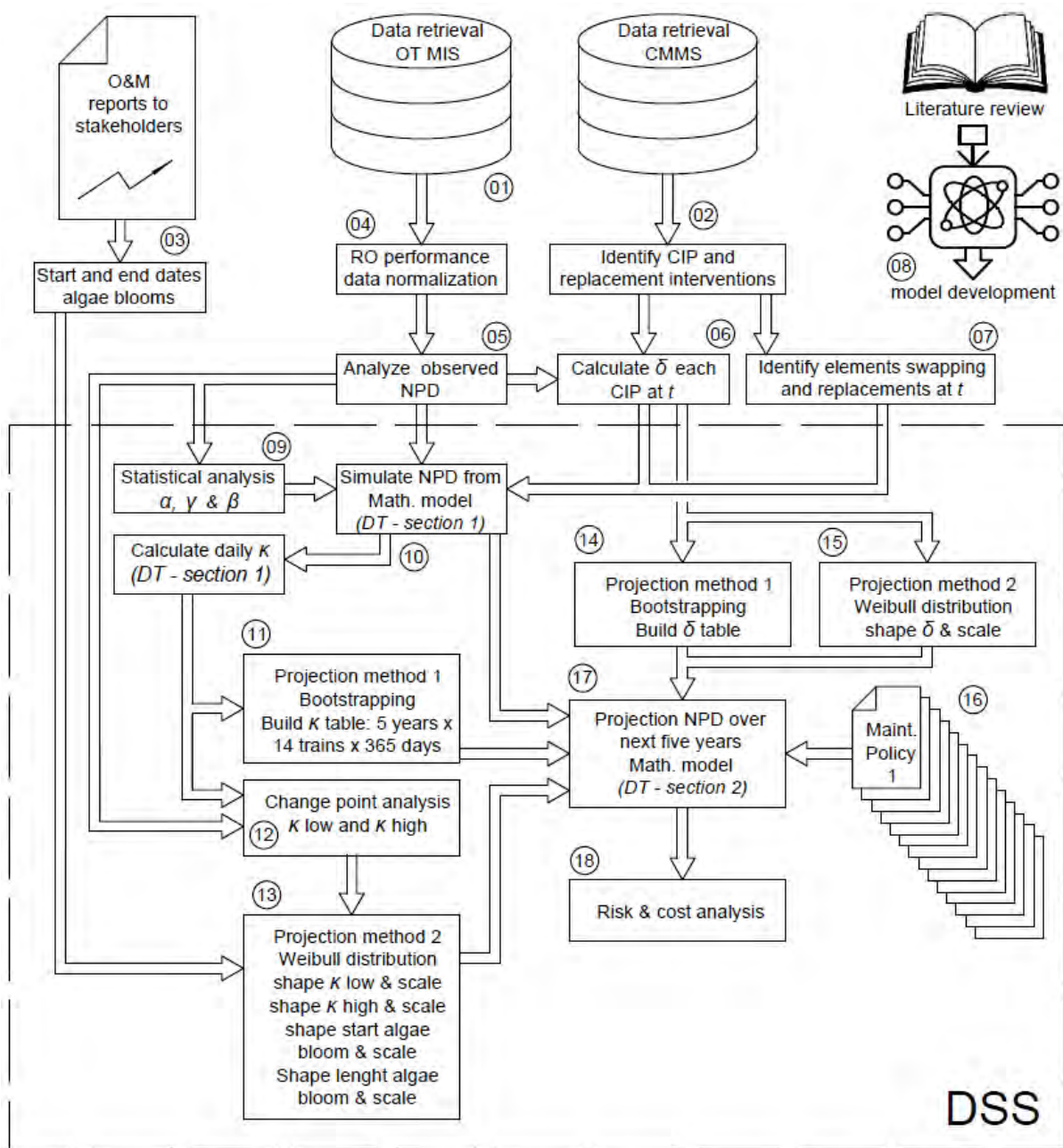


Figure 3-3. Experiment setup

Items 09 to 18 of the experiment (see Figure 3-3) are generated in MATLAB. The full code is too long to attach as an appendix to this thesis. However, the most crucial part, modelling the historical state-space and the projections, is included in Appendix D. The code is available on request. Some supporting subsequences are performed in MS excel, as are the inputs and output of the DSS. Analysis and discussions of the sections shown in the flow chart are detailed in the thesis's main content. In this section, the researcher limits himself to technical procedures, which are not addressed in the main body of the thesis. These procedures involve the following:

- Data collection;
- RO performance data normalization;
- MATLAB applications as part of the experiment and;
- Instructions to download the MATLAB applications and run the DSS for experiment replication.

3.3.1 Data Collection

All data collected is secondary data. Data has been collected from November 8, 2015, until September 30 2020. The most extensive is operational data retrieved from the Historian database (01 Experiment setup, Figure 3-3). The Historian database is a time-series dataset. Further, data on maintenance activities are collected from the CMMS (02 Experiment setup, Figure 3-3). Finally, dates on the start and end of algae blooms, membrane autopsy reports, production demand and delivery are retrieved from monthly reports to the stakeholders (03 Experiment setup, Figure 3-3). Figure 3-4 shows a slightly simplified diagram of the operational data collection. Field sensors provide real-time data to the remote input/output (RIO) modules of the Programmable Logic Controllers (PLC).

Data applicable for this research is analogue data transferred to the Analogue-to-Digital converter modules at the RIO. The converted digital data is polled by the PLC's Central Processor Unit (CPU) at every program scan. Program scans of PLCs vary, but in the case of this case study, they are approx. 25 mili-seconds. The PLC has only real-time data storage. The PLC provides control sequences, like Proportional, Integral, and Derivative (PID) controls and interlocking. From the PLC, the data is transferred into different channels.

The data is polled from the PLC by the Supervisory Control and Data Acquisition (SCADA) and displayed as part of graphical presentations of the process for the operator. The SCADA incorporates a dedicated database from which the operator can retrieve time-series data trends. Data retrieval by SCADA is not utilized in this research and is omitted

from the diagram in Figures 3-4.

Besides SCADA, the data is further retrieved by an independent OPC server. OPC (Open Platform Communications) is a well-known group of standards and specifications for industrial telecommunication. The OPC server collects data from the PLCs using Alan Bradley EtherNet/IP protocol and converts it into SQL server protocol. The OPC functions as an intermediary between the PLC and the Management Information System (MIS).

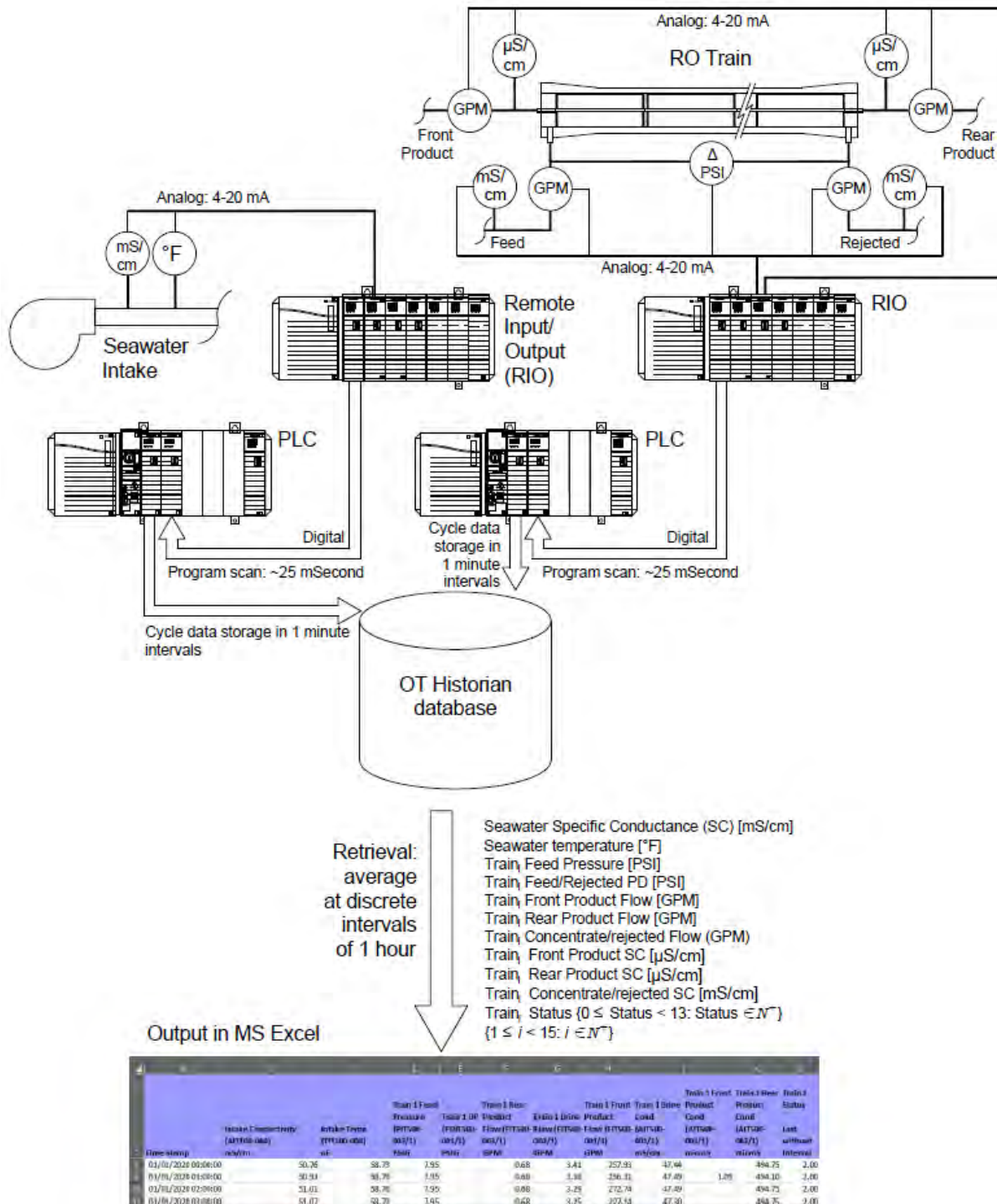


Figure 3-4: Operational data retrieval from Historian database

The agent of the MIS at the OT network level collects the data in cycle or delta retrieval from the OPC and stores it in a relational database. Most commonly, as is with the data utilized in this research, the data is stored in cycle intervals of one minute. The database is replicated from the OT to an identical database at the corporate level through a Unidirectional Security Gateway, a more recent type of data diodes. A data diode means that the data can only leave the OT network, and no reverse traffic is possible (Ginter, 2012). Reporting and data analysis are conducted at the mirrored MIS. A reference will be made simply to MIS when referring to the mirrored database in this research. Table 3-1 shows the data collected from the MIS, involving SWRO performance data.

Table 3-1. Data collection of SWRO performance data from the MIS operational database

| Variable | units | Retrieval interval | Data type and range |
|---|------------|--------------------------------------|---|
| <i>Common for all SWRO trains</i> | | | |
| Seawater Specific Conductance (SC) [<i>SWSC</i>] | mS/cm | 1h weighted average | $40 < SWSC \leq 52.2 : SWSC \in \mathbb{R}^+$ |
| Seawater temperature [<i>T</i>] | °F | 1h weighted average | $57.2 < T \leq 95 : T \in \mathbb{R}^+$ |
| <i>For each individual train i: $0 < i \leq 14 : i \in \mathbb{N}^+$</i> | | | |
| Train _{i} Feed pressure [<i>PF</i>] | PSI | 1h weighted average | $300 < PF \leq 1130 : PF \in \mathbb{R}^+$ |
| Train _{i} Feed-Rejected pressure differential [<i>PD</i>] | PSI | 1h weighted average | $0 < PD \leq 50 : PD \in \mathbb{R}^+$ |
| Train _{i} Front Product flow [<i>QPF</i>] | GPM | 1h weighted average | $0 < QPF \leq 3200 : QPF \in \mathbb{R}^+$ |
| Train _{i} Rear Product flow [<i>QPR</i>] | GPM | 1h weighted average | $0 < QPR \leq 1000 : QPR \in \mathbb{R}^+$ |
| Train _{i} Rejected flow [<i>QR</i>] | GPM | 1h weighted average | $0 < QR \leq 6000 : QR \in \mathbb{R}^+$ |
| Train _{i} SC front product [<i>FPSC</i>] | μ S/cm | 1h weighted average | $0 < FPSC \leq 1500 : FPSC \in \mathbb{R}^+$ |
| Train _{i} SC rear product [<i>RPSC</i>] | μ S/cm | 1h weighted average | $0 < RPSC \leq 2000 : RPSC \in \mathbb{R}^+$ |
| Train _{i} SC rejected [<i>RSC</i>] | mS/cm | 1h weighted average | $0 < RSC \leq 150 : RSC \in \mathbb{R}^+$ |
| Train _{i} Status | - | Last without interval (each hour) | $0 \leq Status < 13 : Status \in \mathbb{N}$ |

Variables in Real numbers (all of the above variables except Status) are retrieved as the weighted average of the 60 stored numbers per hour. The weighted average is the following: if a stored number is missing, then the MIS conducts an interpolation of that number. Thus, in this case, a weighted average equalizes the frequency of the values in a data set.

The last number is retrieved for those variables with an integer data type, i.e., status since averaging would result in data loss. For example, the status value of a train on standby is two and that in operation five. If a train goes from standby to online halfway the hour, then the average weight would be 3.5. The number 3.5 does not represent a state condition. ‘Last without (w/o) interval’ is to prevent gathering NULL values during the retrieval. The option ‘Last’ gives a value per hour if the value has changed. Those hours without a change, no value is output. ‘Last without interval’, repeat the previous value until the value changes. Therefore no NULL values are generated.

Specific Conductance (SC) is an indication of total dissolved solids (salt concentration) in cold dilute water, whereby the temperature is adjusted to 25 °C. The unit is expressed in Siemens per centimetre (Thomas, 1986). High saline water, like seawater or concentrate (rejected), is expressed in mS/cm. Low saline water is expressed in $\mu\text{S}/\text{cm}$.

For other operational parameters, the MIS uses imperial units. These are pounds per square inch (PSI) for pressure, US gallons per minute (GPM) for flow rate and Fahrenheit (°F) for temperature. In the following data manipulation process, imperial units are converted to metric.

In addition to the above data for SWRO performance normalisation, the status of the primary equipment is collected for the maintenance performance analysis in chapter 2.4. SWRO status data for the maintenance performance analysis is independently collected from the SWRO performance data normalisation data. Table 3-2 shows the data collected from the MIS.

Table 3-2. Data collection of primary equipment status from the MIS operational database

| Variable | units | Retrieval interval | Data type and range |
|--|-------|------------------------|---|
| Intake pump status $IP_i.\text{status}: 0 < i \leq 3: i \in \mathbb{N}^+$ | - | Last w/o interval (1h) | $0 \leq \text{Status} < 6: \text{Status} \in \mathbb{N}$ |
| LPB pump status $LPB_i.\text{status}: 0 < i \leq 4: i \in \mathbb{N}^+$ | - | Last w/o interval (1h) | $0 \leq \text{Status} < 6: \text{Status} \in \mathbb{N}$ |
| HPB pump status $HPB_i.\text{status}: 0 < i \leq 4: i \in \mathbb{N}^+$ | - | Last w/o interval (1h) | $0 \leq \text{Status} < 6: \text{Status} \in \mathbb{N}$ |
| HP pump status $HP_i.\text{status}: 0 < i \leq 4: i \in \mathbb{N}^+$ | - | Last w/o interval (1h) | $0 \leq \text{Status} < 9: \text{Status} \in \mathbb{N}$ |
| ERS status $ERS_j.\text{status}: 0 < j \leq 8: j \in \mathbb{N}^+$ | - | Last w/o interval (1h) | $0 \leq \text{Status} < 12: \text{Status} \in \mathbb{N}$ |
| SWRO Train $i.\text{status}: 0 < i \leq 14: i \in \mathbb{N}^+$ | - | Last w/o interval (1h) | $0 \leq \text{Status} < 13: \text{Status} \in \mathbb{N}$ |
| PWS Pump $i.\text{status} PWS_j.\text{status}: 0 < j \leq 3: j \in \mathbb{N}^+$ | - | Last w/o interval (1h) | $0 \leq \text{Status} < 6: \text{Status} \in \mathbb{N}$ |

The status represents a discrete operational condition, e.g., for all pumps, except the HP pumps, 0 is off-line, not available; 1 is Fault; 2 is standby; 3 is starting up; 4 is running, and 5 is shutting down. For an SWRO train, status 5 is online, and 12 is clean-in-place (CIP).

Maintenance-related data is collected from the Computerized Maintenance Management System (CMMS). As with the MIS, data storage at the CMMS is at a relational database. However, the CMMS in this case study is not directly connected to the OT. All data is entered manually by the Maintenance Planner and other maintenance personnel. Work orders (WO) are automatically generated based on a planned time-based preventative maintenance schedule, condition-based following inspections, or manually issued work order requests by O&M staff.

Appendix B shows examples of WOs for membrane replacement and CIP. The latter is divided into two WOs, first SBS soaking, then another work order for High and Low CIP. A WO comes in some cases with attachments, as is shown with the WO of membrane

replacement, which includes a Standard Operating Procedure (SOP), instructions about which elements to replace and how to swap the element and the serial numbers of the elements. These attachments are stored at the CMMS and automatically pulled up with the WO. WO for membrane replacement or CIP is not automatically generated. The O&M management team decides annually on the membrane replacement plan and on a weekly basis if a CIP is required and applied to which RO train.

Further, the *Carlsbad Desalination Plant Annual Operations and Maintenance Report* for the years from 2015/2016 to 2020/2021 are consulted. The reports cover the annual contract period, including July to June the following calendar year. Data collected from the annual O&M reports are the monthly production demand, delivered volumes and observations on starting and ending periods of algae blooms.

3.3.2 RO performance data normalisation

RO performance data normalisation aims to standardise RO performance data from seasonal and operational effects. As described in chapter 4.4.1, permeate flow, salt passage, and PD vary without deterioration of the membranes due to changes in feedwater temperature, salinity and flows. For example, lowering the feedwater temperature results in compacting the membrane elements, whereby the DP increases, permeate flow reduces, and the salt rejection improves. An increase in feedwater temperature expands the elements, resulting in lower differential pressure, increased permeate flow, and a reduction of salt rejection.

The method of calculating the NPD can differ slightly in the industry. Some membrane manufacturers apply an element-specific version of NPD based on the following equation

$$PD = C \times Flow^B \quad (1)$$

whereby B is typically 1.45 to 1.6⁸ and C is a coefficient specific to the membrane element (Wolfe, 2003).

This research applies normalisation equations used by the O&M company and specified by the membrane manufacturer (internal document). Table 3-1 shows the data required for the normalization calculation. SC affects normalized permeate flow and salt passage. Feed pressure affects the normalized driving pressure calculation. This research only requires NPD calculations. For calculating NPD, SC and feed pressure are not required. However, the parameters could be of interest in future research and are therefore collected. NPD involves only a feed and rejected flow component and a viscosity component. The variable in the

viscosity (μ) calculation is the temperature of the water (T_w). The viscosity equation is given here.

$$\mu = \frac{e^{-3.7188 + \frac{578.919}{-137.546 + T_w + 273.15}}}{1000} \quad (2)$$

The flow (Q) component consists of the sum of the initial feed ($Q_{f,ref}$) and rejected flow ($Q_{r,ref}$) divided by the current sum of the feed ($Q_{f,t}$) and rejected flow ($Q_{r,t}$) to the power of 1.4. The viscosity (μ) component consists of the initial viscosity (μ_{ref}) divided by the present viscosity (μ_t) to the power of 0.6. Initial is referred to the data commencing the operation of the plant. The NPD equation is given here.

$$NPD_t = PD_t \times \left(\frac{Q_{f,ref} + Q_{r,ref}}{Q_{f,t} + Q_{r,t}} \right)^{1.4} \times \left(\frac{\mu_{ref}}{\mu_t} \right)^{0.6} \quad (3)$$

where:

$Temp$ = Feedwater temperature in °C. The conversion from °F to °C is $(°F-32)/1.8$

μ = Viscosity [N s/m²]

Q_f = Feed flow

Q_r = Rejected flow

t = time of data collection (in intervals of hours)

ref = reference condition (initial data)

PD = Measured PD (Feed pressure – rejected pressure)

NPD = Normalized pressure differential

RO performance can only be calculated when the RO train is in stable operation. Thus, the calculations are only performed when the RO train status is five, normal operation.

To reduce noise at the NPD from, e.g., stoppages, at 00:00 hrs every day, the mean over the previous 24 hours of the hourly NPD is calculated, excluding periods when the train was not operating. The mean over 24 hours is the NPD used in the analysis of the research. In this way, the pressure is adjusted for temperature and production hourly, and degradation is monitored daily.

3.3.3 MATLAB

The main functionality of the DSS and the DT module is developed at the app platform in MATLAB. The platform provides complete flexibility for writing code and, at the same time, has built-in tools for the creation of the Human-Machine-Interface (HMI). The DSS can be shared as a stand-alone application for stakeholders who do not have a MATLAB license or as a MATLAB app. The application, including the supported data files, can be accessed at https://drive.google.com/drive/folders/1eUCKvJkl2rn7Qu_J6kfx-1ikpaWI9z-u?usp=sharing.

MATLAB is a proprietary programming Language of MathWorks. It allows matrix manipulations and plotting of functions and data, creation of user interface, and importantly various algorithms can also be implemented. MATLAB has a substantial audience in the applied mathematics community. It supports languages, including C, C++, Java, Fortran and Python (UpSkill, 2016). The MATLAB coding language is similar to *structured text* (ST), an imperative language defined by the open international standard IEC 61131-3 for PLCs. ST is one of the five standard programming languages for the software development of PLCs.

Further, MATLAB/Simulink models can be migrated directly to ST and *Continuous Function Charts* (CFC), another standard PLC language defined in IEC 61131-3 (Wenger and Zoitl, 2012). MATLAB was first adopted by researchers and practitioners in control engineering. The researcher, a practitioner in control engineering himself, is highly knowledgeable in the programming and development of PLC/SCADA and DCS systems due to more than 25 years of experience in this field as a Control System Integrator.

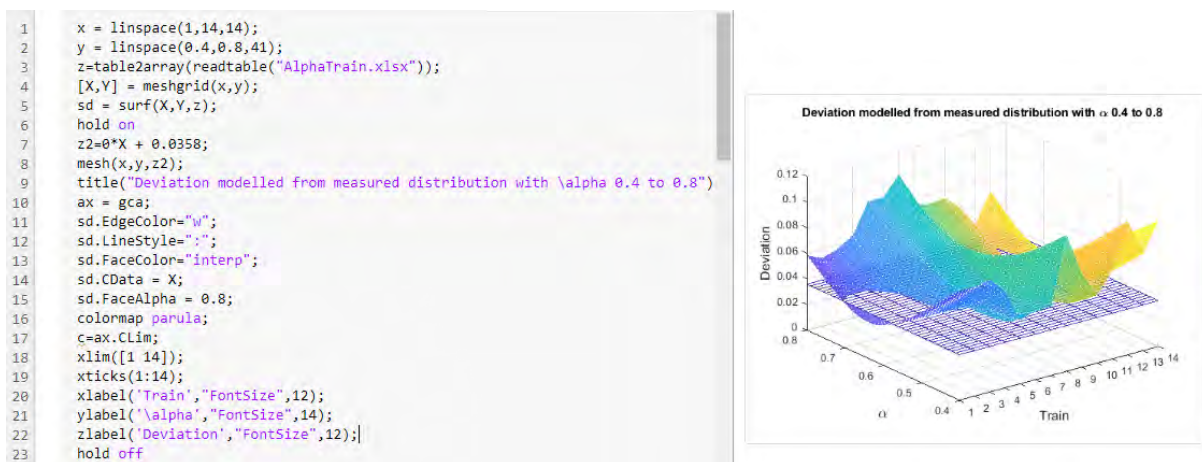


Figure 3-5. Surface plot of the difference between inspected biomass and modelled wear distribution at parameter α values 0.4 to 0.8 for the 14 RO trains

Besides the app platform, Live Editor was utilised for statistical analysis of the parameter estimation and risk analysis of the various maintenance policies. There is no difference in code between the application platform and Live Editor. The difference, as the word 'Live'

already indicates, is that the code can be directly executed while developing the program. Figure 3-5 shows an example of code in Live Editor that visualizes the difference between inspected biomass and modelled wear distribution at parameter α values 0.4 to 0.8 for the 14 RO trains in a surface plot. Code developed in Live Editor can be downloaded from the same link above.

3.4 Research ethics

Early at the commencement of this research, the researcher has undertaken an online Module on Induction & Research Ethics and completed an ethics approval request, application SBSR1920-014. Confirmation of approval was sent on 22 May 2020. The research is conducted following the principles of good ethical standards outlined by the Academic Ethics Policy (V1.0) of the University of Salford (UoS). These principles, although not restricted by it, include the following:

- *The dignity, interests, rights, safety and well-being of all actual and potential participants, observers and all others involved in the academic activity.*
- *The welfare and interests of those carrying out the activity.*
- *The welfare and interests of the University's partners and collaborators and the individuals associated with those organisations.*
- *Animal welfare.*
- *Cultural Heritage.*
- *The natural environment.*
- *The reputation of the University and the wider academic community.*
- *The welfare and interests of the wider community.*

(Associate Director Research UoS, 2017, p. 4)

This research involves only secondary data retrieved from an engineered system. Therefore the research does not include any data collection of individuals. However, the researcher recognizes that there are other ethical responsibilities as outlined above. These responsibilities are towards humanity in general and further to the company that allowed to conduct the research and provided partial compensation for the research. The researcher will not violate the required confidentiality regulations. Secondary data retrieved will not be published without solid approval.

Ethical responsibilities towards humanity are honest scientific research to contribute to the scientific knowledge in general, avoiding plagiarism. A consequence of this research is the extension of the useful life of a RO membrane not only for the plant in this case study but

potentially for other plants subjected to the same conditions. Therefore the research promotes sustainability in contributing both ethically and physically to reducing waste. The research further does not contribute to the unethical use of technology.

3.5 Summary

This research addresses general requirements of a decision support system (DSS) for restoration so that the DSS is fit for purpose. The researcher demonstrates this with the development and implementation of the DSS in a novel case study. A seawater desalination plant in California, where the wear of the Reverse Osmosis (RO) membranes was higher than initially expected due to biofouling accelerated by seasonal algae blooms.

This research considers the maintenance modelling of an engineered object. Therefore, this management improvement study is engineering-based in character and founded on applied natural science involving deducted formal science. Data collection is limited to secondary data of a technical system. No data collection of individuals is involved. The data is quantitative.

Maintenance modelling is objective. Although the research involves projections of uncertain outcomes, frequentist statistical probabilities are applied, which again are objective in character. The researcher presents Positivist Deductive research involving quantitative secondary data. The strategy followed in the research is that of a virtual experiment: the demonstration of a DSS powered by a DT.

The philosophical approach of the presented methodology should be evaluated against this background. The researcher is of the opinion that the philosophical approach taken in this study is based on the most workable scientific method for this specific problem. The next chapter concentrates on the main aspect of RO membrane degradation, biofouling, from a process engineering point of view.

4 Reverse Osmosis seawater desalination

This research uses a practical example of a decision support system (DSS) for the long-term maintenance planning of reverse osmosis (RO) membranes in seawater desalination, affected by biofouling due to seasonal algae blooms. This chapter describes reverse osmosis desalination to provide the required process engineering background. First, the need for seawater desalination and the current lack of research in RO maintenance management are evaluated. Before the specifics of membrane degradation are addressed, the principle of RO and its practice application is clarified. Then, this chapter concentrates on membrane degradation and algae blooms. Finally, the mitigation of membrane degeneration is addressed.

4.1 Desalination to combat water shortage

We refer to the Earth as the water planet. We cannot live without water. Our planet has more water than land. Seventy-one percent of the earth's surface contains water. However, 97.5 percent of the water is saltwater. Thus, not suitable for human consumption, land animals or plants. Only 2.5 percent is freshwater.

Nevertheless, two-thirds of this freshwater is frozen in snow, ice and permafrost. Only one-third of the total freshwater is available from aquifers below the ground, springs, lakes, rivers, and reservoirs collecting rainwater and melted ice. Reoccurring draughts over the last decennia has put freshwater resources under stress. Although the root cause of drought is still not fully understood, climate change has a substantial impact, which is expected to increase during this century. Besides the increase in droughts, freshwater resources are further stressed due to growing water demand (Haile et al., 2020).

Water scarcity affects currently 40% of the population worldwide (Jamieson et al., 2021). The limited freshwater resource must be shared by about 7 billion people worldwide. Over a period of 50 years, from 1967 to 2017, the world population has doubled. At the same time, freshwater per capita has fallen by half over this period (Zapata-Sierra et al., 2022). The world population is expected to grow further to 8 billion by 2025 and 9 billion by 2040 (Gaskin-Reyes, 2016). It is estimated that by 2030, 700 million people will potentially become displaced due to drought (Jamieson et al., 2021).

Urbanisation has resulted in further deterioration of freshwater resources and, in some cases, resulted in the depletion of lakes, rivers and aquifers. The United States' Southwestern region comprises seven water resource regions. These regions are the Pacific Northwest, the

Great Basin, California, Upper Colorado, Lower Colorado, the Rio Grande and the Texas Gulf regions (see figure 4-1a). Water demand is now outpacing supply in much of this drought-stricken region., While the water supply is decreasing, water demand, on the other hand, is growing. Except for the Texas Gulf regions, the water supply relies primarily on the dwindling seasonal snowpack (Miller et al., 2021). The cross border flow of the Colorado River into Mexico (see figure 4-1b) has shrunk by nearly 75% in less than 15 years due to significant overuse of domestic and agricultural water demand (Day et al., 2021). Nowadays, the river is sometimes dry when it reaches the outlet in the Gulf of California. Decades of sinking levels of the Great Salt Lake in the Great Basin resulted further in additional environmental damage (Miller et al., 2021). Freshwater reductions at the Colorado delta have resulted in hypersaline conditions and widespread wetland death (Day et al., 2021).

In other areas, increased demand for freshwater has a devastating effect on ancient aquifers. Parts of Houston, Texas, are sinking at 5 centimetres per year due to excessive groundwater pumping. Like Jakarta, the capital of Indonesia, which is even sinking up to 17 centimetres per year, the sinking results from the depletion of aquifers beneath it. Both Jakarta, Houston and nine other sinking cities could disappear by 2100 (Lakritz, 2019).

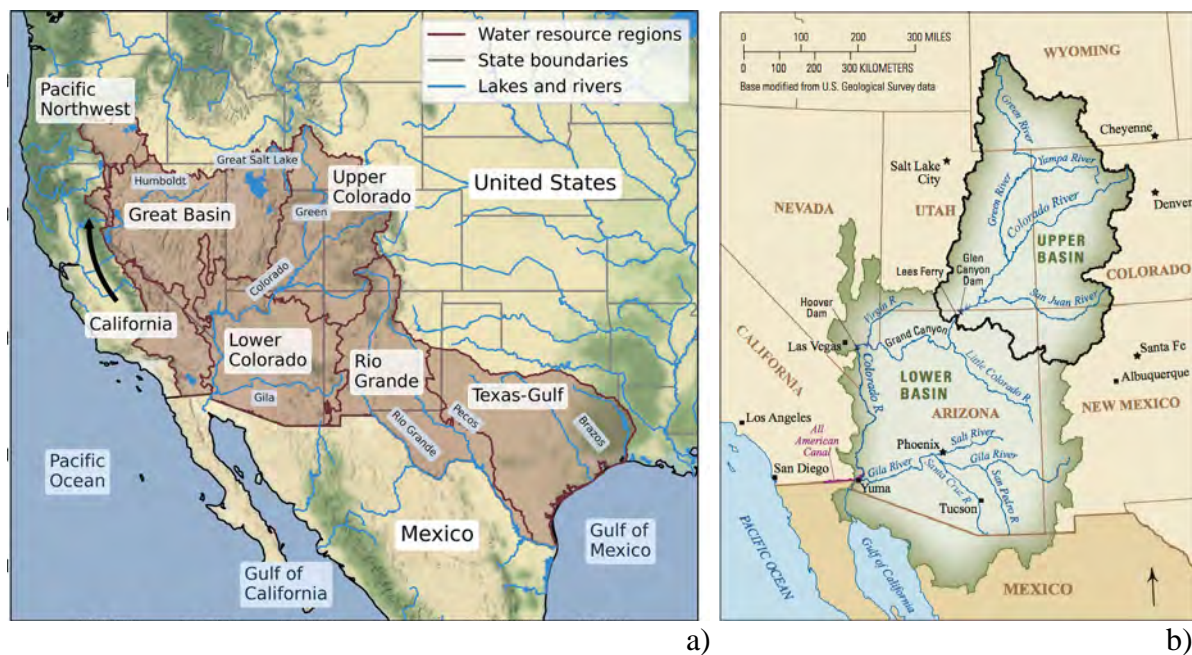


Figure 4-1 a) Seven water resource regions Southwestern region of the United States. Map data ©OpenStreetMap contributors, available under the Open Database License (<http://www.openstreetmap.org/copyright>), accessed through Stamen OpenSource Tools (<https://stamen.com/open-source/>). b) Drainage basin of the Colorado River in the Southwestern United States and Mexico (Public domain image from USGS).

The shortage of freshwater sources around the globe has led to an increased focus on RO desalination to meet clean-water demand for industrial and domestic use. By 2015

desalination, both seawater RO (SWRO) and thermal provided only around 1 percent of the world's drinking water. Approximately 18,000 desalination plants exist worldwide. Nearly half of this capacity is in the Middle East and North Africa (Voutchkov, 2016). By 2020 the total contracted capacity has reached 100 million m³/day (Bashitialshaaer, 2020), and desalination is now a multi-billion industry. The growth of desalination over the next decade is expected to be Asia, the US and Latin America. An important factor is cost breakthroughs. The energy needed to produce freshwater from seawater for one household per year is less than that used by the household's refrigerator (Voutchkov, 2016). Rejected brine is returned to the ocean. Thus Desalination is sustainable, identical to ocean evaporation and rainfall.

The number of scientific productions available further emphasises the interest in desalination. The Scopus database generated 35,845 results of publications on the topic of Desalination in the period between 2000 and 2020, with a peak of more than 3000 publications in 2016. Most publications originated from China, the USA, India, Iran and South Korea, followed by Saudi Arabia, Australia, Spain, Egypt and the United Kindom (Zapata-Sierra et al., 2022).

4.1.1 What is Reverse Osmosis

Reverse Osmosis (RO) is a membrane-based separation technology used to remove dissolved solids from a liquid. It is predominantly applied in water treatment. Osmosis is an essential process in animal and plant cells. Osmosis is the natural, spontaneous migration of a solvent such as pure water through a semipermeable membrane into a solution of higher solute concentration, e.g., seawater (see figure 4-2a).

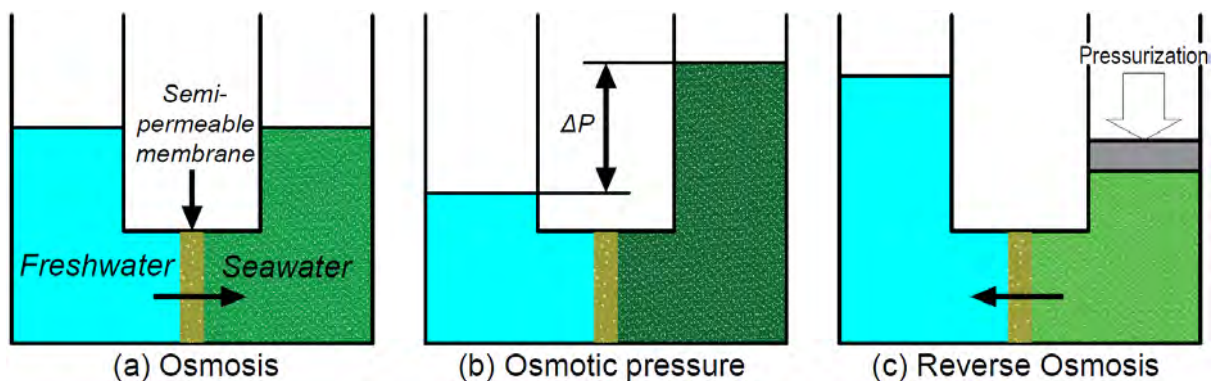


Figure 4-2. Principle of reverse osmosis

This flow continued until the pressure difference between the low solvent, and high solvent side of the semipermeable membrane reached an equilibrium. This equilibrium is called the osmotic pressure (Figure 4-2b). The process can be reversed by applying pressure

at the high solute concentration above the osmotic pressure. The smaller water molecules pass the semipermeable membrane, but the larger salt molecules are rejected. This process is called reverse osmosis (Figure 4-2c).

The University of California, Los Angeles (UCLA) began developing the first RO membrane in the 1950s. The research was encouraged by President John F. Kennedy, then a senator, who advocated the idea of largescale desalination. In the aftermath of World War II, it became evident that the United States would increasingly struggle with water shortages. In 1959 researchers Sidney Loeb and Srinivasa Sourirajan created the prototype of a RO membrane (Wiles and Peirtsegaele, 2018; Takabatake et al., 2021).

Due to the initial high operating costs, energy consumption, and poor performance of the membranes, SWRO desalination plants could not compete with plants based on the thermal desalination process. However, the improvement of SWRO membrane technology has exponentially expanded since the 1990s. SWRO desalination now has replaced thermal desalination as the preferable process. The preference for SWRO desalination follows continuing technological improvement, decreased production costs of SWRO membranes, and the introduction of energy recovery systems. Almost all new desalination plants since 2000 were SWRO membrane desalination plants. Particularly large scale plants of over 100,000 m³/day (Takabatake et al., 2021).

4.1.2 RO Desalination in practice

The original Loeb-Sourirajan membrane was of a flat sheet format in a plate-and-frame module and was far less efficient than current element types. Nowadays, the most common membrane element construction for RO applications is the multi-leaf spiral-wound element.

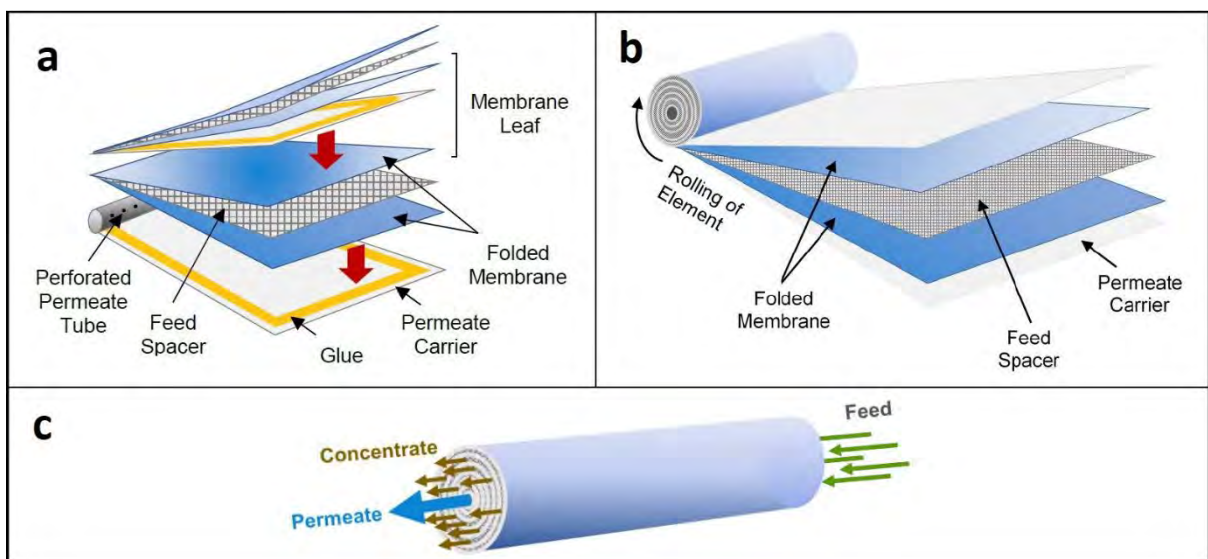


Figure 4-3. Spiral-wound element construction (courtesy Wiles and Peirtsegaele, 2018)

A leaf consists of two sheets of flat-sheet membranes. The active side is faced outwards, and a permeate carrier separates the sheets. The leaves are glued on three sides so the permeate can only exit at the permeate collector, a perforated tube (Figure 4-3a). Multiple leaves are laid on top of each other, separated by a feed spacer (thickness of 0.7 mm), so the feed water is able to pass through the element. The leaves are then rolled around the permeate collector (Figures 4-3b and 4-3c). The spiral wounded element is finally covered with a fibreglass outer wrap to maintain its cylindrical shape (Wilf, 2015; Wiles and Peirtsegaele, 2018).

Concentration polarization is controlled by limiting the recovery rate between 10 to 20% per element (Wilf, 2015). This polarization leads to a decrease in the available driving force and reduces the overall efficiency of separation. Concentration polarization is the accumulation of the retained salt ions and depletion of the water molecules at the boundary layer adjoined to the membrane. (Bhattacharya and Hwang, 1997). Combined with colloidal fouling, this can lead to cake-enhanced concentration polarization, resulting in flux decline and decreased salt rejection (Hoek and Elimelech, 2003). Thus, in order to operate at a higher recovery, multiple elements are interconnected in series in the pressure vessel. Vessel configurations vary between three to eight membrane elements per vessel (Wilf, 2015).

The number of elements and element types varies per plant design. However, at the Carlsbad Desalination Plant (CDP), the 1st Pass RO is configured with single type membrane elements. Thus, multiple elements are loaded into a pressure vessel with permeate connectors between them. Each vessel is loaded with eight identical (when new) FilmTec™ SW30HRLE-400 Elements (Figure 4-4). The active area of an SW30HRLE-400 element is 37 m²; permeate flow rate of 28 m³/day and a salt rejection of 99.8%.

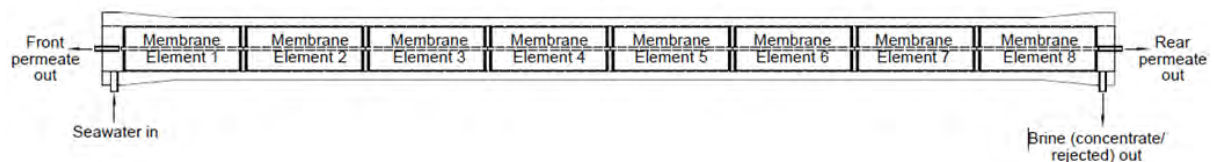


Figure 4-4. A single first pass RO vessel with eight membrane elements

There are more than 2000 pressure vessels at CDP. Of these, 1932 vessels belong to the 1st Pass RO system, and of these, 1792 are filled with membrane elements. The rest are spare for future expansion of production. The vessels are divided into 14 stacks, and each stack is referred to as an RO train. Thus, there are 128 vessels in parallel in each train. Clarified seawater enters at the feed (left at Figure 4-4), and the concentrated rejected brine is

discharged at the tail of the vessel (right at Figure 4-4). The front permeate goes directly to the post-treatment for re-mineralization. The rear goes first to a brackish water RO system for further desalination.

Although each train is subject to identical operating conditions and maintenance interventions, from the maintenance perspective, each train is operated and monitored independently of every other. Demand for permeate (drinking water) is typically met when 13 of the 14 trains are operating. More precisely, the plant's mean peak demand for water is 204 Km³/day and recommended maximum allowable supply per train is 631 m³/hour.



Figure 4-5. A view of the 14 RO trains of the case study

4.2 Biofouling the Achilles' heel of desalination plants

However, membrane fouling significantly threatens the efficiency of RO technology (Kerdi et al., 2020; Jafari et al., 2021; Jamieson et al., 2021). Biofouling is regarded as the most severe and the most difficult to manage (Jiang et al., 2017; Kerdi et al., 2020), and algal blooms are the principal root cause of biofouling in RO membranes (Chiou et al., 2010; Villacorte et al., 2015; Li et al., 2015; Villacorte et al., 2017). In particular, desalination plants on the Pacific coast (California and Chile), the Middle East (the Red Sea and the Persian Gulf coasts) and China report that operations are impacted by algal blooms (Villacorte et al., 2015a).

Degradation or wear of membranes caused by biofouling manifests as a loss in pressure, and maintenance is required. Otherwise, membranes will fail. Biofouling results in a shortening of the membrane life. Membrane replacement is an essential contributor to the cost of operations and maintenance (O&M). Matin et al. (2020) estimate that biofouling costs the desalination industry \$15 billion annually. Jafari et al. (2021) noted that O&M companies do not provide a breakdown of biofouling costs. However, besides loss of revenue due to production interruption, maintenance cost is primarily membrane replacement since clean-in-place (CIP) is just a fraction of the former.

4.2.1 Lack of research in RO maintenance management

Despite the potential severity of biofouling and the costly consequences, little attention has been given so far in the literature to the management of membrane maintenance. The bibliometric study carried out by Zapata-Sierra et al. (2022) on publications related to desalination between 2000 and 2020 does not mention membrane maintenance management. To the author's knowledge, only Koutsakos and Moxey (2007) describe a maintenance protocol for membranes. However, while their system records the position of every element in an RO vessel, it quantifies neither the states of elements nor the long-run costs of interventions. Membrane replacement requires careful planning and should involve computer modelling (Duranceau, 2000). To the author's knowledge, the latter has not yet been addressed.

This research presents a unique maintenance management approach for RO membrane maintenance restoration under biofouling conditions. In doing so, we first must address membrane fouling in general and that biofouling in particular. We will explain from a process engineering stance why biofouling does not cause equal wear over all the elements in an RO vessel. This unequal distribution of wear profoundly affects the maintenance decision for swapping membranes and which elements to replace. The unequal distribution of wear over the vessel's elements justifies the thesis author's point of view to regard a RO pressure vessel as a multi-component system. Further, we provide the reasoning for varying intensity of degradation over time. Both aspects will be captured in the wear increment and restoration equation in chapter 6.

Maintenance planning is interesting because membrane elements can be replaced, swapped, cascaded, or cleaned, and these different interventions have different restorative effects.

Cleanings and replacements are standard practices in the industry, and section 4.4.2

Restoration addresses these practices. However, this research differs from the usual approach

of first cleaning and replacing the most fouled membranes if that is not enough. This research models membrane wear and maintenance in a novel way, describing the hidden states through time of individual membrane elements in a RO pressure vessel. Thus, we can evaluate the effects of the various maintenance choices beforehand.

4.2.2 Membrane degeneration due to fouling

Degeneration of the membranes due to fouling manifests as a decrease in permeate flow, an increase in the salt passage and an increase in the pressure differential (PD) (Li et al., 2015; Jiang et al., 2017; Kim et al., 2017; Villacorte et al., 2017). Membrane fouling is inevitable (Landaburu-Aguirre et al., 2016; Jiang et al., 2017; Qasim et al., 2019). The relevance of the topic is emphasised by the results of a search request at Google Scholar on the topic RO membrane fouling for the year 2020, limited only to Elsevier publications. The response was nearly 2300 articles. The fouling type and behaviour are, however, particular to the application. Fouling of RO membranes in water reclaim of wastewater is fundamentally different from seawater RO applications. Calcium phosphate scaling on membrane surfaces in water reclaim plants is a big problem. However, calcium phosphate scaling in SWRO is minimal. Common types of fouling in SWRO are colloidal fouling, inorganic scaling, organic fouling and biofouling (Jiang et al., 2017; Qasim et al., 2019).

Colloids are fine suspended particles. The size ranges from a few nanometres to a few micrometres. Fouling results by depositing of these colloids on the membrane surface. Colloidal foulants can be divided into inorganic foulants and organic. Common inorganic foulants in seawater are minerals, e.g., calcium carbonate, calcium sulphate, magnesium, aluminium, iron and silica, e.g., silt particles (Jiang et al., 2017; Qasim et al., 2019; Gutiérrez Ruiz et al., 2020). Organic macromolecules in the water mainly consist of materials such as polysaccharides, proteins, carbohydrates, and some other natural organic matter (NOM) (Jiang et al., 2017; Qasim et al., 2019). The colloidal fouling potential of RO feedwater is commonly measured by the silt density index (SDI). SDI is a measurement of the fouling potential of suspended solids (Gutiérrez Ruiz et al., 2020). Colloidal fouling is reversible (Qasim et al., 2019). Pre-treatment filtration can mitigate colloidal fouling (Jiang et al., 2017; Qasim et al., 2019).

Like colloidal fouling generally, inorganic scaling is the deposition of substances on the membrane surface, however inorganic. The most common scalants are calcium sulphate and calcium carbonate. Since minerals are rejected during the RO process, the concentration of these minerals is the highest at the tail of the vessel. Inorganic scaling occurs when these

minerals become supersaturated and undergo homogenous or heterogeneous crystal growth processes. The formation of a cake layer due to the inorganic precipitation could prevent water from permeating through the membrane (Jiang et al., 2017; Liu et al., 2019; Qasim et al., 2019). Physical damage due to the gypsum crystals' perforations of membrane surface can occur. These perforations are exposed after cleaning when the crystals are dissolved (Benecke et al., 2018). The latter then results in decreased salt rejection. Inorganic scaling can be mitigated by adding a scaling inhibitor to the RO feed (Jiang et al., 2017; Liu et al., 2019; Qasim et al., 2019).

Organic fouling in seawater desalination is caused by NOM. NOM in RO seawater feed includes, e.g., algal, transparent exopolymer particles (TEP), proteins and humic acids. NOM with low molecular weight is difficult to remove from the RO feedwater by conventional pre-treatment (Jiang et al., 2017; Qasim et al., 2019).

4.2.3 Biofouling

Biofouling, in particular, increases the PD due to the build-up of the biofilm at the membrane surface and the feed water carrier (Bereschenko et al., 2010; Matin et al., 2011; Villacorte et al., 2015a; Villacorte et al., 2017; Badruzzaman et al., 2019). Therefore, the PD provides a measure of the level of degeneration (wear) of an RO train.

Nearly half of all membrane fouling is due to biofouling (Qasim et al., 2019). The effect of bio-fouling is continuous and long-lasting and regarded as the most severe and the most difficult to manage. Living microorganisms cause biofouling. Initially, organic macromolecules, mainly anionic biopolymers, settle on the surface of a clean membrane and form a conditioning film. Due to its flexible character, TEP has explicitly the ability to pass through pores much smaller than its size. There is a direct correlation between TEP concentration in the feed and the severity of fouling. TEP provides a conditioning layer on the membrane. The latter provides a stable environment for bacteria to proliferate and develop biofilms. (Jamieson et al., 2021). The conditioning film increases the capacity of the surface to absorb and concentrate nutrients from the RO feed water. This organic adsorption is a precondition for bacterial attachment (Baier et al., 1968). Bacterial species that produce large amounts of extracellular polymeric substances then colonize the surface, forming a slime layer known as a *biofilm*.

A biofilm is a community of surface-attached microbial organisms. Their phenotypic and biochemical properties are distinctly different from floating planktonic cells. The switch from

a planktonic phase to a surface biofilm formation is thought to be triggered when the bacteria sense environmental conditions for this (Kadouri and O’Toole, 2005).

Worldwide, Proteobacteria and Actinobacteria are frequently the most dominant organisms identified within the feed water and on fouled membranes. Proteobacteria have the ability to dominate SWRO biofilms as they are small enough (0.22 μm) to bypass all the pre-treatment systems within the plant. Observations show that both α - and γ - proteobacteria increased in their relative abundance after pre-treatment. α -proteobacteria are often the primary colonisers within biofilms. The physiological and phenotypic traits of surface-associated bacteria differ from those in a planktonic state. The cells undergo a range of phenotypic switches throughout biofilm formation. As the bacteria respond to their surrounding environment, concentration gradients, diffusional processes, signalling compounds, and waste result in a heterogeneous structure within the biofilm.

Consequently, the cells within the biofilm are physiologically distant from planktonic bacteria. Proteobacteria are known for forming biofilms and producing unique and individual EPS/TEP products, potentially leading to further settlement of the organic matter and accumulation of microorganisms to spread the biofilm further (Jamieson et al., 2021).

The latter was examined at CDP, where a study independent of this research observed a high abundance of *Shewanella* species on membrane samples. These metabolically versatile species belongs to γ - proteobacteria species and are known to form biofilms. The *Shewanella* species were nearly absent prior in samples from the cartridge filters (Podar et al., 2021).

Attachment of the biofilm is irreversible. Depending on the supply of nutrients, the biofilm can grow in a matter of days or even hours. Figure 4-6 shows the lifecycle of the biofilm. When the biofilm has matured, and the colony gets overcrowded, some bacteria disperse and starts to colonize the next area of the membrane surface (Stoodley et al., 2002; Bereschenko et al., 2010; Matin et al., 2011; Villacorte et al., 2015a; Badruzzaman et al., 2019). Trulear and Characklis (1982) refer to detachment as the partial detachment of the biofilm by shearing.

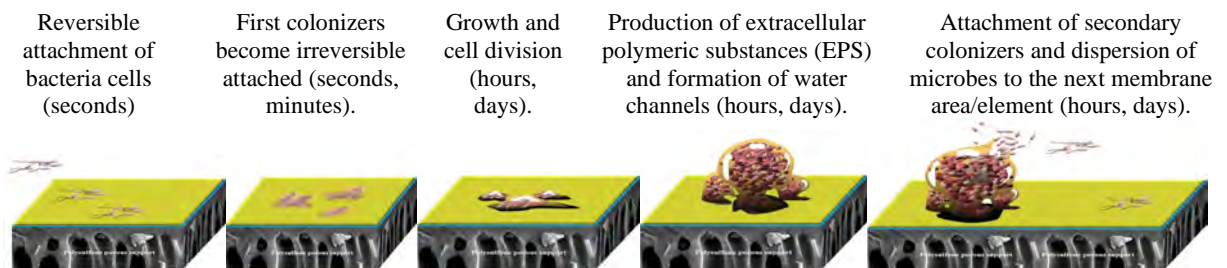


Figure 4-6. Lifecycle of the biofilm (Modification of work by American Society for Microbiology).

When this biofilm starts affecting the RO system, we speak of biofouling (Li et al., 2015; Jiang et al., 2017; Villacorte et al., 2017; Qasim et al., 2019). Membrane autopsies by elements throughout a vessel by Fortunato et al. (2020) at an SWRO desalination on the Red Sea confirmed the gradual spread of biomass over the elements, depending on the module position in the vessel.

Scale inhibitors are also prone to contribute to biofilm growth (Landaburu-Aguirre et al., 2016). However, most importantly, biofouling in RO membranes accelerates due to algal blooms. The direct cause of this acceleration of deterioration is not the algae cells themselves but Algal Organic Matter (AOM), particularly Transparent Exopolymer Particles (TEP). Pre-treatment can reduce the amount of TEP in the RO feed water, but low amounts will still reach the SWRO membranes.

Dead algae cells disintegrate and release AOM, which like TEP, adheres to clean membranes and even more so to AOM-fouled membranes. Thus, by settling these organic macromolecules on the surface of a clean membrane, the surface is conditioned, increasing the capacity of the surface to absorb nutrients. This surface conditioning helps the initial bacteria adhesive to the surface and form micro-colonies. (Li et al., 2015; Villacorte et al., 2017). Therefore, AOM facilitates the onset of wear, resulting in the formation of a biofilm by the bacteria. Besides AOM, organic macromolecules occur as TEP. High absorption of TEP can be observed as a slimy substance sticking to surfaces when coming into contact. Dinoflagellates, a group of phytoplankton responsible for algal blooms, generate large quantities of TEP once nutrients have been exhausted (Zamanillo et al., 2019).

After the onset of wear, AOM and TEP then accelerate the growth of the biofilm by delivering the required nutrient source. Previous studies have observed the presence of TEP on fouled membranes. However, how far TEP is brought in by the source water or produced by bacteria remains unclear. In matured biofilms, the dominant TEP source is bacteria (Jamieson et al., 2021).

A high proportion of the biofilm is exopolymer material. The latter is essential in maintaining the structural integrity of the biofilm matrix. As the biofilm develops, the exopolymer content changes (Trulear and Characklis, 1982).

The complexity of the ecosystem promotes the coexistence of organisms creating niches and increasing the diversity within the communities. The biofilm also provides an environment for settlement and growth for other organisms such as diatoms, dinoflagellates, and ciliates. Due to their complementary lifestyles, a collaborating relationship develops between diatoms and bacteria (Jamieson et al., 2021).

Therefore, a biofilm is a complex ecosystem that protects the settled communities. Biofilms mitigate attacks by *Bdellovibrio*, a bacteria predator species. The survival rate of planktonic cells by a *Bdellovibrio* attack is much lower (Kadouri and O'Toole, 2005). Among other functions, the biofilm deals with nutrient transport and storage (Battin et al., 2003) and oxygen to the biofilm's lower levels (Trulear and Characklis, 1982). Thus, the degeneration due to bio-fouling continues beyond the period of an algal bloom. The decay is exponential (Agawin et al., 2000).

4.3 Monitoring membrane fouling

As mentioned in section 4.2.3, PD provides a measure of an RO train's level of degeneration (wear). However, permeate flow, salt passage and PD vary without deterioration of the membranes due to changes in feedwater temperature, salinity and flows.

For example, lowering the feedwater temperature results in compacting of the membrane elements, whereby the DP increases, permeate flow reduces, and the salt rejection improves. An increase in feedwater temperature expands the elements, resulting in lower differential pressure, an increase of permeate flow, and a reduction of salt rejection.

Before we can monitor the actual membrane deterioration, the effects of feedwater temperature, salinity and flows must be filtered out. The process of standardizing RO performance data is defined in the industry as *normalization*. Data normalization enables the performance of the RO data at a specific time to be compared against the initial performance. The American Society for Testing Materials (ASTM) defines the standard practice for standardizing RO performance data in ASTM Methods 4516. However, there is no specification for PD normalization in this standard (Wolfe, 2003).

A normalization equation has been adopted, specified by the membrane manufacturer. RO real-time performance data is monitored continuously and recorded in intervals of 60 seconds. The normalized pressure differential (NPD) is calculated from the hourly means of the recorded data. Then, to reduce noise from, e.g., stoppages, at 00:00 hours every day, the mean NPD is calculated over the previous 24 hours. So, this daily mean NPD provides a measure of the level of deterioration of the vessels in an RO train (Figure 4-7). Interruptions of the NPD (red pen) and product (blue pen) are due to the train being offline.

The observed NPD's first sudden acceleration started around June 2016 (week 30). The first maintenance action took place in February 2017 (week 66/67). Therefore, up to month 14 of operation shows the initial deterioration of the membranes without interventions.

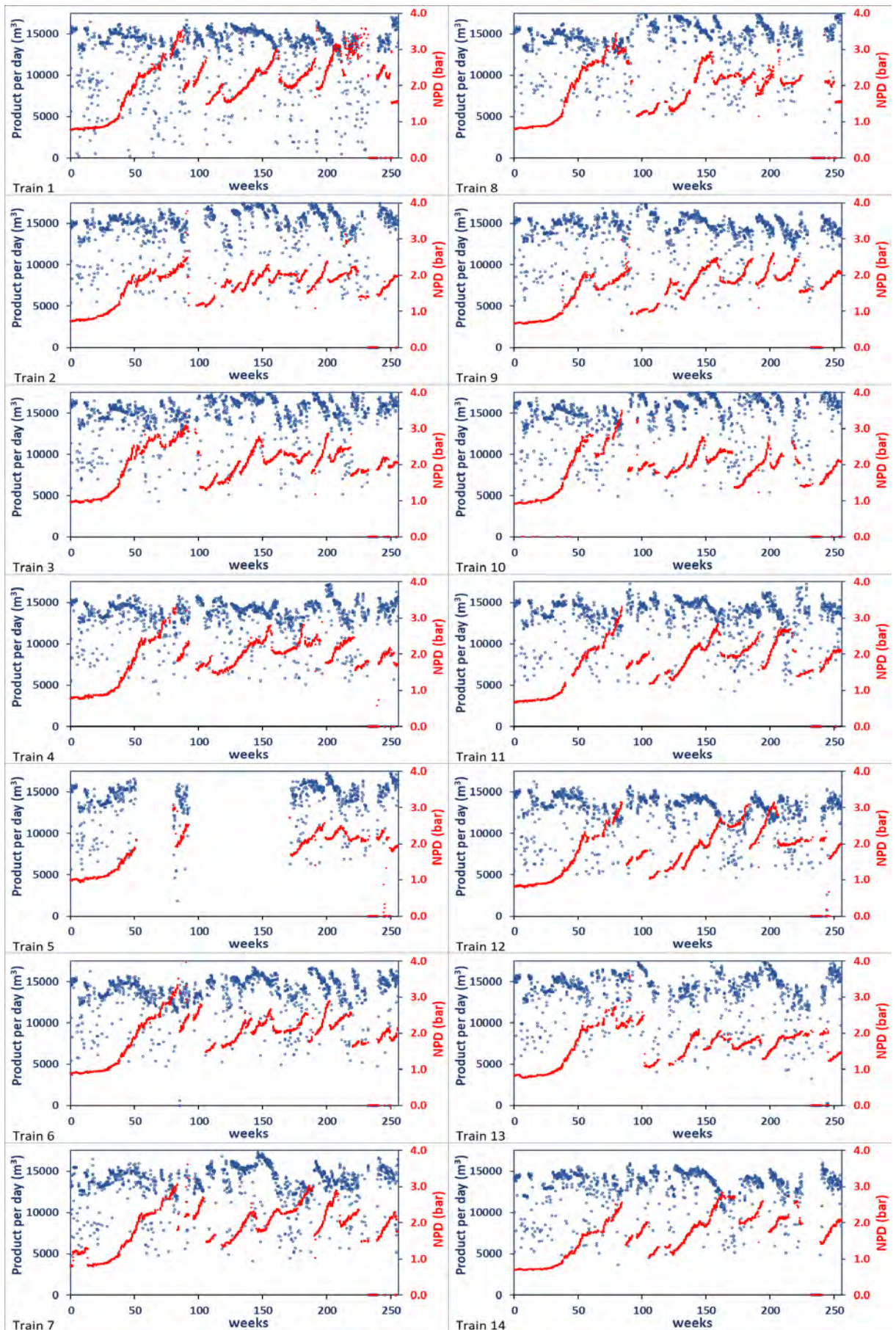


Figure 4-7. Normalized DP (pressure) for each train from the start of operation of the plant.

4.3.1 Membrane Autopsy to determine the fouling type

The only way to examine what is taking place inside the membrane element is to cut it open and have a look (Fortunato et al., 2020). This destructive inspection technique is called membrane autopsy. Membrane autopsies are performed as long as synthetic membrane elements exist. Specialized laboratory services usually perform membrane autopsies (Dalton et al., 2004).

In October 2016, a front membrane and a tail membrane of one of the trains was removed and sent to an external Lab for membrane autopsy. The front membrane weighed 18 kg. A new element is expected to weigh between 13.5 and 16 kg. The element was coated with an orange gelatinous material. The foulant was denser on the element's feed end, and increased foulant streaks were noted on all the membrane leaves in areas furthest from the permeate tube. A slight biological odour was noted upon dissection. The feed spacer material was lightly coated in orange-coloured material and was more heavily coated on the feed end of the element. The foulant was identified as 91% organic (bio-slime, fungi, algae, bacteria) with particles embedded in the organics. The remaining 9% represents inorganic particulates.

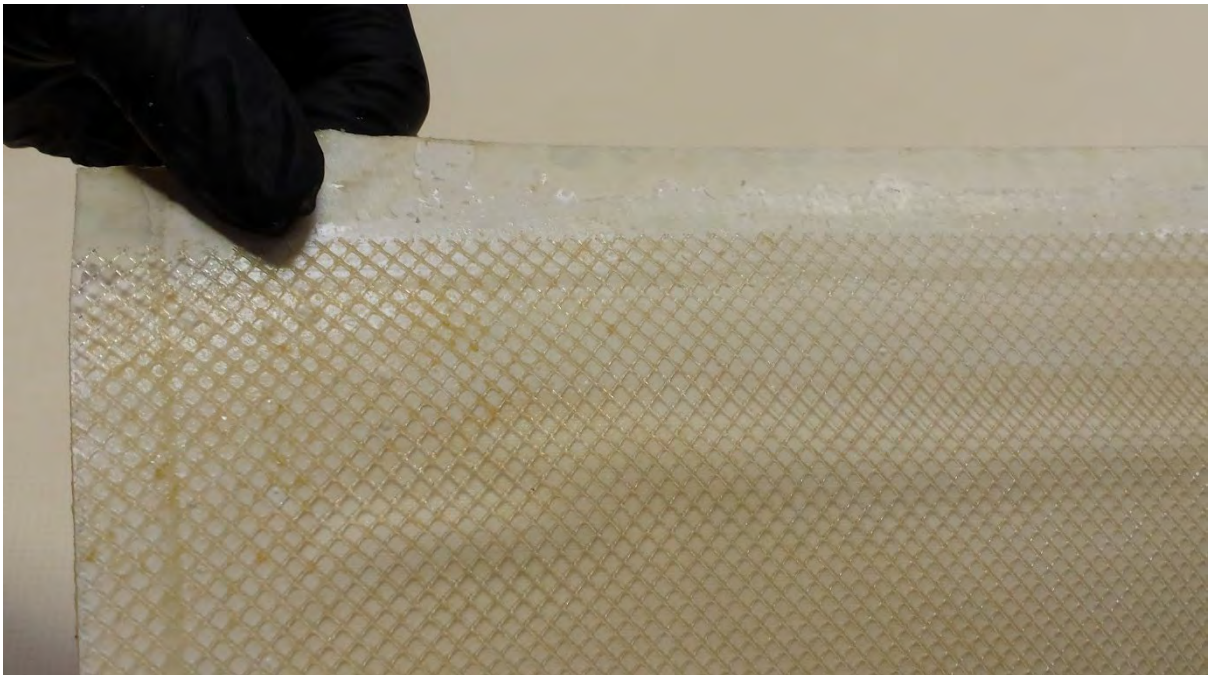


Figure 4-8. Membrane surface of the front element and feed spacer during the autopsy.

The tail element weighed 16 kg. Minimal foulant was observed on the tail membrane, only trace salts and organics. Testing under brackish water conditions of both elements separately showed that the pressure drop of the front element was more than double than the tail element.



Figure 4-9. Membrane surface of the tail element and feed spacer during the autopsy.

4.3.2 Seasonal algal blooms

As mentioned above, algal blooms amplify biofouling. So far, algal blooms have affected the desalination plant mainly during the spring season and close to the spring season. The timings of algal blooms are shown in Table 4-1.

Table 4-1. Dates of algal blooms (week number of operation of the plant in brackets)

| Detected change in <i>P</i> | Reported start | Reported end | Detected end effects |
|-----------------------------|----------------------|----------------------|--------------------------|
| June 8, 2016 (30) | N/A | N/A | November 20, 2016 (54) |
| March 12, 2017 (70) | April 12, 2017 (74) | April 27, 2017 (76) | July 30, 2017 (90) |
| April 8, 2018 (126) | April 8, 2018 (126) | April 9, 2018 (126) | August 26, 2018 (146) |
| April 9, 2019 (178) | April 9, 2019 (178) | April 13, 2019 (179) | |
| | June 6, 2019 (186) | June 12, 2019 (187) | September 23, 2020 (202) |
| | April 10, 2020 (231) | May 5, 2020 (234) | |

Fluctuations in environmental conditions can explain the seasonal occurrence of algal blooms. The desalination plant of the case study is positioned at the Southern California Bight (SCB) above San Diego (see map Figure 4-10). The SCB is a significant portion of the Californian west coast. The coastal islands act as a buffer of the southern California coast from the direct impact of the oceanic California Current and meteorological effects (Smith et al., 2018).

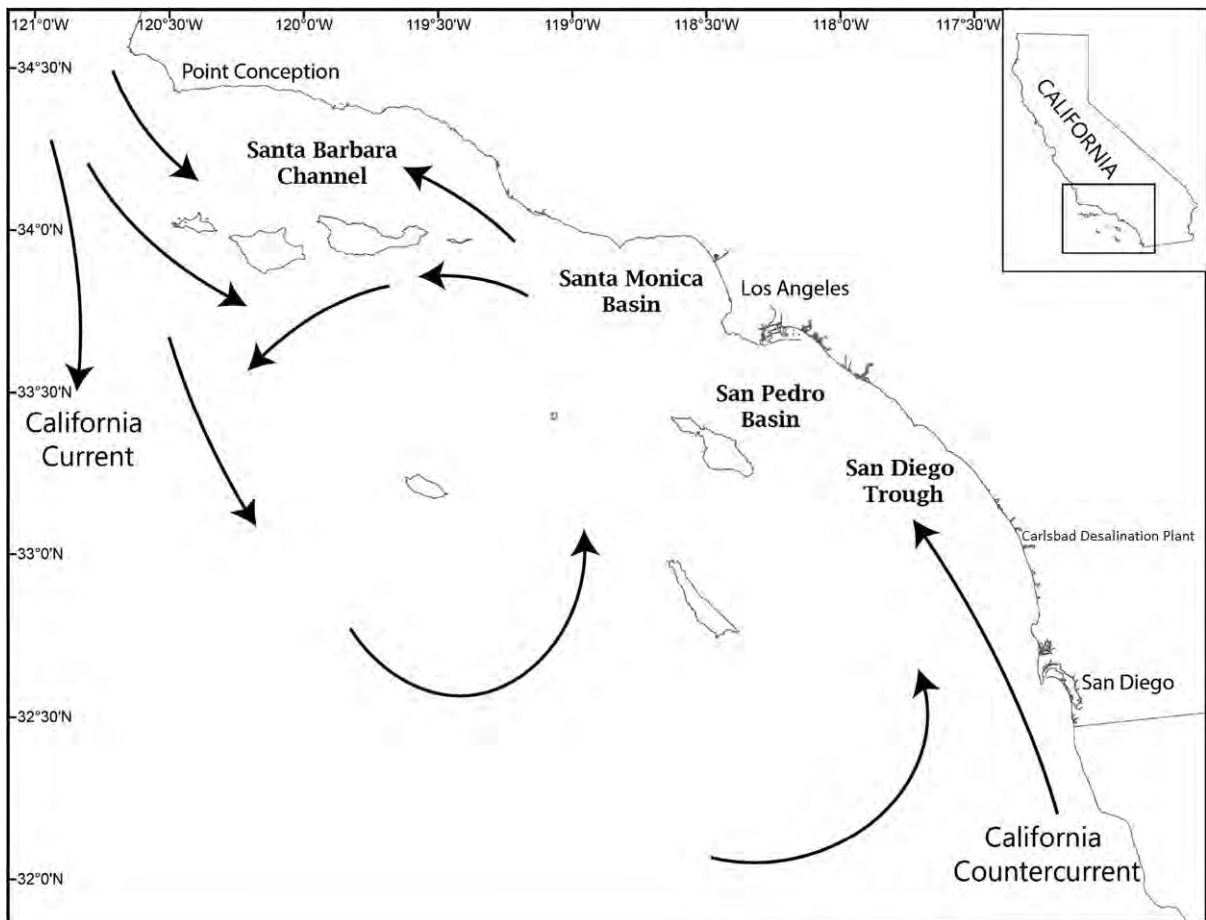


Figure 4-10. Map of the Southern California Bight. Courtesy Smith et al. (2018).

The most hazardous group of algae identified at CDP, contributing to the biofouling of RO membranes, are dinoflagellates. Besides AOM from disintegrating algae cells, an essential trigger for biofouling is also the TEP, produced by some algae. However, not only dinoflagellates but also diatoms generate large quantities of TEP once nutrients have been exhausted (Zamanillo et al., 2019).

Dinoflagellates are a group of phytoplankton. Phytoplankton is concentrated at the upper sunlit layer of the ocean, called the euphotic zone that supports net photosynthesis. The depth of the euphotic zone is defined as *the depth at which the photon flux equals 1% of the flux measured just above the air-sea interface* (Letelier et al., 2004, p. 508). These photoautotrophs species harvest light to convert inorganic to organic carbon. Phytoplankton requires, therefore, light and nutrients (Sigman and Hain, 2012).

The increase in seawater temperature and the mild UV radiation at shallow waters explains the occurrence of algal blooms during the spring season. As the waters warmed in early spring and wind reduced, conditions appeared perfect for developing widespread algal blooms (Anderson and Hepner-Medina, 2020). However, although these are essential

conditions for inoculation into the planktonic phase, other dependencies exist. Rengefors et al. (1998) suggest that the composition of the food web is one of the triggers of an algae bloom. Nutrient charging differs significantly throughout the SCB. An essential source of nutrients at the SCB is the North Pacific Subtropical Gyre, the largest contiguous ecosystem on earth (Di Lorenzo et al., 2008). Observations undertaken in the North Pacific Subtropical Gyre exhibited an upper region of the euphotic zone (0-90 m) that is almost permanently under nutrient limiting conditions. Blooms in the upper euphotic zone at this oceanic region are stochastic and short-lived. The lower euphotic region (90 – 200 m) is seasonal richer in nutrients, which supports better conditions for annual algae blooms. (Letelier et al., 2004). Spring phytoplankton blooms are caused in this period when the upwelling of deeper water delivers nutrients to the well-lit surface layer (Anderson and Hepner-Medina, 2020).

The source of nutrients supplied by the California Current from the North Pacific Subtropical Gyre at the SCB is only one part of the supply. Nutrients are further supplied from the shores. The demographic diversity of the coastal region, a mixture of agricultural and highly urbanized regions, results in variability of magnitude and type of nutrient loading to the near-shore waters. Therefore, an essential source of nutrients is the effluent discharge of public wastewater treatment plants (Smith et al., 2018).

The algae bloom of Spring 2020 occurred after heavy rainfall in March, which resulted in high storm drain effluent from the shore to the lagoon. The lagoon is connected to the Pacific Ocean, and CDP receives its source water from this lagoon. The Southern California coast experienced precipitation levels of 200 to 400% above average (Anderson and Hepner-Medina, 2020). The seawater colour at the lagoon became a caramel brownish. The inlet turbidity increased above the plant's operations and maintenance (O&M) contractual limit. The following months, April and May 2020, saw the worst algae bloom since 1983, when the systematic recording of chlorophyll concentrations started (Anderson and Hepner-Medina, 2020). This algae bloom was referred to as a Red Tide. The seawater was dark rust-brown. 95% of abundance were dinoflagellates, with *Lingulodinium polyedra* as the dominant group. There was an intense odorous sulphur smell from water, foam, and numerous dead fish (Carter, 2020). Similar conditions were observed at the intake lagoon of the plant (Figures 4-11, 4-12 and 4-13). The algae bloom conditions were so severe that the plant was forced to shut down for weeks. Large quantities of TEP, observed as slime, were noted during Net Tow sampling on some days and nearly absent on others.



Figure 4-11. Intake Lagoon condition during Red Tide in Spring 2020



Figure 4-12. Net Tow sample seawater



Figure 4-13. Observed dead fish at the Intake Lagoon associated with the Red Tide in Spring 2020

Table 4-2. Average RO feed source water condition during algae bloom and non-algae bloom conditions between 2017 and 2020 (ND = non detect). In those cases, SDI > 5 or Turbidity > 0.35 NTU, RO feed water supply is interrupted.

| | SDI | Turbidity (NTU) | 2-5 μ m particle (counts/ml) | ORP (mV) | DOC (ppm) | TOC (ppm) |
|-----------------|------|-----------------|----------------------------------|----------|-----------|-----------|
| non-algae bloom | 3.08 | 0.07 | 41.59 | 222.51 | ND | 0.71 |
| algae bloom | 4.62 | 0.13 | 157.47 | 232.12 | 1.88 | 2.21 |

Lingulodinium polyedra is an armoured bioluminescent dinoflagellates species associated with fish and shellfish mortality events (Dodge, 1989). Following the algae bloom in 2020, CDP started monitoring residual algae species of the source water in-house. Figure 4-14: showing several algae species observed by CDP internal lab utilizing a 40X-1500X Trinocular Inverted Infinity-corrected Phase-contrast Microscope with Koehler Illumination. Magnification is 40x. The algae observed in Figures 4-14 are from the same seawater sample taken on 30 March 2021 (pre-bloom conditions).

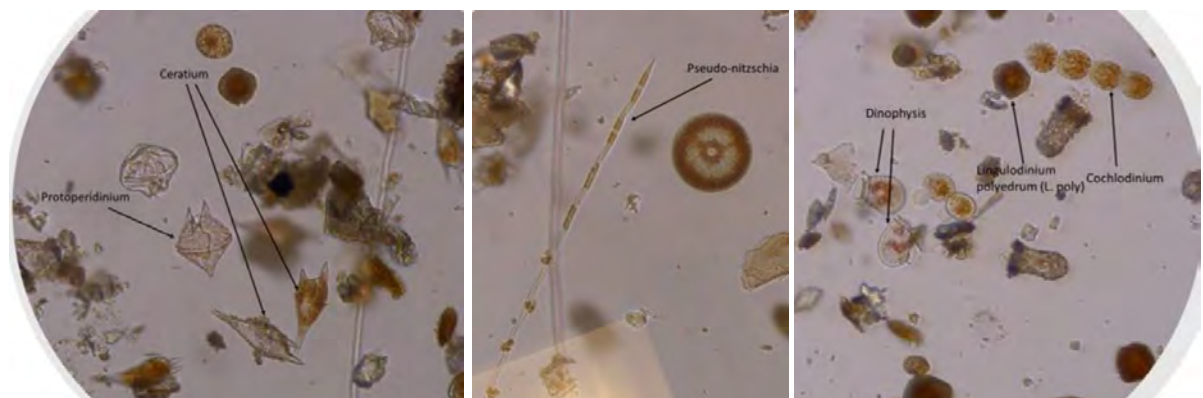


Figure 4-14. Protopteridinium and Ceratium species (left), Pseudo-nitzschia species (middle) and Dinophysis, Lingulodinium polyedra and Cochloclonium species (right).

The *Lingulodinium polyedra*, see figure 4-14 at the right, is among the dinoflagellates species that has a resting cysts stage (Lewis, 2018). A significant number of marine dinoflagellate species undergo a benthic phase in their lifecycle. During unfavourable vegetative conditions, the planktonic dinoflagellates lose their flagellate and produce a cyst. The cysts settle in the sediment layer of the benthic zone and reinoculate the water column when favourable conditions are restored, resulting in bloom. This survival strategy is to protect the species from unfavourable conditions. The latter can be a multitude of factors, e.g., temperature, depletion of nutrition, UV radiation, avoidance of grazing or defence against parasitic attack. The benthic phase can last several hours to several years (Bravo and Figueroa, 2014).

The fundamental dynamics of planktonic blooms have not been established yet. Patterns of seasonal algal blooms can further change in the future due to climate change (Hallegraeff, 2010). Increasing ocean temperature has been linked to the intensification of algal blooms (Gobler et al., 2017; McKibben et al., 2017). Although algae blooms seem to occur mainly in the spring season, blooms in later seasons cannot be excluded. For instance, the whole coastline of the SCB was hit by a dinoflagellate bloom during the summer-fall period of the year 2005. Recently in 2021, a bloom of *Lingulodinium polyedra* occurred in November.

The National Oceanic and Atmospheric Administration, a US governmental institution, is developing a forecast for harmful algae blooms (HOB). The focus is on algae, which are toxic for marine animals, birds and humans (Smith et al., 2018). However, algae resulting in excessive biofouling at RO membranes are not limited to HOB species. This research considers that algal blooms affecting the desalination plant will mainly occur in the spring season, considering that an algal bloom could occur in the summer-fall period.

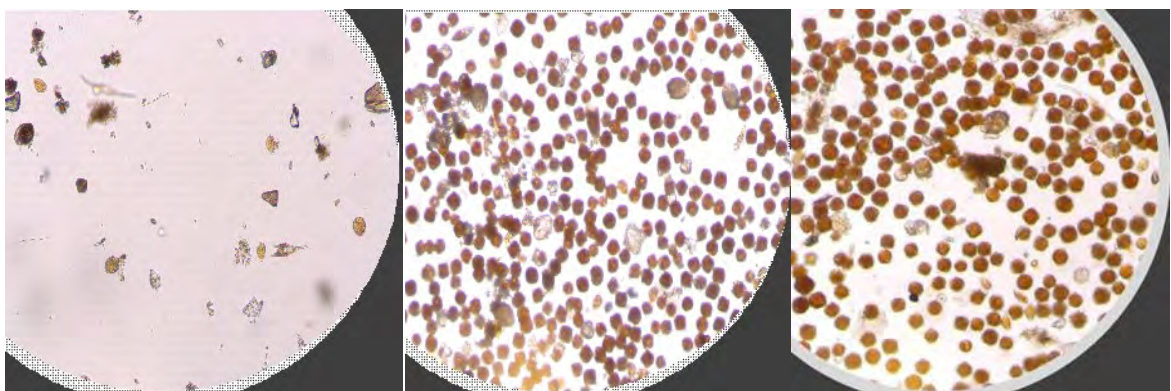


Figure 4-15. Feedwater CDP, magnification 10x Left 5 May, Middle 8 Nov., Right 18 Nov. 2021

4.4 Mitigation of Membrane degeneration

Mitigating biofouling by improving the pre-treatment should be considered first (Matin, Khan, Zaidi, and Boyce, 2011; Villacorte et al., 2015; Jiang et al., 2017; Badruzzaman et al., 2019). Pre-treatment aims to filter out organic and inorganic foulants from the feed water to the RO. Granular media filtration is the most common applied source water pretreatment process for RO desalination. However, over the last decade, the application of membrane filtration as a pretreatment strategy has increased (Voutchkov, 2017).

4.4.1 Prevention

According to Villacorte et al. (2017), granular media filtration is unable to deal with an algae bloom attack. Although granular media filtration is still the most common, ultra-filtration (UF) has made significant inroads. UF requires less footprint, provides better filtration and is less affected by changes in seawater quality. On the other side, the operation of UF is more complex. It requires a delicate balancing of coagulation, run time, controlling filtration flux, backwashing and chemically enhanced backwash to prevent irrecoverable fouling (Brover et al., 2022).

Membrane-based methods such as microfiltration (MF) and UF are better in preventing biopolymers from reaching the RO membranes. However, consequently, MF and UF undergo rapid biofouling themselves during an algae bloom. As with granular media filtration, low molecular weight organic compounds, e.g., humic-like substances, are also poorly rejected by MF/UF membranes (Villacorte et al., 2017). A pilot study by Nakaya et al. (2021) showed that UF reduced living biomass by 75%. That means 25% survive the UF and continue towards the RO membranes.

Although MF and UF are now standard in RO desalination plants, in addition to disinfectants and chemical dosing, these treatments only temporarily improve mitigating biofouling. Colonization of RO membranes by microorganisms is inevitable. Research by Jamieson et al. (2021) showed that only selective bacterial groups are removed. Pre-treatment systems can become niche environments for the proliferation of adaptable bacteria due to the steady inflow of nutrients. These environments potentially become a reservoir for diverse microorganisms. Even limited amounts of microorganisms passing the pretreatment have serious results due to proliferation and biofilm formation (Jamieson et al., 2021).

Franks et al. (2006) reported on a pilot study of several years at the SCB that involved conventional pre-treatment, MF and UF. During the three years of the pilot test, heavy rains

and red tide occurred. The pre-treatment systems studied were all unable to prevent biofouling during heavy rainfall and algae bloom conditions.

Dissolved air flotation (DAF) incorporating filtration (DAFF) is the most promising solution to improve filtration in the case of algae blooms (Badruzzaman et al., 2019). However, biofouling mitigation is often limited for economic, environmental or practical reasons, e.g., available footprint. Even with reasonably healthy pre-treatment performance, organic and biofouling are practically unavoidable (Karanasiou et al., 2021). The use of additional cartridge filters as a final safety net to catch particles that escaped the pre-treatment exacerbates biofouling. Cartridge filters provide a unique ecosystem for microorganisms (Jamieson et al., 2021). A study by (Fortunato et al., 2020) at an SWRO plant on the Red Sea showed similar observations. Water samples collected after cartridge filters had a significantly higher biomass activity than water samples after pre-treatment. Jamieson et al. (2021) proposed removing the cartridge filters as an additional safety net.

4.4.2 Restoration

So, O&M teams often must accept a degree of biofouling. Cleaning of membranes in-situ, so-called clean-in-place (CIP), is the most apparent initial maintenance action to reverse membrane degeneration. The CIP method depends on the membrane fouling layer composition (Jiang et al., 2017). In this case study, the O&M team started CIP after confirming biofouling as the main reason for membrane degeneration (see section 3.5). Since the dominant fouling occurred at the lead membranes in the vessel, the cleaning direction was configured as reverse, i.e., cleaning flow direction from the tail (brine) to the lead (feed) side of the vessels (Andes et al., 2013). Initially, the cleaning solution used was standard in the industry when dealing with biofouling. Consecutive high pH (NaOH solution) and low pH cleaning (HCl solution). This CIP activity gave a poor to a moderate reversal of the degeneration. The high and low CIP procedure is shown in Table 4-3.

Table 4-3. Procedure high and low pH CIP (C1)

| | pH | Chemical | Stage 1 low flow per vessel | Stage 2 high flow per vessel | Stage 3 Soaking | Stage 4 high flow per vessel |
|---------|----|----------|--------------------------------|---------------------------------|--------------------|---------------------------------|
| High pH | 12 | NaOH | 4 m ³ /h (15 min) | 7 m ³ /h (60-90 min) | 60 min | 7 m ³ /h (60 min) |
| Low pH | 2 | HCl | 4 m ³ /h (15 min) | 7 m ³ /h (30-45 min) | 30 min | 7 m ³ /h (60 min) |

Sodium Bisulfite (SBS) is commonly used for dechlorination and dechloramination of RO feed water (Kucera, 2019). Farooque et al. (2002) reported using SBS as a low pH solution for cleaning biofouled nano-filtration (NF) membranes, however, without success.

Nevertheless, SBS removes oxygen from water (Kucera, 2019) and therefore suffocates bacteria. An SBS treatment to kill the bacteria, followed by high and low pH cleanings to remove the biomass, improves the restoration significantly. Therefore, the O&M team mainly conducted soaking the membranes with SBS (1% SBS solution, 0.7 m³/h per vessel for 24 hr) followed with a high and low pH CIP from August 2018 onwards. This maintenance action gave, on average, better restoration of membranes than the standard high and low cleaning. Initially, also a third method was conducted. This experimental cleaning method would remove the lead element from the vessel and clean it externally. This method was only applied to two trains and was discontinued after that.

Furthermore, when biofouling is severe, CIP is insufficient to restore an RO train to an acceptable state over time. Replacement of the most fouled membrane elements then becomes unavoidable (Koutsakos and Moxey, 2007). Membrane maintenance can become costly when the number of elements to be replaced surpasses significantly that of the initial projection during the plant-design phase. These unforeseen costs are not limited to the cost of new elements but also labour and downtime (Jafari et al., 2021).

Some authors report a cost of membrane replacement of a 5% figure (Miller, 2003; Younos, 2005), others 10% (Poullikkas, 2001; Stover et al., 2017). Emamjome et al. (2019) report the percentage of membrane replaced annually at 10%. This rate of membrane replacement is according to the recommendations of membrane manufacturers. However, the estimates of Miller, Younos, Poullikkas, Stover et al. and Emamjome et al. do not consider the variations in feedwater quality at different locations in the world. Considering the design and feedwater conditions, Jiang et al. (2015) estimate the annual membrane replacement cost at 15 to 20% of total operational expenses (OPEX). A recent study of fouling cost as a fraction of OPEX by Jafari et al. (2021) of two surface water RO plants and one secondary industrial wastewater effluent RO plant in the Netherlands concluded that the figure was approx. 24%. Membrane replacement was the main cost factor.

Despite the potential severity of biofouling and the costly consequences, little attention has been given so far in the literature on the management of membrane restoration. Mitra et al. (2009) reported a decision to replace 25% of membrane elements in a plant in one go after three years of operation. They discussed the performance effect but not the cost-efficiency of this intervention. Vrouwenvelder et al. (2007) and Bartman et al. (2011) developed a simulation tool for monitoring biofouling in spiral-wound membranes. This tool notionally monitors the first element in a vessel so that a complete picture of the states of all elements in the vessel is missing. Koutsakos and Moxey (2007) describe a protocol for membrane

maintenance. The first step is CIP, and the second step is the replacement or swapping of elements if CIP is not sufficiently effective. However, as stated earlier, while their system records the position of every element in an RO train, it quantifies neither the states of elements nor the long-run costs of interventions.

This research presents a new approach in which the (degradation) states of all elements in RO are quantified throughout the life of the train. Furthermore, in this research approach, the degradation of trains is continuously monitored, and the cost and effectiveness of interventions (cleaning, replacement, swapping) are measured. The state of the elements is quantified by modelling the evolution of degradation, and hence performance, of a train. Thereby, the feed water quality (extent of algal contamination) and the effects of cleaning, swapping and replacing elements are accounted for. The ordering of the components is also called permutations (Miller and Childers, 2012). Except when a distinct difference is made between cascading and swapping of components, a reference to permutations is made further onwards.



Figure 4-16. Membrane replacement

4.5 Summary

Seawater desalination has become an essential solution to deal with the increase in droughts and, at the same time, growing water demand. With seawater accounting for 97.5 percent of all water, the available resources are substantial. Improved reverse osmosis (RO)

membrane technology and energy recovery has made RO affordable. Thus in the last decade, the capacity of SWRO has increased significantly, as has the academic interest.

However, membrane fouling is the Achilles' heel of desalination plants. Biofouling is the most challenging, and algae blooms are the principal root cause of biofouling in RO membranes. We have seen reports from operators of several desalination plants worldwide that algal blooms impact their operations. Biofouling manifests itself in increased hydraulic pressure differential (PD) between the feed and concentrates side of the membrane elements due to biofilm growth at the membrane surface and feedwater spacers. When this PD over the vessel exceeds the limit of 3.5 bar, elements can fail irreversibly.

Biofouling is a physical-, biochemical reaction by settling of planktonic bacteria at the surface of the membrane and thereby switching to surface-attached microbial organisms. Surface adjustment by organic fouling is a precondition. The switch from a planktonic phase to a surface biofilm formation is triggered when the bacteria sense environmental conditions for this. A biofilm is a complex ecosystem that supports surface-attached microbial organisms. Attachment of the biofilm is irreversible. Natural organic matter (NOM) that first adjusted the surface of the membrane now becomes nutrients for the microbial organisms. Depending on the supply of nutrients, the biofilm can grow in a matter of days or even hours. When the colony becomes too big, some bacteria disperse and colonize the next area of the membrane surface. So, biofouling starts at the first element's feed then spreads to the tail.

Standard in an SWRO desalination plant, a pre-treatment is preseeding the RO process to mitigate biofouling and fouling in general. Pre-treatment aims to filter out organic and inorganic foulants from the feed water to the RO. However, filtration cannot entirely remove NOM due to its physical molecular size. The latter is especially the case when only traditional granular media filtration is applied for pre-treatment.

During algae blooms increase in nutrients occur not by algae cells escaping the pre-treatment, but Algal Organic Matter (AOM), which is released after dead algae cells disintegrate. An additional source of nutrients is the Transparent Exopolymer Particles (TEP) produced by some algae species under stress. TEP can be observed as a slimy substance sticking to surfaces when coming into contact. Due to its flexible character, TEP has explicitly the ability to pass through pores much smaller than its size. Algae blooms mainly occur during spring. However, rarely blooms have been observed in autumn. Patterns of seasonal algal blooms can change in the future due to climate change, especially increasing ocean temperature, which has been linked to the intensification of algal blooms.

So, operation and maintenance (O&M) teams often must accept a degree of biofouling. Cleaning membranes in-situ, so-called clean-in-place (CIP), is the most apparent initial maintenance action to reverse membrane degeneration. CIP is a physical-chemical process to remove the biofilm. However, CIP can only partially remove a matured biofilm. Therefore this is an imperfect maintenance procedure. Over time, the most fouled membrane elements must be replaced. Despite the potential severity of biofouling and the costly consequences, little attention has been given so far in the literature on the management of membrane restoration. The literature to date generally describes a membrane system and its associated wear as a single system. In this research, an RO vessel is approached as a unique multi-component system describing the hidden states through time of the individual elements. The next chapter will evaluate this unique multi-component system from a maintenance engineering point of view.

5 A RO vessel as a multi-component system

The previous chapter explored the degradation and restoration of a reverse osmosis (RO) pressure vessel from an RO process engineering perspective. This chapter evaluates the degradation and restoration of RO membranes compared to other systems in the maintenance theory literature. The previous and this approach are both essential, but one cannot be seen as a sheer extension of the other. Thus, both comprehend different approaches to the research. Suppose the EO would be a centrifugal pump, then a mechanical and specific hydraulic engineering understanding would be required instead of physical-biochemical processes. Maintenance engineering, however, would look at both EOs from a similar perspective.

Maintenance engineering must not be seen of how an EO is to be disassembled and reassembled, but how the maintenance of an EO is planned. It deals with reliability, maintenance requirements analysis and establishing suitable maintenance policies. An essential part of maintenance engineering is maintenance modelling. Maintenance modelling gives insight into the potential degradation and restoration projections when both degradation and restoration are stochastic.

In this chapter, first, the definition of multi-component systems is explored. Following different degradation dependencies and models are evaluated. Finally, the management of restoration is evaluated. The chapter concludes with a summary.

5.1 Multi-component systems in maintenance theory

Maintenance optimization involves developing and analysing mathematical models to improve or optimise maintenance policies (de Jonge and Scarf, 2020). In their review paper, de Jong and Scarf (2020) referred to single- and multi-component systems. Zhang et al. (2016, p. 159) defined a multi-component system as *a structural system consisting of a certain number of components of specific form, a container and the supporting structure that interconnects the components and the container for its integrity*. The components can be connected in series, parallel, or as a combination of both. The components themselves can be complex structures or single mass-produced components (Birnbaum et al., 1961). Wang and Chen (2016) refer to multi-component systems as complex systems consisting of several individual assets, e.g., a group of pumps as part of a common system or an engineered object (EO) consisting of more than one component, e.g., a pump itself.

Chapter 4.2 described the SWRO system consisting of vessels, each with eight identical membrane elements in series. A vessel corresponds precisely with the definition of a multi-

component system as defined by Zhang et al. (2016). As Figure 4-3 shows, a spiral-wound element construction is a complex structure in itself. However, in this research, a membrane element is regarded as a single component since it cannot be taken apart and re-assembled.

On the other hand, the train is a multi-component system of 128 vessels interconnected in parallel. Finally, the RO plant design is configured as a common pressure centre, meaning that the inlet and outlets of the trains are connected to common headers. Therefore, while the individual trains are in operation, the RO system is a multi-component system of various trains in parallel. The RO system itself is part of a broader multi-component system, as shown in Figure 5-1. This research concentrates on the RO train. Production-wise, vessels are in parallel, but reliability-wise, they are in series. A failure of any vessel component results in the train's complete failure. It is unlikely that a failure of this type results from biofouling, except if the train is operated at a pressure differential above 3.5 bar.

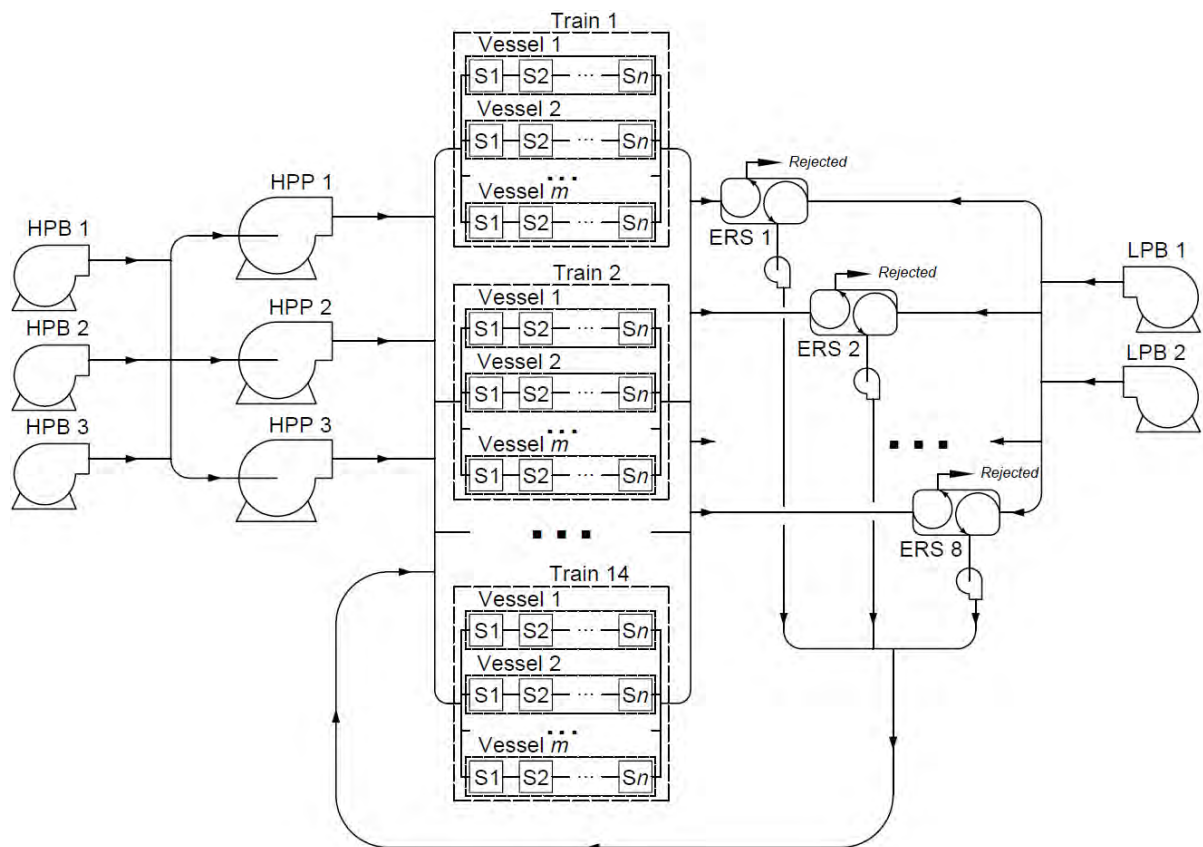


Figure 5-1. Multiple stacks (trains) of vessels in parallel with multiple membrane elements in series.

This chapter first concentrates on the basic multi-component system, the pressure vessel loaded with multiple membrane elements in series. Later on, the RO train as a multi-component unit and the RO system acting as a multi-component system is addressed. For now, we can state that it is essential to balance the wear of the vessels equally due to the

hydraulic process. Vessels with less wear have a higher permeate flux and therefore work harder. Due to the increased hydraulic load, the components of these vessels deteriorate faster, whereafter some time, an equilibrium of wear is reached between the vessels.

So, from the perspective of maintenance modelling theory, we can classify an RO vessel as a novel multi-component system. The fouling of an RO train, observed mainly as an increase of observed NPD (section 4.3 and 4.4), is approached as the *wear* of the components.

The maintenance literature distinguishes between three types of dependence. These are economic dependence, structural dependence and stochastic dependence (Dekker et al., 1997; Vu et al., 2015; Shi and Zeng, 2016; Olde Keizer et al., 2017; de Jonge and Scarf, 2020). In the early days, models for multi-component maintenance only considered one category of dependence since combining all categories would make the model too complicated (Dekker et al., 1997). Shi and Zeng (2016) argue that the components have both structurally and stochastic interdependence in complex largescale systems. Therefore, a model should not be limited to only a single dependence. This research considers all three categories of dependence, with the main emphasis on stochastic dependence.

The complexity is simplified by classifying the dependencies into two separate groups. In this research, the dependencies are classified as affecting deterioration and affecting maintenance. Camci (2009) refers to functional dependence instead of structural dependence. He describes functional dependence as causing other system components to stop due to the failure or maintenance of one of the components. In the presented RO vessel as a multi-component system, each component has a functional dependence from the other components. A component cannot be taken offline individually, and a failure of one component will result in the need to take offline the complete system. However, this thesis will not differentiate between functional and structural dependence since the structure does not allow a single component to be taken offline separately.

5.2 Dependencies affecting degeneration

Stochastic processes are generalizations of families of random variables. The interpretation of a stochastic process usually involves modelling a random characteristic of a system over time. Every stochastic process can be expressed as a function of the two variables, time (t) and the random variable κ : $X_t(\kappa)$ (Žitković, 2010).

Dependencies affecting degeneration are stochastic (Dekker et al., 1997; Gorjian et al., 2010). Jolly and Wreathall (1977), cited by Carfagno and Gibson (1980), distinguish between

internal or intrinsic causes and external or extrinsic causes of wear dependencies. Intrinsic wear dependence means that the state of a component affects the wear rate of other components (Dekker et al., 1997). If more than one dependency affects the degradation, we speak of multivariate dependencies.

Common mode degradation can be defined as dependencies due to a common mechanism, applying to both extrinsic and intrinsic wear dependencies. This type of failure is referred to as gradual failure, soft or degradation failure. An EO fails when the degradation reaches a specific failure threshold (Gorjian et al., 2010). The latter is called soft failure since the EO often can still be operated (Balali et al., 2020). The maintenance interventions in this case study intents to prevent reaching this threshold.

There is a distinct difference between common mode failures and random failures. Random failures have an utterly random probability. The failure cannot be detected by condition monitoring or measuring age. The EO fails without prior indication and is termed sudden or hard failure (Gorjian et al., 2010). The latter often apply to the classic “bathtub” curve of failure change over time. Unlike common-mode degradation, the classic bathtub curve does not consider extrinsic and intrinsic wear dependencies (Carfagno and Gibson, 1980).

As with age-related failure processes, the degradation of membrane elements in a vessel is both random and deterministic to some extent. If degradation was limited to a single RO train, in this case, we could define the wear process as random. However, since it co-occurs at all 14 trains, we speak of common-mode degradation.

According to Carfagno and Gibson (1980), dependencies of wear, common to components, can originate from several types of shared similarities. Carfagno and Gibson proposed the following classification of common failure mode types:

- i. Conceptual or engineering design error or inadequacy.
- ii. Manufacturing error; shortcoming or poor practice.
- iii. Testing or qualification error or omission.
- iv. Installation error, omission or lack of validation of proper installation.
- v. In-service ageing or deterioration due to environmental or operational stress.
- vi. Operational misuse.

In the case of this research, stochastic dependencies of wear of a component involve both extrinsic and intrinsic dependencies belonging to the class v. Besides the wear dependence, the effect of wear is further dependent on the structural dependence from a performance point of view. The latter was first introduced by Olde Keizer et al. (2017) and involved the

configuration of the components when the performance is not just the sum of wear of the individual units.

In the case of an RO pressure vessel, the vessel's performance is dependent on the position of the component with specific wear. The vessel's performance is worse if a component with high wear is positioned in the first socket rather than the last socket. The latter is an example of structural dependence from a performance point of view. In chapter 6.1, the structural performance dependence of components in an RO vessel is addressed from a hydraulic perspective.

However, although the effects of wear are improved in the short term by moving the component with high wear to the tail, the latter increases the intrinsic wear dependence. The intrinsic wear dependence is addressed in section 5.1.3.

5.2.1 Extrinsic and intrinsic wear

Olde Keizer et al. (2017) reviewed publications on stochastic dependencies. They classified stochastic dependencies as failure-induced damage, load-sharing and common-mode deterioration. Failure-induced damage involves one-time damage of a component if one or more other components fail. An example given was when a propeller of an aeroplane comes off and pierce the fuselage. Failure-induced damage in an SWRO train would occur following a sudden rapid depressurization due to an endcap blown off or the common header dislocating. Although this does happen in practice, this is not part of membrane degradation due to biofouling.

Load sharing involves the degradation of components, having to work harder due to failure or degradation of another component. The latter is defined as intrinsic wear, addressed under section 5.1.3 Rate-state interactions. Finally, common-mode or external shared deterioration is the dominant cause of degeneration due to biofouling in RO membranes.

Wear dependencies that result from external shared or common causes are referred to as extrinsic dependencies. Extrinsic dependencies originate from shared physical or environmental stresses (Zhou et al., 2020). Although extrinsic dependencies like oxidants can result in chemical degeneration of seawater RO membranes (Sandin et al., 2012), such dependencies are strongly related to operational decisions. On the other hand, physical stress, like telescoping, can be a direct result of environmental stress (Bristow et al., 2020). This research concentrate on extrinsic environmental dependencies, i.e., biofouling amplified by seasonal algae blooms. As has been highlighted in the literature reviewed in chapter 4, these extrinsic dependencies are difficult to mitigate.

Observing the degradation during the first 500 days after the plant was taken into operation will give the impression that the degradation is non-monotonic (Figure 5-2). However, when a train is taken offline for some days, the membranes are flushed with permeate, i.e., low salinity. The reason to perform a low salinity flushing is to replace seawater with permeate water to preserve the membranes and keep them hydrated. Low salinity flushing can be considered a hydraulic physical cleaning method whereby flushing water through the membranes in a forward direction remove unintentionally part of the accumulated biomass and organic foulants. The partially removed biomass provides short-term restoration of the lead element. However, it can cause further biofouling as the removed biomass are pushed downstream, where they form nearly instantly new biofilms (Bucs et al., 2018).

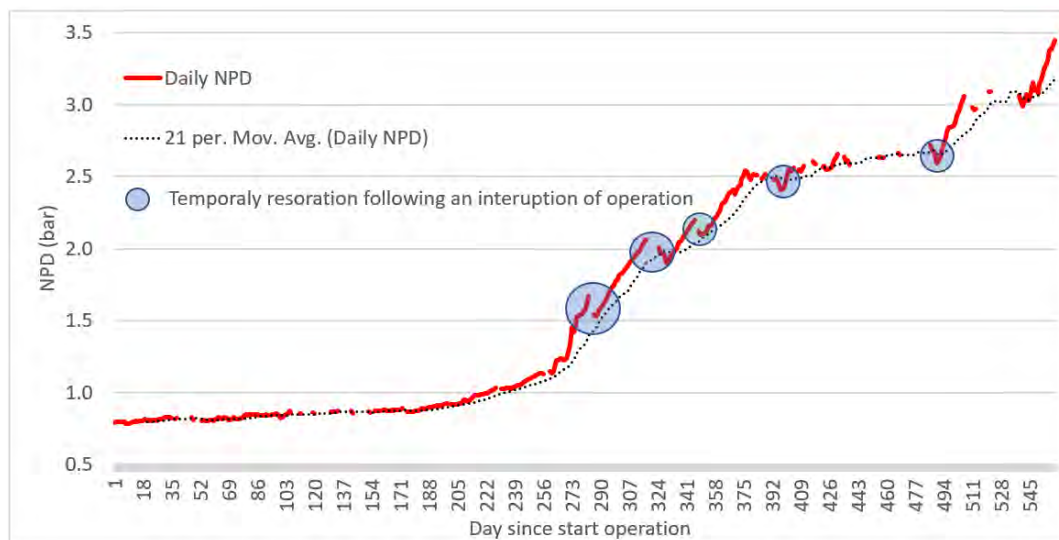


Figure 5-2. Train 8: Observation of limited restoration following an interruption of operation due to low salinity flushing after stopping the train.

Thus, the small restorations following a low salinity flushing can be considered a mechanical cleaning, whereby parts of the matured biofilm can be sheared off from the most fouled elements. However, low salinity flushing is intended to preserve the elements and is not a conscious maintenance intervention. Further, as described earlier, the effects of restoration are short-lived and result in spreading the biofilm to the elements downstream. The deterioration is a stochastic process with independent non-negative increments, also known as a gamma process (van Noortwijk, 2009; Balali et al., 2020).

According to Ben-Daya et al. (2016), there are two categories of failure mechanisms: overstress and wear-out. Overstress means that the stress which is subjected to an engineered object (EO) exceeds its maximum strength. If the stress is below the strength threshold, no permanent damage occurs. In case of wear-out, stress causes damage that usually irreversible

cumulates until the EO is weakened to a threshold above its endurance limit and subsequently breaks. Typical examples of wear-out stress are material loss due to friction and corrosion. As mentioned earlier, these are typically gamma processes. Examples are the erosion of the height of dikes due to crest-level decline, the thickness of steel coating and car brake pads (van Noortwijk, 2009).

This research adds an additional degradation category, the buildup of foulants as an obstruction. The latter is a known phenomenon in pipes and heat exchangers. Biological growth, mineral scaling or heavy organic precipitation reduces the effective diameter limiting flow and sometimes blocks the pipe or tubes and shells in case of a heat exchanger (Mansoori, 2001; Hoang et al., 2007; Nebot et al., 2007).

In the case of this research, the space to transport seawater along the high salinity side of the membrane is blocked due to biofilm growth at the membrane surface and the feedwater spacers (see Figure 5-3 and Figure 4-3 spiral-wound element construction). As a result, the hydraulic pressure loss increases. The individual components do not necessarily reach the point of failure, even after severe fouling. However, when cascaded, the sum of the differential pressure exceeding the threshold could result in unrecoverable failure of the individual components. So, in this case, failure occurs due to stress but not due to applying additional force. Further, the sum of the differential pressure depends on the position of the components. Section 6.1 will provide the theoretical reasoning of the latter.

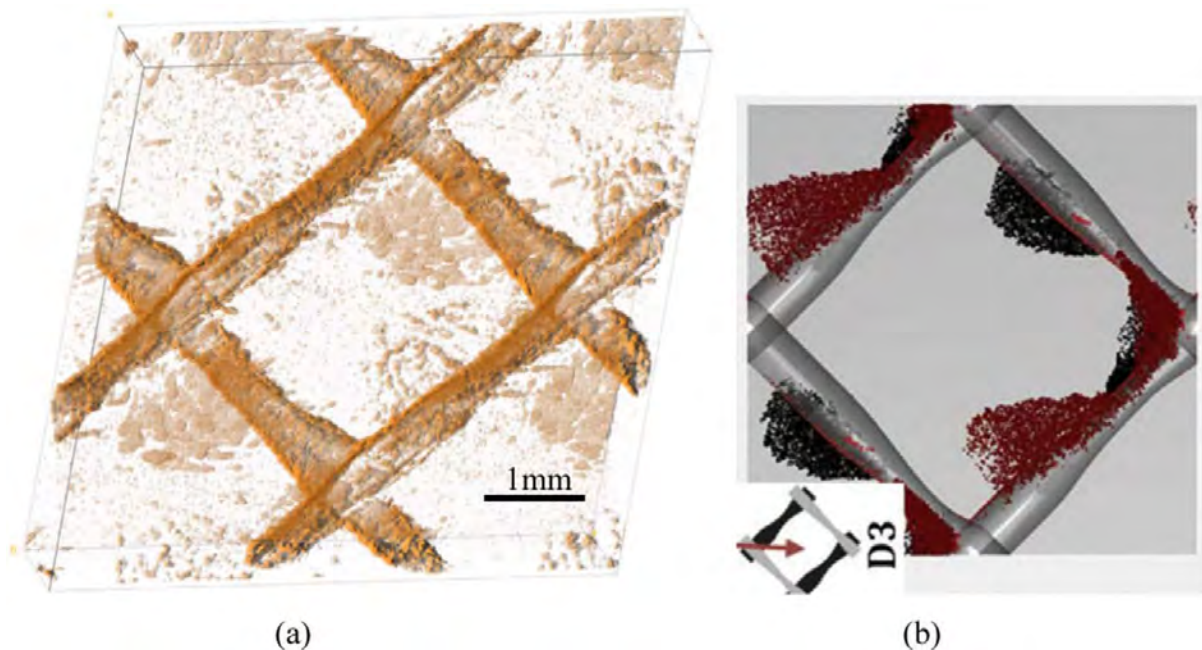


Figure 5-3. (a) Three-dimensional Optical Coherence Tomography image with biomass (brown colour), feed spacer, membrane. (b) Three-dimensional simulation of particle deposition on top (red) and bottom (black) membranes in a spacer-filled feed channel. Source Bucs et al. (2018).

The literature on biofouling accelerated by algae blooms, reviewed in section 4.2, describes that the surface is conditioned by organic fouling. This surface conditioning only occurs in the initial state when the element is new. Following an algal bloom, the organic macromolecules from AOM and TEP amplify these conditions. After biofilm-producing bacteria have colonized the surface, the membrane surface is irreversibly changed. Organic macromolecules no longer condition the surface of the membrane elements but now provide nutrients for bacteria.

Since the initial stage of surface conditioning of a new element is difficult to quantify and in the case of increased AOM and TEP concentration of the feedwater during increased algae abundance, this process is assumed to be instant. This research acknowledges that surface conditioning is a necessary first step, the surface conditioning is also inevitable. The latter is therefore not taken into account in the degradation model.

Thus, the extrinsic or common-cause wear dependency in this research is the feed water condition, supplying nutrients. The extrinsic wear dependency is specifically the concentration of NOM in general and the organic macromolecules from AOM and TEP. Therefore, the degeneration continues to occur post-bloom.

The changes in nutrients are random and can be defined as a Markov process (Kim et al., 2020). Markov processes are widely used in engineering, science, and business modelling. They are used to model systems that have limited memory of their past (Ibe, 2014). The annual nutrient load, as observed over the previous five years (see chapter 6, section 6.2.3), follow a reoccurring pattern with a typical Weibull right-skewed distribution. As described in chapter 4.4.3, the extrinsic dependence is seasonally influenced due to algae blooms. The annual start of an algae bloom, intensity and duration can be considered a Weibull distribution. Section 6.2.3 provides the reasoning for the Weibull characteristic of the extrinsic dependence data.

Biofouling causing degeneration of an EO can have various forms, from bacterial-influenced corrosion in the form of stainless steel pitting (Brenna et al., 2014; Adumene et al., 2020) to barnacle settlement (Ip et al., 2021). Figure 5-4 is an illustration of the latter. Most models involving degradation due to ageing or, in particular, degradation due to biofouling are based on a Markov process, applying Markov chains, Poisson, Petri nets and Bayesian networks (Carfagno and Gibson, 1980; Adumene et al., 2020). Despite the randomness of the feedwater quality, and although biological processes, like biofilm growth, are typically random to a degree, the wear process is gradual and monotone, following a gamma process (van Noortwijk, 2009). Thus, this research considers the extrinsic dependence

a stochastic continuous-time Markov process, but the associated wear, a gamma process, is modelled deterministically.

After the wear increase model has been determined, we can then derive the feedwater quality parameter from the history between maintenance interventions, i.e., cleaning activities and permutations of the components. Statistical methods, i.e., Weibull distribution or bootstrapping, can then be applied to project future feedwater conditions.



Figure 5-4. Biofouling at a 15.5 thousand m³/h submersible Brine dilution pump at CDP after one year of operation. Left: Pump body covered by mussels and barnacles. Middle: Pump discharge covered with barnacles. Right: Close-up of attached barnacles.

5.2.2 A multi-component system with non-identical components

Multi-component systems with non-identical components consist of a system with several assets or an asset constructed out of unidentical components. An example of the first category is the assembly platform Iung et al. (2016) referred to, consisting of a conveyor, a pallet loading station, assembly stations, and a pallet unloading station. The assembly workstations consisted of pneumatic jacks and a pneumatic suction cup. Laggoune et al. (2010) give an example of the second category, a centrifugal compressor. The multi-stage compressor in that research is driven by a steam turbine consisting of a stator, i.e., diaphragms, landings, tightness subsystem and the rotor, consisting of components such as shaft, wheels, equilibrium piston. An example of multi-component systems with identical components has been presented by Scarf and Cavalcante (2010). Scarf and Cavalcante considered an 8-identical component series system consisting of bearings while disregarding other non-

identical components. Assaf et al. (2018) considered a lab bench gearbox consisting of three identical gears.

This research considers a multi-component system of an 8-component series system, a RO pressure vessel with eight elements. When the system is new, all components are new. Thus, the vessel can initially be considered a multi-component system with identical components. Scarf and Cavalcante did not consider interactions between components and considered the components' wear to be stochastic. Although systems consisting of a known number of identical components are standard in the industry, military, and medical sectors, these systems often operate separately, according to Zhang and Zeng (2017). Thus, there is no stochastic dependence among the components in those cases.

The presented multi-component system in this thesis differs from the systems referred to by Zhang and Zeng (2017) and that presented by Scarf and Cavalcante. The presented multi-component system in this research comprises cascaded components in vessels. The vessels are further interconnected in parallel in stacks (a train). Therefore, in the case of this multi-component system, interactions between components exist. The interactions between components are addressed in the next section, 5.2.3 Rate-state interactions.



Figure 5-5. Pressure vessels connected in parallel in CDP. Courtesy WaterWorld 2018.

Biofouling tends to degrade membranes at the lead side faster than membranes at the tail side by the process of attachment, growth and disperse of the bacteria (see section 4.2). Thus,

the wear rate varies with position in a vessel. Although a new vessel is a multi-component system with identical components, the vessel can be considered a multi-component system with non-identical components (Nicolai and Dekker, 2008) as soon it is taken into operation.

The multi-component system of this research differs further from that referred to in the maintenance modelling research. The RO vessel is not a k-out-of-n system with non-identical components (Sharma and Govindaraju, 2020). The components of the RO vessel does not have a discrete good-fail state. The wear increase of the components is continuous. Although the state of the multi-component system can be impaired, therefore, failed, that of the individual components does not necessarily have to fail. A train, impaired due to excessive PD due to significant wear of the lead component of the vessels, can be made operational by moving the most severe deteriorated components to the vessel's tail and pushing the other elements to the front. Permutations of bad components at a critical location to a less critical location at a multi-component system were proposed by Najem and Coolen (2018).

5.2.3 Rate-state interactions

The rate of wear also depends on intrinsic wear conditions. The intrinsic wear of a membrane element depends on the state (level of wear) of the others, particularly the trailing elements. This dependence is because clean elements tend to have a higher flux when trailed by fouled elements. Colloidal fouling of RO membranes is a function of permeate flux and the extrinsic water quality. Under deteriorating feedwater conditions, higher flux accelerates fouling more than under low flux (Singh, 2014).

When replacing the lead element, the new element is therefore always inserted further down in the direction of the tail. Thus, there is stochastic dependence between components in the system in which the rate of wear of one depends on the state of the others. The quantification of interactions of components in the degradation of the multi-element system is the so-called rate-state wear-dependence (Bian and Gebraeel, 2014; Iung et al., 2016; Assaf et al., 2018; Do et al., 2019). Rate-state interaction parameters are estimated using actual data on vessel performance.

A further novel aspect of the multi-component system is that the individual components' degradation states (wear) are hidden (unobservable). In most systems involving condition-based maintenance (CBM), each component has its dedicated sensors, and the extrinsic and the component health can be individually monitored from the sensor data (Camci, 2009). In an RO vessel, the components are hidden, and only the combined health state of the multi-component system can be observed.

Nonetheless, the model presented in chapter 6 can estimate the individual components' deterioration state and quantify the effect (on performance) of components replacements and swaps. The details of these innovations are further presented in chapter 6. Although this research focuses on biofouling, the presented model is not limited to this and potentially can be used in cases of mineral scaling.

Commonly in CBM, maintenance performance optimization involves the prognostics of the Remaining Useful Life (RUL) before undertaking the maintenance (Camci, 2009). Thus, in RO membrane maintenance practices, the standard is to perform maintenance if the normalized RO performance parameters have passed the recommended threshold (see chapter 2.2 Establishing the baseline). The difference in the presented research is that this research aims not to project when to undertake the following maintenance but what the cumulation of maintenance practices, i.e., which policy, will be the most effective.

Shi and Zeng (2016) presented an RUL model by applying statistical analysis to condition data. Their motivation was that a purely statistical analysis approach fitting the available data under probabilistic and mathematical properties would not require relying on physics or engineering principles. However, as mentioned earlier, the sensor data only provides an overall presentation of the degradation in this case. The individual degradation of the components can not directly be interpreted from the sensor data. Therefore the presented model in this research does require applied physics and engineering know-how.

5.2.4 Degradation models

Degradation modelling is the core activity in reliability engineering. Many degradation models have been developed to predict the current state of degradation of an EO. Since degradation is a kind of stochastic phenomenon, this process can be modelled in multiple ways. Commonly, an EO degrades due to ageing or specific degradation dependencies, also termed covariates. In normal degradation models, a distinction is made between models that involve and do not involve stress. Degradation processes that do not involve stress are entirely random. A popular method to model random degradation involves the Wiener Process model. A Wiener process model is a stochastic process that randomly projects the degradation based on shift and drift parameters of a Brownian motion (Balali et al., 2020).

This research refers to stress factors as degradation dependencies. Previously, extrinsic and intrinsic degradation dependencies were defined. Therefore the presented model in this research involves stress factors (Gorjian et al., 2010). The dependencies affecting the EO's degradation addressed in this research are covered in the above sections.

Gorjian et al. (2010) classified degradation models in various groups. The classification is based on the prognostic approaches of degradation. The four main groups are experienced-based, model-based, knowledge-based and data-driven approaches. From these groups, model-based and data-driven approaches involve performance data for reliability assessment.

The simplest form of fault prognosis is experienced-based, requiring less detailed information than other approaches. The Weibull distribution is the most popular approach among the traditional experienced-based models. These models only require historical repair and failure data.

The traditional knowledge-based approach is based on human specialism and is, therefore, qualitative. A knowledge-based approach can be used as a prognostics level in combining other quantitative approaches, like data-driven approaches. The latter is the approach for condition-based maintenance of centrifugal pumps applied by the maintenance practitioner in this case study (see also Chapter 9.2). However, knowledge-based approaches are automated using expert and fuzzy logic systems. Like expert systems, the physical model approach in this research is limited to the current knowledge base of degradation. Nevertheless, unlike expert systems, the presented model is not the primary automation of human expertise.

Recently, expert systems have undergone increased competition from artificial intelligence (AI). AI is a data-driven approach based on learning techniques involving pattern recognition. Typically AI uses Artificial Neural networks (ANN) and Hidden Markov Models (HMM) (Gorjian et al., 2010). The arrival of the Industrial Internet of things (IIoT) has increased data availability. Increased data availability is one of the conditions that have made AI possible (Balali et al., 2020; Zonta et al., 2020).

Model-based approaches use mathematical modelling based on physical laws or statistical methods. A typical example of a physics-based model is the initiation and propagation of cracks and other anomalies in an aircraft. Statistical models are developed from collected input and output data, and then a Bayesian posterior Probability density function (PDF) is applied (Gorjian et al., 2010).

Most data collected by conventional DCS and PLCs are sensor data, such as pressures, flows and vibrations. IIoT provides additional data. However, nor sensor data nor data from IIoT provides direct information on the failure. As long as the failure mechanism is understood, the underlying degradation process can be visualised before the actual failure occurs (Balali et al., 2020). Thus, this data needs to be interpreted. Interpretation can be made by a mathematical model derived from expertise knowledge or by recognising patterns in the case of AI.

The model presented in this research is data-driven in combination with engineering expertise. The mathematical model is based on engineering expertise, while the parameters for the model are data-driven. The advantage of this approach against AI is that the latter would need a much larger set of data for training. Nevertheless, in cases where the physics of a system are well known, mathematical equations can model the degradation (Balali et al., 2020).

This research concentrate on a biochemical-physical model-based approach. As illustrated in this chapter, engineering know-how of the specific degradation processes is used to formulate mathematical equations describing the extrinsic degeneration process due to biofouling with the intrinsic rate-state dependence. Thus, a deterioration function is developed and applied in this research instead of a model based on a purely stochastic process (van Noortwijk, 2009).

5.2.5 Economic dependence from operational performance

Similar to structural dependence from technical and operational performance, we also can consider economic dependence from operational performance. According to Bereschenko et al. (2010), Matin et al. (2011), Jiang et al. (2017) and Jafari et al. (2021), membrane fouling increases specific power consumption (SPC). In this case study, an investigation has been conducted to see if increased NPD of the combined trains results in increased SPC. In the study by Jafari et al. (2021), increased SPC was the second fouling cost factor. Although between January 2017 and September 2019, a substantial variation in the average NPD can be observed, the SPC is almost constant, as shown in Figure 5-6.

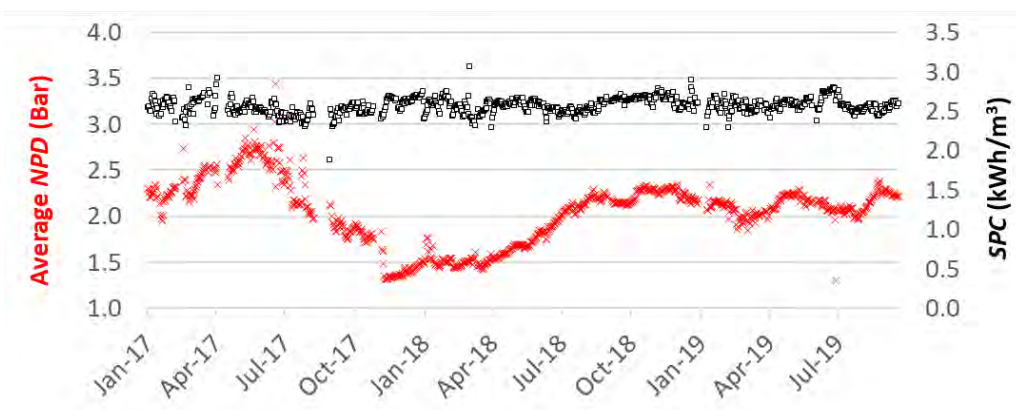


Figure 5-6. Average NPD vs the SPC (intake and product pumps excluded).

The small fluctuations in SPC do not correlate with the significant changes of NPD due to the wear and maintenance restoration activities. The increase in NPD is insignificant for power consumption. No correlation between differential pressure and specific power consumption

can be noted. Jafari et al. (2021) investigated brackish water RO, where increased NPD has a higher impact in relation to the feed pressure. The feed pressure at brackish water RO is approximately a tenth of that of SWRO, despite the differential pressures being equal. Adding the SPC costs due to the NPD increase would slightly increase the model complexity. This cost is an operational cost increase due to wear, and the reduction should be subtracted from the maintenance cost. The latter requires data to model the relationship, which would benefit brackish water RO. In SWRO, however, there is no incentive for restoration for the purpose of lowering power consumption. Thus, in the presented model, the impact on SPC is ignored.

5.3 Management of restoration

Turning now to the management of restoration, the state of the vessel can be improved by various methods. Dependencies affecting maintenance are economic dependencies and structural dependencies from a technical point of view (Olde Keizer et al., 2017). Typical economic dependencies are fixed setup costs to perform maintenance (Scarf and Deara, 2003). This research refers to structural dependencies from a technical point of view when other components have to be removed before the component being maintained can be accessed.

The improvement of the state of a vessel is hereby called restoration. Restorations are typically partial restorations (Pham and Wang, 1996). A vessel can be partially restored by various methods.

- (i) Cleaning is maintenance whereby biomass is partially removed from all elements (without removing an element from a vessel). For example, two cleaning methods were used for the trains in Figure 4-7. The first (C1) is a standard cleaning method that uses high pH cleaning followed by low pH cleaning. The second (C2) first soaks the elements with sodium bisulphate and then follows C1 (see also section 4.4.2).
- (ii) Cascading is a permutation that involves a combination of partial replacement and component reallocation (Fu et al., 2019) that focuses on the replacement of elements with the most accumulated biomass. Here, typically, the membrane element in the leading socket (S1) is replaced by the element in the second socket (S2), that in S2 by that in S3, and so on, and a new element is placed in S8. In general, r elements can be replaced, and $8-r$ cascaded.

- (iii) Swapping is another permutation that involves component-reallocation intervention that partially restores a vessel. Elements in leading sockets are systematically swapped with elements in trailing sockets, and no new elements are used.

5.3.1 Structural dependence

Structural dependence from a technical perspective entails the physical, static relationship between different components. Structural dependence implies that replacing a component requires removing or replacing other components (Dekker et al., 1997; Nicolai and Dekker, 2008; Olde Keizer et al., 2017; de Jong and Scarf, 2020).

Nguyen et al. (2015) present a model involving technical, structural dependence based on a fictive complex Reliability block diagram of a 14-component system. Zhou et al. (2015) present a fictive multi-component machine tool model. Do et al. (2019) demonstrate a lab experiment of a gearbox system consisting of two interacting gears. The presented case study is unique since it involves an actual production facility with both technical-structured dependence and structurally dependence from a performance view (see Figure 5-1).

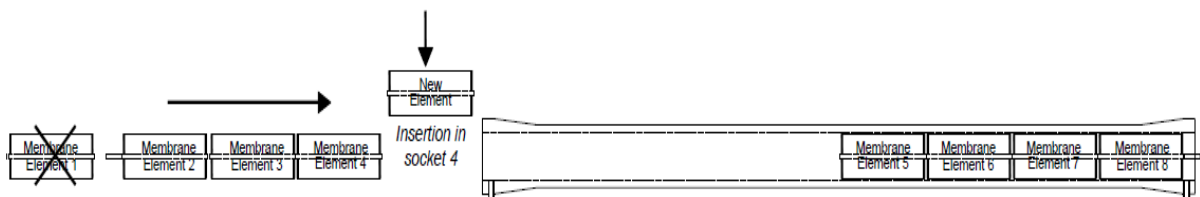


Figure 5-7. Membrane permutation. The first element is discharged, and the new element is inserted at socket 4. Elements 2, 3 and 4 need to be removed before the new element can be inserted.

With membrane interventions, elements are always inserted from the lead to the tail side of the vessel to prevent displacement or damage to the O-rings of the element permeate interconnectors. So, when an element in S_n is removed, elements from S_1 to S_{n-1} must be removed. The latter is structural dependence seen from a technical point of view (Geng et al., 2015; Dao and Zuo, 2017), while the positional dependence, discussed previously, is structural-performance dependence (Olde Keizer et al., 2017).

Figure 5-8 shows all components of a RO vessel. Each element contains a brine seal at the front end of the element in the form of a flexible o-ring. The function of this brine seal is to prevent feedwater from bypassing the element. Shortcircuiting of the feedwater means less water flows through the element, resulting in a high recovery per element. The permeate tubes of the elements are interconnected through a permeate connector, whereby the permeate tubes of all the elements form a common permeate tube. The permeate tubes of the feed of the first element and the rear of the last element are connected to the vessel permeate outlets

utilizing end adapters. The head or end cap seals the vessel. The end caps are kept in place with a retaining ring. A thrust cone is installed at the rear of the vessel to absorb the pressure (Wilf, 2015).

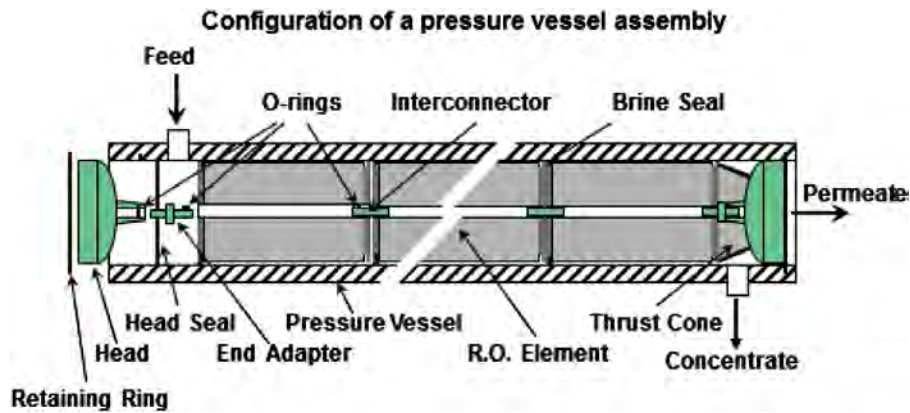


Figure 5-8. Components of a RO vessel. Source: Wilf (2015)

Vessel opening is required before the elements can be accessed for permutations. Due to corrosion and salt settlement at the end cap, it is sometimes challenging to remove it. Permutations are equally performed at each vessel of the train. Therefore 128 end-caps need to be removed before the actual membrane permutations occur. If only the first four elements need to be accessed, only the front of the vessel needs to be opened. However, if cascading involves all the elements, the vessel needs to be opened on both sides. Due to a lower frequency of opening of the rear end-caps, combined with higher levels of corrosion and settlements, the opening of the vessel's rear is the most challenging.

Membrane permutation requires expertise, e.g., to prevent O-rings slippage and shimming to prevent movement of the elements during vessel pressurisation. However, due to the level of expertise by the maintenance crew, the impact of disassembly and assembly operations on the deterioration of the components, as considered by Dinh et al. (2020), can be ignored.

5.3.2 Economic dependence

Permutations are membrane interventions with a fixed set-up cost (vessel opening). These fixed setups cost double when permutations involve elements at the front and tail sides. It is often economical to perform maintenance in groups, so set-up costs need to be considered only once (Scarf and Dears, 2003). It is considered unpractically not to perform all the train vessels simultaneously in this case.

Nevertheless, economic dependence might be less noticeable when scheduling permutations for all trains. However, fixed set-up costs can be minimised when permutations of trains are planned in a continuous sequence. If an external workforce needs to be hired and

trained (Olde Keizer et al., 2017), as happens in this case study, the training only has to be performed once. Also, as the workforce gets more experienced after the first few trains, this would speed up the job and reduce the overall maintenance time. Multiple trains involving multiple vessels have all the same components. Maintenance procedures, preparations, techniques and maintenance equipment are all identical and need to be prepared only once. Further, spare parts inventory can be procured in bulk (Zhang and Zeng, 2017), reducing the shipping cost and can be an incentive for lower cost of the parts. So, the RO plant as a system exhibits economic dependence.

Economic dependence can be negative or positive (Vu et al., 2015; Olde Keizer et al., 2017). Performing membrane maintenance of all the vessels simultaneously at a train, whereby the interventions occur in one sequence train after train, is considered positive economic dependence. The same hired workforce can continue to do the job without replacing each time the crew and train them all over again. However, performing the maintenance simultaneously at all trains would result in negative economic dependence due to production losses. No economic losses result from taking one train offline when permutations are planned during the winter months when the demand for production is lower.

5.3.3 Block replacement

Scarf and Deara (2003) considered block replacement policies for a two-component system, having the components in series. Their block replacement policy is considered a perfect restoration or complete restoration. Complete restoration, in theory, is the replacement of all n elements in a vessel by new elements. The latter should only be considered if this results in an economic benefit or is dictated by human safety.

However, in the case of an RO plant, complete restoration is prohibitively expensive since it cannot be limited to a single vessel because the states of the vessels must be balanced. When vessels operate parallel with different states, a vessel with minor wear has a higher flux than other more worn vessels. It so degenerates faster (see also section 5.2.3 Rate-state interactions). This accelerated wear then brings the vessel to the same state as the other vessels over time. The latter is also the case when operating trains in parallel in a pressure centre configuration (multiple trains sharing the same pump), as is the case at the Carlsbad plant. Therefore trains are managed collectively whereby trains are operated and maintained to keep both the flux and the state of the trains balanced.

An example was Train 5. The Train was since mid-2017 out of operation due to a construction failure. Failure-induced damage to the membranes occurred following a sudden

rapid depressurization after the common header dislocated (see also chapter 5.2.1 first paragraph). All membranes were disposed of, and the insurance covered the cost. Following the repair of the train at the beginning of 2019, the membranes of Train 10 were shared with train 5. Both trains received new membranes for the remaining membranes. Although both trains had half new elements, the NPD were similar to that of the other trains due to performed permutations.

Nonetheless, some differentiation between trains is unavoidable. This unavoidability is because trains must be taken offline for maintenance or due to demand reduction. Note: when a train is offline for several days, it is flushed with permeate water, which has low salinity (LS). As described in chapter 5.11, an LS flushing can be considered an ineffective mechanical cleaning. Further, biofouling is temporally slowed down since the nutrient-rich seawater is displaced with nutrient-poor LS water. As mentioned before, for this reason, the effect of LS flushing in the presented model is ignored.

Thus, the permutations and cleanings are identically for all vessels of a train. However, between trains, there are some differences in operation and maintenance. Thus, in the model, we assume that the states of vessels in the same train are identical, but trains are not. Therefore, the model we build considers a single, idealized vessel in a train.

Dekker and Smeitink (1991) developed an opportunity-based block replacement applied in the Royal Shell's process industry. In contrast to the discrete industry, performing maintenance may cause problems in the process industry because the equipment is required continuously. Dekker and Smeitink considered thereby the long-term cost. Reflecting this methodology on a RO vessel, replacing additional elements than the lead element will not make much of a difference in the short term but could increase the length of time between permutations and reduce the rate of membrane replacements. On the other hand, it could not make much of a difference in the need for maintenance interventions and unnecessarily increased membrane replacement rate. The DSS presented in this research allows testing these options. Opportunistic replacement of several components per vessel simultaneously will be tested against other policies involving only the most deteriorated element. The reader should be aware that this research considers a niche industry, and other industries require a different approach.

5.4 Summary

A simplified description of a reverse-osmosis (RO) vessel is a container that holds multiple components, RO membrane elements, in series. Therefore from the perspective of

maintenance theory, an RO vessel can be seen as a multi-component system. Although some RO plants have a hybrid configuration, whereby a vessel contains a combination of different element types, in this case, the vessels contain eight elements of an identical type.

The maintenance theory framework applied to this research is outlined in the maintenance principles and sub-principles in Chapter 1.2. Level 2, Principles of planned maintenance, defined that maintenance should use knowledge of both degradation and the effects of restoration. Level 4, Principles for the design of a decision support system (DSS), stated that a DSS should monitor degradation or the indicators of degradation. This chapter went into more detail about the specific degradation process, the indicators of degradation, e.g., extrinsic and intrinsic dependencies, and restoration management.

Multivariate dependencies are affecting the degradation. These dependencies are stochastic and are both intrinsic and extrinsic. Although the intrinsic and extrinsic dependencies are stochastic, these are common-mode degradations rather than random deterioration. Intrinsic dependencies are defined as rate-state interactions, and the degradation of the components is due to the load-sharing mechanism. Specifically, in this research, the degradation rate of a component depends on the state of wear of the succeeding components. The higher the wear of the succeeding components, to higher the load on the preceding components.

The extrinsic dependency is the load of nutrients in the RO feedwater. Algae blooms amplify the latter. Although seasonal waves of algae blooms are observed, the fundamental dynamic of these planktonic blooms has not yet been established. The change in nutrients can be considered a continuous-time Markov process.

The unique characteristics of this Markov process are also known as a gamma process. Both the intrinsic and extrinsic degradation process is monotonic with independent non-negative increments. Intentional and unintentional maintenance interventions can explain the negative increments over the degradation timeline.

There are different methods to model stochastic degradation processes. Although biological processes like biofilm formation are stochastic, deterministic rules are applied to determine the degradation. This research has opted for a model-based approach using mathematical modelling based on physical laws. The mathematical model is based on engineering know-how, while the parameters for the model are data-driven. Statistical methods, i.e., Weibull distribution or bootstrapping, are applied to project extrinsic feedwater conditions. The intrinsic degradation component has been considered fully deterministic.

Although the thesis author acknowledges the stochastic degradation process, this is a practical, workable solution.

There are various restoration methods. A partial restoration can be accomplished by removing the biofilm from all elements without removing the elements from the vessel. The latter is a clean-in-place (CIP). CIP is a partial restoration since the biofilm can not be entirely removed. Another restoration method is a permutation of the elements, whether or not discharging the most deteriorated elements and replacing them with new ones.

Permutations involve both structural and economic dependence. A vessel needs to be opened before the elements can be accessed. When relocating an element, at least some of the elements need to be removed. Economic dependencies involve fixed set-up costs and economics of scale. Economic gain can be achieved by planning the permutation interventions in an interruptible continuous sequence of one train after another. Fixed set-up cost involving vessel opening is of minor importance for a RO train. In this case, it is considered impractical not to perform all the train vessels simultaneously.

The DSS presented in this research allows testing the efficiency of opportunistic block replacement involving multiple renewals of degraded elements. In theory, complete restoration replaces all elements with new elements in a vessel and is prohibitively expensive since it cannot be limited to a single vessel. The states of the vessels must be balanced to prevent unbalanced load sharing. However, some differentiation between trains is unavoidable due to the need to take individual trains offline for maintenance and reduced demand for water. Thus, the model assumes that the states of vessels in the same train are identical, but trains are not.

6 Modelling degeneration and restoration of an RO vessel

The degeneration of the elements in an RO vessel has been presented in Chapter 4. That chapter provided the theoretical background of membrane degeneration due to biofouling in the presence of seasonal algae blooms. Chapter 5 presented the degradation processes from the perspective of maintenance theory. This research opts for a physical, mathematical model of degradation and restoration, while statistical methods estimate the model dependencies after reviewing the various methods of modelling the degradation.

In this chapter, the mathematical model is first outlined, involving the manifestation of the wear, that is, the pressure distribution over the individual components, the wear increments, and the membrane restoration. Then in the second part, the statistical methods are outlined for the model parameter estimation.

6.1 Mathematical model

Based on the novel multi-component characteristics described in chapter 5, a mathematical model is defined that provides a digital replica of the wear and the repair of the cascaded membrane elements in an RO vessel. Conceptually, a vessel has n sockets in series and in each socket is placed an element. It is convenient to define sockets and elements (components) in this way because the sockets are fixed while elements can be replaced or swapped. This conceptual notion of sockets and elements is standard terminology in maintenance modelling that was first articulated by Ascher and Feingold (1984).

The wear state of the element in socket i is continuous and at time t is $X_{i,t}$, and the (unobserved) pressure-differential across the socket i is $P_{i,t}$, $i = 1, \dots, n$. The pressure-differential across the vessel (and hence all parallel vessels in the train), which is observed, is given by

$$P_t = \sum_{i=1}^n P_{i,t}. \quad (4)$$

where n is the total number of elements in a vessel. When an element is new, the model supposes that its state is $X_0 = 1$, and $X_i \geq 1$ afterwards. When a vessel is new (all elements are new), its pressure-differential is P_0 .

Note that a reference is made to pressure differential (PD) when discussing this conceptual model. However, when discussing the reality, a reference shall be made to the normalized

pressure differential (NPD), which is the observed pressure differential after the pre-processing discussed in Chapter 3.3.2.

6.1.1 Modelling pressure distribution

The hydraulics of saline flow in an RO vessel (Figure 6-1) implies that the pressure-differential $P_{i,t}$ across socket i depends both on the state of the element in socket i and the position of the socket. Assuming

$$P_{i,t} = \omega_i P_0 X_{i,t}, \quad i = 1, \dots, n, \quad (5)$$

with ω_i a set of known (dimensionless) position constants such that $\sum_{i=1}^n \omega_i = 1$. This set of constants will be called the pressure distribution. This models pressure variation across the socket.

The variation ω_i arises broadly because the salinity of the feed at each element increases along the vessel. In simplified terms, a vessel has a feed/brine (saline) side and a permeate (drinking water) side. A vessel is a sequence of elements in series. Seawater is pumped into a vessel under high pressure and flows first into element one, then into element two and so on. Water passes through a membrane element provided there is a positive net driving pressure (NDP), i.e., the pressure on the feed-side (P_{feed} in Figure 6-1) is higher than the osmotic pressure (Π in Figure 6-1). The net driving pressure at element 1 is

$$P_{feed} - \frac{P_1}{2} - \Pi_1 - P_{permeate} \quad \text{and at element } i \quad (i = 2, \dots, n) \text{ is}$$

$$P_{feed} - \sum_{j=1}^{i-1} P_j - \frac{P_i}{2} - \Pi_i - P_{permeate}, \quad (6)$$

where Π_i is the osmotic pressure of the feed/brine side minus the osmotic pressure of the permeate side of the element.

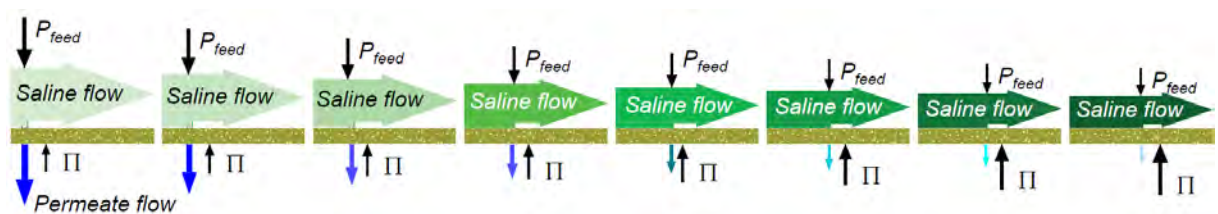


Figure 6-1: Hydraulic representation of an RO vessel with eight membrane elements. The stronger the shade of green, the stronger the salinity.

P_{feed} decreases from one socket to the next. This decrease is the pressure differential across a socket and is a function of the state of the membrane element in that socket. The osmotic

pressure is a function of the relative salinities of the feed and the permeate, noting that the permeate is not perfectly desaline. Thus, the osmotic pressure is that pressure difference across a perfect membrane such that water just starts to pass to the permeate side and salt is retained on the feed side. The higher the salinity, the higher is the osmotic pressure. As a membrane wears, that is, as it becomes biofouled, its pressure-differential increases. Now, assuming there is permeate flow, that is, the feed pressure is sufficiently high, as water flows on the feed-side from one element to the next. The salinity of the feed-side increases from one element to the next so that the osmotic pressure increases from one element to the next, and the permeate flow rate through each element correspondingly decreases. The permeate flow rate of an element depends on the difference between the feed-side pressure and the osmotic pressure.

Now, consider a vessel with a set of new elements. The saline flow per element can be defined as Q_i and the permeate flow per element as \bar{Q}_i . Recovery is defined as

$$R_i = \bar{Q}_i / Q_i. \quad (7)$$

An assumption is made that the recovery reduces proportionally with the increase of salinity of the feed. Furthermore, the salt rejection rate is 99.8% (see chapter 4.1.2). Therefore, the salinity of the feed for socket i relative to socket $i-1$ increases by the factor sR_{i-1} ($s = 0.998$), and so $R_i = R_{i-1} / \{1 + sR_{i-1}\}$ and so

$$R_i = R_1 / \{1 + (i-1)sR_1\}, \quad i = 2, \dots, n. \quad (8)$$

The system recovery is given by $R = \sum_{i=1}^n \bar{Q}_i / Q_1$, and since $Q_i = Q_{i-1}(1 - R_{i-1})$, the following can be derived

$$R = R_1 + \sum_{i=2}^n \left\{ \frac{R_1}{1 + (i-1)sR_1} \prod_{j=2}^i \frac{1 - (1 - (j-2)s)R_1}{1 + (j-2)sR_1} \right\}. \quad (9)$$

Because R is known (it is continuously monitored at train level), R_1 can be calculated numerically using Eq. (9), and the recoveries for each trailing element can then be obtained from Eq. (8). In this way, we obtain

$$\omega_i = R_i / \sum_{i=1}^n R_i, \quad i = 1, \dots, n, \quad \sum_{i=1}^n \omega_i = 1. \quad (10)$$

These constants represent the variation of PD across the sockets in an as-new vessel and correspond with the Darcy-Weisbach head-loss model that describes the relationship between

flow and pressure loss (Brkić, 2012): if the flow reduces, the pressure loss reduces. The constants ω_i do not depend on the states of the elements. The latter is a reasonable assumption for a typical vessel under normal operation, although it would not apply under unusual operating conditions, which themselves would jeopardize the integrity of a vessel.

6.1.2 Modelling wear increase

Time is for convenience discretised, and the day is used as the unit of time to model the evolution of the wear state of the element in socket i over time. The increment of wear in the element in socket i is denoted from day $t-1$ to day t by

$$\Delta X_{i,t} = X_{i,t} - X_{i,t-1}. \quad (11)$$

The wear increment of an element is being supposed to be given by

$$\Delta X_{i,t} = \kappa_t \alpha^{i-1} \left\{ \sum_{j=i+1}^n X_{j,t-1} / (n-i) \right\}^{R\gamma}, \quad (12)$$

for $i=1, \dots, n-1$, and

$$\Delta X_{n,t} = \kappa_t \alpha^{n-1}. \quad (13)$$

where

- κ_t is the extrinsic (common-cause) wear effect due to the feed water quality on day t . Notice that when all elements in the vessel are new (either when the plant is new or hypothetically when all the elements in the vessel are replaced), the wear increment in the element in socket 1 ($S1$) is precise κ_t because the other terms are equal to 1.
- $\alpha \in (0,1)$ quantifies the variation in biofouling along a vessel due to preferential attachment of bacteria, and hence the growth of biomass, to leading elements, as discussed in Section 4.4. This exponential decay is a specific way to model the biofouling-position effect with a single unknown parameter.
- $\left\{ \sum_{j=i+1}^n X_{j,t-1} / (n-i) \right\}^{R\gamma}$, with γ as a decay factor, models the wear in an element that accrues because the trailing elements, elements further along the vessel, are worn. This wear interaction is the multi-component rate-state effect as described in section 5.3. A vessel generally works harder when its recovery is higher, and so R here represents the operational extrinsic wear component. When the elements in trailing sockets are all new, this term is null. The latter is justified because the effect of varying recovery is

negligible when the vessel is as-new. Notice that when the system is not operating, $R = 0$, and so that $\Delta X_{i,t} = \kappa_t \alpha^{i-1}$.

When a train is offline, it is flushed daily with seawater (to prevent hydrating the elements). In this case, there is neither rate-state dependent wear nor operational extrinsic wear because the recovery is zero. Thus, the term $\{\sum_{j=i+1}^n X_{j,t-1} / (n-i)\}^{R\gamma}$ is unity when the train is offline, and the wear increment is limited to $\Delta X_{n,t} = \kappa_t \alpha^{n-1}$.

Returning to the feed water quality effect, κ_t , there are various ways to model the development of this parameter over time. The simplest supposes that feed water is either good ($\kappa_t = \kappa_1$) or bad (algal bloom is present) ($\kappa_t = \kappa_2$). After the finish of an algae bloom, we observe that the wear rate does not decrease abruptly but slowly decays. This slow decay is exponential due to the initial high availability of nutrients following an algal bloom and the exponential decline at the end (see section 4.2.3). So, when applying a Weibull distribution, the following is assumed. Before an algal bloom $\kappa_t = \kappa_1$ and after an algal bloom,

$$\kappa_t = (\kappa_2 - \kappa_1)e^{-\beta\tau}, \quad (14)$$

where β is the decay factor and τ the days since the finish of the algae bloom. In the case of bootstrapping, κ_t can be sampled with replacement from the historical dataset

6.1.3 Modelling membrane restoration

When the element in socket i is replaced by a new element at time t , it is supposed that $X_{i,t^+} = 1$, where t^+ denotes the time immediately following the restoration. During any restoration (which typically takes one to two weeks to complete for a train), the vessel is not operating, and element states are otherwise unchanged.

When the element in socket i is swapped with the element in socket j at time t , then immediately following restoration we have

$$X_{i,t^+} = X_{j,t^-}, \quad X_{j,t^+} = X_{i,t^-}, \quad (15)$$

where t^- denotes the time of operation immediately prior to the restoration. In this way, the model captures the state of an element in its socket.

Cleaning can be modelled in a number of ways. The thesis author supposes that the cleaning effect is proportional to the wear so that an element in a poorer state is cleaned to a

greater absolute extent. Thus, if a vessel is cleaned at time t , then the state of the cleaned element in socket i is given by $X_{i,t^+} = (1 - \delta)(X_{i,t^-} - 1) + 1 = (1 - \delta)X_{i,t^-} + \delta$, (16)

and the NPD across the vessel (overall) immediately following cleaning is

$$P_{t^+} = (1 - \delta)P_{t^-} + \delta P_0 \quad (17)$$

Thus, the cleaning effect is proportional to the excess NPD above P_0 . Here δ is the cleaning effect parameter. If $\delta = 0$, $P_{t^+} = P_{t^-}$, so cleaning has no effect. If $\delta = 1$, $P_{t^+} = P_0$, so cleaning is as good as a replacement of all elements in the vessel (like new). An absolute cleaning effect would be unnatural because, potentially, this could imply $P_{t^+} < P_0$.

6.2 Parameter estimation

Now that the mathematical model has been determined, the parameters must be estimated based on its goodness of fit, i.e., finding parameter values that best fit the model output with the observed data. Generally, there are two methods to find the goodness of fit, least-squares estimation (LSE) and maximum likelihood estimation (MLE). LSE is a popular choice in linear regression. The proportion of variance can be expressed in r^2 . Unlike MLE, LSE requires minimal distributional assumptions (Myung, 2003). However, the parameters of the model presented does not behave linearly.

The earlier presented degeneration model is continuous, and a first conservative estimate would assume a normal distribution, also called a Gaussian distribution. Gaussian distributions are the most well-known engineering, statistics, and physics assumptions. The Gaussian distribution can be applied in most situations due to the Central limit theorem (CLT), a probability theorem (Park et al., 2013). According to CLT, the sampling distribution of the sum or mean of size n is approximately normal for large samples of n observations from a population with finite mean and variance (Anderson, 2010). A Gaussian probability distribution can be applied to estimate unknown deterministic or random parameters (Park et al., 2013).

The presented mathematical models involve the following parameters:

- The variation of PD across the sockets, parameter ω , is directly derived from the recovery R by eq. (10). No other estimations are required.
- Biomass distribution parameter α .
- The severity parameter κ of the extrinsic feedwater quality.
- The decay of the severity of κ following the end of an Algae bloom, parameter β .

- The severity of the rate-state interactions, parameter γ . Note that the severity of the rate-state interactions also depends on R . However, the latter is known.
- The imperfect restoration following a cleaning, restoration parameter δ . There are two different cleaning methods, so δ must be estimated separately for C1 and C2.

Although parameters α , β and γ are stochastic to a degree, they are approached as deterministic in this research for practical reasons. The parameters are estimated once but separately per train. Parameters κ and δ are stochastic and varying constantly, both parameters following a Gaussian distribution and can be estimated by a probability distribution (Park et al., 2013). MLE can, in this case, find the goodness of fit and is widely applied in parameter estimation and inference in statistics. The MLE is explained by Myung (2003), where also MATLAB codes are given for MLE and LSE. We will return to the probability distribution of κ in sections 6.2.3 to 6.2.5 and δ in section 6.2.6. First, the deterministic parameters α , β and γ must be estimated.

6.2.1 Results wear parameters α

First, the biofouling-wear distribution parameter α (see Eq. 12) is estimated from the deterministic parameters. Once α is specified, the particle filter method (Kantas et al., 2015) can be utilized to estimate γ and β using a restricted set of values for κ_t .



Figure 6-2. Inspection of biomass accumulation at the elements by weighting.

Before estimating parameter α , we must inspect a random vessel per train, remove all elements and identify them in the same order as they were at their last location in the vessel. We estimate α per train. Sampling several or all vessels per train will give a better result, but the time required does not allow that. Selecting only one vessel during the start of membrane replacement is not time-consuming. The vessel must be opened regardless. So this is a reasonable compromise. We can revisit cases like train 8 with a poor fit by repeating the inspection during future membrane replacement interventions. Then, the elements are weighed individually to determine the element's accumulated biomass. The original weight of the elements is required to determine the biomass. However, this information is not available. As was mentioned in chapter 4.4.2, a new wet element is expected to weigh between 13.5 and 16 kg. So, we cannot use the weight of a new element instead. As a compromise, the biomass distribution is estimated as follows:

$$w_i = \frac{W_i - \min \{W_1, W_2, \dots, W_n\}}{\min \{W_1, W_2, \dots, W_n\}} \quad (18)$$

where W_i is the element's weight, and w_i is the proportional biomass. This assumption neglects any biomass build-up at the element with the lowest weight. Therefore an unknown factor should have been included. The error in the distribution of the biomass is, for this research, neglectable.

The parameter α is estimated by comparing the modelled wear distribution across individual elements with the measured distribution of biomass obtained at vessel inspections when a vessel is opened, and individual elements are weighed. This method is as follows. We fix $\gamma = 1$ (the effect of γ on the outcome of α is small, so it is being neglected). Eqs. (1-2, 8-9) imply that

$$\kappa_t = \frac{P_t - P_{t-1}}{P_0 \sum_{i=1}^n \alpha^{i-1} f(x, i)^{R\gamma} \omega_i}, \quad (19)$$

where,

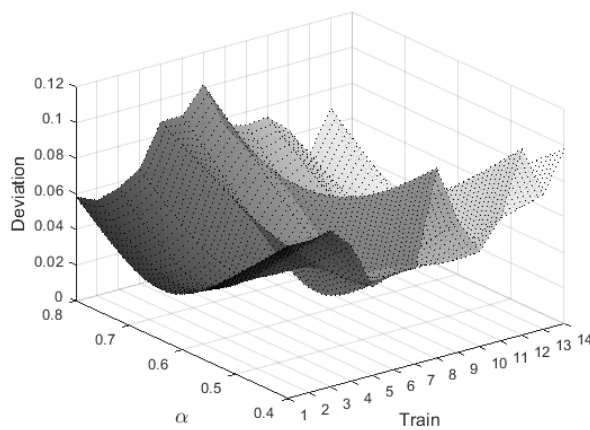
$$f(x, i) = \begin{cases} \frac{\sum_{j=i+1}^n X_{j,t-1}}{n-i} & i < n, \\ 1 & \text{else.} \end{cases}$$

Then, κ_t can be calculated recursively as follows. On day $t=1$, $X_{i,0} = 1$ (all elements are new), $P_1 - P_0$ is observed (this is the NPD increment), R is known, the constants ω_i are known, and α is specified (and $\gamma = 1$). Therefore, κ_1 can be calculated using Eq. (19) and

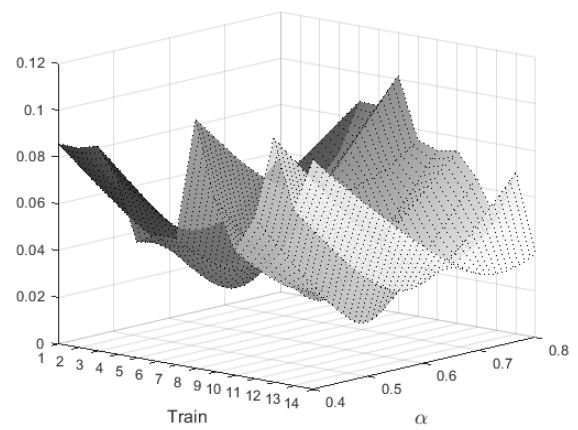
$X_{i,1}$ ($i = 1, \dots, n$) can be calculated using Eqs. (11, 12). Then, in turn, κ_2 can be calculated using $P_2 - P_1$ (observed) and the known $X_{i,1}$ ($i = 1, \dots, n$), and so on. When elements are swapped, Eq. (15) is used to update the wear-states. Then, on day τ when elements in a vessel are weighed, we know the weights w_i and the states $X_{i,\tau}$ of each element (Figure 6-4), and the deviation

$$\sum_{i=1}^n \left(\frac{X_{i,\tau}}{\bar{X}_\tau} - \frac{w_i}{\bar{w}} \right)^2, \tag{20}$$

can be calculated. The procedure is repeated for different values of α , and this researcher's estimate is the value of α that minimizes this deviation. Figure 6-3 (a) and (b) show a plot of various values of α and the resulting deviation from the inspected biomass distribution. Figure 6-3 (c) shows a surface plot of the deviation of all 14 trains. The numerical values per train for α are shown in Table 6-2. The fit between the biomass and modelled wear distribution is good overall, as shown in Figure 6-4. However, this is not always the case, like train 8. There are multiple reasons for this. First, the vessel inspected could have undergone additional maintenance, e.g., a failed element was replaced. Secondly, the model uses a deterministic equation for biomass distribution. In the real world, there is probably also a stochastic element.



(a)



(b)

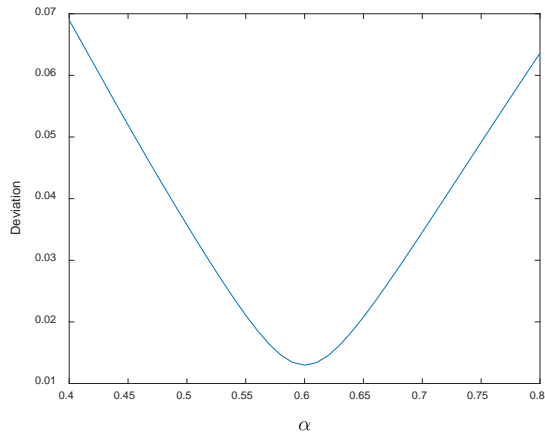


Figure 6-3, (a) and (b) Deviation from the measured distribution with α from 0.4 to 0.8 for all 14 trains. The surface plot is shown at different angles.

(c) Deviation from the measured distribution with α from 0.4 to 0.8 for train

(c) 11.

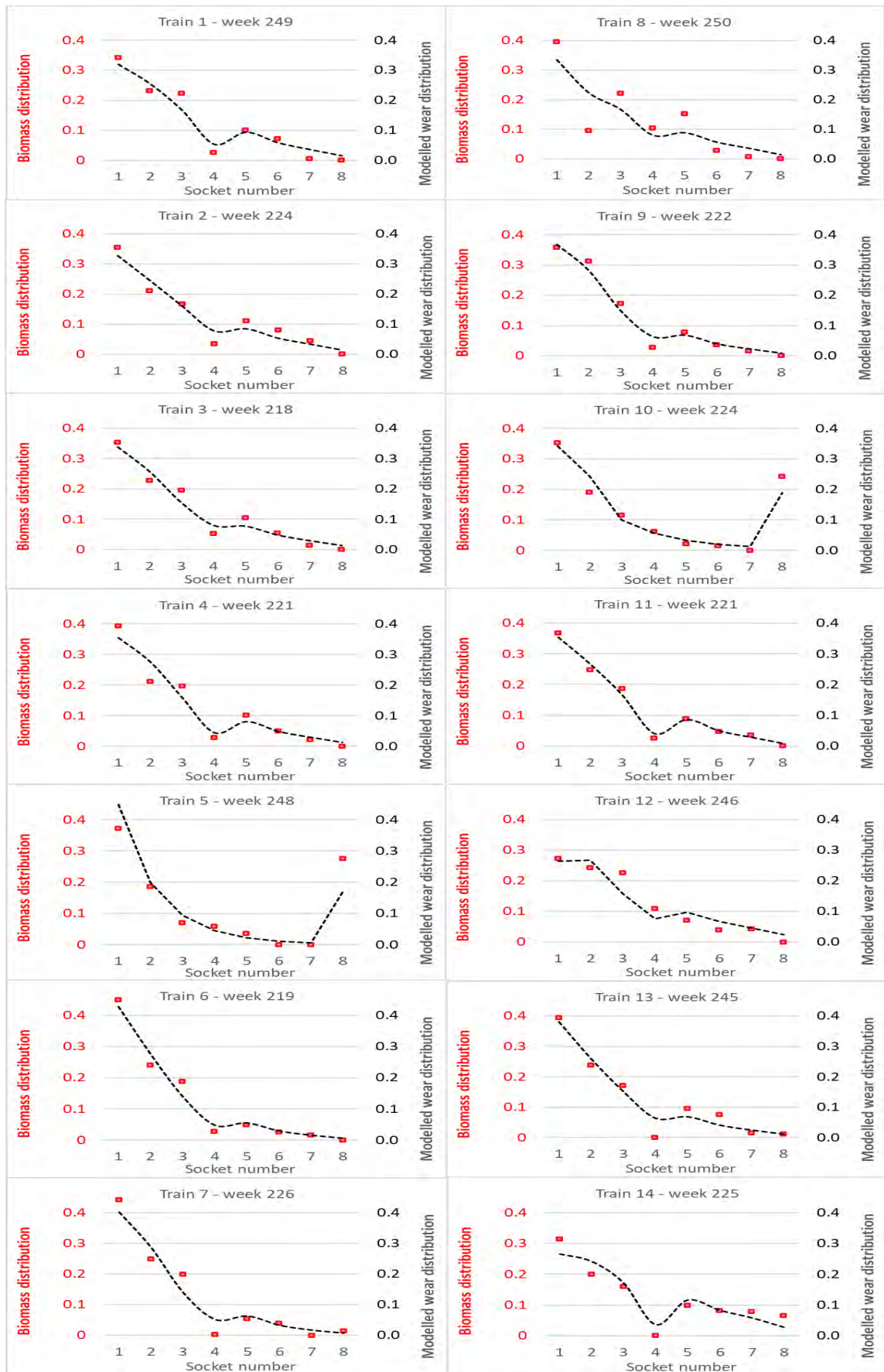


Figure 6-4: Relative element weights (▪) and relative modelled wear-states (---) for all trains (train number and time of weighing indicated with α at the best value for the specific train).

6.2.2 Results wear parameters β and γ

Next, the other parameters are estimated using the particle filter (Doucet et al., 2001; Candy, 2007; Kantas et al., 2015; Elfring et al., 2021). The primary purpose of Particle filtering (PF) in this research is to estimate parameters β and γ . Further, the mean value for κ before the first algae bloom occurred (κ_1) and the mean value for κ afterwards (κ_2). By establishing a κ_1 or κ_{low} for non-algae bloom conditions and a κ_2 or κ_{high} for algae bloom conditions, a probability distribution function can be applied for random values of κ with seasonal variation. The seasonal variation, thereby, is the algae blooms. The implementation is presented in the next section, as is an alternative method of probability given. Here we estimate only κ_1 or κ_{low} and κ_2 or κ_{high} .

PF has emerged as the most successful method for parameter estimation when confronted with nonlinear non-Gaussian state-space models. PF is suitable for parallel implementation, as is the case of this research, where we need to estimate four parameters. Further, PF is often more accurate than standard alternatives such as the Extended Kalman filter (Kantas et al., 2015). Widespread tutorial material and code examples are available, making PF easy to implement (Elfring et al., 2021).

A prevalent example of PF is the localization problem of domestic robots, like the type that vacuum the floors of a house, using a Lidar sensor to identify obstacles or walls.

Simplified the procedure of the PF estimation is as follows:

1. Take multiple samples (particles) from an original uniform distribution.
2. Weight the sampled particles against the observed data.
3. Discard the low-weight particles and resample with replacement of the high-weight particles. Then return to step 2.

The PF uses the Bayesian probability theorem for particle filtering (Candy, 2007; Elfring et al., 2021). In contrast to the robot example, where the particles can be directly weighed against the observed data, the PF estimations applied here are indirect. The particles represent the parameters and need to be applied to the mathematical model, whereby the weighting is based on the model output versus the observed NPD.

The implementation of FT is as follows, a function (Eqs. 2,5-9) that seeks to model the data (observed NPD) has been specified. Given the data, some parameter values are more probable than others, and this defines a probability distribution over the parameter space (the set of all possible values of the parameters). PF uses sequential simulation to approximate this distribution. Then, this distribution can then be used to determine the best estimate (e.g. the mean value of the parameter vector). Figure 6-5 presents the principle of implementation.

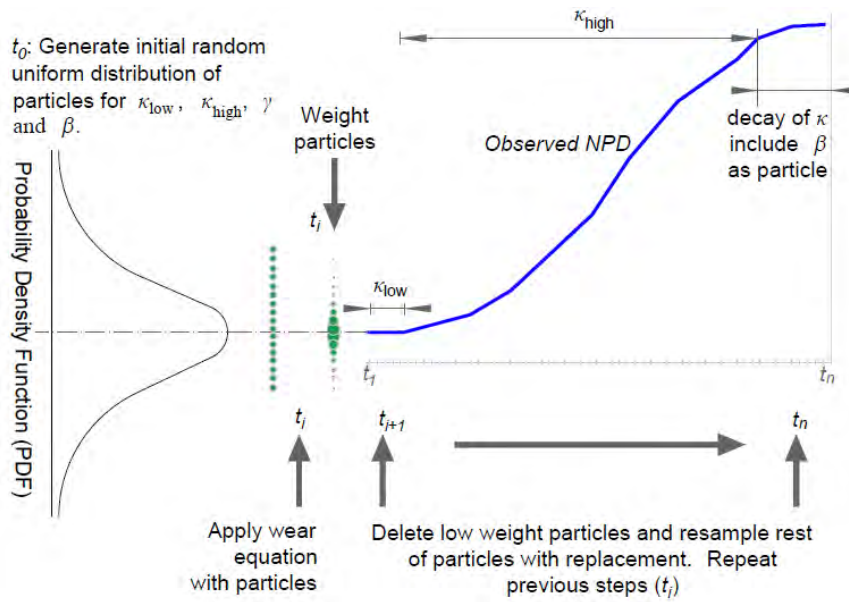


Figure 6-5. Principle of PF for parameter estimation

PF was run for each train separately for the first 500 days. Up to the first 500 days, there were no element permutations up to that time. To simplify the problem, now a fixed value κ_1 is assumed up to day 213 (the known start of the first algal bloom) and a different fixed κ_2 after that. The decay in NPD increments after the finish of an algae bloom, κ_t decays with $\kappa_t = (\kappa_2 - \kappa_1)e^{-\beta\tau}$ (see section 6.1.2). This way, the estimates of γ , β , κ_1 and κ_2 for each train are obtained. PF has not been utilized to estimate α since the method described in section 6.2.1 is preferred, whereby information about α that is available in the measured biomass distribution at the time of the inspection is utilized.

One of the issues with PF is the chance of failure to provide an output due to particle weight loss. An example of a failed run of the PF is shown in Figure 6-6. The modelled NPD in figure 6-6 starts to divert from the observed NPD between days 200 and 250. The initial deviating is such that the particles, in general, lose weight, the continuing increase in deviation results in the collapse of the particles. As a remedy, first, the range of the parameters has been limited to a realistic range. The configured ranges are shown in Table 6-1.

Table 6-1. Limitations parameters for the PF.

| | γ | β | κ_1 | κ_2 |
|-------------|----------|---------|------------|------------|
| Lower limit | 0.40 | 0.01 | 0.001 | 0.014 |
| upper limit | 1.10 | 0.10 | 0.005 | 0.040 |

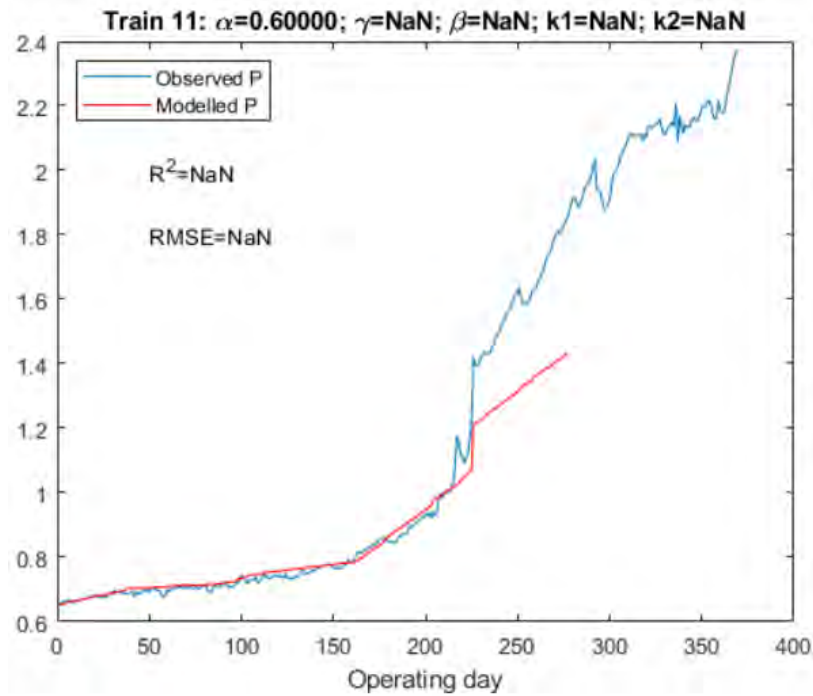


Figure 6-6. PF collapse

Bengtsson et al. (2008), Doucet and Johansen (2009), and Robinson et al. (2018) recommend smoothing and filtering to minimize the change of collapse of the PF. Thus, before using the PF, the NPD has been smoothed using the Savitzky-Golay (S-G) filter to improve its accuracy by removing various partial spikes in NPD. These spikes arise when a train is taken offline for a brief period and are likely related to low salinity flushing at this time. An S-G filter is a polynomial lowpass filter originally developed by Savitzky and Golay to smooth noise data obtained from a chemical spectrum analyser. The filtering is done by local least-squares polynomial approximation. A least-squares polynomial approximation is a procedure to fit a curve by finding the least-squares of the vertical offsets of the data points to the curve (Hamming, 1973).

The S-G filter works as follows, a sequence of input data points is fitted with a polynomial trend curve based on the least-square approximation. The polynomial degree and the approximation interval are configuration inputs of the filter. The advantage of an S-G filter, in contrast to a moving average smoothing, is that the S-G filter reduces the noise while maintaining the shape and height of the waveform peaks. Therefore, the input dataset must behave as a (semi)-Gaussian process (Schafer, 2011).

The “Smooth Data” function in MATLAB supports several smoothing options, of which the moving average and the S-G are applied in this research. The performance of the S-G filter is illustrated in Figure 6-7.

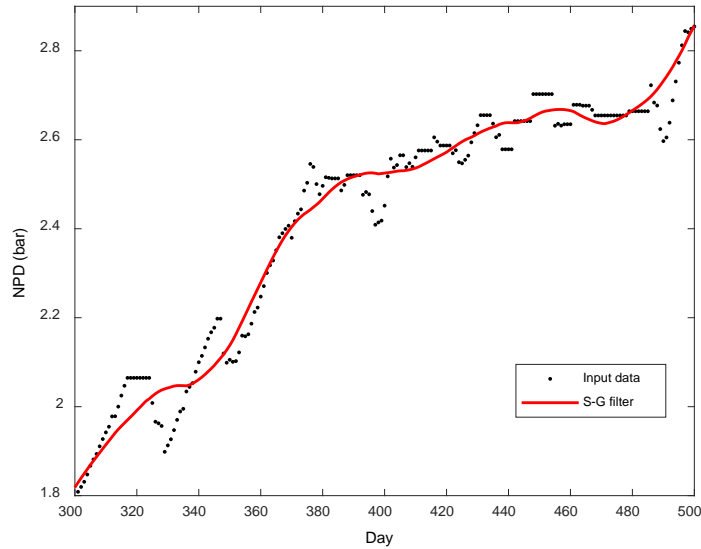


Figure 6-7. Illustration of the S-G filter for the NPD of Train 8. The polynomial degree of the filter is 4, and the approximation interval by a moving window of 150

A polynomial degree of 4 and a moving window of 150 were used for the PF's input data S-G filter. Smoothing and limiting the range of the parameters reduces the change of the PF collapses but does not prevent that. In some cases, the PF collapse or gives an unsatisfied output is computed with a low r^2 . Consequently, the running of the PF is repeated multiple times per train until ten results are attained where the r^2 is above 0.95. Then the mean of γ , β , κ_1 and κ_2 are taken. Figures 6-8, 6-9 and 6-10 show the histograms using ten bins for 200k particles of γ , β , κ_1 and κ_2 and fits a normal density function. The result per parameter is the sum of the particles times the weight. The histograms selected per train are for the PF run with the highest r^2 .

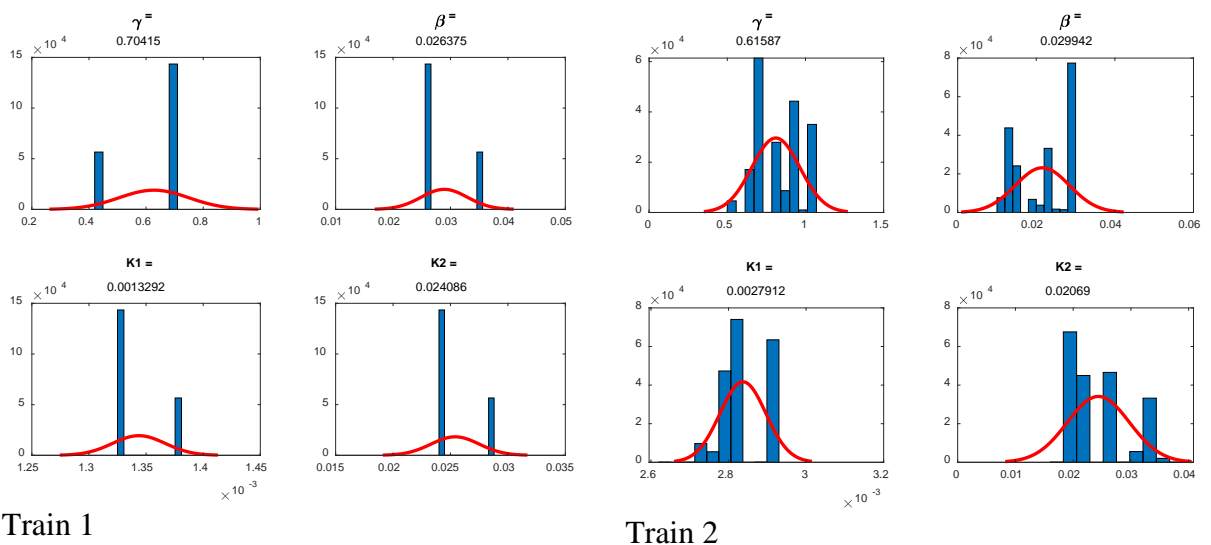
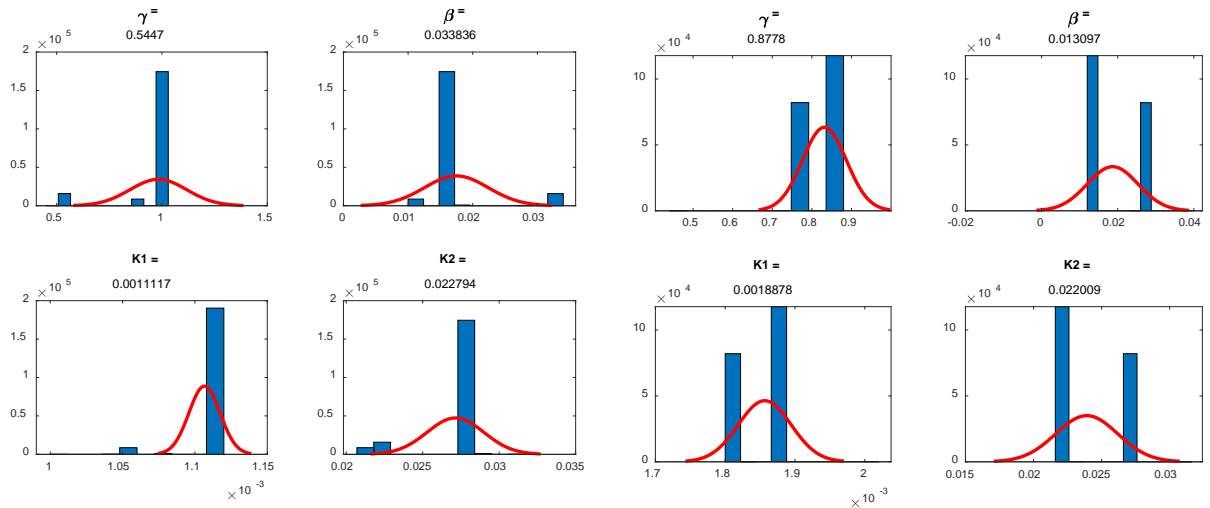
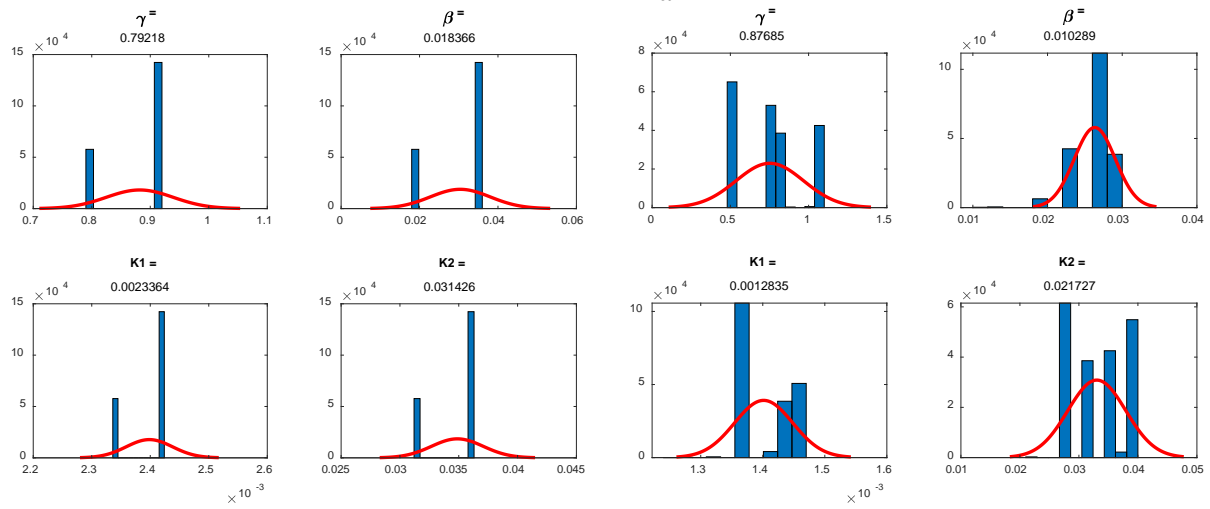


Figure 6-8: Histogram using ten bins for 200k particles of γ , β , κ_1 and κ_2 and fits a normal density function. The result per parameter is the sum of the particles times the weight. Plots train 1 and 2.



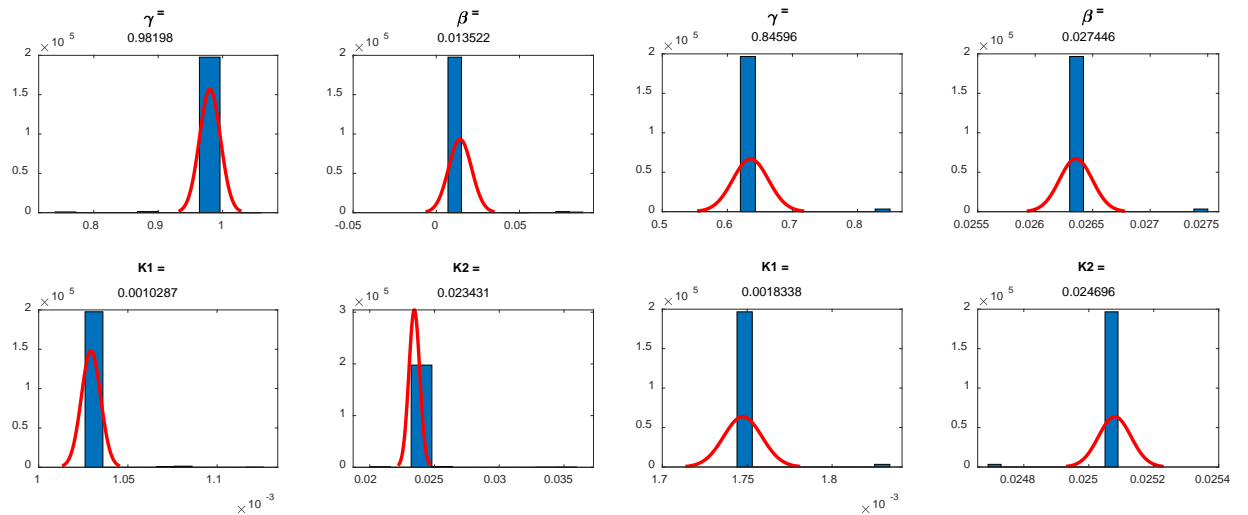
Train 3

Train 4



Train 5

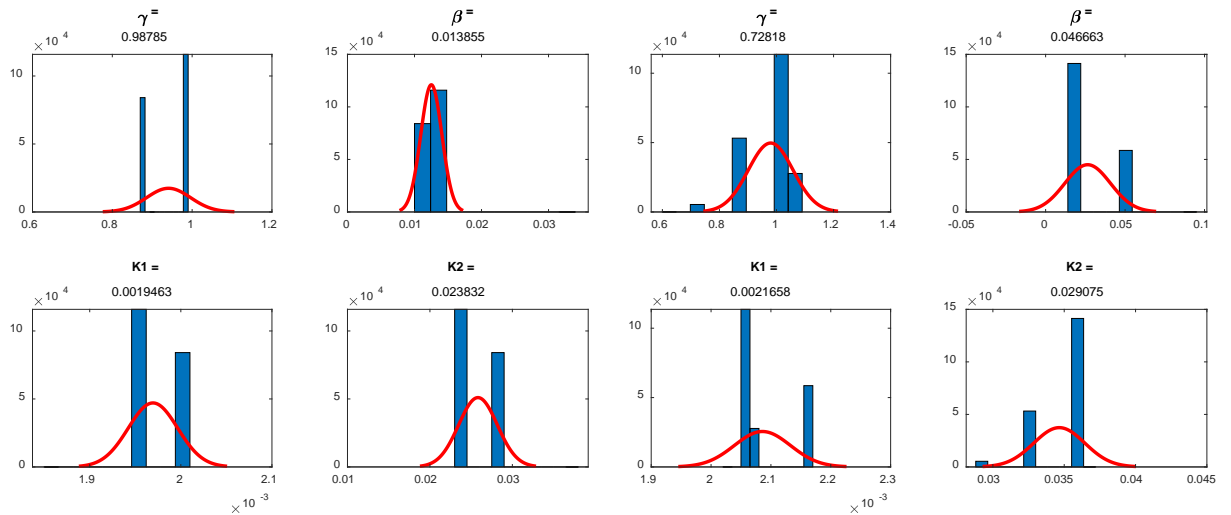
Train 6



Train 7

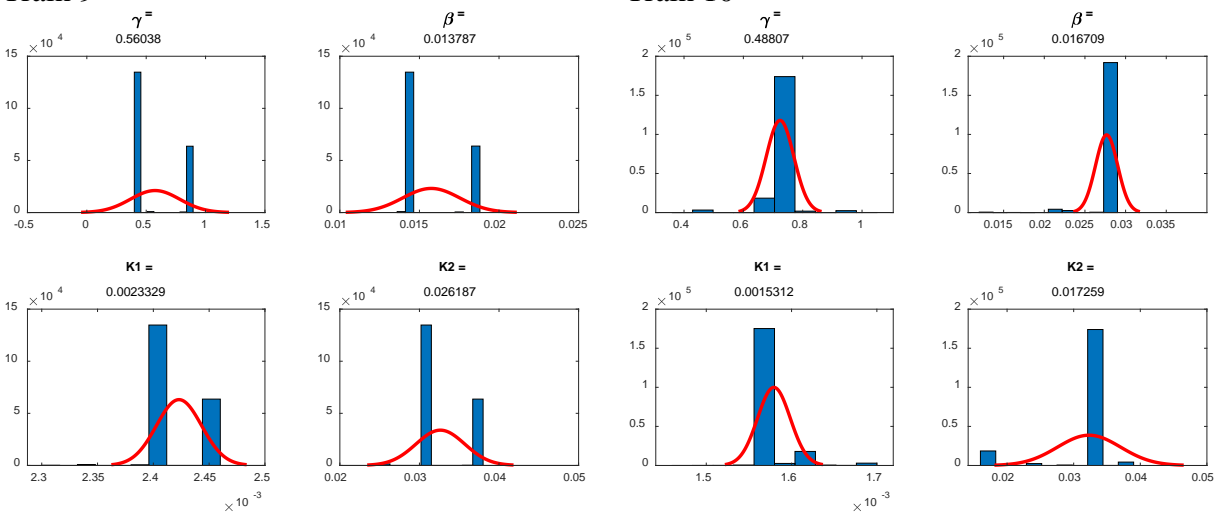
Train 8

Figure 6-9: Histogram using ten bins for 200k particles of γ , β , κ_1 and κ_2 and fits a normal density function. The result per parameter is the sum of the particles times the weight. Plots train 3 to 8.



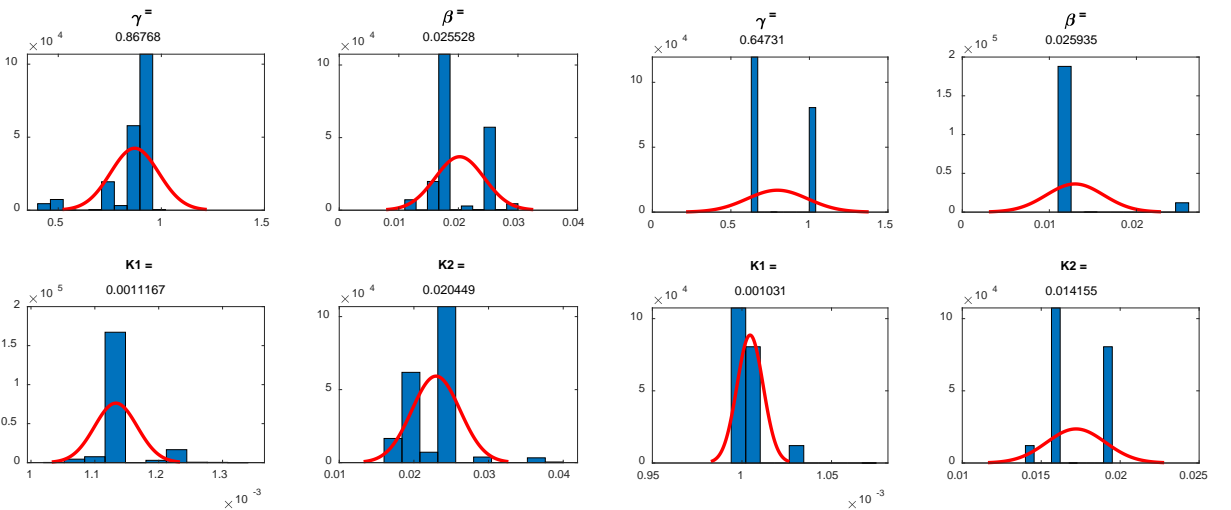
Train 9

Train 10



Train 11

Train 12



Train 13

Train 14

Figure 6-10: Histogram using ten bins for 200k particles of γ , β , κ_1 and κ_2 and fits a normal density function. The result per parameter is the sum of the particles times the weight. Plots train 9 to 14.

6.2.3 The (non)-Gaussian character of wear parameter κ

The introduction of chapter 6.2 stated that the parameter κ is stochastic, follows a Gaussian distribution and can be estimated by a probability distribution. The equation to calculate the state-space values of κ has been presented in section 6.2.1 (eq 15). Now that α and γ are estimated, the state-space values of κ can be more precise re-calculated. The state-space values of κ resulted in 365 days over five years, covering 14 trains. Therefore, we have 70 values for each day of the year from which we can sample. February 29th is ignored.

Figure 6-11 (top left) shows a plot of all state-space values of κ (grey dots) ordered according to the year's day. Further, the daily mean of κ ($\mu\kappa$ –blue dots) is calculated. As can be observed, both κ and $\mu\kappa$ are somewhat random. No visual pattern recognition can be established of periods of increased κ due to algae bloom conditions and periods where this condition is absent.

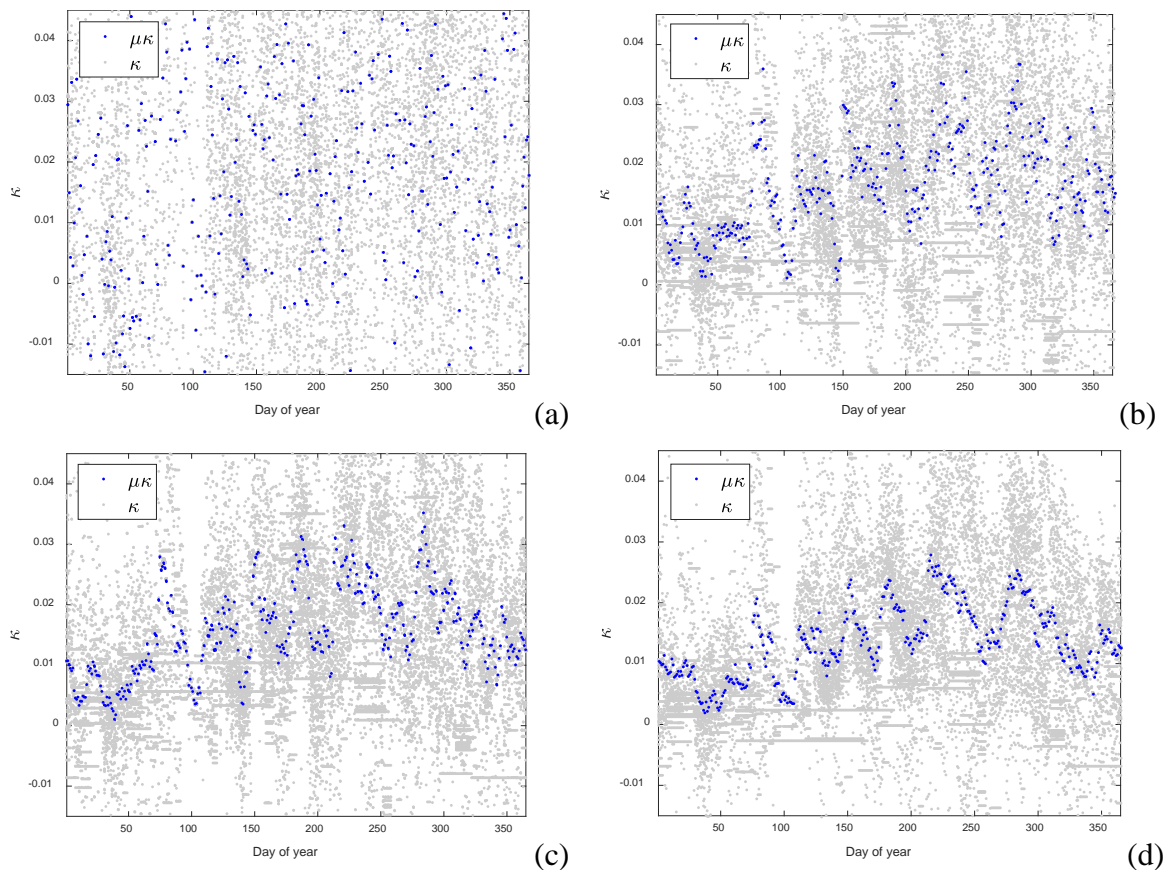


Figure 6-11. State-space values of κ (grey dots) and daily mean of κ ($\mu\kappa$ –blue dots) ordered according to the year's day. Top left (a): unsmoothed, top right (b): smoothing of -1,4, bottom left (c): -2,8, and bottom right (d): -4, 16.

A moving average with different strengths has been applied to intensify the contrast. Three different smoothing windows are applied to ensure the results are robust to the smoothing one

before, four after (-1,4), (-2,8), and (-4, 16), corresponding to windows of width 5, 10 and 20 days, respectively. The results of smoothening κ (grey dots) ordered according to the year's day and the corresponding daily mean of κ ($\mu\kappa$ –blue dots) are shown in Figure 6-11, where (top right) represents a smoothing of -1,4, (bottom left) -2,8, and (bottom right) -4, 16.

Further, a cumulative distribution function (CDF) and the PDF are applied and plotted in Figure 6-13 to demonstrate a Gaussian distribution. Diagrams at the left are the distributions of κ with a smoothing of -1,4, -2,8, and -4, 16. The diagrams at the right are the distributions of $\mu\kappa$ following the same smoothing.

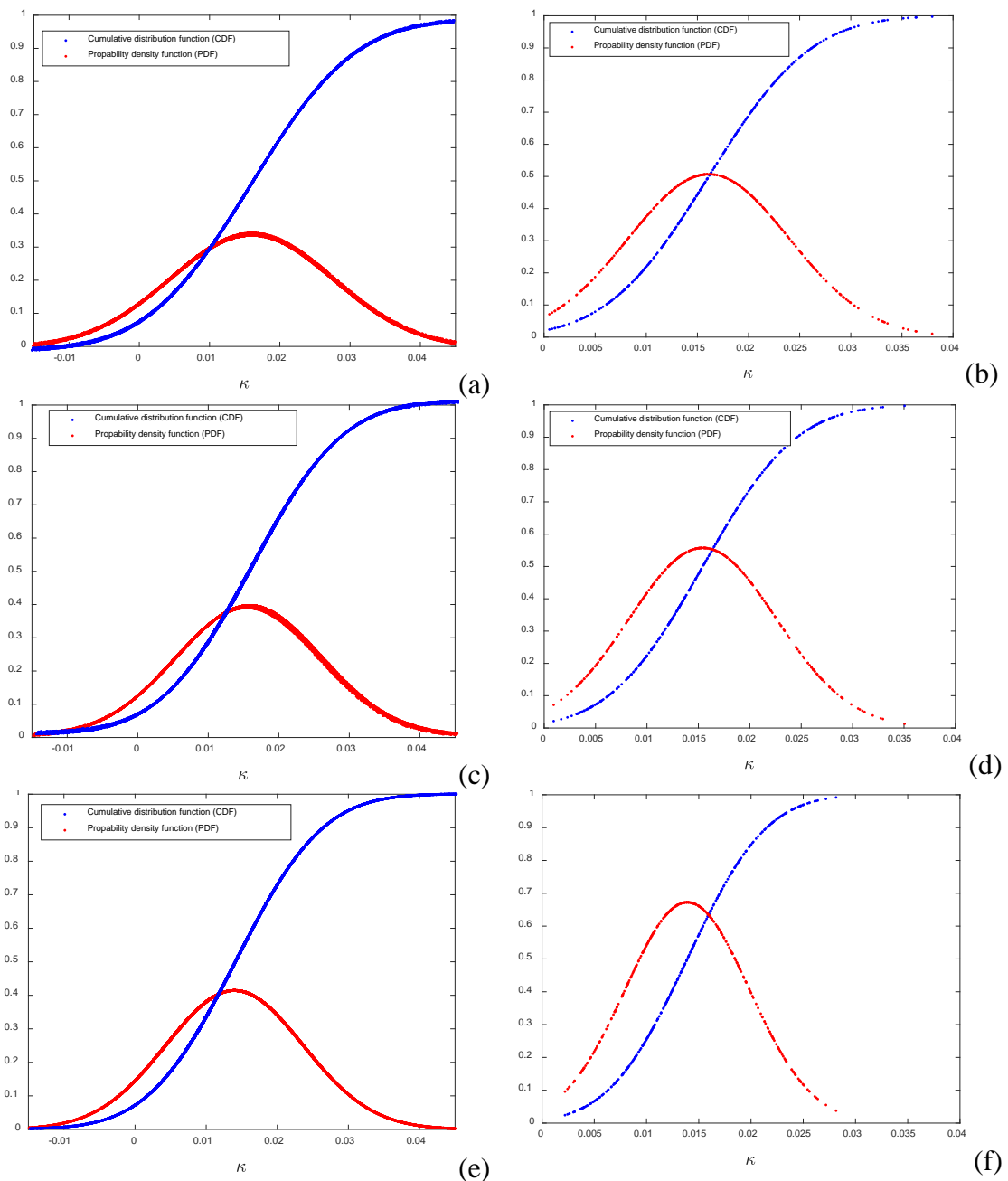


Figure 6-12. CDF and PDF with top smoothing of -1,4, (a) κ and (b) $\mu\kappa$. Middle smoothing of -2,8 (c) κ and (d) $\mu\kappa$. Bottom smoothing of -4, 16 (e) κ and (f) $\mu\kappa$.

Observation of Figure 6-12 gives an impression of a Gaussian distribution for κ , but the PDF of the daily average skews slightly to the right. A histogram has been plotted for the data using a smoothing of -1,4 to verify this. Then, the MLE is added to the plot and shown in Figure-13 on the left. We observe that the MLE is symmetric while the histogram skews slightly to the right.

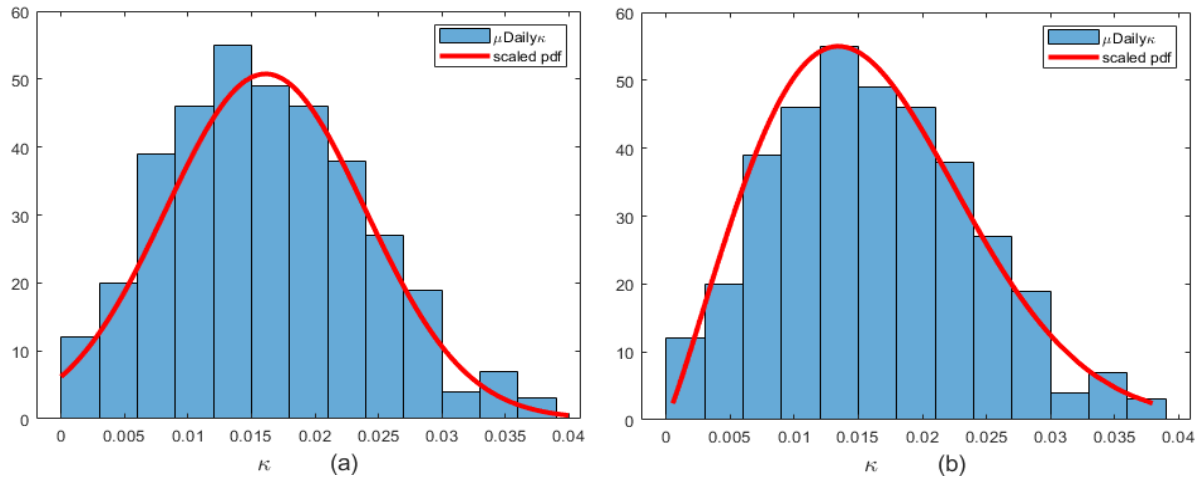


Figure 6-13. Histogram and PDF of daily κ (a) MLE for parameters with normal distribution, (b) MLE for parameters with Weibull distribution

The same histogram is shown on the right side of Figure 6-13. However, the MLE is following a Weibull distribution. We can observe that the MLE with a Weibull distribution fits the right-skewed histogram. If we can utilize a normal distribution to project a random distribution for the probability of κ , the slight deviation of the MLE would be neglectable. However, we must incorporate the stochastic seasonal effect of algae blooms. Therefore additional normal distributions must be applied for the start day and length of the algae bloom in days.

The limited data on algae blooms' annual start and duration gives a high standard deviation. Because Normal distribution is unbounded, a too-large standard deviation results in nonphysical sampled values at the lower tail (Mishra and Datta-Gupta, 2017). The reported duration of algae blooms between 2017 and 2020 (see Table 6-2 chapter 4.3.2) provides a mean for the algae blooms of 23.5 days and a standard deviation of 33.7, which is excessive for the mean. Generating random values for the projection of the length of algae blooms utilizing a normal distribution resulted in a range of -59 to +115 days (see Figure 6-14). A negative value is problematic. A Weibull distribution is, therefore, more practically. The equation below gives the PDF of the Weibull distribution (Mishra and Datta-Gupta, 2017).

$$f(x) = \frac{k}{\lambda} \left(\frac{x}{\lambda}\right)^{k-1} \exp\left\{-\left(\frac{x}{\lambda}\right)^k\right\}; k, \lambda > 0, 0 \leq x \leq \infty$$

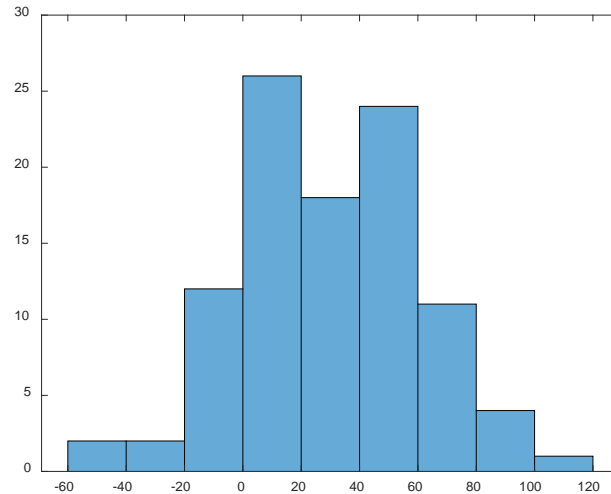


Figure 6-14. Random duration algae bloom by Normal Distribution with a mean of 23.5 and σ of 33.7

where k is the shape parameter, and λ is the scale parameter.

A function to fit the PDF of a Weibull distribution and the corresponding Weibull distribution of random values are available in MATLAB and is derived from the above equation. The code used to generate Figure 6-13 (b) is shown below. The parameter estimation for the Weibull fit will be addressed in section 6.2.5. First, we concentrate on the other method this research applies for sampling stochastic parameters, bootstrapping.

```
% Weibull fit
[KappaHat, KappaCi]=wblfit(DailyKappa);
h = histogram(DailyKappa);
hold on
Y = wblpdf(sort(DailyKappa),KappaHat(1),KappaHat(2));
yScaled = Y * (1/max(Y)) * max(h.Values);
% Plot scaled pdf (the pdf should overlap with the hist)
plot(sort(DailyKappa), yScaled, 'r-', 'LineWidth', 3)
legend('\muDaily\kappa', 'scaled pdf')
hold off
```

6.2.4 Bootstrap sampling

Finding the parametric confidence intervals, standard errors, and bias of state-space spatial structures can sometimes be challenging. In 1979 Brad Efron introduced a nonparametric statistical approach that he called the bootstrap. Bootstrap is a resampling method that does not need a mean and standard deviation in the case of a normal distribution or a shape parameter k , and a scale parameter λ in the case of Weibull distribution. At its foundation, bootstrapping involves a Monte Carlo approximation of a sample from an original observation with a population of n with replacement, so a bootstrap sample of a population of $n!$ can be generated. Mathematically n^n permutations can be made from a population of n .

However, some results would be equivalent since they are permutations of each other. Therefore the bootstrap sample $n!$ does not grow as fast as n^n (Chernick and LaBudde, 2011).

Bootstrap then generates the MLE of the bootstrap sample without defining parameters (Hinrichsen and Holmes, 2009). This research intends to project the entire possibility of the likelihood instead of the MLE. So, of interest is the bootstrap sample rather than the bootstrap itself. When we apply Bootstrapping in MATLAB utilizing the “bootstrp” function, this results in the MLE of the bootstrap sample from the original data. The bootstrap sample itself is temporal for applying the bootstrap and is not accessible.

On the other hand, the function “datasample” is identical to the bootstrap sampling step and needs to be utilized to compute the bootstrap sample. The MATLAB code below illustrates the differences between the original data, bootstrap sample and the bootstrap function. Figure 6-15 gives the output.

```
%Bootstrap sample
DayKappa=Kappa(:,55); % Sample of a random day: 55
Bootstrapsample=datasample(DayKappa,100); %Bootstrap sample n!=100
HisBootstrapsample=histogram(Bootstrapsample); %Histogram
[bootstat,bootsam] =bootstrp(100,@mean,DayKappa); % MLE Bootstrap
hold on
HisObs=histogram(DayKappa); % Histogram observed data
HisBootstrap=histogram(bootstat); % Histogram MLE Bootstrap
HisBootstrap.FaceColor="k";
legend('Bootstrap sample','Original', 'Bootstrap @mean');
xlabel('\kappa','FontSize',14);
hold off
```

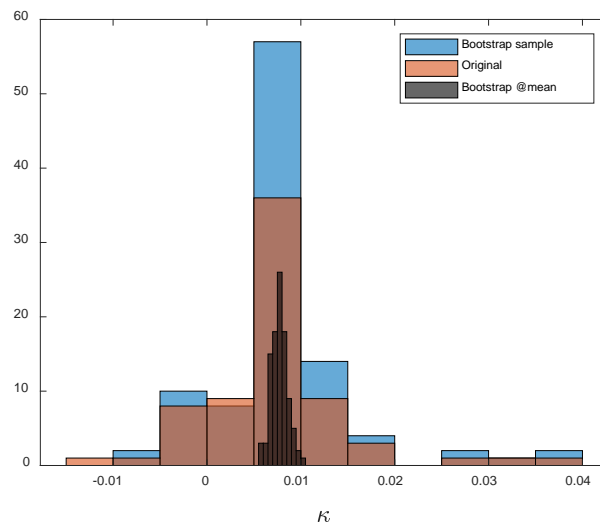


Figure 6-15. Histogram of the population on a random day 55 of κ smoothen -1,4 dataset, bootstrap sample and Bootstrap at the mean.

In the previous section, the daily κ were ordered as a multivariate state-space model. Assumed that the years are statistically identical, five values are obtained for each day and

each train with five years of observed data in total. Estimates for trains are then pooled, yielding a bootstrap sample of size 70 (5x14) for each day of the year and, therefore, a 70x365 bootstrap sample matrix. The daily κ_t for each train has been smoothed using a moving average. Three different smoothing windows were applied, -1,4, -2,8, and -4, 16, to ensure the results were robust to the smoothing. The effect of algae blooms is automatically included in the multivariate state-space model, as shown in Figures 6-11.

These three datasets with different smoothing provide the original observation for projections (see chapter 7) involving bootstrap sampling as a forecasting method. In the latter case, bootstrap samples of δ are generated separately for clean-in-place (CIP) methods C1 and C2 (see section 6.2.6).

6.2.5 Results wear parameter κ utilizing Weibull distribution

Weibull distribution as an alternative for Bootstrap sampling was presented in section 6.2.3. We recall from section 6.2.2 that κ needs to be separately estimated during Algae bloom (κ_2) and non-bloom periods (κ_1). Utilizing PF (see section 6.2.2), κ_1 and κ_2 were estimated over the first 500 days of operation, whereby κ_1 covers the period up to the first signs of membrane fouling. However, the first 500 days might not represent the severity of κ_2 over the entire state-space. Of interest are the mean values of κ during periods of algae blooms.

Although the records of the O&M team mentioned the start and end dates of the algae blooms since 2017 (see Table 4-1), the recorded days might not cover the full extent of the duration. Therefore, change-point analysis is applied to the NPD to find the starts and finishes of the algal blooms effect. The changepoint analysis aims not to define the number and duration of algae blooms but to identify periods that allocate κ_2 . After segments of κ_2 have been allocated, the mean κ over the segment is calculated. Then the maximum mean value of κ_2 over the state-space of the individual train is recorded. So, similar to the PF analyses, 14 new values of κ_2 are estimated, covering the entire state-space instead of the first 500 days.

A changepoint analysis is a method that identifies within a dataset of points where the statistical properties change (Killick et al., 2012). These changes in statistical properties can be a change in the mean, variance or a combination of these parameters within a Gaussian distribution (Lavielle, 2005; Killick et al., 2012) or a known number of changepoints (Picard et al., 2005).

MATLAB has a standard function, “ischange”, for changepoint analysis. The “ischange” function has been utilized in this research to identify periods where κ can be identified as κ_1

or κ_2 . Besides mean or variance, defining the statistical properties of the change, a linear change detection method can be applied. The latter is helpful for non-Gaussian distributions and detects abrupt changes in the slope and intercept of the data. Additional parameters can be a threshold or the maximum number of changepoints⁴, similar as mentioned by Picard et al. (2005). A threshold, when specified, will adjust the change point detection sensitivity.

Smoothing of the NPD was applied beforehand to filter out noise. The smoothing method was the S-G filter with a polynomial degree of 4, and a smoothing factor of 0.1 was applied.

First, a linear regime (black pen in Figures 6-16 to 6-18) is applied to the NPD (red dotted pen). Then change points are determined based on changes in the linear regime. Change points reflect the end of an algae bloom or maintenance interventions. After obtaining the changepoint times, the mean of the daily κ between these times is calculated. The daily κ is first smoothed by moving mean of one before and one after. Following the mean κ between changepoints is calculated from the daily κ . The highest mean as κ_2 per train is recorded.

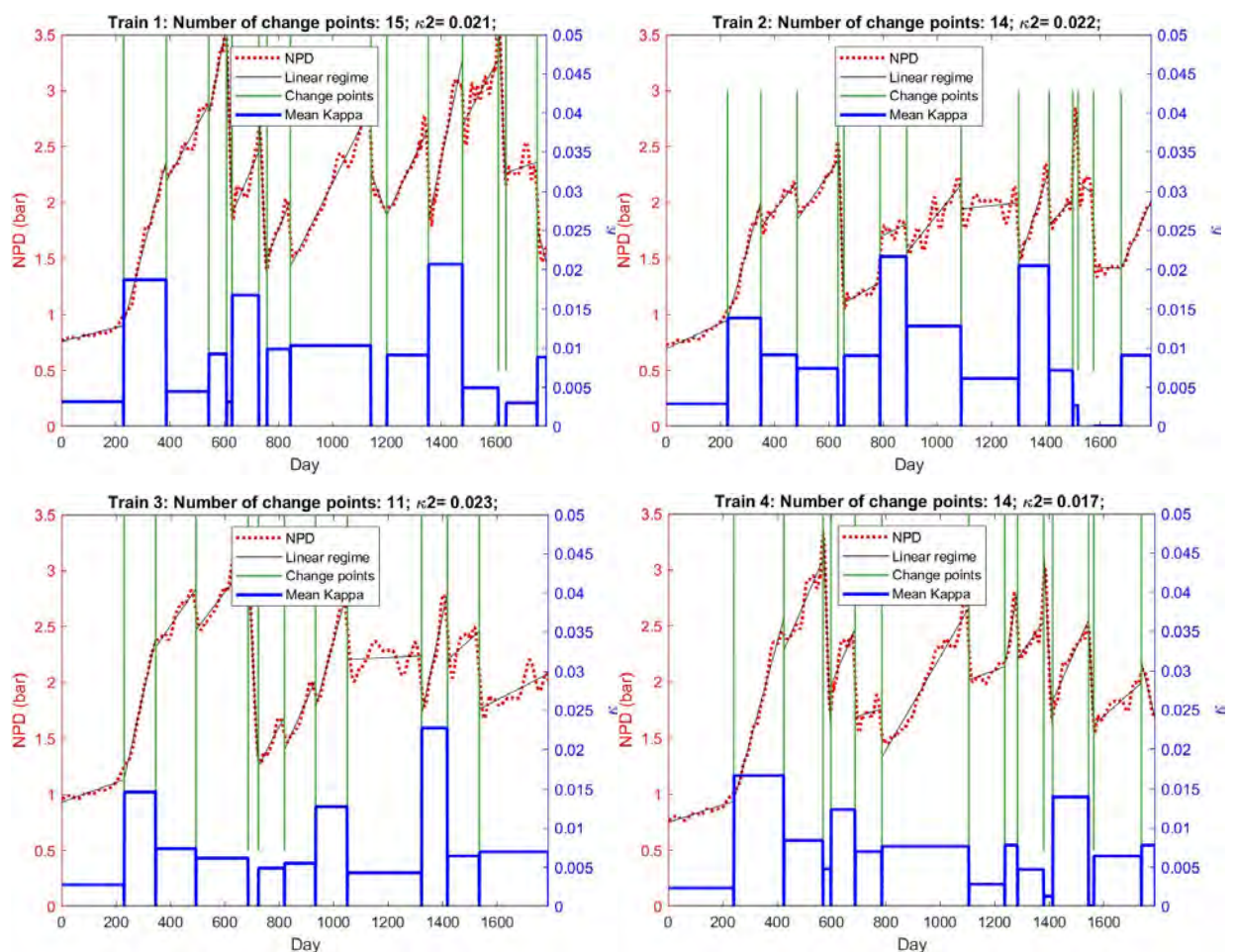


Figure 6-16: Outputs of the change-point analysis of RO trains 1 to 4

⁴ MathWorks Help Center

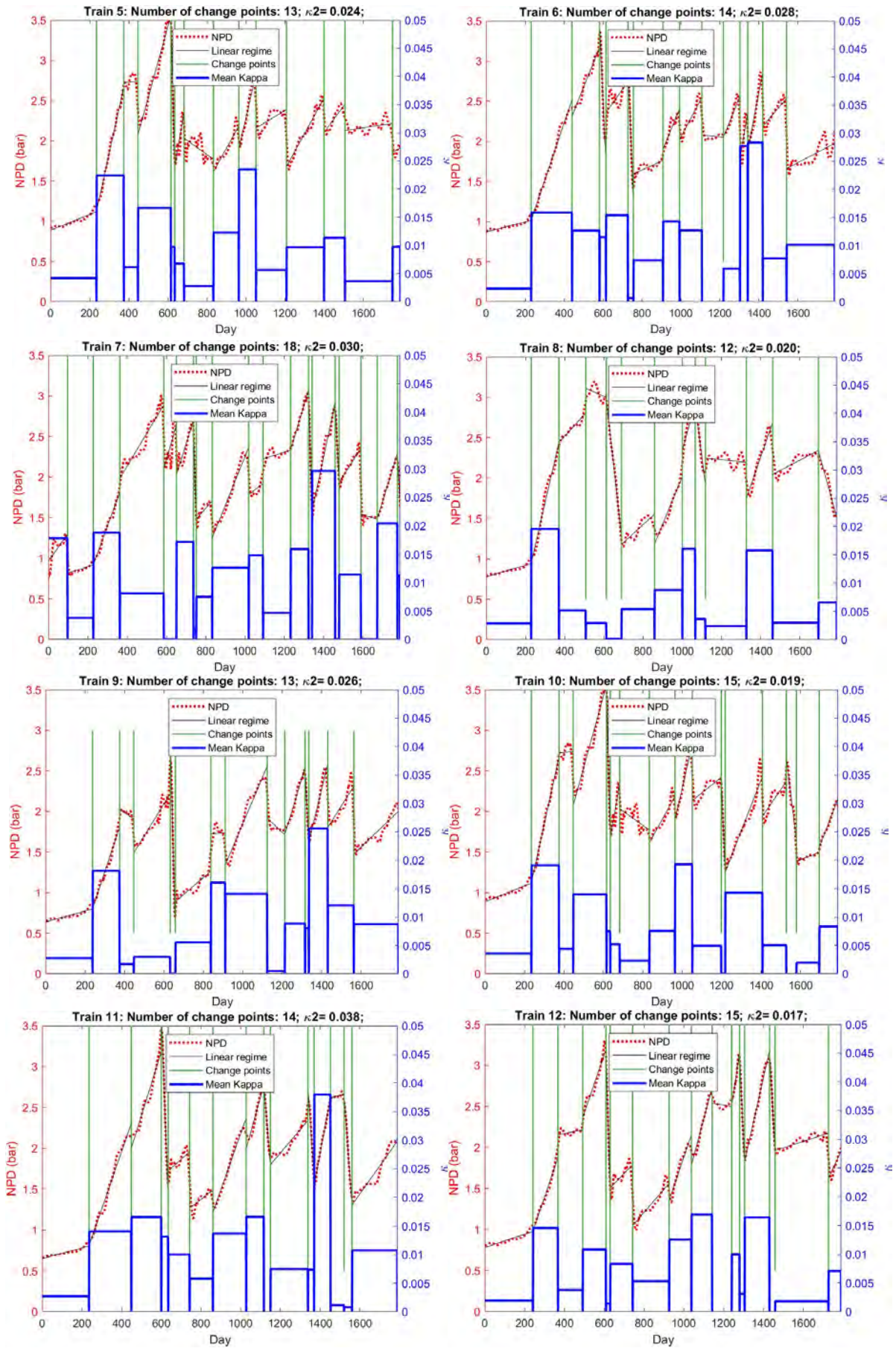


Figure 6-17: Outputs of the change-point analysis of RO trains 5 to 12

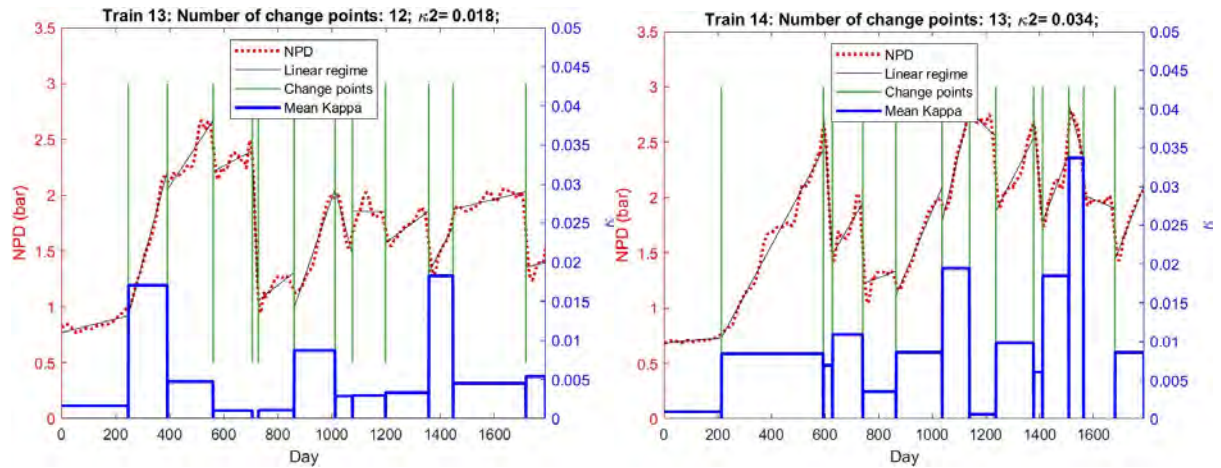


Figure 6-18: Outputs of the change-point analysis of RO trains 13 and 14

Multiple reasons exist for the variation of the changepoint output between the trains. First, there are different intervals of changepoints between trains. These changepoints are triggered due to the slope of the observed NPD. The time the trains are in operation varies; therefore, the trains are not exposed equally to extrinsic feedwater conditions. Further, after the first 500 days of operation, the trains underwent different maintenance schedules. While some trains operate during worsening extrinsic feedwater conditions, other trains are offline, flushed with nutrient-poor low salinity water or underwent a CIP. The results of the parameter estimation are given in table 6-2.

Table 6-2: Estimates of parameters.

| Train | r^2 | RMSE | α | γ | β | κ_1 | κ_2 |
|-------|-------|-------|----------|----------|---------|------------|------------|
| 1 | 0.992 | 0.06 | 0.65 | 0.74 | 0.026 | 0.0014 | 0.021 |
| 2 | 0.964 | 0.10 | 0.65 | 0.73 | 0.026 | 0.0028 | 0.022 |
| 3 | 0.975 | 0.10 | 0.64 | 0.66 | 0.031 | 0.0011 | 0.023 |
| 4 | 0.980 | 0.09 | 0.62 | 0.86 | 0.023 | 0.0017 | 0.017 |
| 5 | 0.984 | 0.08 | 0.47 | 0.80 | 0.023 | 0.0025 | 0.024 |
| 6 | 0.988 | 0.06 | 0.55 | 0.72 | 0.017 | 0.0016 | 0.028 |
| 7 | 0.983 | 0.07 | 0.53 | 0.73 | 0.020 | 0.0010 | 0.030 |
| 8 | 0.983 | 0.09 | 0.66 | 0.92 | 0.023 | 0.0018 | 0.020 |
| 9 | 0.975 | 0.07 | 0.60 | 0.90 | 0.026 | 0.0019 | 0.026 |
| 10 | 0.979 | 0.09 | 0.55 | 0.82 | 0.028 | 0.0021 | 0.019 |
| 11 | 0.990 | 0.06 | 0.60 | 0.86 | 0.014 | 0.0023 | 0.038 |
| 12 | 0.973 | 0.09 | 0.70 | 0.55 | 0.021 | 0.0015 | 0.017 |
| 13 | 0.979 | 0.08 | 0.61 | 0.70 | 0.020 | 0.0011 | 0.018 |
| 14 | 0.969 | 0.07 | 0.74 | 0.54 | 0.034 | 0.0010 | 0.034 |
| mean | 0.980 | 0.08 | 0.60 | 0.75 | 0.023 | 0.0017 | 0.024 |
| min | 0.969 | 0.06 | 0.47 | 0.54 | 0.014 | 0.0010 | 0.017 |
| max | 0.990 | 0.09 | 0.74 | 0.92 | 0.034 | 0.0025 | 0.038 |
| Std | 0.006 | 0.010 | 0.078 | 0.126 | 0.005 | 0.0005 | 0.0062 |

For Weibull distribution projections, we need to calculate the shape parameter k and scale parameter λ to forecast the stochastic parameter κ . The parameters are determined separately for κ_1 and κ_2 by utilizing a Weibull fit function at MATLAB. For κ_{low} $\lambda = 0.0019$ and $k = 3.3567$. For κ_{high} $\lambda = 0.0265$ and $k = 4.0043$.

We must also forecast the annual start of algae bloom and the duration of the forecast method utilising Weibull distribution. The recorded start and end dates are used from the O&M records. Since there are no recorded data for the first year of operation, the observed beginning of the rapid degeneration and the observed end for the first year is considered.

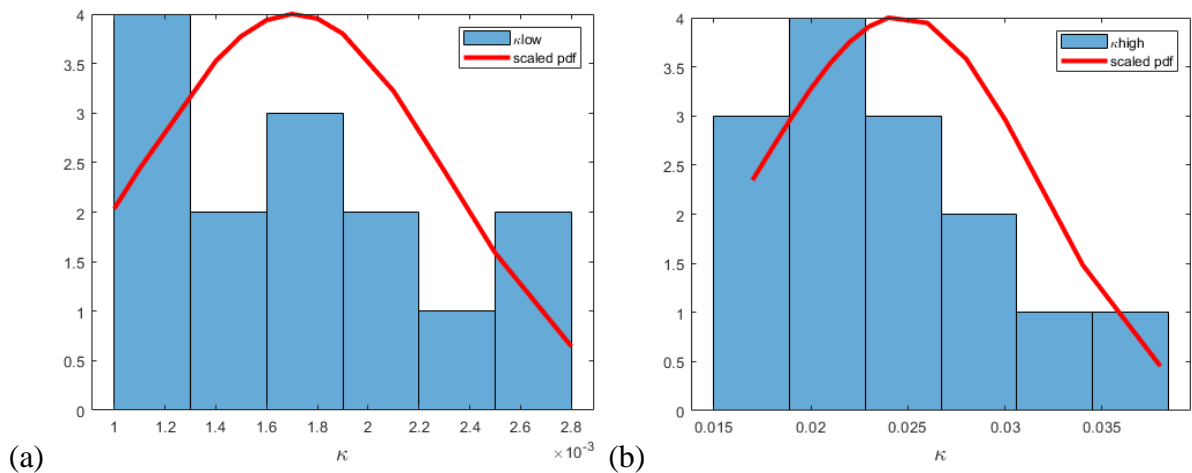


Figure 6-19. Histogram of κ with scaled PDF from the Weibull fit, (a) κ_{low} and (b) κ_{high}

Considered are further the records for the remaining period from 2017 to 2020 (see Table 4-1 in section 4.3.2). Based on this data, a Weibull fit has been applied. For the annual start day $\lambda = 122$ and $k = 3.88$. For the duration in days $\lambda = 20$ and $k = 0.76$.

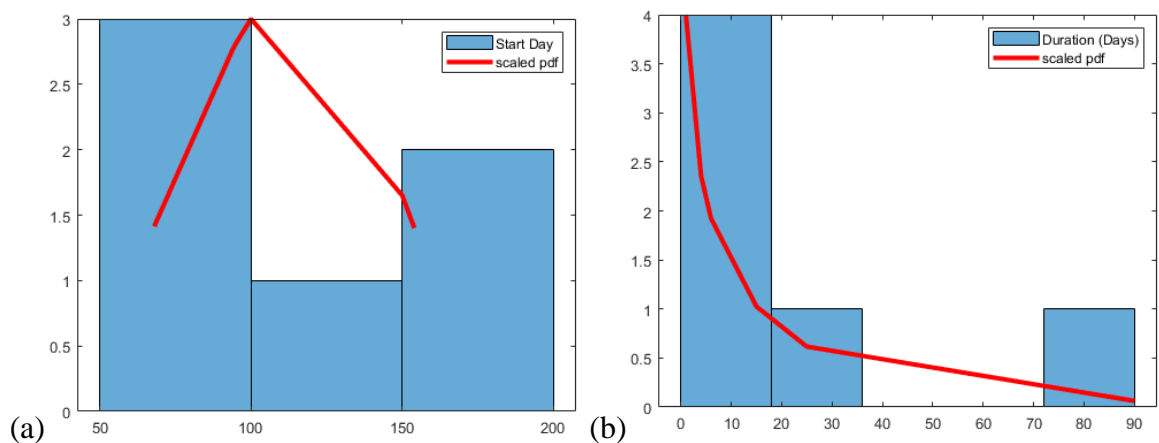


Figure 6-20. Histogram of (a) day of year start algae bloom and (b) duration in days with scaled PDF from the Weibull fit

6.2.6 Results restoration parameter δ for C1 and C2

The cleaning effect δ was calculated using Eq. (17) for each cleaning operation. Note, the effects of cleaning can have a lag of a few days after a train returns to normal operation, so P_{t^+} must be carefully specified. In total, 64 CIP restorations were performed up to September 2020, of which 33 were C1 (standard high and low pH cleaning), and 31 were C2 (soaking with Bisulphate then a standard high and low pH cleaning). C1 gave, on average, a reduction of NPD of 14%. However, it was less than 10% in one-fifth of the cases. C2 gave, on average, a reduction of NPD of 26%. Only 4% of the cases was the reduction less than the average reduction by C1. For C1, $\lambda = 0.2625$ and $k = 1.7476$. For C2, $\lambda = 0.4211$ and $k = 3.9152$. (figure 6-20).

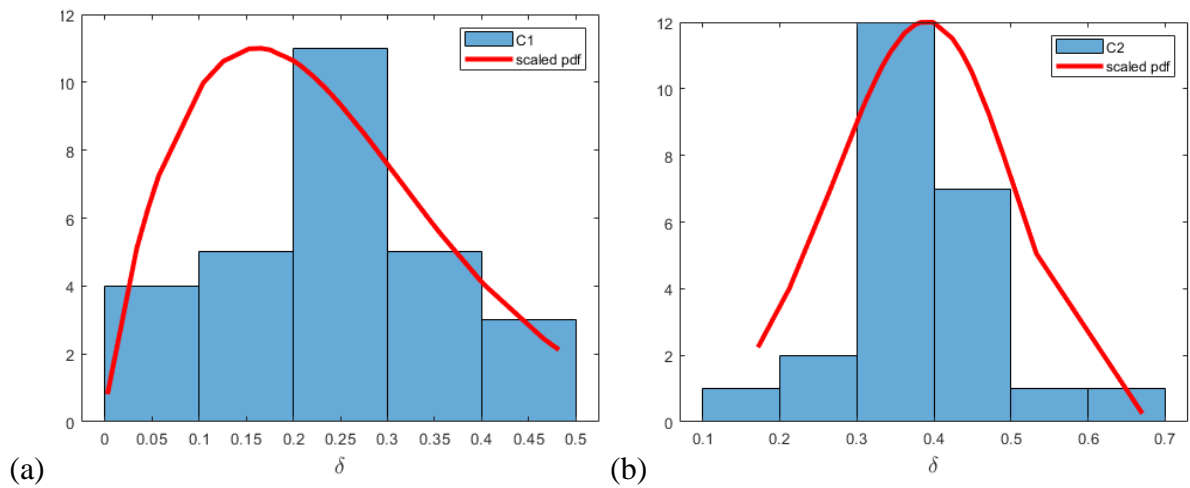


Figure 6-21: Histograms with scaled PDF from the Weibull fit of the observed effects for cleaning-in-place for cleaning modes C1 (a) and C2 (b)

6.3 Summary

A mathematical model of degradation (in the presence of biofouling) and restoration of membrane elements have been presented. The degradation is due to the built-up of biomass and is denoted as the degradation or wear X . Although the wear is a continuous process, the vessel is approached at discrete intervals per socket for practical reasons. The wear state of the element in socket i at time t is $X_{i,t}$, and this wear variates.

The wear manifests in operational conditions of the vessel as an increase of normalized pressure differential (NPD) over the feed inlet and the concentrate or reject outlet. The NPD of a vessel is the sum of the NPD of the elements. When the element is new, $X_i = 1$ and when all elements are new, P_t is P_0 .

Despite equal wear, the NPD per succeeding elements decreases due to hydraulic laws, known as the Darcy-Weisbach head-loss model that describes the relationship between flow and pressure loss. Thus, although the components, the membrane elements, are cascaded, the manifestation of the wear as NPD is not simply the sum of the individual wear X_i but distributed with ω_i a set of known (dimensionless) constants such that the sum is unity. This set of constants will be called the pressure distribution due to the decreasing flow.

The feed flow to each succeeding element reduces, and the salinity increases due to permeation from a discrete perspective. The permeation of the succeeding elements decreases relatively due to increased salinity resulting in higher osmotic pressure and lower net driving pressure. The recovery is the permeate flow divided by the saline flow. Since the overall vessel recovery and the salt rejection are known, the recovery and the pressure distribution constants per socket can be calculated.

The thesis author supposes the wear increment of an element when the vessel is in operation is given by the extrinsic dependency κ , the wear distribution dependency α and the rate-state dependency (see equation 9). When the vessel is offline, there is no longer a rate-state dependency. The recovery is zero, and this part of the wear increment equation $\{\sum_{j=i+1}^n X_{j,t-1} / (n-i)\}^{R\gamma}$ becomes unity.

Restoration is done by permutations and clean-in-place (CIP). When swapping, X_i moves with the element to the new socket. Furthermore, if replaced with a new one, the wear state becomes unity ($X_i = 1$). CIP is an imperfect restoration that reduces the wear increase partially (see equations 12 and 13). Thus, the cleaning effect is proportional to the excess NPD above P_0 . So we partially remove the biomass. Here δ is the cleaning effect parameter.

The parameters of the model are estimated using statistical analysis. First, biofouling-wear distribution parameter α is estimated. The parameter α is estimated by comparing the modelled wear distribution across individual elements with the measured distribution of biomass obtained at vessel inspections when a vessel is opened and individual elements are weighed. The value of α from the logical range of 0.4 to 0.8 minimizes this deviation.

Once α is specified, the particle filtering (PF) method is utilized to estimate γ and β using a restricted set of values for κ_t . The input data to the PF is first smoothed with a Savitzky-Golay (S-G) filter to reduce noise. The time series is limited up to day 500, which includes exposure to an algae bloom, but no maintenance actions have been performed up to this day. Up to the algae bloom, a fixed value for κ_1 is assumed and a different fixed κ_2 after that. To account for

the decay in NPD increments after the finish of an algae bloom, the model supposes that κ_t decays according to equation 14.

Finally, the daily values of κ_t are calculated to predict future NPD, where κ_t is assumed to be a random value retrieved by bootstrap sampling or Weibull distribution. Bootstrapping involves random sampling from a 70x365 matrix composed of daily values of κ_t from 14 trains over five years. Eq. (19) is used to re-calculate κ_t daily for each train and smooth these using a moving average. Three different smoothing windows are applied to ensure the results are robust to the smoothing, one before, four after (-1,4), (-2,8), and (-4, 16), corresponding to windows of width 5, 10 and 20 days, respectively.

The shape parameter k and a scale parameter λ of κ_1 for the Weibull distribution are fitted from the PF results. However, fitting the parameters for κ_2 from the results of the PF will not cover the whole range of the state-space. Therefore changepoint analyses are being applied to identify periods of κ_2 . Then, the maximum value of the means of these intersections is used for the value of κ_2 per train. The individual values of the 14 trains are used for the Weibull shape parameter k and a scale parameter λ of κ_2 . Note that the value of κ is common in the projections for all the trains since they see the same source water. The trigger for applying κ_1 or κ_2 depends on the projection of the start and duration of an algae bloom. A Weibull fit has been applied to the algae bloom recording of Table 4-1 in chapter 4.3.2.

The cleaning effect parameter δ is sampled in the same manner. Each cleaning method, C1 and C2, has its dedicated parameter δ . Of the 64 performed CIP restorations, 33 were C1 with five just before a permutation, and 31 were C2 with six just before a permutation. The latter gives 28 known values for C1 and 24 known values for C2. The cleaning results provide two vectors for bootstrap sampling. Further, Weibull fits have been applied to the vectors.

7 The Digital Twin

The Mathematical equations of degradation and restoration of RO membranes set out in Chapter 6 are the basis of a simulation application for projecting an RO vessel's long-term degradation and restoration. Thus, the simulations are founded on mathematical modelling based on physical laws (see Chapter 6.1) and statistical methods. The forecast methodology includes Monte Carlo simulation (Wilks & Vannitsem, 2018) and discrete-event simulation (Lawson & Leemis, 2008). The extrinsic parameter κ of the equations provides the common feedwater quality dependency for degradation and varies continuously. The cleaning parameter δ that gives the effect of imperfect restoration by clean-in-place (CIP) varies per intervention. Both parameters are stochastic and projected from data over the previous five years. The parameters κ and δ are fitted to a Weibull distribution and used when predicting future projections by sampling from these distributions. Alternatively, the simulation allows bootstrap sampling directly from the previous data (see Chapter 6.2). This chapter concentrates on the simulation application deployed as a digital twin (DT).

7.1 Industry 4.0 and smart maintenance

Pintelon and Parodi-Herz (2008) stated nearly one and a half decades ago (chapter 2) that maintenance had been recognized as one of the pillars of business strategy. A scientific approach toward maintenance management started in the 1950s and 1960s. Time-based preventative maintenance was encouraged to reduce failures and unplanned downtime. Condition-based maintenance was developed in the 1970s as a cost-effective alternative to large time-based preventative maintenance programs. Computerization of maintenance started in the 1980s with the introduction of the PC, initially for administrative purposes, followed by the application MAINOPT as the first maintenance analysis program (Dekker, 1996). Computerised maintenance analysis gave rise to predictive forecasting maintenance.

The importance of maintenance has not diminished. Recently, in 2016, US manufacturers spent an estimated \$50 billion on maintenance and repair, which corresponds to between 15% and 70% of the costs of produced goods (Brundage et al., 2019). Zonta et al. (2020) estimate the maintenance costs between 15 and 60% but notes that companies often mismeasure the spending ratio. The growing complexity of the supply chain, i.e., the interactions between different production segments in an increasingly extended manufacturing environment, has given maintenance even more importance. An interruption of one production segment can have severe consequences for other manufacturing processes (Zonta et al., 2020).

An example is the recent semiconductor shortage that interrupted car production, phones, entertainment consoles, and TVs. Loss of revenue in the automobile industry due to the chip shortage is estimated at around \$61 billion for 2021. Apple estimated a loss due to a chip shortage of between \$3 to \$4 billion in the second quarter of 2021 (Voas et al., 2021). Therefore, it is unsurprising that maintenance improvement is emphasized again in the current orientation towards the digital transformation of the industry, also referred to as Industry 4.0.

The term *fourth industrial revolution* originated from German Industries to meet the demand for innovation in response to new technologies (Zhou et al., 2015). These new technologies, e.g., connectivity, big data, and new devices, especially the Industrial Internet of Things (IIoT), is expected to provide further inventory reduction, customisation, and production control. The philosophy behind this innovation is that predictive decisions can be made from information involving big data.

Internet of Things (IoT) is an intelligent device that can communicate wireless over the internet with other intelligent devices using Internet Protocol (IP) without interference from computers or humans. A vital business application is the tracking of goods in the supply-chain network. The industrial variant is the IIoT, involving intelligent devices that communicate wireless or wired through the internet or the local ethernet. IIoT devices do not necessarily communicate between themselves but can be linked to a service platform, an operational technology system. Besides the feedback of their actions, IIoT devices can give a multitude of additional information, e.g., their health status (Jaidka et al., 2020). The manufacturing sector's share of deployment of IoT devices will be 33% by 2025. A smart connected factory can produce approximately one Petabyte of data per day (Liu et al., 2019).

Although Industry 4.0 mainly focus on addressing data analytics and machine learning methods to change production processes (Zonta et al., 2020), a critical part of Industry 4.0 is the digitalization of maintenance from both a technological and a management perspective (Silvestri et al., 2020).

Digitalization of maintenance involves maintenance modelling. The prominence of maintenance modelling in operational research goes back decades (Pidd, 2004). Academic publications on maintenance modelling started in 1965. Of notice of these early publications are a book *The Mathematical Theory of Reliability* by Barlow and Proschan (1965, cited in Cho and Parlar, 1991) and the papers, *Maintenance Policies for Stochastically Failing Equipment: A Survey* by McCall (1965), *A Survey of Maintenance Models: The Control and Surveillance of Deteriorating Systems* by Pierskalla and Voelker (1976, cited in Cho and

Parlar, 1991) and *Optimal Maintenance Models for Systems Subject to Failure* by Sherif (1982). The models were categorized by the knowledge of the system's state or the model relevance to the maintenance problem (Cho and Parlar, 1991).

With the evolution of maintenance strategy from time-based and condition-based maintenance to predictive and prescriptive maintenance, the role of maintenance modelling has increased in importance. Predictive and prescriptive maintenance is fed by field data but driven by mathematical modelling (Errandonea et al., 2020). Lately, a focus on artificial neural networks (ANN) has become popular due to increased data acquisition (Zonta et al., 2020). This tendency is reflected in the discussions about digital twins (DT) in maintenance. After production planning and control, the primary utilization of DTs is in maintenance (Kritzinger et al., 2018). This focus on DT in maintenance has increased in the last years (Errandonea et al., 2020).

7.2 A different approach towards a digital twin

The digitalization of physical systems goes back some two decades and since then has been referred to as digital twins (Grieves and Vickers, 2017). A digital twin (DT) was first conceptualised as a finite-element model of an aircraft structure (Tuegel et al., 2011) but is now understood as any virtual representation of an engineered object on a computer for the purpose of product or process planning. Another term for DT being used is the Cyber-Physical System (CPS), introduced around 2006 by the National Science Foundation (NSF) in the United States. It is referred to as the next generation of engineered systems (Zonta et al., 2020). However, the concept of the DT is still undetermined (Kritzinger et al., 2018).

A prominence in predictive and prescriptive maintenance research has resulted so far in the domination in the literature of the DT for maintenance modelling, focusing on early failure prediction and diagnosing the causes of failures and the symptoms (Errandonea et al., 2020; Silvestri et al., 2020; Zonta et al., 2020). This approach of a DT is mainly driven by Artificial Intelligence (AI) based on artificial neural networks (ANN). Adaptation of advanced maintenance strategies by implementing technology is oriented towards reducing unplanned corrective work and assistance to operators and maintainers. Academic research has further predominately addressed maintenance scheduling (Brundage et al., 2019).

Following the above, the DT functions as a short-term controller of an EO. Thus, probably seen from this perspective, Kritzinger et al. (2018) and Errandonea et al. (2020) claim that a true DT should involve all aspects of the physical system. Further, both the physical system and its DT should have fully automated interaction. In the thesis author's opinion, this is a

narrow view. That opinion is also supported by Liu et al. (2021). They conclude that a DT is not a specific technology but an idea that can be implemented with many advanced technologies. Therefore, the concept of a DT should be kept to its core, a digital entity that reflects the behaviour of the physical entity and keeps updating through the whole lifecycle (Liu et al., 2021).

So far, the DT in maintenance has been used to analyse the health condition by monitoring failure or modelling the reliability of the asset. Further, lifecycle optimization from the design phase onwards mirroring the physical object. A practical example of health condition monitoring is the aerospace industry, where aircraft reliability is simulated according to flight hours, integrating historical data and maintenance history (Negri et al., 2017).

The thesis author recognizes the vital role of the DT in monitoring failure and modelling the reliability of the asset, and mirroring the lifecycle for maintenance. However, another functionality a DT has to offer has been overlooked so far. This research proposes an additional role of a DT for maintenance modelling and projections. Besides projecting causes of failure, asset lifespan, and when to schedule interventions, modelling simulations can be applied to model maintenance effects in the presence of stochastic degradations, complicated by the fact that the maintenance interventions are imperfect repairs. To the thesis author's knowledge, no research has been published on this role of a DT so far.

A DT, in this case, does not need to represent all characteristics of the physical counterpart but can be limited to the specifics being investigated, using only relevant data and models (Haag and Anderl 2018). Similar, referring back to chapter 3.2.5, testing and validation, Pidd (2004) refers to a lumped model in computer modelling as a definitive and simplified version of the base model, the complete comprehensive hypothetical model.

The DT, as here proposed, bears some similarity to accelerated life testing (Elsayed, 2003) because a DT can show degradation and failure behaviours without having to wait for the real system to degrade and fail. Accelerated life testing has extensively been conducted in the weapons and space programs, where the lifetime requirements are limited to five to ten years. Compared to the nuclear power industry, where accelerated ageing testing is preferred due to safety concerns, the desired lifetime expectation is up to 40 years. Although accelerated life testing is supposed to speed up this process, this testing is still time-consuming for systems with long life expectancy (Carfagno and Gibson, 1980). Thus, safety concerns of systems with a long life expectancy can be tested in a much shorter time with a DT than with conventional accelerated life testing.

Equally, interventions that may slow degradation, prevent failure, restore functionality, and thereby reduce risk and increase performance, can be investigated quickly. Such interventions may extend over the entire product life cycle. The primary purpose of the here presented digital twin of an RO vessel is to study such interventions.

Maintenance modelling on its own has limited value. It must have a practical, workable connection with practitioners in the field. The latter is not always the case in academic publications, where published research, evaluated by their peers, often have no access to real-world problems. Consequently, part of the scientific literature on maintenance optimisation models is incompatible with an engineering mindset. The presented models are too specialist and lack an overall systems engineering viewpoint (van Rijn, 2007). According to the quoted author, a research manager at Shell in Amsterdam for decades, the real value of maintenance modelling lies in using a DSS, which helps the practitioner select a course of action among various alternatives.

This research, therefore, demonstrates a different approach to maintenance modelling. A DT is presented as a Decision Support System (DSS) engine. A DSS involving a DT was presented in the health care sector by Patrone et al. (2018). The purpose was to improve the management of operating rooms. Zhou et al. (2021) presented a DSS involving a DT for maritime port resilience analysis. Neto et al. (2021) presented a DSS involving a DT for opportunistic preventive maintenance scheduling. Here, the DT is a model of the shop floor. That DSS aims to exploit unexpected opportunities in the shop floor that resulted in low production throughput to undertake maintenance pitstops.

The presented DSS involving a DT in this thesis aims to establish the most effective maintenance requirements for (a subsystem) of an engineered object (EO). Therefore, the DT must simulate the current wear of the EO and further project the prolonged long-term state of the EO under stochastic wear conditions and uncertain imperfect repair.

In contrast to the black-box approach, i.e., a DT is driven by AI, the methodology of the proposed DSS and its underlying DT involves a combination of expertise in operational research and maintenance modelling with that of the specific engineering expertise of the system. The mathematical model and the DT derived from the model must collaborate these two fields of expertise. Process engineering expertise identified the unequal distribution of wear due to the amount of nutrition fed to the biofilm-developing microorganism, additional wear due to fouled trailing membranes and the restoration methods (chapter 4). Operational research identified the system as a unique multi-component system with stochastic extrinsic wear dependencies, intrinsic rate-state wear dependency, and stochastic imperfect repair

(chapter 5). Maintenance modelling expertise translated the mechanisms of degeneration and restoration into mathematical equations (chapter 6) and estimated the model parameters (chapter 6.2). Therefore, the DT, the thesis author developed, is a computer simulation of the model described in chapter 6.

With this simulator, we can investigate the effect of alternative restoration policies upon performance criteria of interest. These criteria are specifically the pressure and the cost rate (restoration). Without maintenance, the pressure differential (PD) will exceed the critical threshold of 3.5 bar, resulting in irrecoverable failure of the elements (see chapter 8.3). If the PD exceeds this threshold, the operation is no longer possible. Also, importantly, since decision-making about policies must acknowledge that there exist uncertainties about system behaviour and our knowledge of the system encoded in the model, and hence the DT, sensitivity to model parameters can be studied so that robust policies can be developed.

7.3 The architecture of the DSS

A DSS involving a DT of an RO vessel has been built using the mathematical model of degradation described previously. Figure 7-1 presents a schematic view of the DSS.

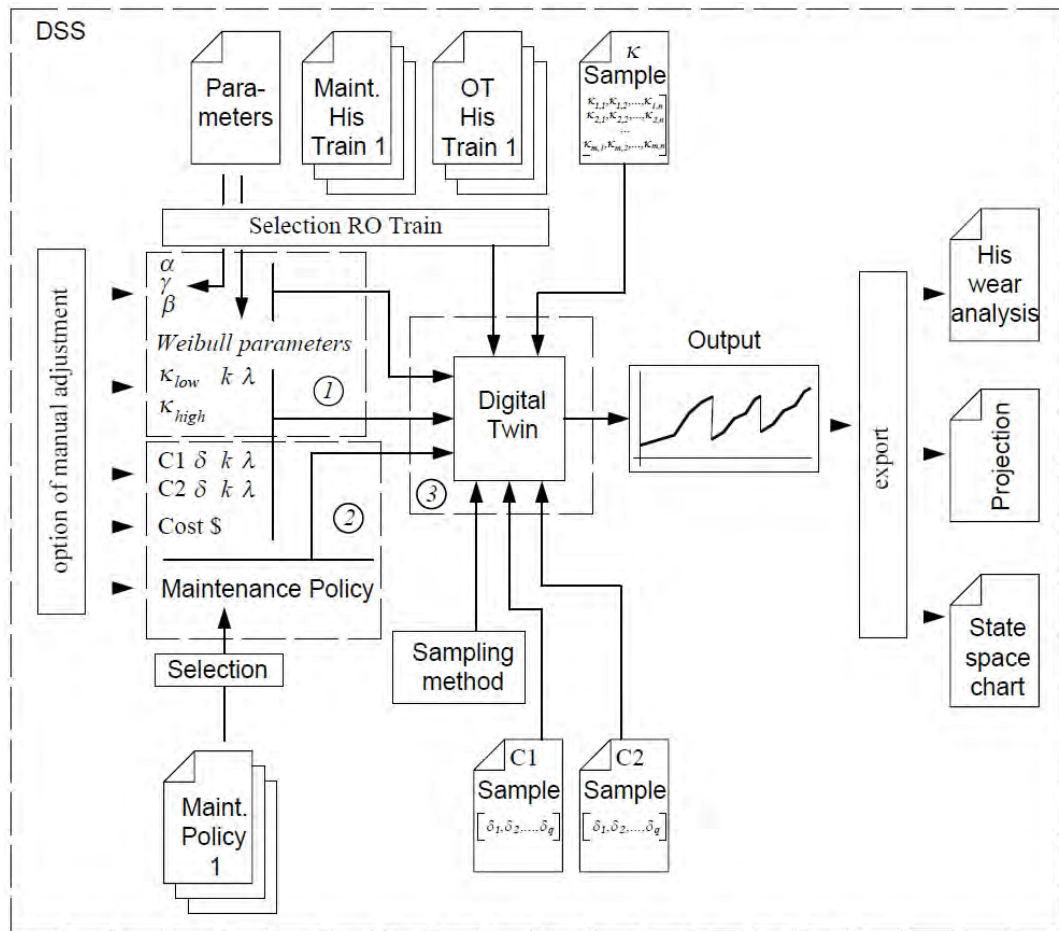


Figure 7-1. The architecture of DSS. (1) Data analyse module, (2) Planning module, and 3) DT.

The DSS is data-driven, and the data source can be updated as needed. The DSS selects what data is required for the task and sends that to the DT. The modelling output of the DT is then returned to the DSS, where it is visualized and can be exported for external processing.

The DSS and its DT have been built in MATLAB utilizing App Designer, an object-oriented programming platform that includes a Graphical User Interface (GUI). MATLAB is a proprietary programming language that supports programs written in other languages, e.g., C, C++, Java, Fortran and Python. MATLAB was first utilized by researchers and engineers in control engineering (UpSkill, 2016). Besides the object-oriented programming of GUIs, there is further no difference in approach between App Designer and the standard or Live editor. The App Designer code of the DSS can be transferred to the MATLAB editor with the same results. A comprehensive explanation on how to program with MATLAB, including the App Designer, has been presented by Attaway (2018).

The user interface of the DSS is graphical, showing tables, numeric inputs, trend plots and buttons. The DSS is presented as a typical computer application, with the coding hidden behind the interface. So, the practitioner does not need any programming skills, nor is deterred by a presented programming code. The GUI of the DSS is shown in Figure 7-2.

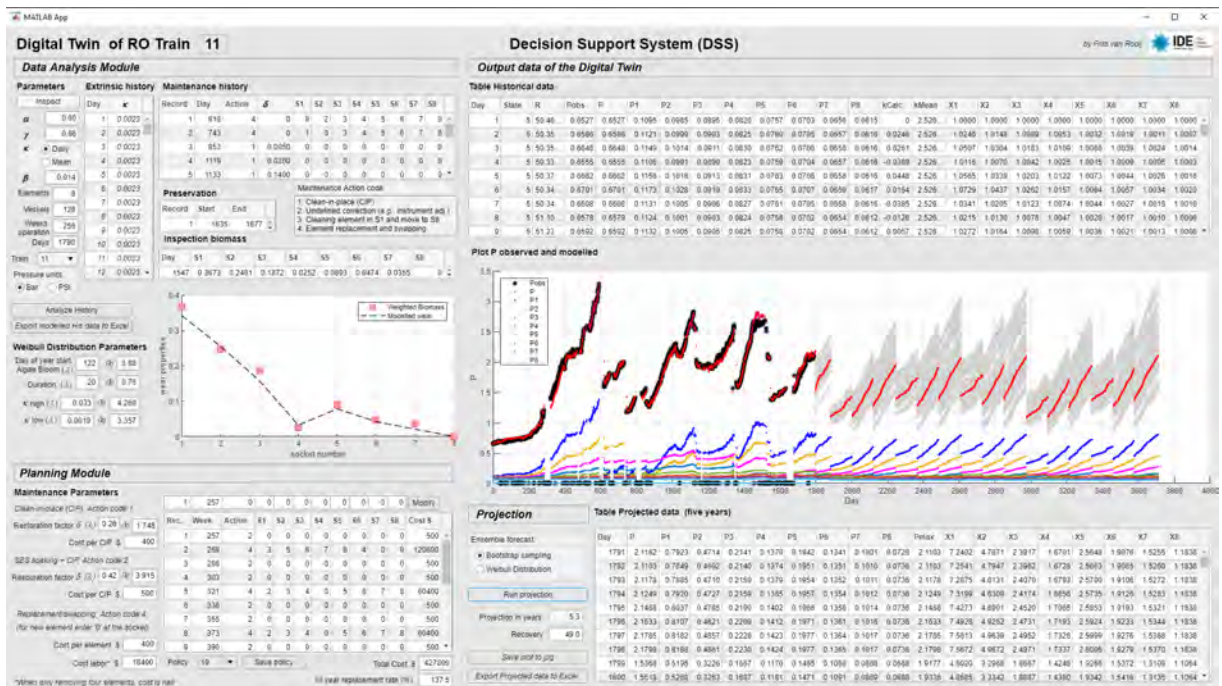


Figure 7-2. Interface (GUI) of the decision support system (DSS).

A functional presentation of the GUI will follow. Here is a brief architectural presentation. Each item displayed is a user interface (UI). Some of the UIs are shown here.

UIFigure

Method

matlab.ui.Figure

matlab.ui.container.ButtonGroup

| | |
|----------------------------|------------------------------------|
| Ensembleforecast | matlab.ui.control.RadioButton |
| MaintHistory | matlab.ui.control.Table |
| DataAnalysisModuleBanner_2 | matlab.ui.control.TextArea |
| DSSLabel | matlab.ui.control.Label |
| RunHis | matlab.ui.control.Button |
| TrainDropDown | matlab.ui.control.DropDown |
| Vessels | matlab.ui.control.NumericEditField |
| DataAnalysisModuleBanner | matlab.ui.control.TextArea |

The program in App Designer is ordered in sub-programs. Triggers (events) are radio buttons, buttons, and dropdown lists. Each event is a UI (see above). These UIs, having an event, are separate sub-programs. An example of an event exporting the Modelled variables of a train is presented below.

% Button pushed function: HisDataToXLS

```
function HisDataToXLSButtonPushed(app, event)
    switch app.DigitalTwinofTrain.Value
        case 0
            % No action
        case 1
            writetable(app.UITableHis.Data, 'Train1.xls');
            ...
        case 14
            writetable(app.UITableHis.Data, 'Train14.xls');
    end
end
```

A flowchart of the DSS program in MATLAB App Design is shown in Figure 7-3. Any variable declared in a sub-program is considered local and not transferred to the next program section. The notation “app.” is placed before the variable name to enable a variable to be retrained and transferred throughout the program. These app variables must be declared at the beginning of the program under properties. For example, the following program command contains local variables, x , i , j and a global variable, $app.Xhis$.

```
x = x - app.Xhis(i-1,j);
```

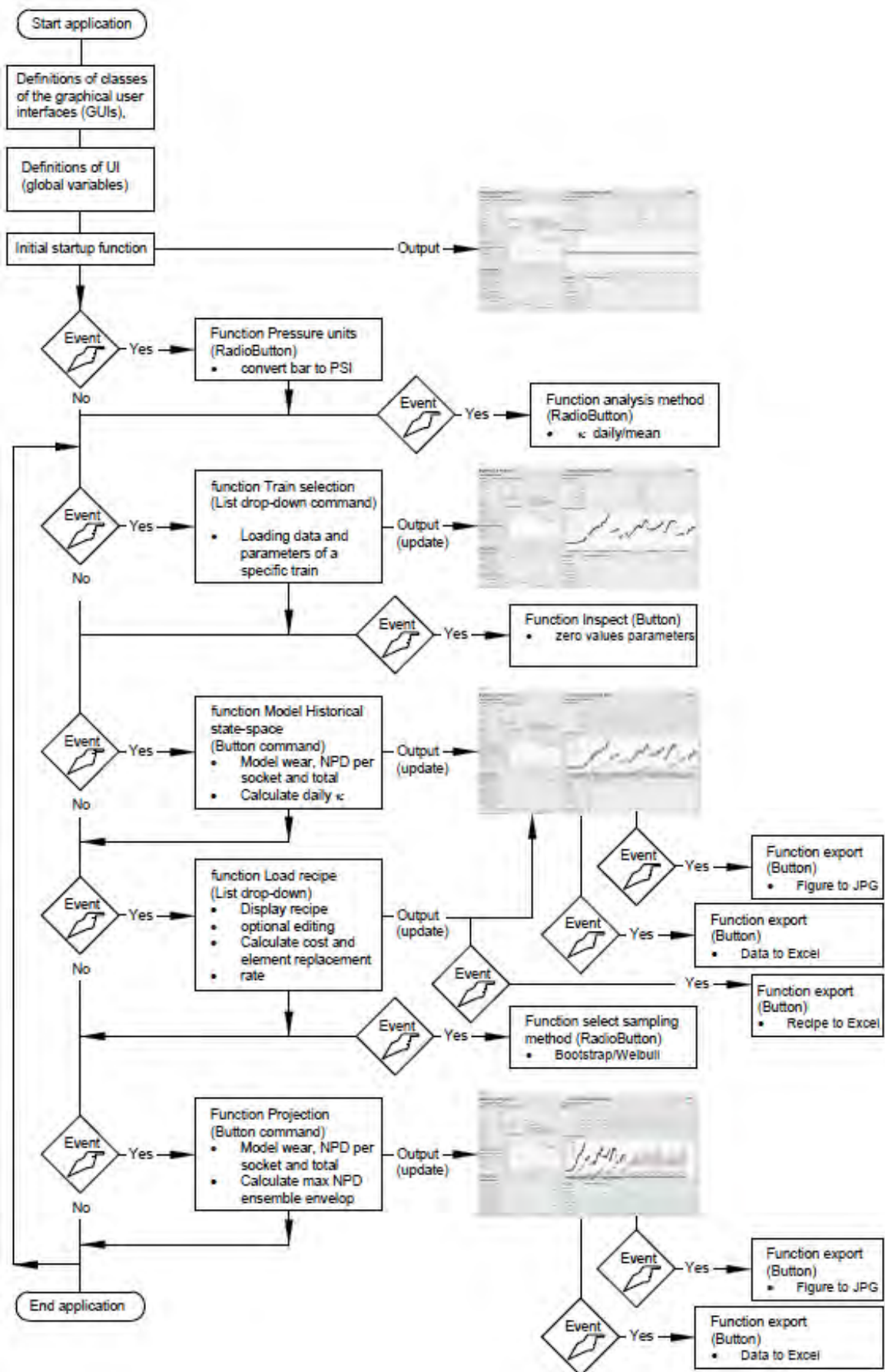


Figure 7-3. Flowchart App Design DSS

7.3.1 Data sources

The data being fed to the DT is in Microsoft Excel format. Importing data from excel files allows the practitioner to review and make modifications beforehand. Similarly, the OT management information system (MIS) data and the CMMS are produced in excel. Besides the MIS and the CMMS data, separate excel files containing the parameters for the model and the bootstrap matrixes and maintenance policies. The supporting excel files of the DSS are shown below. The extensions of the excel files are omitted:

1. CIPHIS, containing the bootstrap vectors of δ for CIPs with C1 and C2 methods.
2. InspectTi, $\{1 \leq i \leq 14\}$, containing the day and results from the membrane inspection.
3. Traini, $\{1 \leq i \leq 14\}$, containing the historical OT data of the train.
4. MaintHisTraini, $\{1 \leq i \leq 14\}$, containing the maintenance data from the CMMS.
5. PresvTi, $\{1 \leq i \leq 14\}$, containing the CMMS data of day and length of SBS preservation of the train.
6. Kappai, $\{1 \leq i \leq 14\}$, containing mean κ between changepoints.
7. Parameters containing the parameters α , β , γ , and κ_1 and κ_2 for Weibull distribution.
8. Policyi, $\{1 \leq i \leq 12\}$, containing the maintenance policies.
9. KappaMatrix, containing the bootstrap source matrix of κ .

The DT gives a separate output of the state-space data analysis and the projections. The DT allows for sensitivity analysis used in this research (see section 7.6.1. Data analysis module). Further, data can be exported from the DSS to excel.

The state-space analysis is rewritten to the excel file Traini, $\{1 \leq i \leq 14\}$, where the daily κ , X_j , ΣP , and P_j $\{1 \leq j \leq 8\}$ are added to the table. X_j is the modelled wear per element, ΣP is the modelled NPD of the vessel, and P_j is the modelled NPD per socket. The DT projection is simultaneously exported into two excel files.

1. EnsembleTraini, $\{1 \leq i \leq 14\}$, provides a matrix of the ensemble envelope.
2. ProjectionTraini, $\{1 \leq i \leq 14\}$ provides the mean of X_j , ΣP , and P_j $\{1 \leq j \leq 8\}$ and the max ΣP of the ensemble envelope. ΣP , and P_j $\{1 \leq j \leq 8\}$ can also be exported as a plot figure, which includes the modelled historical state-space.

MATLAB makes it easier to perform computations on matrices instead of tables. Therefore the tables are converted to a native matrix format. Excel file read command and conversion to a native matrix format is presented below, followed by a write command.

```
Table = readtable("Table.xlsx");
```

```
Matrix = table2array(Table);
writetable(Projection, 'ProjectionTrain1.xlsx');
```

7.4 Modelling Historical State-Space

The functions ‘Model Historical State-Space’ and ‘projections’ (See Figure 7-3) are of most interest for the discussion of this chapter. The source code of these two functions is presented in Appendix D. Below (Figure 7-4), a simplified block diagram of the function ‘Model Historical State-Space’ is presented.

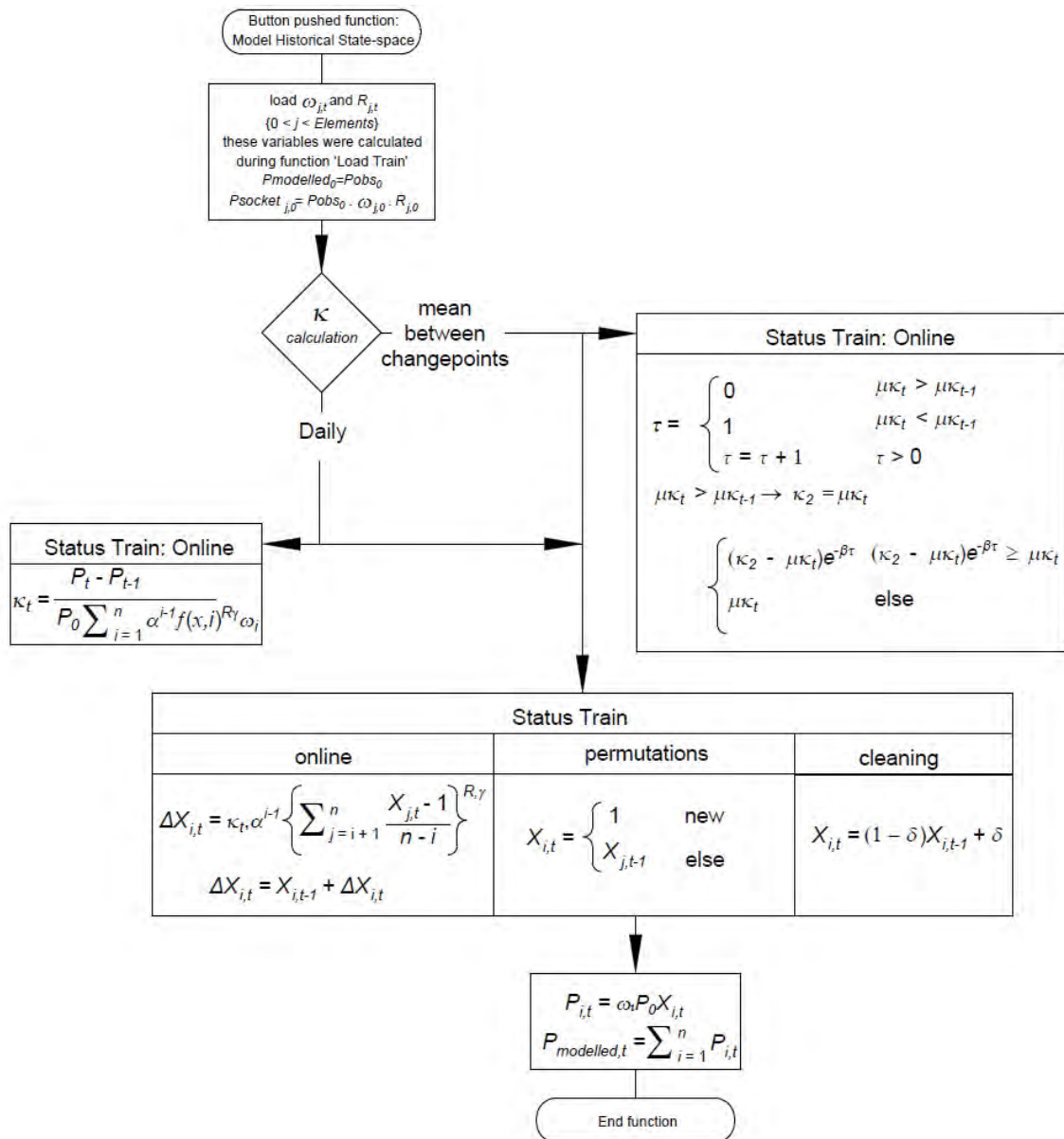


Figure 7-4. Flow chart diagram function ‘Model Historical State-Space.’

The purpose of the function ‘Model Historical State-Space’ is to build a virtual replica of the observed NPD by modelling the degradation $X_{i,t}$ per element. Knowing the latter is

essential for any decision-making and refers to the first principle of level 4 of the Maintenance theory framework presented in chapter 1.2.1 (see also Figure 1-1). The modelled NPD over the elements and the sum, the modelled NPD over the vessel, are derived from the modelled $X_{i,t}$.

The state $X_{i,n}$, where n is the last day of the modelled State-Space, is the point of departure for the projections, so this function must be performed before projections occur.

There are two methods to derive κ for modelling the state-space. *Daily*, the first method derives κ at discrete daily intervals from the difference between the observed NPD from one day to the next, using eq. (19). Since the observed NPD is only known when the train is in operation, κ can only be defined during this state.

As mentioned in chapter 5.1.1, a sudden reduction of NPD can occur after a train has been offline. This reduction is expected to be a reaction to Low Salinity (LS) flushing, which can be considered an unplanned hydraulic physical cleaning. Consequently, the modelled NPD will continue from the last observed NPD and do not compensate for the effect of LS flushing. A maintenance event can be included to correct this behaviour, modelled the same as cleaning. The maintenance or action code “2” (see below) marks that this was not a planned intervention. The daily κ method further gives the best fit between modelled and observed NPD.

The alternative method is by mean κ between changepoints. The mean κ between changepoints must be defined before the modelling occurs. Section 7.6.1 Data analyse module presents methods for configuring the mean κ between changepoints.

Since this method intends to fit κ over longer discrete intervals, based on observed changes in the slope of the observed NPD or by changepoint analysis, this method provides a lesser fit than the former method. This method aims to provide another tool for parameter estimation to that presented in chapter 6.2.

As described in chapter 6.2.2, κ becomes κ_{low} before and between algae blooms and as κ_{high} during algae blooms. The severity of κ_{low} and κ_{high} can change at each new event, i.e., bloom or non-bloom. These events do not have to follow the recorded algae bloom events of the O&M reports but can be based on the observations of the observed NPD. Then a new period where κ_{high} is replaced with κ_{low} , κ_t decays using eq. (14), where τ the days since returning to κ_{low} .

The daily and the mean κ methods generate a vector κ_t at discrete daily intervals with identical properties. The vector length is $1 \leq t \leq n$, where n is the end day of the state space.

Thus, the following model sequence is identical, regardless of the method defining κ .

Four options are possible: the train is online, offline standby or offline undergoing permutations or cleaning, depending on the state of the train and if the maintenance history records an action. The status of the train is an integer that represents the following conditions:

0. Shutdown, Train set to not available by operator
1. Master Fault
2. Standby
3. Individual Seawater (SW) filling/flushing
4. Individual Pressurization or bacterial sampling off-spec
5. Operation
6. Individual depressurization
7. SW Flushing
8. Waiting for Low Salinity (LS) Flushing
9. LS flushing
10. Cold startup (Full RO Plant common startup)
11. Cold shutdown (Full RO Plant common shutdown)
12. CIP (not including C3)

The DT needs to know when the train is online; therefore, only state 5 is of interest. An integer representing a maintenance action code identifies maintenance actions from the maintenance history file. The action code stands for the following:

1. CIP.
2. Unidentified correction, e.g., LS flushing or instrument adjustment.
3. C3, a discontinued cleaning experiment (see chapter 8).
4. Permutations.

The wear $X_{i,t}$ is calculated as follows, if online eq. (12) followed by eq. (11) are executed. In case of a maintenance intervention, when performing permutations, eq. (15). In the case of a CIP or an unidentified correction, eq. (16). C3 involves permutations and an externally cleaned lead element placed in socket 8. Since we cannot measure the effect of the single element cleaned, an approximation of this elements degradation is given as $X_{8,t} = 1.1$; The modelled NPD per socket and overall are then derived from eq. (5) and eq. (4).

7.5 Modelling Projections

A simplified block diagram of the function ‘Projection’ is presented below (Figure 7-5). Essentially the modelling of the projections is identical with the modelling of the historical state-space, with two differences, instead of deriving κ from the changes in the observed NPD by eq. (19), κ is a probability estimation, and a hundred different estimations per day are generated. The latter also applies to the cleaning effect δ . When modelling the historical state-space, δ is calculated from the changes in observed NPD before and after the

intervention utilizing eq. (17). For the projection, δ is a probability estimation, and a hundred different estimations per cleaning event are generated. A hundred samples of these stochastic dependencies will result in a forecast envelope from the most likely best to the worst outcome.

The dependencies κ and δ are derived in two different methods, bootstrap sampling and Weibull distribution, discussed in chapter 6.2. The results are similar matrixes for κ and δ , in the case of κ , a 100 rows, 365 columns matrix. In the case of δ , a vector of 100 is generated separately for every cleaning event. The estimations of the dependencies are further equally applied for the wear estimation $X_{i,t,m}$, and restoration by cleaning.

The projection covers five years. Each year is probably different with the different occurrence of algae blooms. The seasonal variation is built into the source sample in bootstrapping sampling method. Each of the 365 columns of the source matrix provides 70 elements. Bootstrap sampling converts this to 100 samples per day. For the cleaning, bootstrap sampling provides 100 samples from the 28 usable C1 cleaning results and another 100 samples from the 24 usable C2 cleaning results.

In the case of the other method, Weibull distribution, first, the total projection span must be divided into lumps of a year. Then probabilities for the start and duration of algae bloom must be forecasted from a Weibull distribution. The start and duration of the blooms provide change points of periods where κ_{high} can be applied from a Weibull distribution, and the other parts decay from algae bloom conditions to κ_{low} , applying eq. (14). This procedure is then reapplied for every calendar year.

The wear $X_{i,t,m}$ is calculated equally to the historical state-space model. The model assumes the train is online if no maintenance is scheduled, resulting in eq. (12) followed by eq. (11). The dimension m represents the 100 probabilities. The number 100 is a compromise between the accuracy of the probability uncertainty and the computing load of the projections. In case of a maintenance intervention according to the policy under evaluation, when performing permutations, eq. (15) is applied to each preceeding probability $X_{i,t,m}$. In the case of a CIP, eq. (16) is applied to each preceeding probability $X_{i,t,m}$, selecting a different sample m from the vector $\delta C1$ or $\delta C1$, depending on the policy.

The modelled NPD per socket and overall are then derived from eq. (5) and eq. (4), for each probability of $X_{i,t,m}$. For the indicative purpose only, a mean estimation is given. The complete DSS application with the source files of this research is available on request. The application is shared as a stand-alone application for stakeholders who do not have a MATLAB license or a MATLAB app (see appendix A).

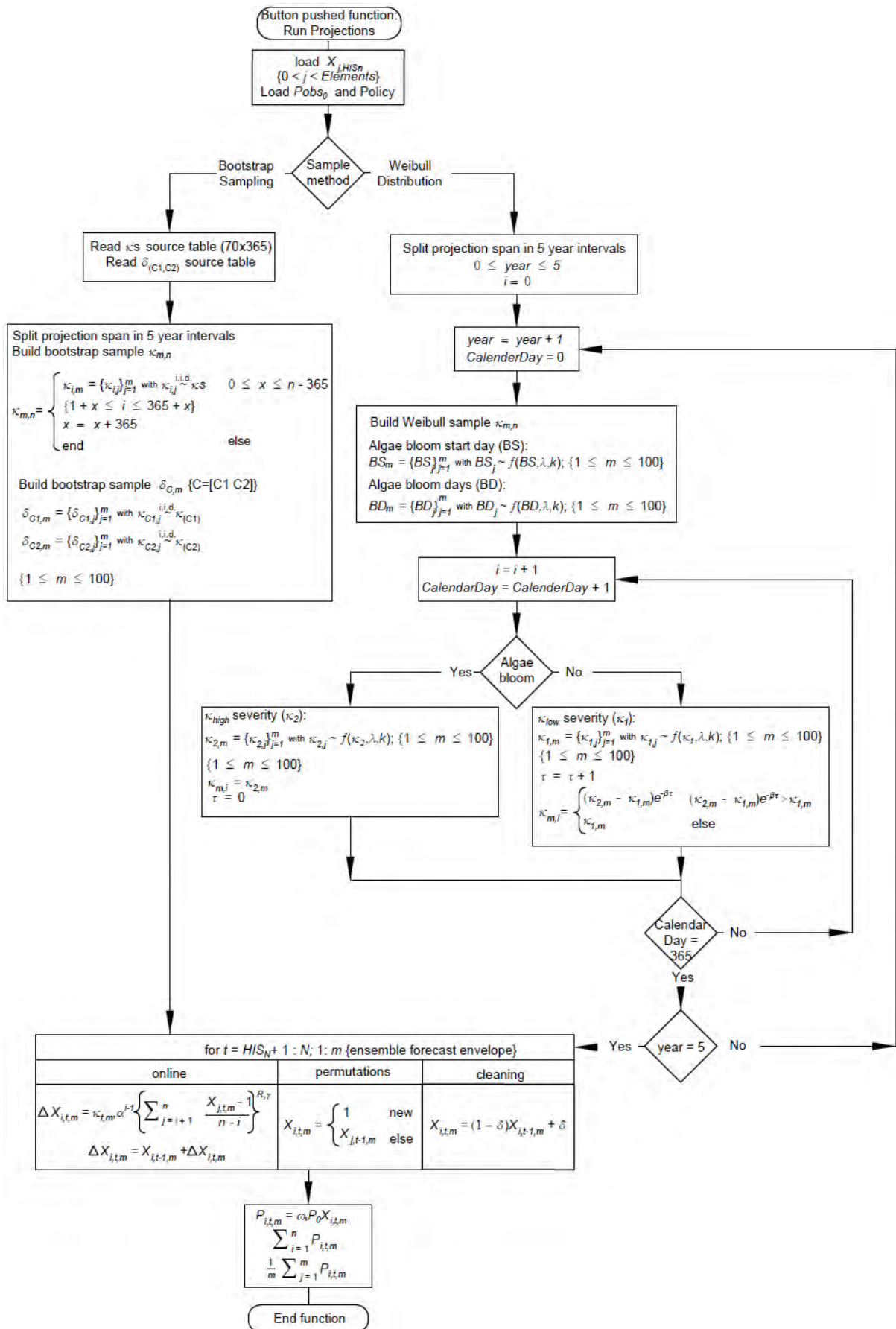


Figure 7-5. Flow chart diagram function 'Projection'.

7.6 Modules of the DSS

The DSS has three modules: a data analysis module, a planning module, and the DT. The planning module allows for different restoration policies to be studied. It uses the DT to simulate NPD and cost trajectories for a specific policy. The DSS runs the DT in the background. The DT first models the NPD according to the model parameters (red pen in figure 7-2) and compares that against the observed NPD (black pen). According to the modelled wear per element, the DT calculates the NPD per socket (other coloured pens). The planning module allows for different restoration policies to be studied.

7.6.1 Data analysis module

The data analysis module lets the user select a train, and consequently, the corresponding historical state-space data from the OT, parameters and maintenance history are loaded into the DT. Updated data files can be placed into the working folder before starting the DSS.

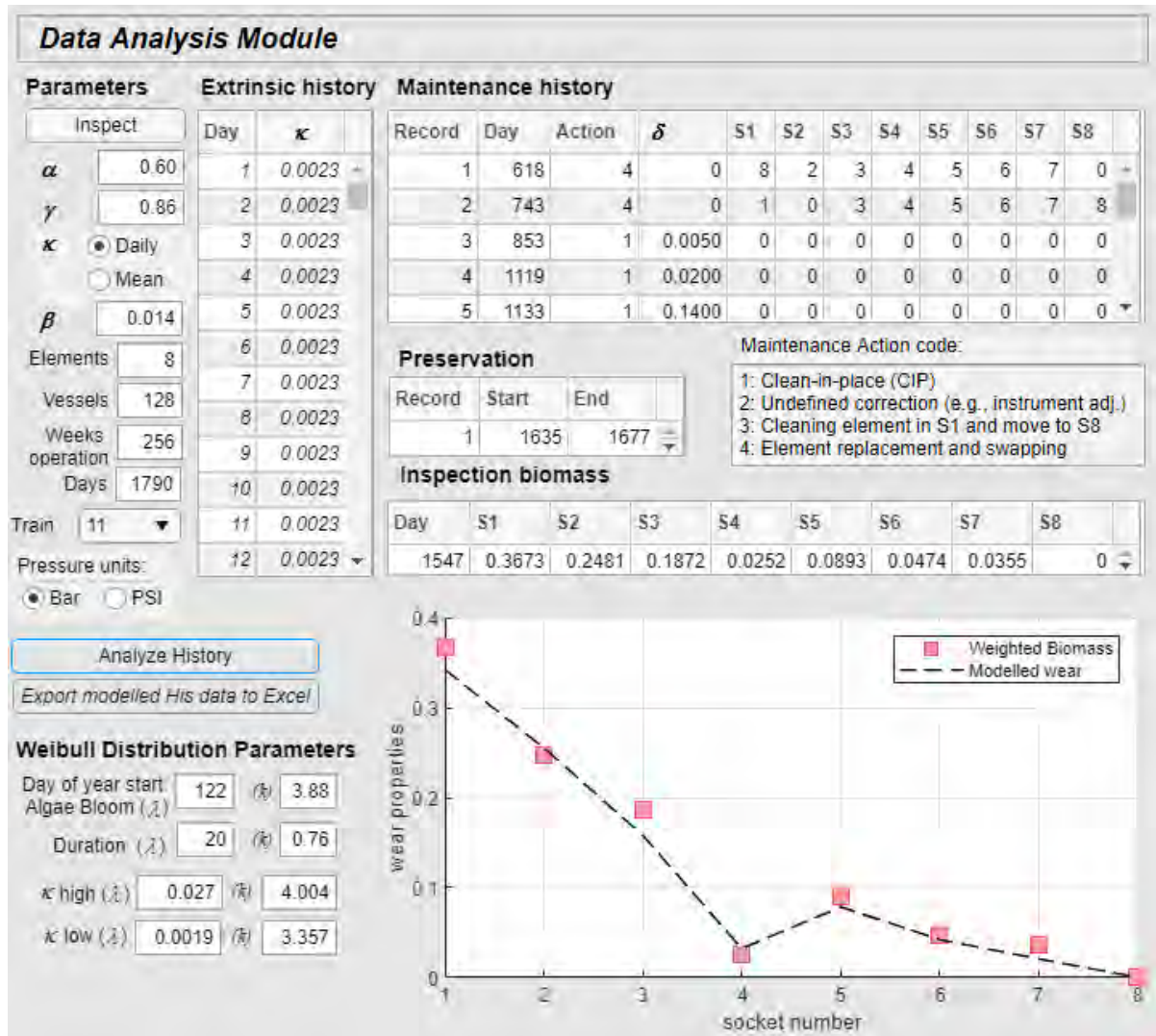


Figure 7-6. Data analysis module of the decision support system (DSS).

Several excel files are imported from the background by selecting a train from the drop-down menu. These files are tables of pre-configured data and are located in the working folder of the application. The tables being loaded are as follows:

- Historical RO performance data, including the day of operation, daily NPD, Train state, and recovery.
- Maintenance history of CIP with corresponding δ value; element replacements and relocations.
- Biomass inspection with the day of inspection and distribution of biomass per element.
- Periods of prolonged preservation with SBS (from April to May 2020).
- Mean values κ from the changepoint analysis.
- Deterioration parameters α , γ , β , κ_1 and κ_2 .
- Matrix of daily κ (70,365) for bootstrapping.
- Vector of C1 cleanings and vector of C2 cleanings for bootstrapping

Except for bootstrapping, all imported tables are presented at the DSS output screen. Although the imported NPD data is in bar, the DSS converts the units to PSI if preferred. Radio buttons for bar or PSI units are provided (see figure 7-6).

Besides adjusting the parameter file externally in advance, the parameters can be updated interactively from the screen. The parameters α , γ , β , the number of elements in the vessel, vessel quantity per train and the Weibull parameters for κ can be interactively updated from the screen. Manual manipulation allows for exploring the effects of the parameters. These updates are, however, not saved. Saving of parameters must be done directly at the parameter excel file. When another train is selected, the parameters are overwritten for the newly selected train. Therefore the entered values in the data analysis module are lost, except if they are updated in the parameter excel file (see Figure 7-1).

The purpose of the data analysis module is for sensitivity analysis of the parameters. A reference for sensitivity analysis is the preparation for estimating α (see chapter 6.2.1). During this estimation, the historical State-Space was modelled for discrete values of α between 0.4 to 0.8. The plot in the data analysis module gives a visual impression of the fit. To demonstrate, below the plots for α 0.4, 0.6 and 0.8 at train 11 are presented in Figure 7-7. Another sensitivity analysis example is the value assigned to γ for the above procedure. From the sensitivity analysis, setting $\gamma = 1$ will not significantly influence α , as stated in chapter 6.2.1. Figure 7-8, generated by the data analysis module, confirm this.

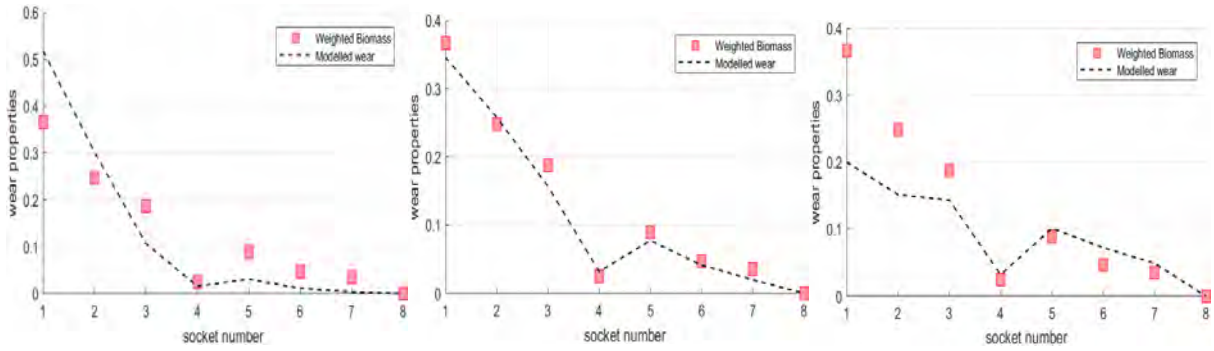


Figure 7-7. Model – biomass fit plots for train 11 at the Data analysis module. For α left 0.4, middle 0.6 and right 0.8.

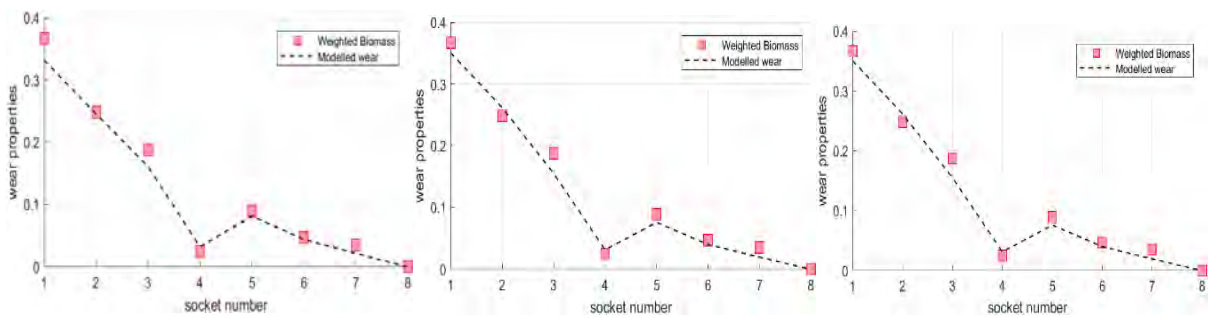


Figure 7-8. Model – biomass fit plots for train 11 at the Data analysis module with $\alpha=0.6$ and γ left 0.4, middle 0.8 and right 1.2.

The estimation of the Weibull parameters for κ_{low} , κ_{high} and β can be evaluated, whereby the modelled or simulated trajectory is compared against the observed historical state-space. The Weibull distribution parameters for κ are intended for the projection and do not affect the historical state-space modelling. However, sensitivity analysis allows comparing the bootstrap sampling method against the Weibull distribution for projection.

The mean κ option must be selected to perform this approximation. Two radio buttons are provided at the data analysis module to select the method (see Figure 7-6). In this option, the parameter β is utilized. This method for defining κ utilizes the imported mean values κ from the changepoint analysis. Any changes must be made at the $Kappai$, $\{1 \leq i \leq 14\}$ import file and then reloaded. However, the mean values of κ give a less precise fit between modelled and observed NPD, and the purpose is mainly for sensitivity analysis.

The modelled or simulated trajectory and the actual trajectory are visualized in the plot and table at the right of the data analysis module. The DSS runs the DT in the background. As described in section 7.3, the DT first models the wear X and after that, the NPD according to the model parameters (red pen in Figure 7-9) and compares that against the observed NPD

(black pen). According to the modelled wear per element, the DT calculates the NPD per socket (other coloured pens).

After executing the DT, by clicking on the “Analyse History” button, the wear per element at each socket, the overall modelled NPD and that per socket are calculated per day. The results are shown in the table above the plot (see Figure 7-9). Further, the observed NPD and the modelled NPD of the vessel and per socket are plotted. The modelled data of the data analysis module can be exported to excel by clicking on the “Export His data to Excel” (see figure 7-6). The excel file will be stored in the working folder of the application.

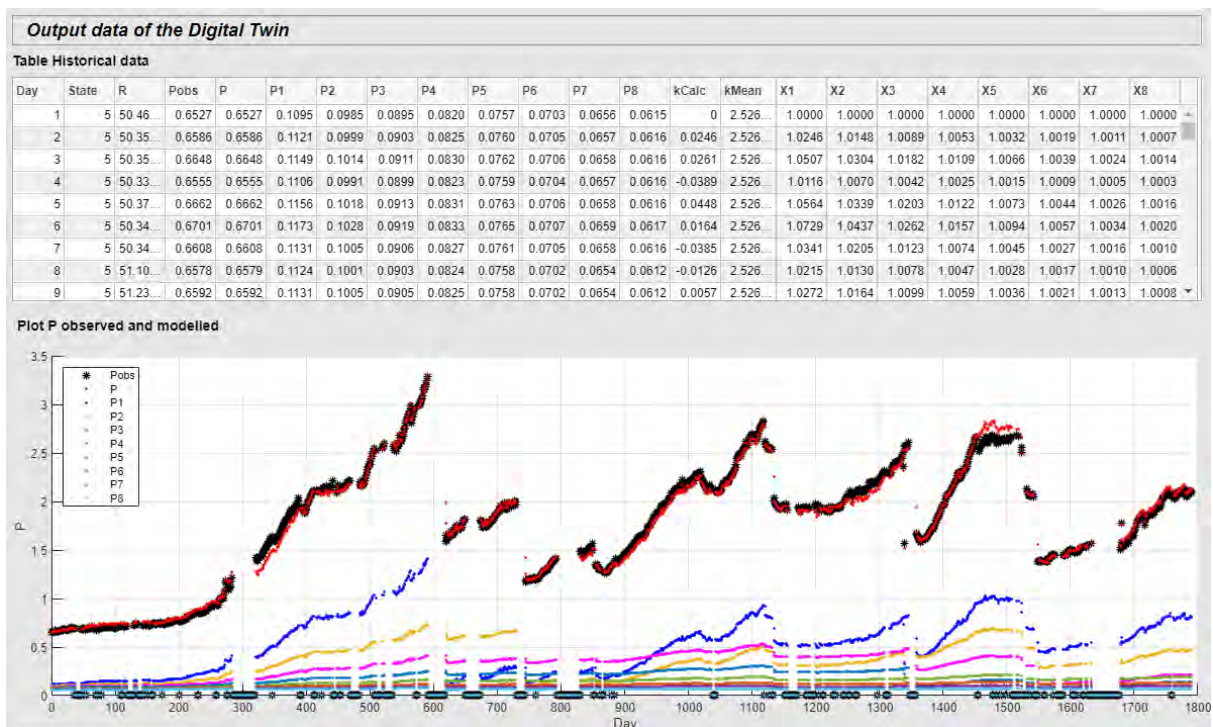


Figure 7-9. The output of the DT of the modelled state-space. Top in a table, bottom a plot.

7.6.2 Planning module

The planning module allows for different restoration policies to be studied. Thus, neither the DT nor the DSS generates a policy. The DSS uses the DT to simulate NPD and cost trajectories for a specific policy. The Planning module allows drawing various maintenance policies. Maintenance parameters for δ at CIP methods C1 and C2; the cost of CIP according to the method; the cost of a new membrane element; and the labour cost for membrane replacement/relocation can be adjusted at the planning module. The application loads the default values for CDP at the time of the building of the simulator. Maintenance policies can be created directly by interacting with the planning module, or pre-defined policies can be loaded from the dropdown menu. These predefined policies are Excel files located in the

working folder of the application. The maintenance policies can be adjusted externally or in the planning module. In the latter case, the policy can be saved by clicking “save policy”. The policy is stored again in the working folder.

According to the policy, the corresponding costs per maintenance activity are calculated, and the total sum is shown below the table. Besides the cost, the 10-year element replacement rate is also calculated based on the policy and train history (see Figure 7-10).

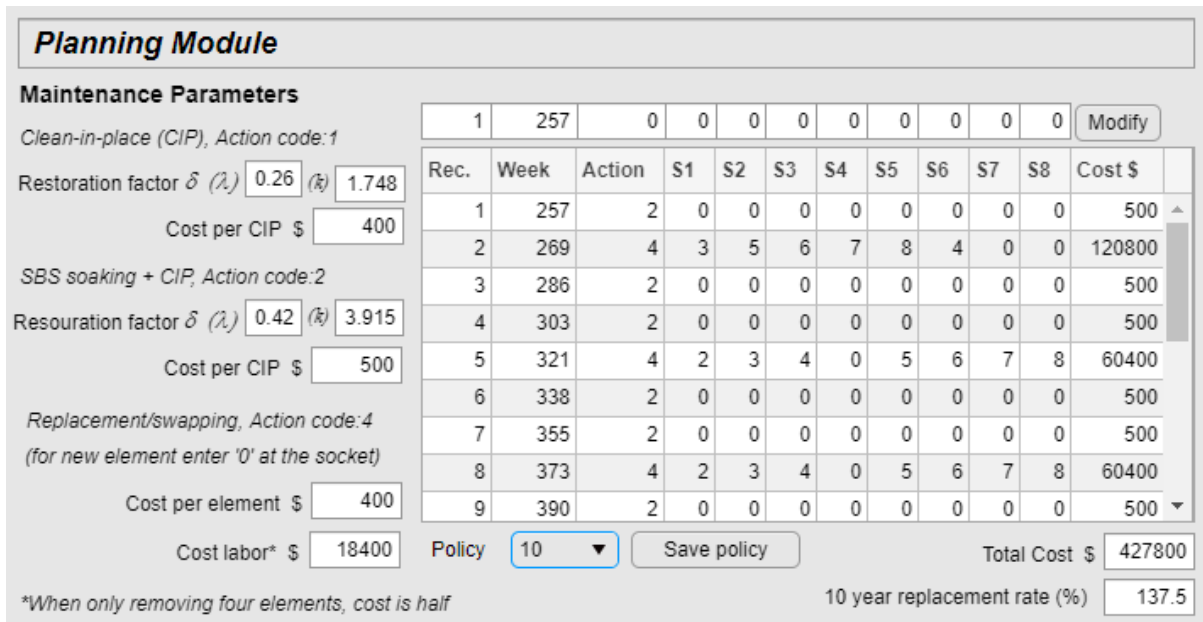


Figure 7-10. Data analysis tool and planning module of the decision support system (DSS).

As mentioned, the planning module does not require updating the external excel file and importing the updated file again to make any changes to the policy. Figure 7-10 shows a random policy. Any row can be edited from the editing row at the top of the table. The cells of the editing row correspond with the table header.

If the button “Modify” is pressed with the current input, the first record will be overwritten, whereby the action “2” will be deleted. The update from the editing row is as follows:

Cell 1: Record of the table to be updated.

Cell 2: Week of maintenance intervention.

Cell 3: Maintenance action code. An explanation follows.

Cell 4 to 11: Permutations. An explanation follows.

The maintenance action code represents the following intervention types:

1. CIP using method C1.
2. CIP using method C2

3. Discontinued cleaning method C3 (see chapter 7.3)
4. Permutations.

The above selection of maintenance actions can be easily adapted if additional maintenance actions become available.

When planning permutations at each socket S_i , the number of the elements' previous location S_j is entered. So, for example, if an element is moved from socket S_4 to socket S_1 , the cell corresponding to S_1 gets the value 4. If a new element is placed in a socket, say, S_4 , the cell corresponding to S_4 gets the value 0.

The cost of the maintenance intervention, the overall policy cost and the ten-year membrane replacement rate are automatically recalculated. If for any reason, only the cost of the elements is required, then \$0 can be entered for the cleaning and labour costs. It is not required to save the policy update for running the projection. However, if saving is preferred, this can be done by clicking “save policy” (see Figure 7-10). The updated policy will be exported to an excel file with the same name as the selected policy and stored in the working directory. If the loaded policy file was located in the working directory, then the previous excel file of the policy will be overwritten with the modified file.

7.6.3 Projection

Ensemble forecasting is a method to improve projections with uncertainties (Zhu, 2005; Hollyman et al., 2021). Ensemble forecasting is applied in various fields of research. Zhu (2005) presented ensemble techniques for weather forecasting. Shahriari et al. (2020) presented an ensemble forecast method for traffic flow prediction. Pan et al. (2022) presented an oceanic storm surge model utilizing ensemble forecast. The ensemble spread or envelope reflects the uncertainty and provides possible probability variation (Zhu, 2005; Pan et al., 2022).

This research applies ensemble forecasting to reflect the spread of probability of the projected NPD. Each discrete time interval, 100 random values from a distribution of κ are selected. The increase in degeneration from t to $t+1$ can vary due to variation of the extrinsic dependency from κ_{max} to κ_{min} probability. In successive n intervals, this is repeated. So the spread of probabilities from one day to another generates new probabilities, and the uncertainty is multiplied. The latter is expressed in the ensemble forecast envelope of Figure 7-12.

Equally, following an imperfect restoration, i.e., cleaning, the decrease in degeneration can vary from δ_{max} to δ_{min} probability. In the case of imperfect restoration, 100 random values

from a distribution of δ are selected. When applying permutations, those elements which are replaced, the state is fully restored, so there are no uncertainties. However, the other elements not replaced will transfer their previous variation of probabilities with them. So, if all elements were replaced during a maintenance intervention, there would be no uncertainties, $X_{i,t+} = 1$. This spread in the uncertainty of the probability over time is the ensemble envelope.

Following a “Run Projection” command (see Figure 7-11), the DT compute an ensemble forecast for the following years. The outcome of the projection depends on the train’s operational and maintenance history, the specific degeneration parameters of the train, i.e., α , γ and β and the selected maintenance policy.

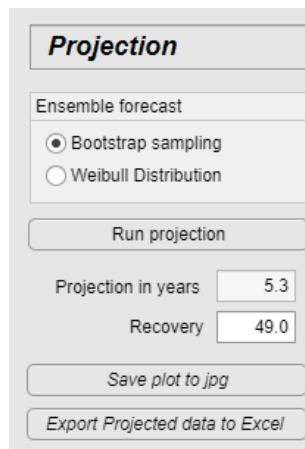


Figure 7-11. Projection control box

Figure 7-12 shows the output of the DT as a plot of the modelled NPD (left part of the plot) and the projection (right part of the plot). A grey area plot can be seen at the right part of the plot. This grey area is the ensemble envelope. The red pen, which divides the ensemble envelope approximately halfway, is the projected mean NPD of the vessel. The left part of the plot shows the observed and modelled NPD of the vessel (see also section 7.4). The mean NPD of the individual sockets is plotted using other coloured pens.

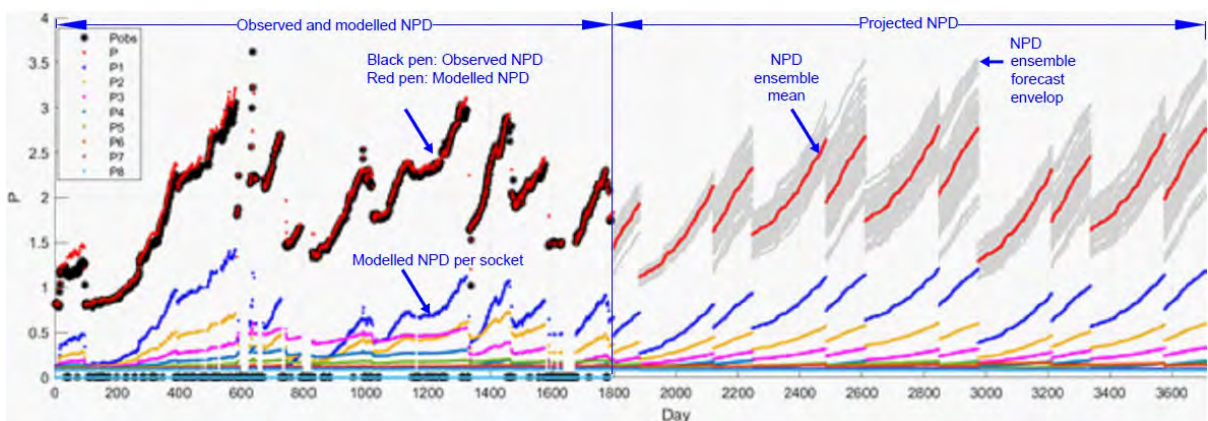


Figure 7-12: NPD projection output from the DT for one of the trains.

The mathematical procedure of the projection is described in section 7.5, involving bootstrap sampling and Weibull distribution for κ_t and δ_{C1} and δ_{C2} . Here is a summary. In the case of projection by bootstrap sampling, κ (feed quality) for each day of the projection is selected at random with replacement from its respective bootstrap sample. That is, κ for Jan 1st in year 1 of the projection is sampled from the Jan 1st bootstrap sample, and so on throughout year 1, repeating the same for year 2, and so on.

Then, clean-in-place is scheduled, and the individual cleaning effects are bootstrapped from each cleaning method's estimated cleaning effects samples (see section 6.2.6). Further, element swaps and replacements are scheduled. Their effects are known and deterministic. Then the wear model is run to obtain the projected states of each element and the implied NPD for the train for each day of the projection, using the estimates of the other parameters for that train and the user-defined system recovery R , which in turn implies ω_i . The projection is repeated 100 times to obtain the ensemble forecast (grey ribbon in figure 7-12) and the ensemble mean (red pen).

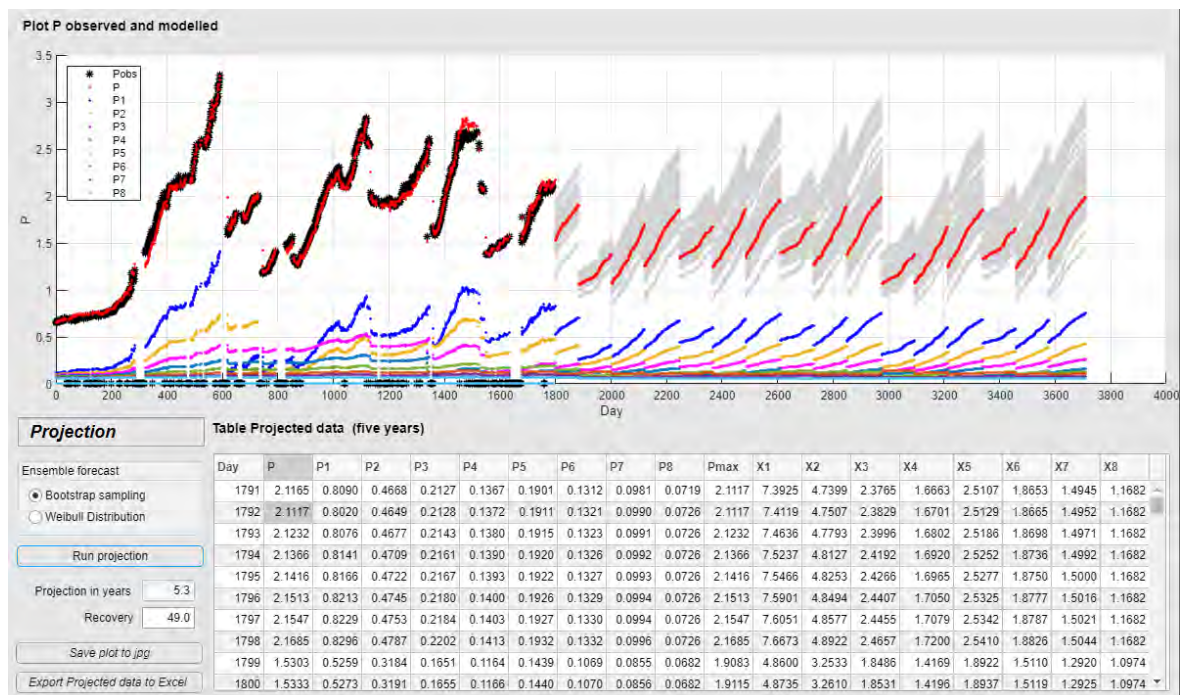


Figure 7-13: Projection interface of the DT.

In the case of projection by a Weibull distribution, κ_t (feed quality) for each day of the projection is selected at random based on the Weibull shape parameter k and scale parameter λ for both κ_1 and κ_2 . From the shape parameter k and scale parameter λ of the start day and the duration of the algae bloom, defined at the DSS (see figure 7-2), random start day and duration are calculated based on Weibull Distribution. This defines the period where $\kappa_t = \kappa_2$

or $\kappa_t = (\kappa_2 - \kappa_1)e^{-\beta\tau}$ is utilized.

After this, the daily wear is modelled over the projected period applying the selected maintenance policy (see chapter 8). In the case of a CIP, a random Weibull distribution is applied of δ per intervention, with $\delta \sim N(\delta_1, \lambda_1)$ for C1 and $\delta \sim N(\delta_2, \lambda_2)$ for C2. Finally, the daily NPD per socket is calculated and the vessel NPD. The output is visualized in a plot, and a table is shown in the visualization (see Figure 7-13).

The projection utilizing ensemble forecast executes nearly 200k calculation, which is understandable, time-consuming. Therefore, an execution progress bar is incorporated into the application to notify the user of the progress (see figure 7-14).

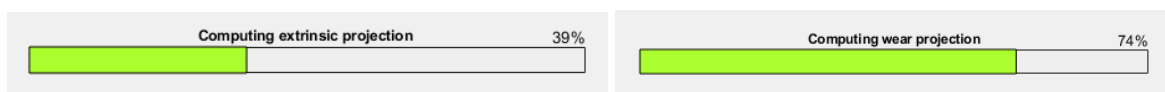


Figure 7-14: Ensemble projection progress bar.

7.7 Summary

Industry 4.0 has once again emphasised maintenance as a pillar of business strategy. The recent global supply chain disruption emphasised how delays in one production segment can be fatal. A breakdown of a vital asset at one production segment would have equal consequences. Industry 4.0 is driven by the objective of increased efficiency, providing further inventory reduction, customisation, and production control against the emergence of new technology. One of these is the increased availability of information from big data and digital technological innovation.

Maintenance through digitalisation has simultaneously developed towards Maintenance 4.0. Maintenance modelling has evolved into new dimensions with the deployment of Digital Twins (DT). The more recent attention on the concept of DTs in academic society has opened the debate of when a virtual representation of a physical object can be called a DT. Some researchers insist that a DT can only be called so if the virtual version includes all aspects of the physical object. Both the virtual model and physical object continuously should interact automatically.

Among the author of this thesis, other researchers maintain a more general definition. The concept of a DT should be kept to its core, a digital entity that reflects the behaviour of the physical entity and keeps updating throughout the whole lifecycle (Liu et al., 2021). The characteristics of the physical counterpart can be limited to the specifics being investigated, using only relevant data and models (Haag and Anderl, 2018). This concept applies to business modelling in general (Pidd, 2004).

The DT so far, among others, has been utilised in design verification, production and scheduling in general and in maintenance, specifically for anomaly detection. This research adds an additional dimension to the DT, the projection of the impact of maintenance on the long-term reliability of an engineered object (EO) against the prospects of stochastic degradation dependencies and imperfect repair. To the thesis author's knowledge, this has not yet been applied nor studied. The DT is embedded into a decision support system (DSS) and acts as its engine. The objective of the DSS is to support the maintenance practitioner in investigating the effect of alternative restoration policies upon performance criteria of interest. This research used a practical example of the degradation, restoration, and costs of reverse osmosis (RO) desalination trains in algae bloom amplified biofouling conditions to demonstrate the proposed concept of the DSS.

There are various approaches to how the DT is driven. Recently a popular approach is towards Artificial Intelligence (AI), involving artificial neural networks (ANN). This research presents a DT based on mathematical modelling. As with AI, the presented DSS is data-driven, and the data source can be updated in time to verify the previously tested policies or new alternatives. According to the selected sub-EO, the DSS sends the data to the DT and receives the modelled output back from the DT. Since the practitioner must consider uncertainties in the projection due to stochastic degradation dependencies and imperfect repair, the sensitivity of model parameters can be studied to develop robust policies.

The DSS and its DT have been built in MATLAB, a popular programming language under researchers and practitioners in control engineering. A Graphical User Interface (GUI) of MATLAB has been utilised, so the practitioner does not need any programming skills, nor is deterred by a presented programming code. Data in the form of excel files are automatically imported. The DT output is visualised at the DSS GUI and can be exported to excel files by clicking on a button.

The DSS has three modules: a data analysis module, a planning module, and the DT. The data analysis module lets the user select a train. Consequently, the corresponding historical state-space data from the OT, parameters and maintenance history are loaded into the DT. The parameters can be updated interactively at the data analysis module. Manual manipulation allows for exploring the effects of the parameters. A simulated trajectory can be compared with an actual trajectory at the visualisation.

The planning module allows for different restoration policies to be studied. Maintenance parameters for imperfect restoration, δ , at clean-in-place (CIP) methods C1 and C2; the cost of CIP according to the method; the cost of a new membrane element and the labour cost for

membrane replacement/relocation can be adjusted at the planning module. Maintenance policies can be created directly by interacting with the planning module, or pre-defined policies can be loaded from the dropdown menu. These pre-defined policies are excel files located in the working folder of the application. These maintenance policies can be adjusted externally or in the planning module. The policy can be saved to the excel file in the latter case. The corresponding maintenance costs are calculated according to the policy, and the total sum is shown. Besides cost, the 10-year element replacement rate is calculated based on the policy and train history.

The DSS runs the DT in the background. It uses the DT to simulate NPD and cost trajectories for a specific policy. The DT first models the NPD according to the model parameters and compares that against the observed NPD. The DT calculates the NPD per socket according to the modelled wear per element. Then, a five-year projection ahead is modelled based on two different sampling procedures, bootstrap sampling or Weibull distribution.

Bootstrap sampling generates a 100x365 matrix for degeneration dependency κ by resampling with replacement from a set of calculated κ from the observed NPD of 14 trains over five years with an interval of one day (70x365). Further, it generates a vector of 100 from a set of results from restoration parameter δ , following performed cleanings.

The Weibull distribution uses the same source sets. However, it splits dependency κ into κ_{low} for non-algae bloom and into κ_{high} for algae bloom conditions. Then additional distributions for the annual start and duration of algae blooms is generated based on records. The 100x365 matrix for degeneration dependency κ is then assembled from κ_{high} and κ_{low} , where after the end of an algae bloom, the decay equation (eq 17) is utilised.

The projection presents a hundred probabilities per daily interval. These probabilities vary according to the distribution of the stochastic severity of the source water quality parameter κ . Then, on a CIP occurrence, 100 probabilities of restoration parameter δ are applied according to its distribution to the 100 probabilities of the state X_i . The combination of degradation and restoration probabilities gives a spread of the reliability probability of the EO, the RO vessel. The spread that can be expressed as a cloud or area is the ensemble forecast envelope.

Ensemble forecasting has been utilised in various research disciplines to improve the probability. The forecasting ensemble envelope expresses the probability variance in this research to provide a better risk assessment. The next chapter, 8, exploring restoration policies, will further emphasise the risk assessment.

8 Exploring restoration policies

Having defined the mathematical model for RO degradation and restoration, following the presentation of the digital twin (DT) in the previous chapter, in this chapter, the decision support system (DSS) is tested practically. As stated in chapter 1, the DT-based DSS has not been developed to generate an optimum maintenance policy. However, a DT-based DSS where various policies drawn up by the practitioner can be tested on long-term wear management and cost. This chapter explores that functionality. The operation and maintenance (O&M) company's current policy is compared to alternative policies having lower costs.

8.1 Current policies of the O&M company and alternatives

The O&M company has an agreement with the membrane supplier for a fixed price of the elements for ten years. This period also covers the warranty agreement. The agreed total membrane replacement over this period is 115%. So, on average, the O&M company replaces 11.5% of the element annually, whereby all elements are replaced over ten years. The membrane supplier guarantees a fixed price for the membranes over that period. Table 8-1 shows the contractual agreement for replacement and the actual renewal for the first five years. In addition, the number of cleanings is provided.

Table 8-1. Membrane maintenance history of the first five years of operation

| Week | Membrane replacement | | | | Cleaning | | |
|----------------------|----------------------|----------------|--------------------|----------------|----------|----|----|
| | Contractual (%) | Cumulative (%) | Actual renewal (%) | Cumulative (%) | C1 | C2 | C3 |
| 1-60 (Years 2015/16) | - | - | - | - | - | - | - |
| 61-112 (Year 2017) | 8 | 8 | 25 | 25 | 10 | - | 2 |
| 113-164 (Year 2018) | 13 | 21 | - | 25 | 23 | - | - |
| 165-216 (Year 2019) | 13 | 34 | 18 | 43 | - | 18 | - |
| 217-268 (Year 2020) | 13 | 47 | 13 | 56 | - | 13 | - |
| Total | | 47 | | 56 | 33 | 31 | 2 |

Besides the standard clean-in-place (CIP), which involves a high pH followed by a low pH cleaning (C1), and the enhanced cleaning (C2) whereby the membranes first are soaked with SBS and afterwards, a high and low pH CIP is performed, the table shows a third cleaning method, C3. The C3 is not considered a CIP but an externally experimental cleaning of the most fouled membrane by a third-party membrane cleaning company combined with cascading membranes. C3 involves the removal of the lead element and shipment to the

cleaning service. The remaining elements all shift one position in the direction of the feed side of the vessel. After receiving the cleaned element back, the element is positioned at the tail socket of the vessel. This experimental cleaning was only performed at two trains and terminated due to the high costs and poor performance. C3 cleanings are not further considered. The effectiveness of C1 and C2 CIPs are given in chapter 6.2.6.

Before turning to the coming years' policies, a brief history is provided of the replacement methodology of the previous years. Besides managing the restoration due to biofouling, we must further consider the warranted lifespan of the elements, which is approximately ten years. The DSS models age-related effects by membrane fouling over time. Future works can add identification for elements reaching warranted lifespan by time since installation. Thus, the practitioner should consider this when designing a policy. The permutations are presented as a block diagram of eight cascaded sockets. As shown at the left of Figure 8-1, the vessel has eight new elements, notated as *N*. At each permutation, instead of *N*, the socket number of the previous position of the element is shown. Again, when renewed, this is shown as *N*. The colour code represents the element age (see Figure 8-1, right).

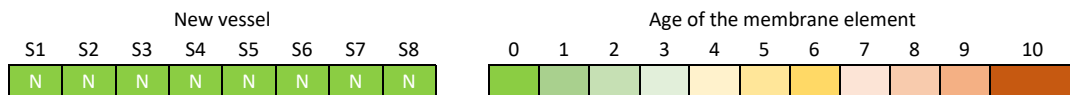


Figure 8-1. left: Notation of a vessel with all new elements, right: element age colour code.

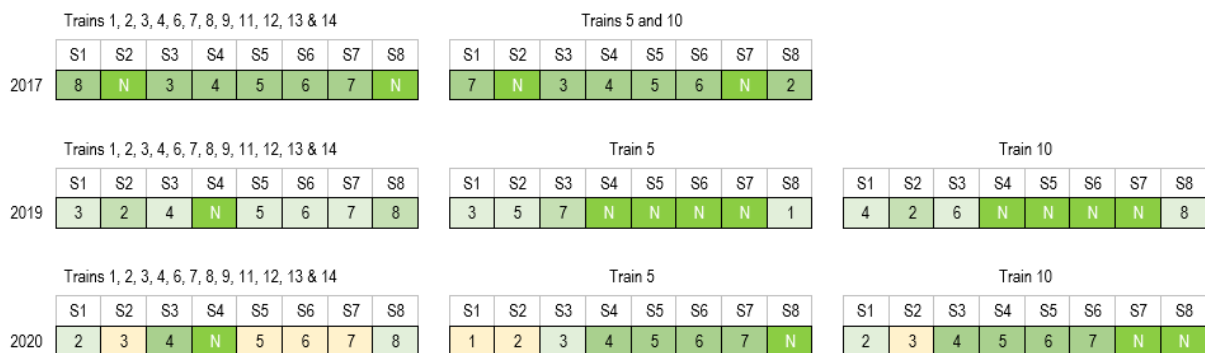


Figure 8-2. Membrane permutations 2017 to 2020

Twelve restoration policies are compared over a planning horizon of five years, beginning in 2021 and ending in 2025, a point in time that will be ten years after the plant was commissioned. These policies use varying types and frequencies of cleaning and permutations and are summarised in Table 8-2.

We start by describing the status quo (Policy 1). Element replacements to date were either one or two elements per vessel at each intervention. Permutations are replicated in all vessels of a train. Having experienced annual algal blooms for five years in a row, the O&M team assumed that 16% of the elements must be replaced over the five-year planning horizon

annually. This means (two elements per vessel for four trains and one element per vessel for the other trains (rotating annually for the five years)).

Further, due to the COVID related restrictions, permutations in 2020 diverged from the plan, and replacement was two elements/vessel for only one train and one element/vessel for the other trains. In 2021, therefore, the plan was to catch up from the previous year. Replacement for 2021 will be two elements/vessel for seven trains and one element/vessel for the other 7. The current cleaning policy is one C2 per train per year. This policy would bring the total element replacement rate to 139% over ten years.

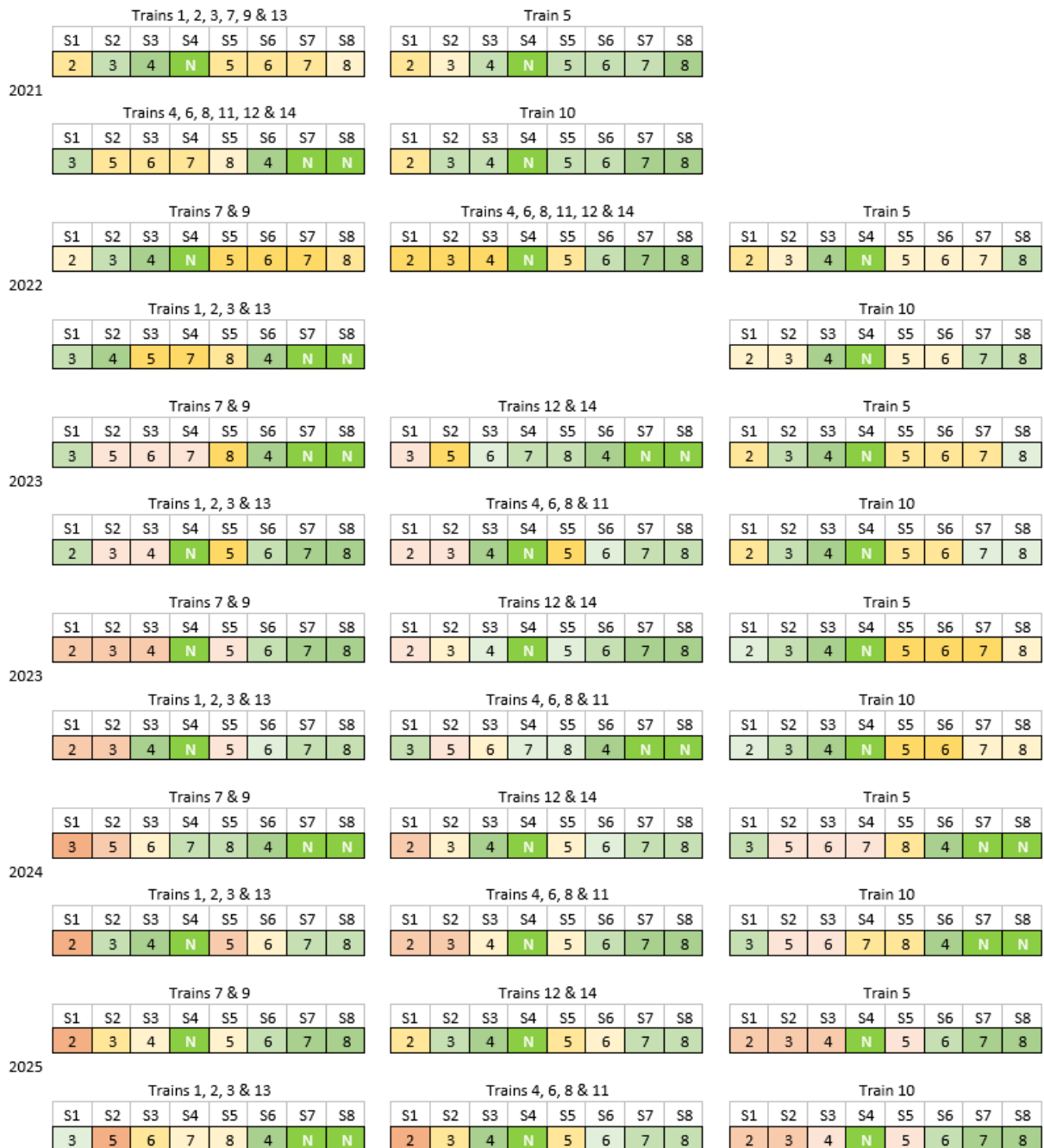


Figure 8-3. Current membrane replacement policies (1 & 10) of the O&M company

Table 8-2. Considered policies with element replacement rate per year, total cleaning frequency per year and cost (\$000s) for each year over the five-year planning horizon.

| Week | Policy 1 | | | | Policy 2 | | | | Policy 3 | | | |
|----------------------------|------------|-----------|------------|--------------|---------------|-----------|------------|--------------|---------------|------------|-----------|--------------|
| | new (%) | C1 | C2 | cost | new (%) | C1 | C2 | cost | new (%) | C1 | C2 | cost |
| 269-320 (Year 2021) | 19 | 0 | 14 | 1,275 | 0 | 0 | 42 | 21 | 0 | 42 | 0 | 17 |
| 321-372 (Year 2022) | 16 | 0 | 14 | 1,094 | 25 | 0 | 28 | 1,705 | 25 | 42 | 0 | 1,708 |
| 373-424 (Year 2023) | 16 | 0 | 14 | 1,094 | 12.5 | 0 | 28 | 860 | 12.5 | 42 | 0 | 862 |
| 425-476 (Year 2024) | 16 | 0 | 14 | 1,094 | 12.5 | 0 | 28 | 860 | 12.5 | 42 | 0 | 862 |
| 477-528 (Year 2025) | 16 | 0 | 14 | 1,094 | 12.5 | 0 | 28 | 860 | 12.5 | 42 | 0 | 862 |
| Total | 83 | 0 | 70 | 5,652 | 62.5 | 0 | 154 | 4,305 | 62.5 | 0 | 0 | 4,312 |
| Total over 10 years | 139 | 33 | 101 | | 118.75 | 33 | 185 | | 118.75 | 243 | 31 | |

| Week | Policy 4 | | | | Policy 5 | | | | Policy 6 | | | |
|----------------------------|---------------|-----------|------------|--------------|---------------|-----------|------------|--------------|---------------|------------|-----------|--------------|
| | new (%) | C1 | C2 | cost | new (%) | C1 | C2 | cost | new (%) | C1 | C2 | cost |
| 269-320 (Year 2021) | 0 | 0 | 42 | 21 | 0 | 0 | 42 | 21 | 0 | 42 | 0 | 17 |
| 321-372 (Year 2022) | 12.5 | 0 | 14 | 981 | 12.5 | 0 | 28 | 988 | 12.5 | 42 | 0 | 991 |
| 373-424 (Year 2023) | 25 | 0 | 14 | 1,698 | 12.5 | 0 | 28 | 1,705 | 12.5 | 42 | 0 | 991 |
| 425-476 (Year 2024) | 12.5 | 0 | 14 | 981 | 12.5 | 0 | 28 | 988 | 12.5 | 42 | 0 | 991 |
| 477-528 (Year 2025) | 12.5 | 0 | 14 | 981 | 12.5 | 0 | 28 | 988 | 12.5 | 42 | 0 | 991 |
| Total | 62.5 | 0 | 98 | 4,663 | 50 | 0 | 154 | 4,691 | 50 | 210 | 0 | 3,982 |
| Total over 10 years | 118.75 | 33 | 129 | | 106.25 | 33 | 185 | | 106.25 | 243 | 31 | |

| Week | Policy 7 | | | | Policy 8 | | | | Policy 9 | | | |
|----------------------------|---------------|------------|-----------|--------------|--------------|-----------|------------|------------|---------------|-----------|------------|--------------|
| | new (%) | C1 | C2 | cost | new (%) | C1 | C2 | cost | new (%) | C1 | C2 | cost |
| 269-320 (Year 2021) | 0 | 42 | 0 | 17 | 0 | 0 | 42 | 21 | 12.5 | 0 | 28 | 988 |
| 321-372 (Year 2022) | 37.5 | 42 | 0 | 2,425 | 0 | 0 | 42 | 21 | 12.5 | 0 | 28 | 988 |
| 373-424 (Year 2023) | 0 | 56 | 0 | 22 | 0 | 0 | 42 | 21 | 12.5 | 0 | 28 | 988 |
| 425-476 (Year 2024) | 0 | 56 | 0 | 22 | 0 | 0 | 42 | 21 | 12.5 | 0 | 28 | 988 |
| 477-528 (Year 2025) | 12.5 | 42 | 0 | 991 | 0 | 0 | 42 | 21 | 12.5 | 0 | 28 | 988 |
| Total | 50 | 210 | 0 | 3,478 | 0 | 0 | 210 | 105 | 62.5 | 0 | 140 | 4,942 |
| Total over 10 years | 106.25 | 243 | 31 | | 56.25 | 33 | 241 | | 118.75 | 33 | 171 | |

| Week | Policy 10 | | | | Policy 11 | | | | Policy 12 | | | |
|----------------------------|---------------|-----------|------------|--------------|---------------|-----------|------------|--------------|---------------|-----------|------------|--------------|
| | new (%) | C1 | C2 | cost | new (%) | C1 | C2 | cost | new (%) | C1 | C2 | cost |
| 269-320 (Year 2021) | 19 | 0 | 28 | 1,275 | 0 | 28 | 14 | 18 | 12.5 | 0 | 28 | 988 |
| 321-372 (Year 2022) | 16 | 0 | 28 | 1,094 | 12.5 | 0 | 42 | 995 | 12.5 | 0 | 42 | 995 |
| 373-424 (Year 2023) | 16 | 0 | 28 | 1,094 | 12.5 | 0 | 42 | 995 | 12.5 | 0 | 42 | 995 |
| 425-476 (Year 2024) | 16 | 0 | 28 | 1,094 | 12.5 | 0 | 42 | 995 | 12.5 | 0 | 42 | 995 |
| 477-528 (Year 2025) | 16 | 0 | 28 | 1,094 | 12.5 | 0 | 42 | 995 | 12.5 | 0 | 42 | 995 |
| Total | 83 | 0 | 140 | 5,652 | 50 | 28 | 182 | 4,000 | 62.5 | 0 | 196 | 4,970 |
| Total over 10 years | 139.25 | 33 | 101 | | 106.25 | 61 | 213 | | 118.75 | 33 | 227 | |

O&M intends to do two C2 per train annually. Two C2 per train is the maximum frequency of C2 that can be conducted with the current CIP system. Thus, Policy 10 is identical to Policy 1 regarding permutations, but with two instances of C2 per train per year instead of one. Since testing the policy on the physical system is impractical, the practitioner can test the effectiveness of increasing the CIP frequency using the DT. The results of wear management for O&M policies 1 and 10, which only differ in CIP frequency, shows the modelled effects and are given in section 8.2.1.

The current O&M procedure, when replacing one element per vessel at an intervention, discards the element in S1 and arranges the other elements in the eight sockets as 234N5678. Thus, the element in S2 is placed in S1, that in S3 in S2, that in S4 in S3, a new element (N) is placed in S4, and the tail of the vessel (S5-S8) is unchanged. As described in chapter 5.2.2, Economic dependencies, locating the new element in socket 4, rather than socket 8, has the advantage that only the vessel's feed (seawater) side needs to be opened and four elements removed. The latter is cheaper and quicker than opening the entire vessel and reduces the labour cost in half. When replacement is two elements per vessel, the elements in S1 and S2 are discarded, and the new and remaining elements are arranged as 356784NN.

The other ten policies are alternatives being investigated to reduce maintenance costs over the next five years. Many more policies could be investigated, and we intend to use the DSS for this as appropriate. For now, we demonstrate the DSS for a set of pre-agreed policies that interest the O&M company. Although the projections are run for each train, and choice can be a multi-criteria one (de Almeida et al., 2015); b), the intention is not to utilize different policies for different trains. As reviewed in chapter 5, both extrinsic and intrinsic degeneration are stochastic. This stochastic character is reflected in the variations of the projections per train to a certain degree. So, by analysing the projections of all the trains, better observation of the projection of the policies is achieved.

All the trains were preserved for almost the whole period of the algae bloom in 2020. The latter was due to the commissioning of a new brine dilution pumping station. Therefore, Policies 2 to 7 and 11 have no replacement in 2021. Their cleaning methods and annual frequencies differ.

In 2022, policies 2 and 3 will discharge the first two elements with a permutation of 356784NN in every vessel. For trains 5 and 10, the permutations are 345678NN. In the following years, one element annually will be discharged with a permutation of 234N5678 in every vessel after that. The permutations are shown in Figure 8-4. Since no permutations occur in 2021, three CIPs, method C2, will be conducted per train. Policy 2 will conduct two CIPs, method C2, per train annually in the following years. Policy 3 will conduct three CIPs, method C1, per train annually in the following years.

Every other policy, except policy 8, uses a permutation of 2356784N (discharging the lead element) at the first replacement and then either a permutation of 2345678N (discharging the lead element) or 345678NN (discharging the two lead elements) after that. A permutation of 2345678N instead of 234N5678 increases the time and labour, but all elements are replaced over time.

| | Trains 1, 2, 3, 4, 6, 7, 8, 9, 11, 12, 13 & 14 | | | | | | | | Train 5 | | | | | | | | Train 10 | | | | | | | |
|------|--|----|----|----|----|----|----|----|---------|----|----|----|----|----|----|----|----------|----|----|----|----|----|----|----|
| | S1 | S2 | S3 | S4 | S5 | S6 | S7 | S8 | S1 | S2 | S3 | S4 | S5 | S6 | S7 | S8 | S1 | S2 | S3 | S4 | S5 | S6 | S7 | S8 |
| 2022 | 3 | 5 | 6 | 7 | 8 | 4 | N | N | 3 | 4 | 5 | 6 | 7 | 8 | N | N | 3 | 4 | 5 | 6 | 7 | 8 | N | N |
| 2023 | 2 | 3 | 4 | N | 5 | 6 | 7 | 8 | 2 | 3 | 4 | N | 5 | 6 | 7 | 8 | 2 | 3 | 4 | N | 5 | 6 | 7 | 8 |
| 2024 | 2 | 3 | 4 | N | 5 | 6 | 7 | 8 | 2 | 3 | 4 | N | 5 | 6 | 7 | 8 | 2 | 3 | 4 | N | 5 | 6 | 7 | 8 |
| 2025 | 2 | 3 | 4 | N | 5 | 6 | 7 | 8 | 2 | 3 | 4 | N | 5 | 6 | 7 | 8 | 2 | 3 | 4 | N | 5 | 6 | 7 | 8 |

Figure 8-4. Permutations of policies 2 and 3.

| | Trains 1, 2, 3, 4, 6, 7, 8, 9, 11, 12, 13 & 14 | | | | | | | | Train 5 | | | | | | | | Train 10 | | | | | | | |
|------|--|----|----|----|----|----|----|----|---------|----|----|----|----|----|----|----|----------|----|----|----|----|----|----|----|
| | S1 | S2 | S3 | S4 | S5 | S6 | S7 | S8 | S1 | S2 | S3 | S4 | S5 | S6 | S7 | S8 | S1 | S2 | S3 | S4 | S5 | S6 | S7 | S8 |
| 2022 | 2 | 3 | 5 | 6 | 7 | 8 | 4 | N | 2 | 3 | 4 | 5 | 6 | 7 | 8 | N | 2 | 3 | 4 | 5 | 6 | 7 | 8 | N |
| 2023 | 3 | 4 | 5 | 6 | 7 | 8 | N | N | 3 | 4 | 5 | 6 | 7 | 8 | N | N | 3 | 4 | 5 | 6 | 7 | 8 | N | N |
| 2024 | 2 | 3 | 4 | 5 | 6 | 7 | 8 | N | 2 | 3 | 4 | 5 | 6 | 7 | 8 | N | 2 | 3 | 4 | 5 | 6 | 7 | 8 | N |
| 2025 | 2 | 3 | 4 | 5 | 6 | 7 | 8 | N | 2 | 3 | 4 | 5 | 6 | 7 | 8 | N | 2 | 3 | 4 | 5 | 6 | 7 | 8 | N |

Figure 8-5. Permutations policy 4.

Policy 4 will start membrane replacements in 2022, replacing only one element with a permutation of 2356784N (discharging the lead element). For trains 5 and 10, the permutations are 2345678N. In 2023 two elements will be replaced with a permutation of 345678NN (discharging the two lead elements). One element will be replaced in the following two years with a permutation of 2345778N (discharging the lead element). The permutations are shown in Figure 8-5. Like the O&M policy 1, only one CIP, method C2, will be conducted per train annually. An exception is the year 2021. Since no permutations occur that year, three CIPs, method C2, will be conducted per train.

Similar to policies 2 and 3, policies 5, 6 and 11 have the same permutations but different cleaning regimes. Membrane replacement starts in 2022, and only one element is replaced each year up to 2025. The permutations for 2022 are 2356784N (discharging the lead element) for all trains, except trains 5 and 10. For trains 5 and 10, the permutations are 2345678N. Then, from 2023 to 2025, the permutations are 2345678N for all the trains. The permutations are shown in Figure 8-6. The cleaning program of policy 5 is identical to policy

2, and that of policy 6 is identical to policy 3. Policy 11 conducts three CIPs with method C2 annually.

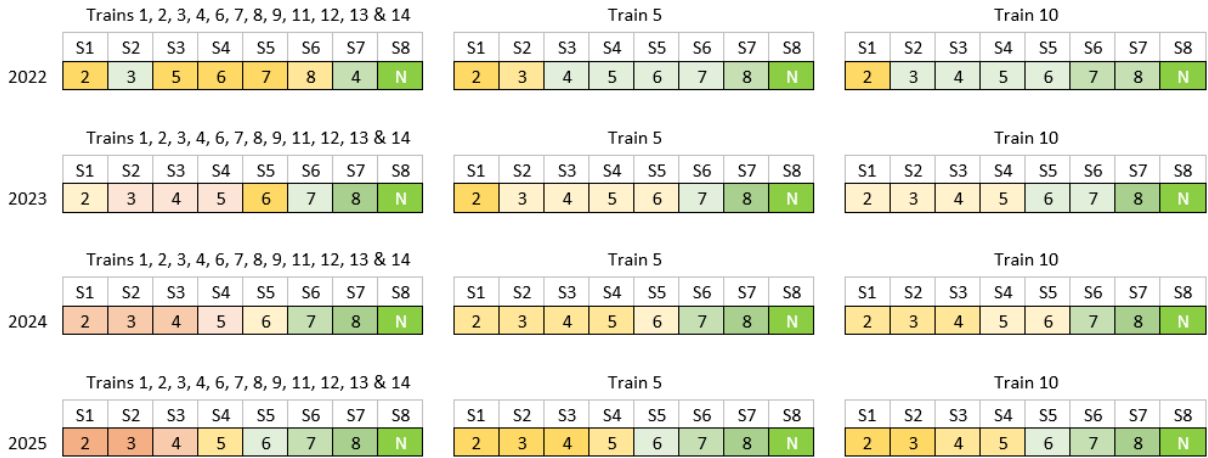


Figure 8-6. Permutations policies 5, 6 and 11.

Policy 7 uses a permutation of 56784NNN for the trains in 2022, discharging the three lead elements, excluding 5 and 10. The permutations for 5 and 10 are 45678NNN. In the following two years, no permutations will take place. Then, in the last year, one element per vessel is replaced with a permutation of 2345678N for all the trains. The permutations are shown in Figure 8-7. For 2021, 2022 and 2025, three CIPs per train, method C1, will be conducted annually. For 2023 and 2024, the frequency is 4 CIPs per train annually, method C1.

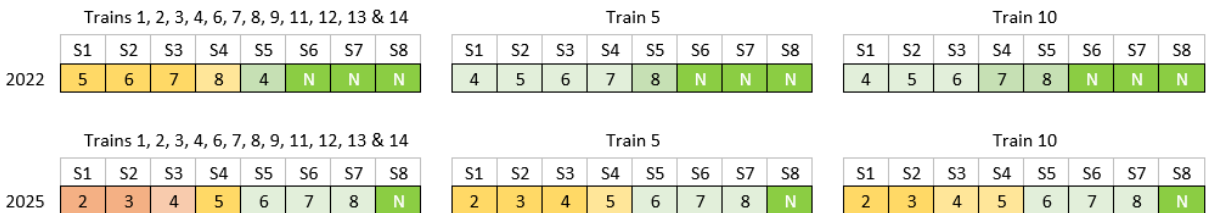


Figure 8-7. Permutations policy 7.

Policy 8 contains only CIP (3xC2 annually). This policy is only theoretically to investigate if only an increase in CIP frequency can control biofouling. As Figure 8-8 shows, the ageing of the membranes after five years is significant.

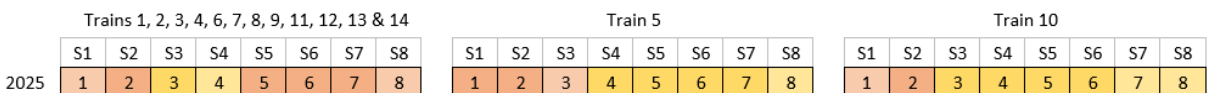


Figure 8-8. Aging of membrane elements after five years (Policy 8).

Finally, policies 9 and 12 will replace annually one element per vessel. The permutations for 2021 are 2356784N (discharging the lead element) for all trains, except trains 5 and 10.

For trains 5 and 10, the permutations are 2345678N. Then, from 2022 to 2025, the permutations are 2345678N for all the trains. The permutations are shown in Figure 8-9.

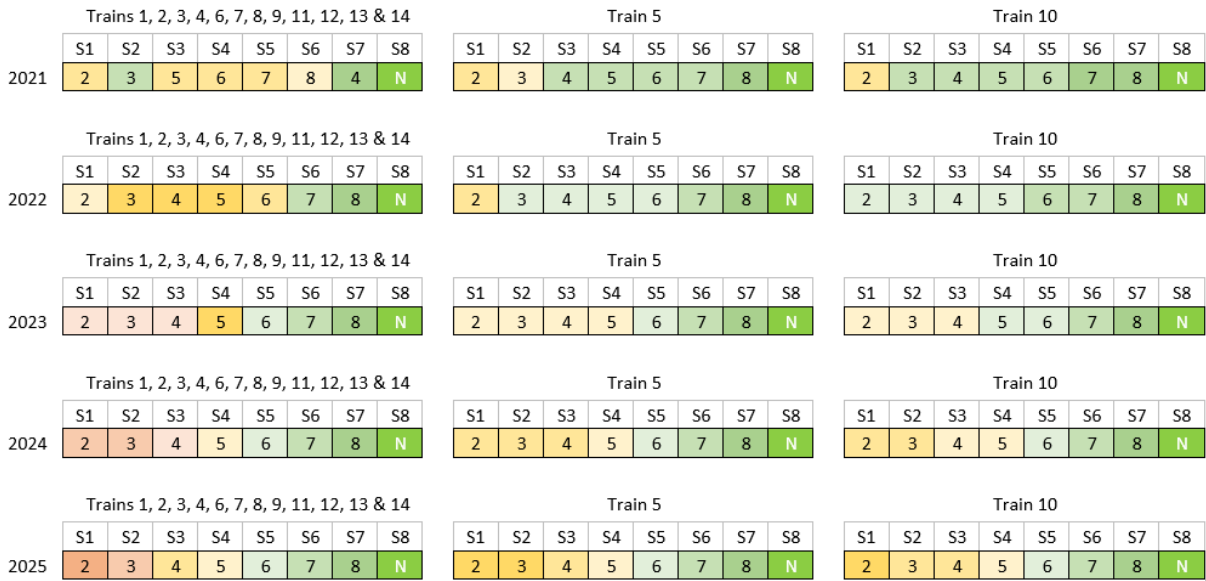


Figure 8-9. Permutations policy 9 and 12

Identical to O&M policy 10, policy 9 involves two instances of CIPs, method C2, per train per year. As with Policy 8 and 11, policy 12 conducts three CIPs with method C2 annually. Currently, the time duration of the discharge of used chemicals is a bottleneck that limits the C2 method of CIP frequency to two per train annually. Therefore, for policies having at least three CIPs method C2, a minor upgrade of the CIP system is required so that the neutralization tank can be used to discharge used cleaning chemicals. Utilizing the neutralization tank will make the cleaning tank directly available after cleaning, reducing delays in preparing new cleaning batches. Policy 11 and 12 consider the first year required to upgrade the system. Therefore, policy 11 will conduct two CIPs, method C1 and one CIP method C2, in 2021. Policy 12 only conducts two CIPs method C2 in 2021.

The annual, total and ten-year replacement rate, cleaning frequencies and associated cost of the policy are shown in table 8-1. Since membrane maintenance activities involving permutations are scheduled during winter when demand is usually lower, this maintenance can be undertaken without affecting the ability to deliver water according to the demand. Therefore, downtime is not included in the cost.

Taking a train offline for a standard high and low pH cleaning (C1) takes only a few hours. In the case of CIP with SBS soaking (C2), an additional day has to be added. However, seasonally, most of the time, this should not affect the ability to produce water according to the demand. During the winter months, the output of a train is reduced due to colder seawater. However, as stated earlier, the demand in these months is mainly reduced.

Further, CIP is undertaken by the operators as part of their daily activities. Cost in the case of CIP is limited to chemicals consumed. If permutations are involved, both costs of elements and labour are considered.

As observed (see chapter 6.2.6), on average, a CIP with method C1 reduced the NPD by 14%. However, it was less than 10% in one-fifth of the cases. C2 gave, on average, a reduction of NPD of 26%. In only 4% of the cases, the reduction was less than the average reduction by C1. Still, policies 3, 6 and 7 utilize method C1 for CIP. These policies investigate if gains can be made utilizing a less effective CIP method but at a higher frequency. Double the CIP frequency can be reached using method C1 compared to C2.

Policy 7 investigate if gains can be made by opportunistic block replacement as described in chapter 5.3.3. By replacing three elements in one go, we should expect that for the next two years, no permutations will be needed for this method to be effective.

8.2 Analysis

Projections have been run utilizing the 12 policies for each train. The number twelve is arbitrary and can be adjusted. For comparison, both forecast methods, bootstrap sampling and Weibull distribution, for sampling the stochastic extrinsic dependence κ and restoration factor δ are utilized. First, the bootstrap sampling method, which has been repeated for the three different smoothing windows, one before, four after (-1,4), (-2,8), and (-4, 16), corresponding to windows of width 5, 10 and 20 days, respectively. After that, the projections are repeated, utilizing the 12 policies for each train for the Weibull distribution forecast method, based on the shape parameter k and scale parameter λ , resulting from the parameter estimation (see section 6.2).

The output of the plots of the combined observed and modelled NPD followed by the projection utilizing the ensemble forecast is presented of each policy for train 11, utilizing the bootstrap method, followed by the Weibull distribution method. Figures 8-10 to 8-12 shows the results with the bootstrap method with four before and 16 after smoothing windows. Figures 8-13 to 8-15 show the Weibull distribution method results. Train 11, as observations of the historical state-space show, is an average-performing train. Additional plots of Bootstrap sampling with smoothening -1,+4, and smoothening -2,+8 are provided in Appendix C. The state-space plots of the projections provide a first impression of the reliability resulting from the various policies. The blue dashed lines indicate the risk thresholds at 3 and 3.5 bar. Section 8.3, Risk Assessment, provides the reasoning behind these risk thresholds and presents a detailed risk assessment.

8.2.1 Projections utilizing bootstrap sampling

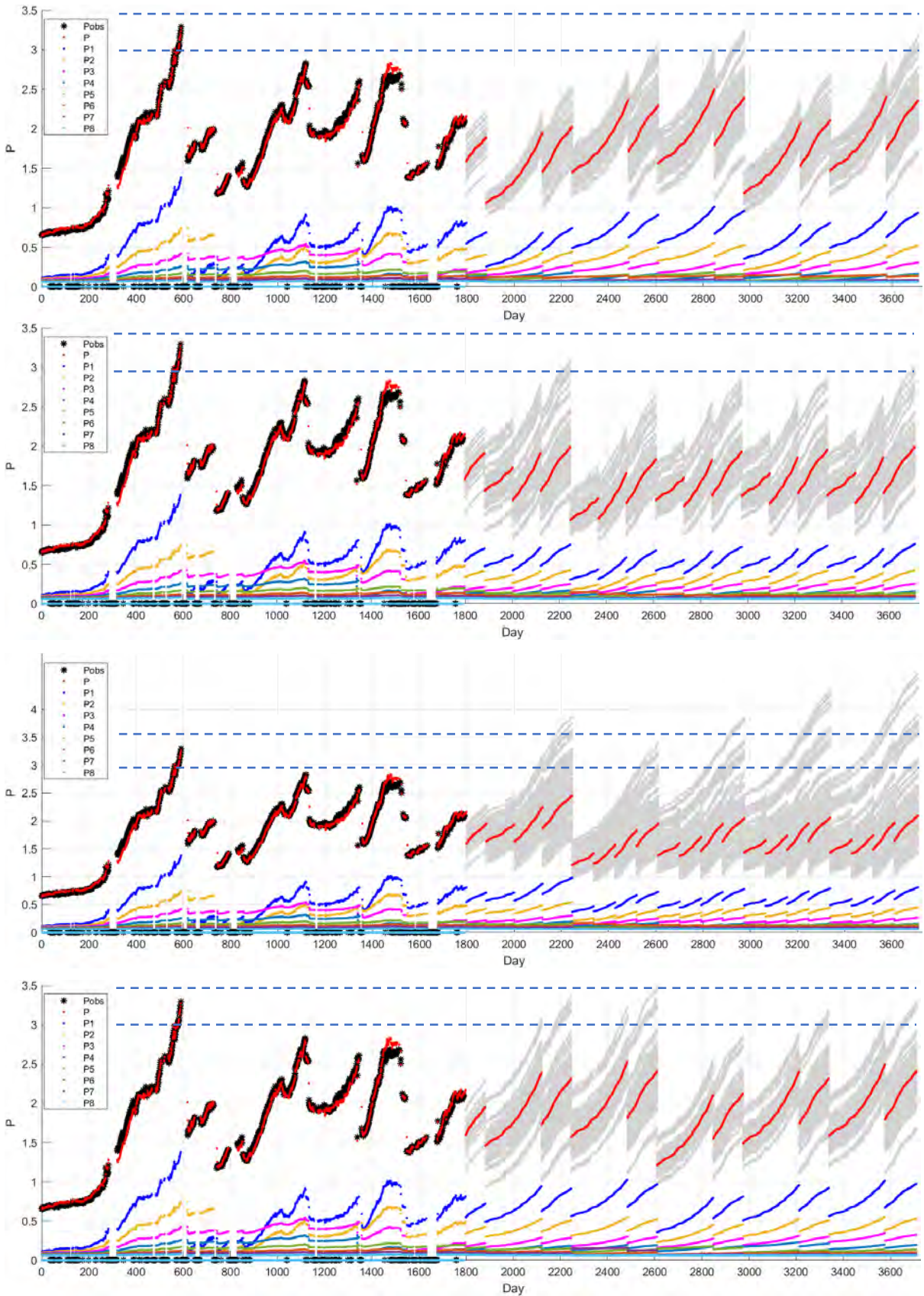


Figure 8-10: DT output of NPD projection based on bootstrap sampling for train 11, policy 1 (top) to policy 4 (bottom).

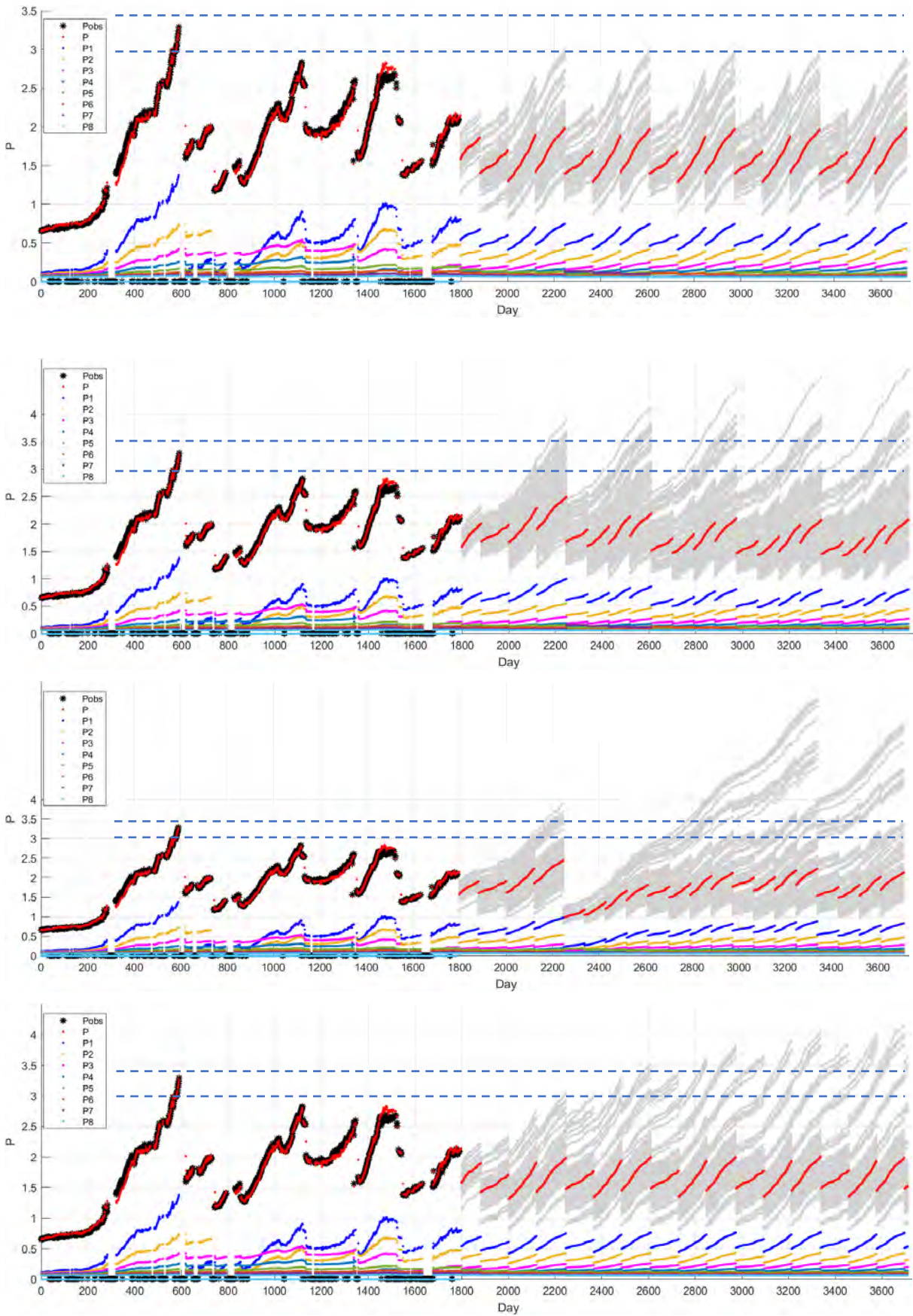


Figure 8-11: DT output of NPD projection based on bootstrap sampling for train 11, policy 5 (top) to policy 8 (bottom).

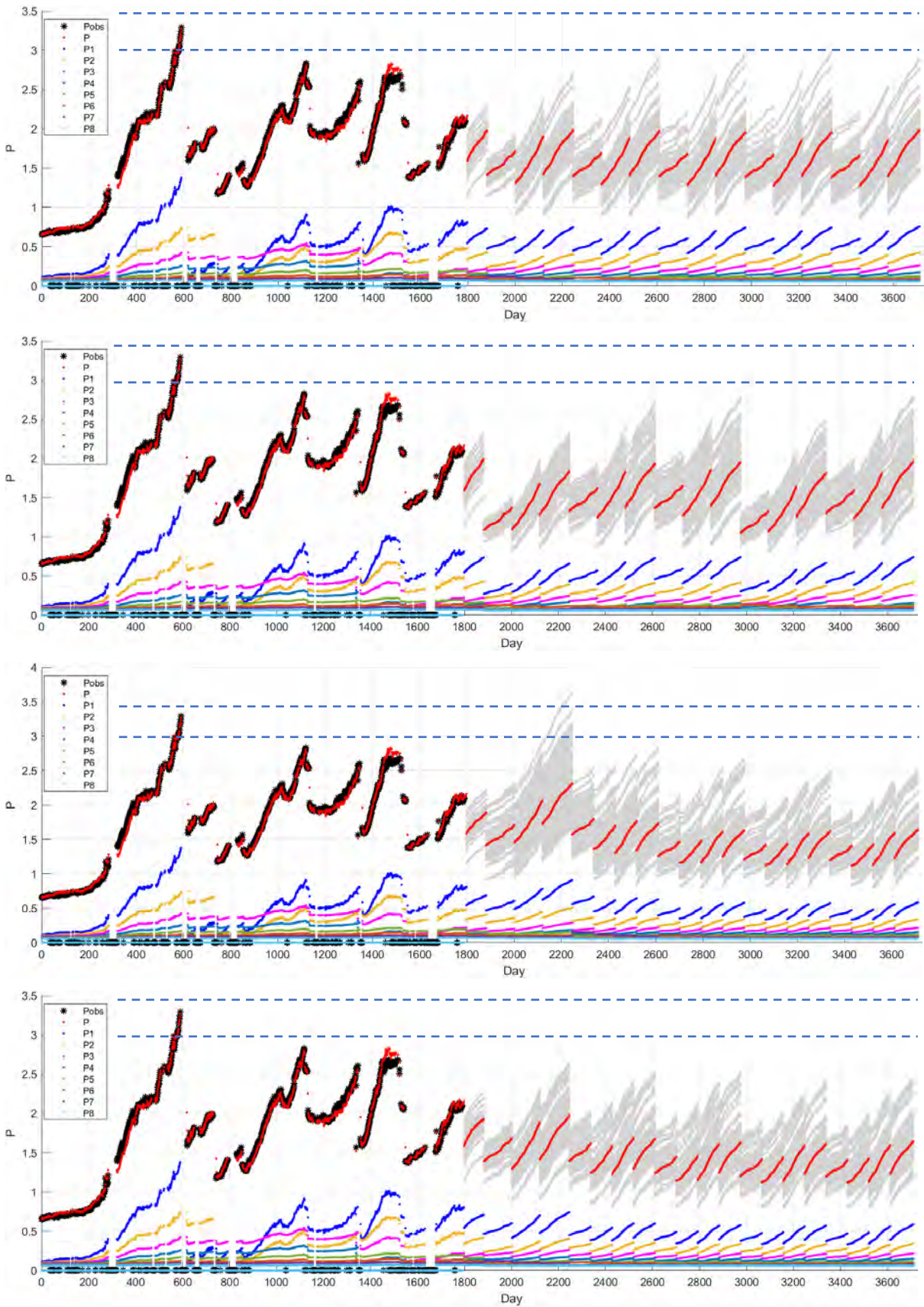


Figure 8-12: DT output of NPD projection based on bootstrap sampling for train 11, policy 9 (top) to policy 12 (bottom).

8.2.2 Projections utilizing Weibull distribution

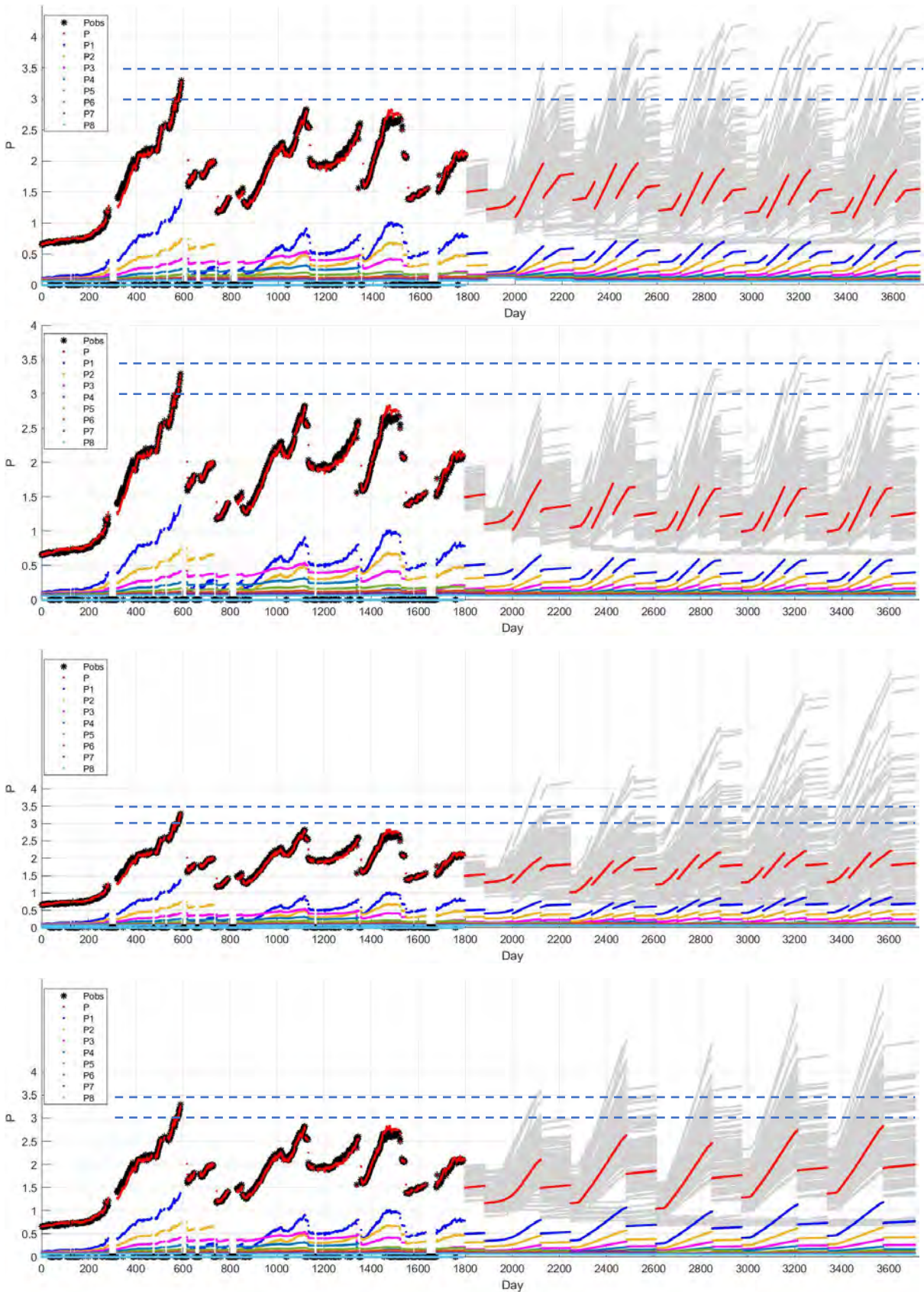


Figure 8-13: DT output of NPD projection based on Weibull distribution for train 11, policy 1 (top) to policy 4 (bottom).

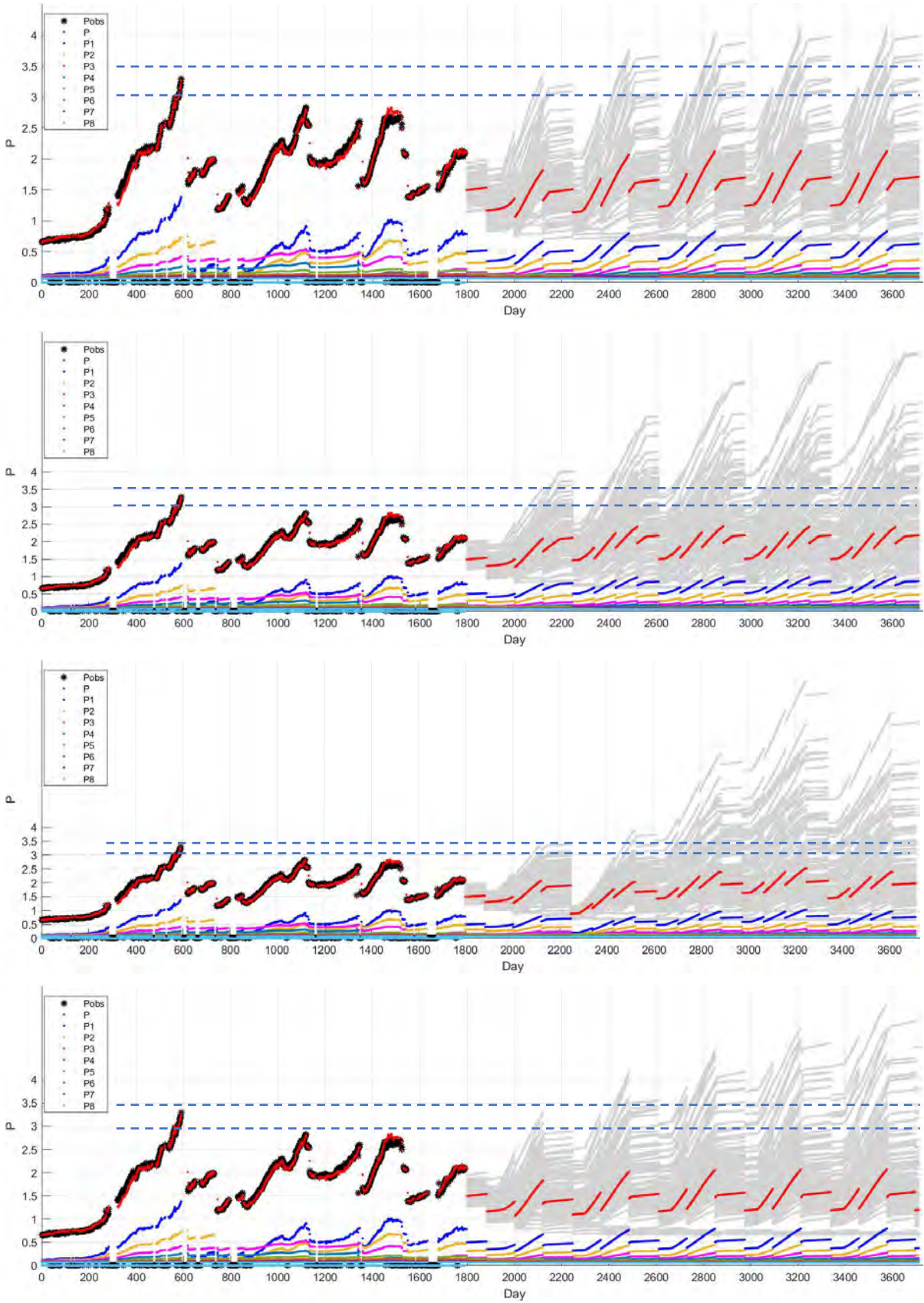


Figure 8-14: DT output of NPD projection based on Weibull distribution for train 11, policy 5 (top) to policy 8 (bottom).

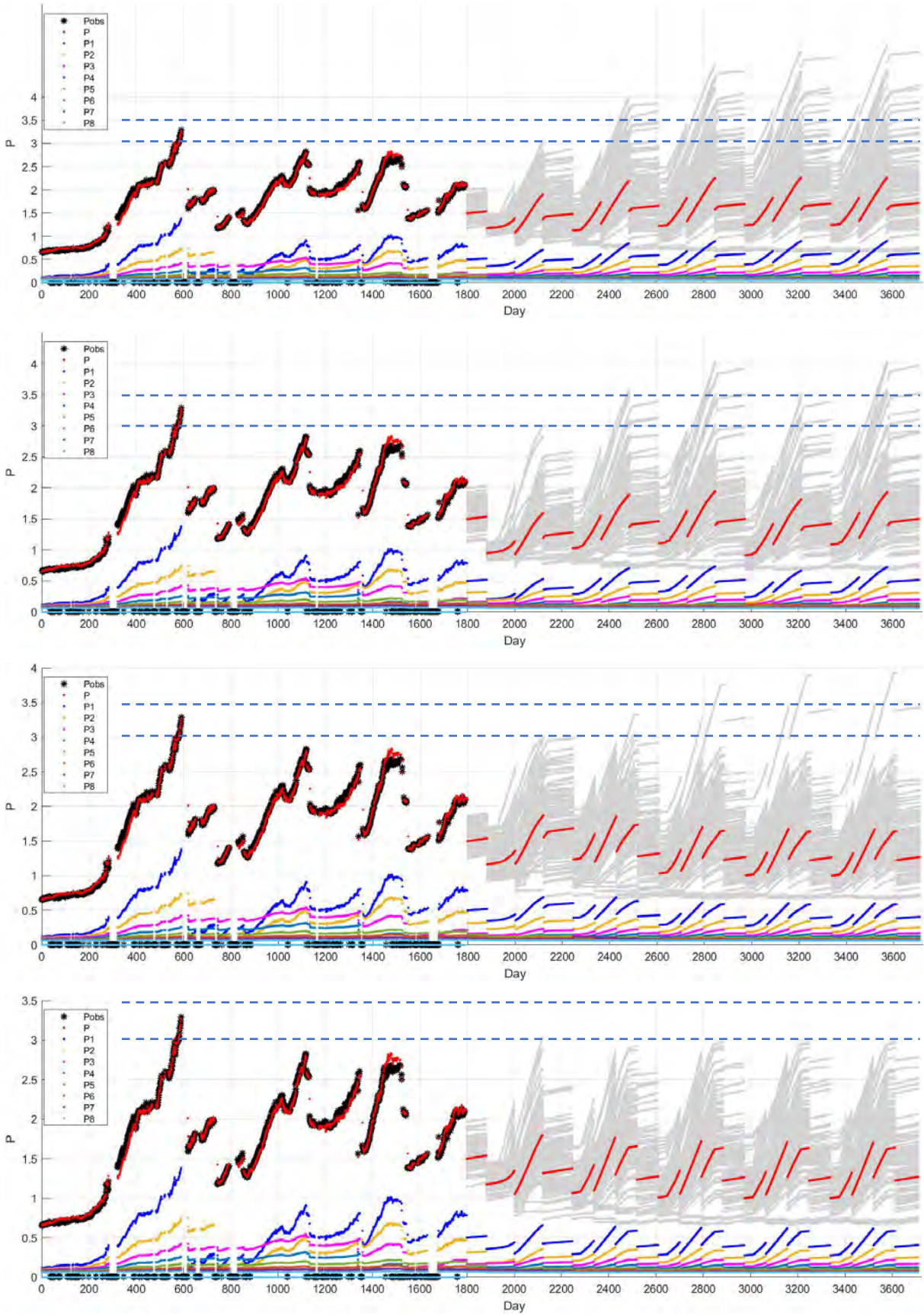


Figure 8-15: DT output of NPD projection based on Weibull distribution for train 11, policy 9 (top) to policy 12 (bottom).

8.3 Risk assessment

A policy is admissible if the PD is always below the critical threshold of 3.5 bar. Above the 3.5 bar, elements can fail irrecoverably. Classically, risk is defined as the probability of an unwanted event's occurrence multiplied by the event's consequence (loss). This research defines risk as the likelihood of the PD crossing this critical pressure threshold. Although this risk measure is essentially *reliability*, O&M company prefers to call this risk. Since there is a slight variance between the NPD and the underlying PD, two risk thresholds at 3 and 3.5 bar are simultaneously considered (Figure 8-16).

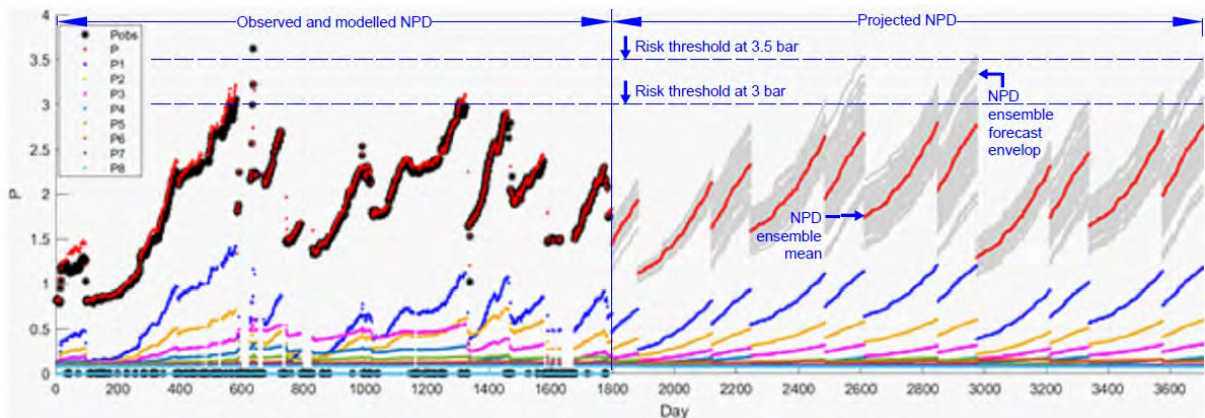


Figure 8-16. DT output with risk thresholds

Figure 8-17 shows a matrix of risk analyses conducted involving 12 policies whereby projections are run for all 14 RO trains per policy. For sensitivity analysis, the latter is conducted for Weibull distribution sampling and bootstrap sampling with three different smoothing regimes of dependencies κ and δ . Thus, 672 projections have been generated in total.

The DSS output the maximum P of the ensemble envelope for a policy. A script at MATLAB Live Editor has been prepared. The script calculates the proportion of the maximum (over the ensemble) projected daily NPD values above each train's threshold. The latter is the risk measure in Figure 8-18. The left column shows boxplots of risk measure of 3 bar and the right column boxplots of risk measure of right, 3.5 bar, across 14 trains. From top to down, risk analysis of the policies with the Weibull distribution sampling method, followed by bootstrap sampling with a smoothing of -1,4; -2,8; and -4,16 smoothing at the bottom. Policies are ranked by the total cost (\$000s) over five years and show downtime per train (%), number of stops per train per year, and boxplots of risk measure.

A boxplot is a standardized way of displaying data distribution based on a five-number summary, minimum, first quartile or 25th percentile, median or 50th percentile, third quartile

or 75th percentile and maximum. It further informs about outliers and their values (see Figure 8-17).

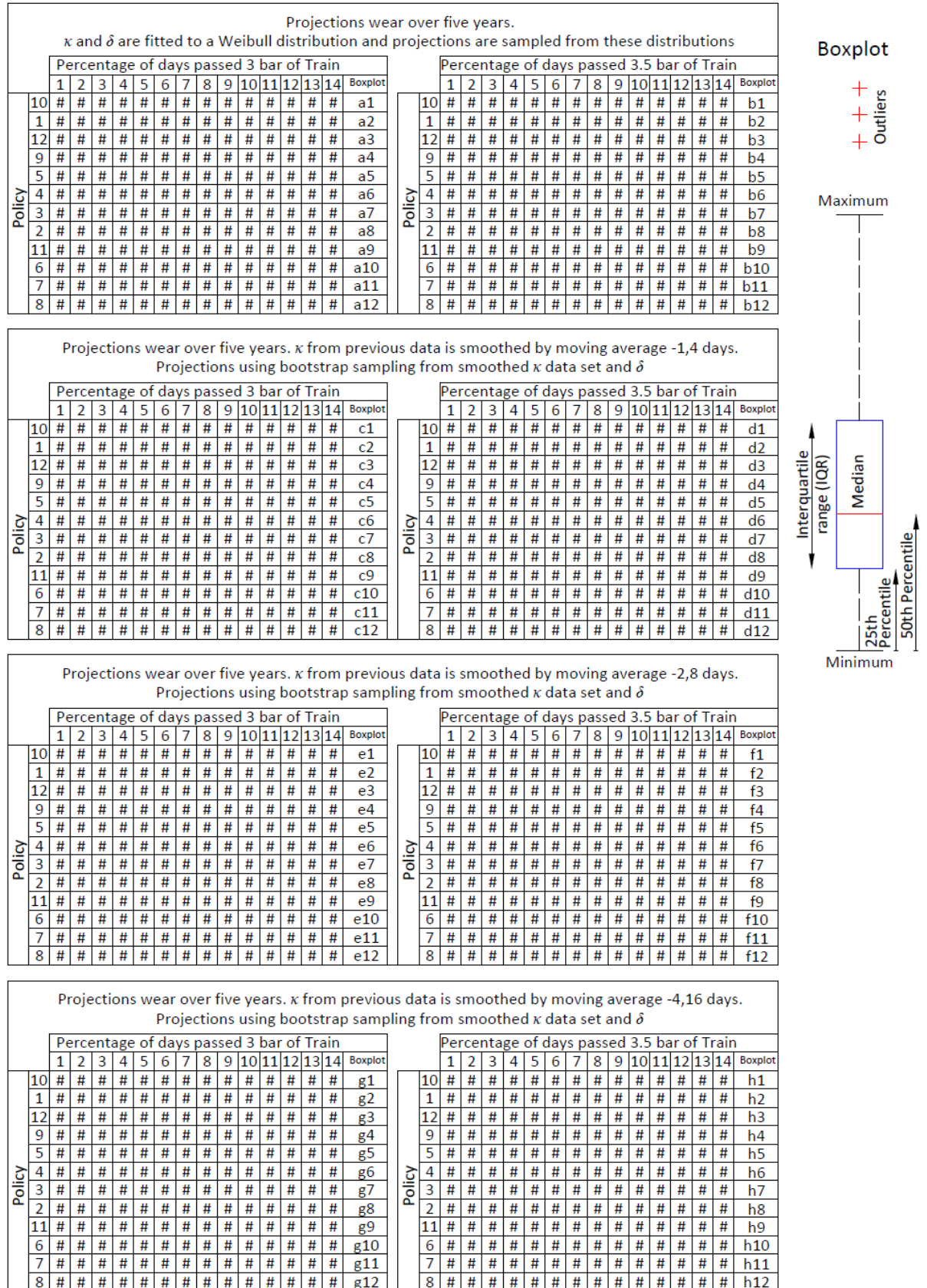


Figure 8-17. Matrix of different risk analyses

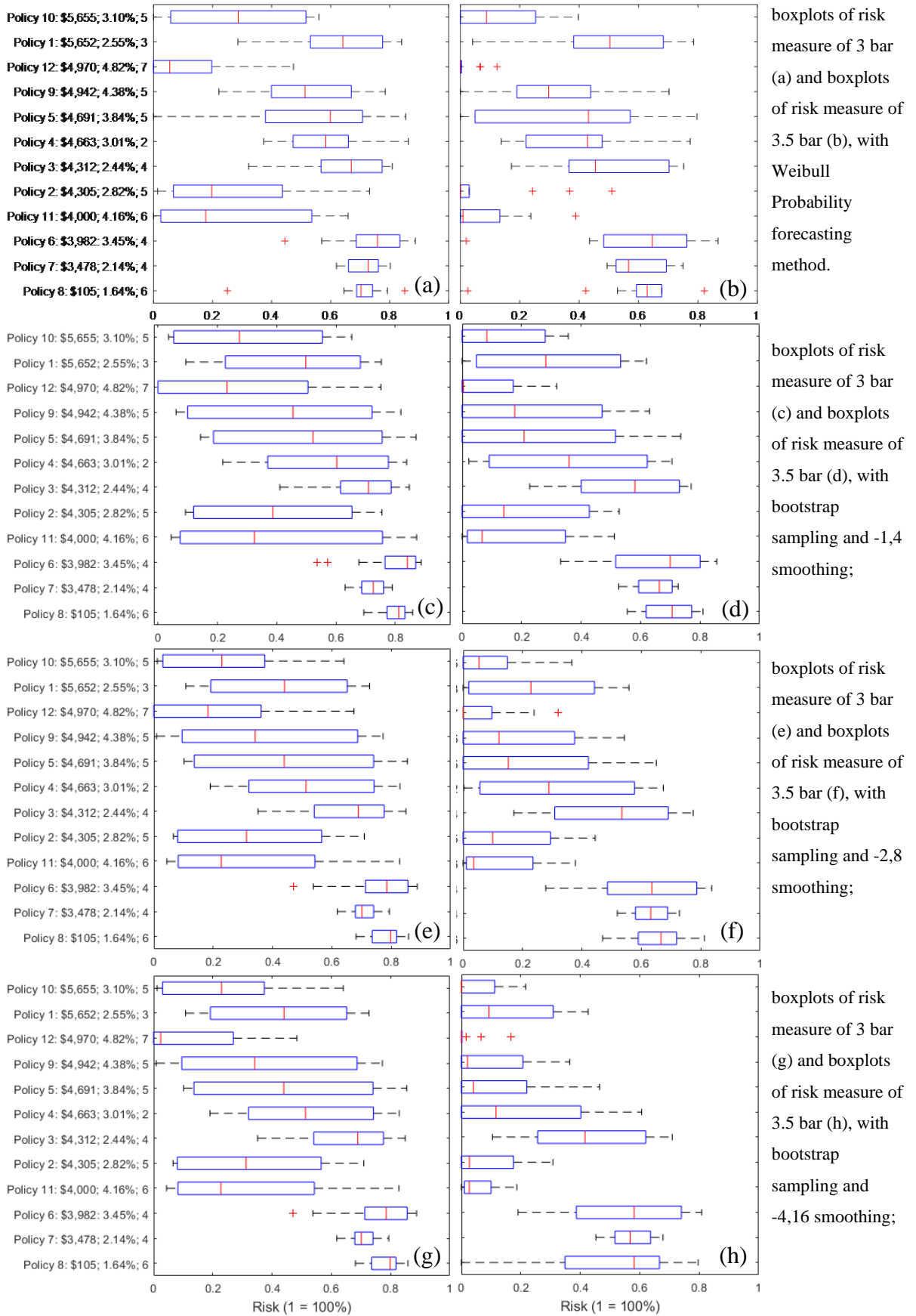


Figure 8-18. Risk analysis of the Policies ranked by the total cost (\$000s) over five years and showing downtime per train (%), number of stops per train per year, and boxplots of risk.

The policies are then ordered in rank based on the median risk measure. The latter is performed for all eight sampling methods and risk measures, then averaged in rank and weight. Figure 8-19 shows the ranking results of the policies as described before.

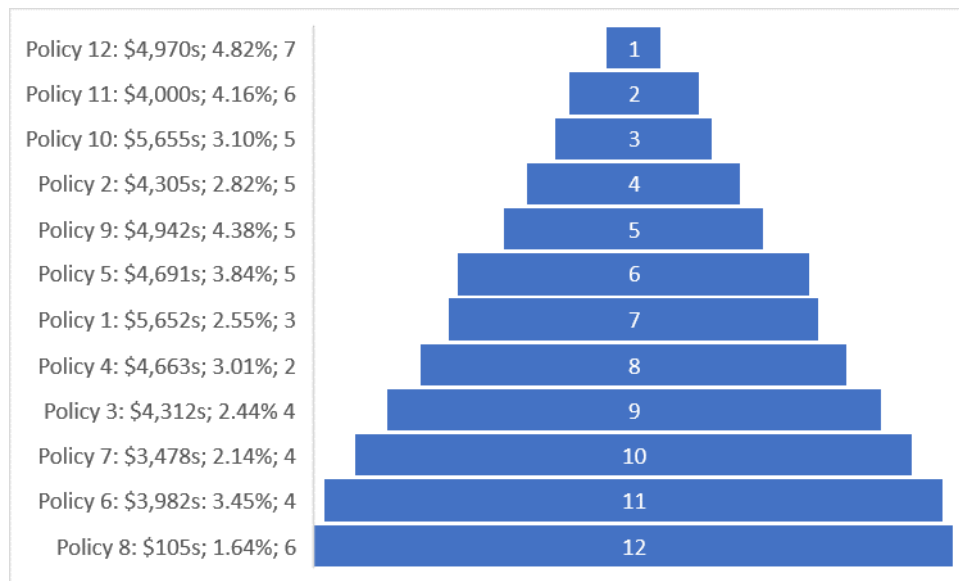


Figure 8-19. Policy ranking based on risk assessment of all eight risk assessments

From Figures 8-18 and 8-19, we can conclude that only Policies 10-12 and 2 have an acceptable risk with a median < 20% (see Figure 8-18) of the eight analyses on average of the eight sampling methods. From this, Policy 12 stands out in terms of risk and cost. Although policy 2 gives an acceptable risk regarding biofouling control, the last four elements will age close and beyond the lifespan of a membrane since permutations have only been applied to the first four elements. Thus, only policies 10, 11 and 12 are sustainable.

| | Trains 1, 2, 3, 4, 6, 7, 8, 9, 11, 12, 13 & 14 | | | | | | | | Train 5 | | | | | | | | Train 10 | | | | | | | |
|------|--|----|----|----|----|----|----|----|---------|----|----|----|----|----|----|----|----------|----|----|----|----|----|----|----|
| | S1 | S2 | S3 | S4 | S5 | S6 | S7 | S8 | S1 | S2 | S3 | S4 | S5 | S6 | S7 | S8 | S1 | S2 | S3 | S4 | S5 | S6 | S7 | S8 |
| 2030 | 2 | 3 | 4 | N | 5 | 6 | 7 | 8 | 2 | 3 | 4 | N | 5 | 6 | 7 | 8 | 2 | 3 | 4 | N | 5 | 6 | 7 | 8 |

Figure 8-20. Ageing of membranes in 2030 following policies 2 and 3.

The current O&M procedure, which applies only permutations at the first four elements when replacing one element per vessel at an intervention, reduces labour cost and downtime of the train. However, this implies that such policy requires complementary interventions involving at least two replacements. The latter is, in this case, not so much to improve biofouling control but to push older membranes to the vessel's front. The cost of additional elements outweighs savings in labour costs.

We can observe that policies 3, 6 and 7, utilizing the less effective CIP method C1, perform inferior despite applying a higher frequency of cleanings. Policy 2 and 3 have similar permutations. However, Policy 3 performs one CIP (C1) per train more than policy 2, which

performs two C2 per train annually. Policy 3 ranks ninth place, while policy 2 ranks fourth place. The cost of both policies is just about the same. Policies 5 and 6 repeat the performance behaviour of policies 2 and 3, with policy 6 at the near bottom rank and policy 5 at the sixth rank.

The purpose of policy 7 was to examine if gains can be made with block replacement. The performance would have been better when utilized C2 instead of C1 in the policy. However, the thesis author believes that it makes no difference regarding the efficiency of block replacement in the case of this study. After replacing three elements, we observe that the vessel looks as good as new. However, the projections show degeneration to the same level as before the permutations in one year (see Figures 8-11 and 8-14).

Figure 8-21 (left) shows the modelled wear of the elements for all 14 trains the day before permutations occur involving the replacement of three elements. A divider is added to the plot at the position of socket 3. The mean of the element wear per socket is presented at the figure's right. We observe an exponential decline of the wear at each succeeding socket. Therefore, the impact of replacing the third element is far lower.

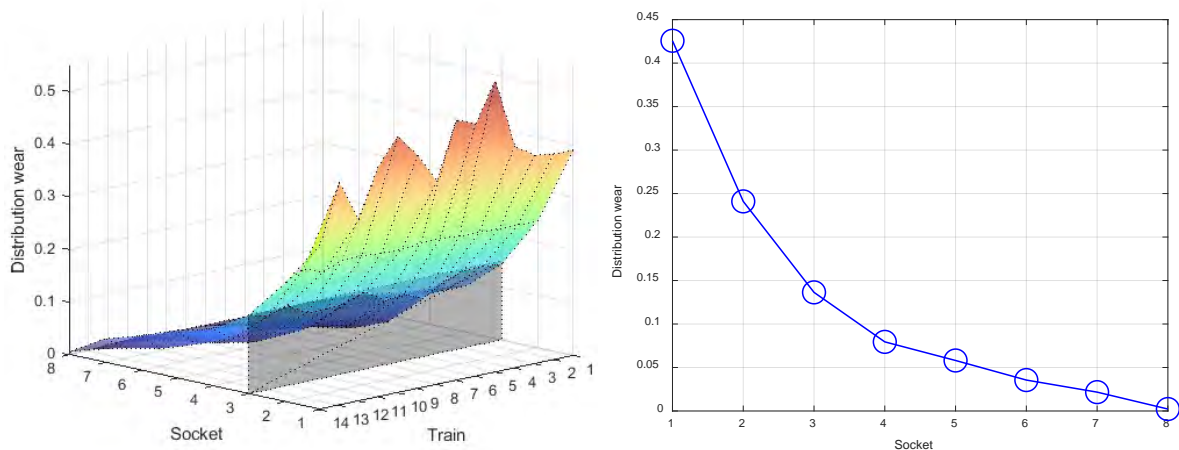


Figure 8-21. Modelled wear on $\tau-1$, where τ is when permutations occur involving the replacement of three elements. Left: surface plot of all 14 trains, right: plot of the mean modelled wear distribution.

Finally, analyses show that maintenance costs can be significantly lowered by lowering the membrane replacement rate, provided a higher frequency of CIP with the more effective method C2 is applied. We can see from the analyses that this does not compromise the reliability of the trains. Results see even better performance with policies 11 and 12 outperforming the most expensive policy 10, reducing the membrane replacement rate back to the original projections of the plant. A higher frequency of CIP with the more effective

method C2 (policy 8) without membrane replacements is not efficient to control the degeneration.

However, the CIP system must be upgraded to enable a frequency of more than two CIPs (C2) per train annually. This upgrade is a minor modification of the current CIP system, and therefore this upgrade is cost-effective. The concept of this research has been published in *Desalination* (van Rooij et al., 2021). Further, the findings have been communicated to the management of the O&M company. As a result, both the O&M company and the owners have agreed to upgrade the CIP system.

Returning to the sampling methods for the DT, although the risk measure decreases with the strength of smoothing, we see no change in the risk ranking of the policies. The latter is also the case when we apply the Weibull distribution sampling method instead of bootstrap sampling. At the same time, a longer smoothing window for the estimated feed quality provides more evident differentiation between algae bloom and non-algae bloom periods when applying the bootstrap method.

Results with Weibull distribution tend to differ when re-running the projection. This variation is significantly less when utilizing bootstrap sampling. The Weibull distribution projections also show the tendency to reach full restoration over time at the lower end of the ensemble forecast envelope (See grey beam at the bottom of Figures 8-13 to 8-15). The latter is unrealistic, except when algae booms disappear. Therefore, bootstrap sampling is preferable if a large dataset is available for sampling. Weibull distribution might be more practicable if limited data is available, as we saw with the start day and lengths of algae blooms. Although three smoothing ranges have been tested for bootstrap sampling in this research, this was only for test purposes. The thesis author recommends using a single smoothing range, in this case, -4, +12.

8.4 Summary

A Decision Support System (DSS) and its Digital Twin (DT), developed in this research by the thesis author, have been utilized to explore several maintenance policies for membrane restoration. The DSS supports two sampling methods for stochastic extrinsic dependencies, κ and cleaning efficiency δ , bootstrap sampling and Weibull distribution. Both methods were utilized. In the case of bootstrap sampling, the projections were repeated for three different smoothing regimes of the extrinsic dependency κ . Further, two risk thresholds were investigated: the projected ensemble forecast envelope exceeds the 3 bar and the 3.5 bar. Thus, the risk analyses of the policies were examined eight times.

Sensitivity analysis by different sampling methods, smoothing regimes, and risk thresholds resulted in similar risk analyses regarding ranking results. Bootstrap sampling gave overall better results than Weibull distribution, independent of the smoothing regimes. The thesis author is of the opinion that bootstrap sampling with a smoothing regime of 4 steps backwards and 16 steps forward is preferable. The reasoning is that a higher smoothing regime accentuates the periods of algae blooms stronger than a low smoothing regime.

When projections utilizing Weibull distribution were repeated, the results were less consistent. The Weibull distribution also tends to project full restoration at the lower ensemble envelope. However, the latter is very unlikely for the system in this case study. Nevertheless, Weibull distribution is a perfect method when available data for sampling is scarce.

The policies, twelve in total, consisted of different permutation regimes, cleaning frequencies and methods. Of these twelve policies, one policy is the current policy of the O&M company, and one is a policy with identical permutations but double the frequency of cleanings. The latter is the intention of the O&M company for the years ahead.

The other policies are alternatives involving fewer replacements and different cleaning frequencies. Three policies that utilise a standard CIP method (C1) that is less effective were tested to evaluate if, by applying a higher frequency of intervention, this method can have better results than the current CIP method (C2) at a lower frequency.

The analyses show that performing standard C1 cleanings is inefficient in controlling the degeneration, even with higher frequency. A standard High and Low pH CIP method will result in a membrane replacement rate excessive to that of the current policies of the O&M company. Neither gives an opportunistic block replacement of three elements simultaneously any improvements.

Alternative policies 11 and 12, involving C2 cleaning frequency of three CIPs per train annually, outperform the current and planned policies of the O&M team regarding cost and risk performance. Policy 12 thereby outperformed all others. These policies return the membrane replacement rate to the original projections of the plant despite being exposed to severe biofouling conditions following seasonal algae blooms. However, policies 11 and 12 require an upgrade of the CIP system to enable the required increase in C2 cleaning frequency to three per train annually. Both the O&M company and the owners have agreed on this upgrade following the outcome of this research.

9 Measuring the results compared to the baseline

In this chapter, we return to the baseline of the research set out in chapter 2. This research started from the objectives expressed by the CEO of the O&M company to reduce shortfall and costs. The baseline consists of three performance indicators, of which membrane maintenance management was one of them. The other two performance indicators were to reduce the shortfall in water delivery and the ratio of reactive corrective maintenance to predictive planned maintenance. By comparing the current performance against the baseline, the impact of the research on the case study can be measured.

The performance analysis described in chapter 2 concluded that system performance improvement should focus on joint production and maintenance planning. This improvement entails three approaches. First, the demand must be forecasted so planned maintenance is performed during pit stops that do not interfere with production demand. Secondly, degradation must be modelled and forecasted. Finally, reducing the time spent on failure-based maintenance will reduce unpredictability so that planned maintenance can be carried out more effectively. The topic of this research, managing the restoration of membranes in reverse osmosis desalination using a digital twin, mainly involves the second approach. Nevertheless, planned membrane maintenance must also be performed during pit stops that do not interfere with production demand.

The thesis presents principles for designing a digital twin (DT) based decision support system (DSS) for maintenance requirements. Next, a case study for the long-term maintenance planning of reverse osmosis (RO) membranes in seawater desalination, affected by biofouling, is used to demonstrate a DSS to solve an actual maintenance problem. The concept of a DT-based DSS is not limited to this practical example. The thesis author intends to demonstrate this with initial research on vibrations anomaly detection and performance analysis of the large centrifugal pumps at the plant. The objective is to identify if the source of degradation is limited to the bearings, which are relatively easy to replace or if the degradation involves components inside the pump casing. The latter requires opening the casing, which is an expensive, time-consuming fixed set-up activity.

The chapter is organized as follows. First, in section 9.1, demand forecasting is addressed. Then in section 9.2, initial research on condition-based maintenance of large centrifugal pumps is set out. Finally, in section 9.3, the results of the current state of the performance indicators are compared against the baseline.

9.1 Forecasting demand

The purpose of the demand forecast is to plan maintenance activities, which will temporally reduce the production capacity. Due to its unreliability, the forecast models give no added value to the decision process. During the period of December to March, the wet season, there is a change of 70% that the water authorities will request a reduced demand. The latter means a 30% chance of a minor shortfall. During the dry season, the demand is 54 MGD 95% of the days from April to November. We must consider that production capacity reduction will always result in a shortfall during these months.

An investigation has been conducted for the possibility of establishing a short-term demand forecast model for the desalination plant in this case study. Short-term water demand predictions for every day of the next week or even just one day in advance will help plan maintenance. Management needs to make decisions such as scheduling of water treatment capacity for short-term maintenance planning. Reduction of capacity for maintenance can have an impact on fulfilling customer demand. Business, industry, and government utilities thus rely on forecasting tools for planning and scheduling tasks.

Although forecasting is a well-established discipline, it has mixed results in the water sector. The reason behind this is the nature and quality of the available data and the numerous variables that affect water demand (Donkor et al., 2014). Forecasting of short-term electrical load by power generation utilities has been more successful. Under- or over-evaluating the required load capacity can result in heavy economic penalties in this sector. It was estimated that a one percent forecast error would result in an additional 10 million pounds per year for the British power system in 1985 (Papalexopoulos and Hesterberg, 1990). Regression analyses, autoregressive moving average (ARMA) and autoregressive integrated moving average (ARIMA) are standard methods for forecasting short-term electrical load demand (Papalexopoulos and Hesterberg, 1990; Che and Wang, 2014).

Various stakeholders, particularly the client, the San Diego County Water Authorities (SDCWA), the project development company representing the owners, further referred to as the asset owners, and the O&M company, have different interests. The first two stakeholders have a commercial agreement for the delivery of potable water. The client has contractually committed to a monthly, quarterly and annually minimum demand. So, if the client can fulfil their water needs from other financially cheaper resources, they are still obliged to request the minimum demand commitment. Therefore, if the delivery capacity is below the client's needs due to the equipment being out of service, the latter immediately requests a demand

corresponding to the designed maximum plant capacity to fulfil their minimum demand commitment even if they do not need that volume.

The incentive of the asset owners for the return on investment is to sell as much water as possible. There is no such incentive for the O&M company. They are paid for their services, independent of the water sold. However, the O&M company has to deliver the water demand of the client. The O&M company is penalized if they deliver less than 95 percent of the water demand. The shortfall can be made up, but no more than five percent above the daily water demand. The above-described stakeholder interests complicate short-term demand forecasting since the latter might not be driven by the actual water demand of the region.

The demand by the client can change up to three times a day with an interval of eight hours. The time slots are 8 am, 2 pm and 8 pm. However, for simplicity in this case study, only one flow change per day is considered. Previous daily averages are used to fit various forecast models. Environmental variables, e.g., daily maximum temperature, probability of rainfall and the season of the year, have been identified to affect water use. However, demand is probably not limited to these variables.

Multi-regression models were analyzed with different combinations of determining variables. The multi-regression analyses were first applied to an extended dataset from January 2016 to April 2019. 95% of the days between April and November, the entire plant design capacity of 54 Million Gallons a Day (MGD) is demanded. The regression analyses were repeated with a reduced dataset to investigate if a better fit could be reached for the winter months, excluding the days when the demand was above 50 MGD. For the period of December to March, there is strong randomness in demand. Additionally, time-series forecasts based on exponential smoothing and a moving average of the demand were tested involving data from January to March 2019.

Water forecasts have been applied to both medium to long-term and short-term demand predictions (Jain and Ormsbee, 2002; Altunkaynak et al., 2005; Caiado, 2010; Donkor et al., 2014). As stated earlier, a short-term demand forecast is helpful for plant operators. Although the medium-term and long-term forecast is expected to be stable for the CDP, this is not automatically the case for short-term forecasts.

Donkor et al. (2014) overviewed selected journal papers on water demand forecasting methods between 2000 and 2010. Of the 33 papers, 15 dealt with short-term demand. Of these 15 papers, ten dealt with daily demand forecasting. Table 9-1 gives the forecasting methods and the determining variables used in these ten studies.

Several researchers concluded that neural networks performed better for short-term forecasts than conventional methods like time-series regression or variate time-series models. This conclusion was, however, not unanimous. According to Jain and Ormsbee (2002), the slight drop in model performance does not justify the time and investment to develop a more sophisticated expert system. Regression analysis is the most frequently used statistical technique for water demand forecasting (Altunkaynak et al., 2005). This research focuses on conventional forecasting methods.

Table 9-1. Forecasting methods and determining variables of daily demand forecast models (source: Donkor et al., 2014)

| Authors | Forecasting method | Period | Determining variables |
|-------------------------|--|-------------------------------|--|
| Jain and Ormsbee (2001) | Regression, time series analysis or artificial neural networks (ANN) | Daily demand | Water demand of previous days, precipitation, max air temperature, sunshine hours |
| Cutore et al. (2008) | ANN, regression and adaptive neuro-fuzzy | Daily demand | Demand of previous day; working day dummy; day of week |
| Jentgen et al. (2007) | Heuristics, regression and ANN methods | Hourly demand Daily demand | Temperature, precipitation and Lag 1 of demand |
| Jain and Ormsbee (2002) | Regression, univariate time series and artificial intelligence (AI) models | Daily demand | Various lags of demand; max temperature; precipitation |
| Alvisi et al. (2007) | Fourier series for seasonal component and Auto-Regression (AR) for residuals | Daily demand hourly demand | Historical data |
| Aly and Wanakule (2004) | regression by adjusting monthly forecasts obtained from a Holt-Winters multiplicative exponential smoothing model | Daily and monthly demand | Precipitation, temperature, humidity, lagged demand |
| Caiado (2010) | Holt-Winters, ARIMA, and GARCH models | Daily demand | Univariate daily consumption |
| Gato et al. (2007a) | Models daily use a function of base use and seasonal where base use is dependent on climatic factors | Daily demand | Thresholds of temperature and precipitation; day of the week |
| Gato et al. (2007b) | Models daily use a function of base use and seasonal where base use is dependent on climatic factors. Uses regression for base use and Fourier series for seasonal use | Daily demand | Thresholds of temperature and precipitation; day of the week |
| Zhou et al. (2000) | Models base and climate components with regression, seasonal with Fourier, and residual with AR (p), where p takes values of 1, 2, and 7 | Daily per capita consumption | Max temperature; occurrence of rainfall; precipitation; evaporation; days since last rainfall. |

Weather patterns typically influence short-term demand (Jain and Ormsbee, 2002; Altunkaynak et al., 2005; Caiado, 2010; Donkor et al., 2014). Determining variables used in previous research for short-term water demand forecast are environmental conditions such as temperature, precipitation, the occurrence of rainfall, days since last rainfall, humidity and evaporation. In addition to environmental conditions, time-series data is used, where seasonal

influence is based on time-series data. San Diego County has a Mediterranean climate. More than 80% of the region’s rainfall occurs between December and March. Beginning 2015, SDCWA serviced 3.2 million residents. The population is expected to be 3.8 million by 2040, an average annual growth of 1%. In 2015 single-family homes accounted for 60% of residential dwellings in San Diego County. Up to 60% of domestic water use in single-family homes accounts for outdoor purposes, e.g., garden irrigation (sdcwa.org, 2016). Water demand is therefore expected to be heavily influenced by seasonal factors. Both environmental determinants and time-series variables have been included in the forecast models.

There are complicating factors that can influence the accuracy of the forecasts negatively. First is the urban structure of San Diego County. Research on water use in Texas showed that small towns have relatively greater randomness in water use than large cities (Zhou et al., 2000). The water authority service area consists of 19 towns⁵ and further rural areas. The largest city is San Diego, with a population of 1.4 million. The smallest is Del Mar, with a population of four thousand. When excluding San Diego, the average population per town is 78.6 thousand. College Station in Texas, where Zhou et al. (2000) refer, has a population of 113.6 thousand.

Table 9-2. Population, home value and household income per town in San Diego County

| | Population |
|------------------------|------------|
| Carlsbad | 113,147 |
| Chula Vista | 264,101 |
| Coronado | 24,053 |
| Del Mar | 4,338 |
| El Cajon | 103,314 |
| Encinitas | 62,595 |
| Escondido | 150,783 |
| Fallbrook ⁶ | 30,534 |
| Imperial Beach | 27,270 |
| La Mesa | 59,479 |
| Lemon Grove | 26,645 |
| National City | 60,715 |
| Oceanside | 174,811 |
| Poway | 49,874 |
| San Diego | 1,390,966 |
| San Marcos | 93,493 |
| Santee | 57,378 |
| Solana Beach | 13,362 |
| Vista | 99,496 |

⁵ <https://www.cleargov.com/california/san-diego>

⁶ <http://www.city-data.com/city/Fallbrook-California.html>

The second complicated factor is that the desalination plant is only one of the various sources of the water supply of the SDCWA. The CDP might not be proportional to the overall water demand of San Diego County. Demand for CDP could also depend on the temporally capacity reduction of the other suppliers the water treatment plants of the member agencies. These 12 plants, with a capacity of 752 million gallons a day (MGD), treat all the water (approx. 90% of the water supply) except the Desalination plant (sdcwa.org, 2016). The local water resources include surface water, water recycling, potable reuse, brackish groundwater recovery, and groundwater. The share of desalination is around 10% of the overall water supply. Table 9-3 below gives an overview of the various water supply sources of the region.

Table 9-3. Water utilities supplying to SDCWA (source sdcwa.org (2016))

| | 2020 | 2025 | 2030 | 2035 | 2040 |
|---|---------|---------|---------|---------|---------|
| Total Projected Supplies (AF/Y) | 587,581 | 648,124 | 676,721 | 694,431 | 718,773 |
| Imperial Irrigation District Transfer | 32% | 31% | 30% | 29% | 28% |
| Metropolitan Water District | 23% | 28% | 31% | 32% | 35% |
| Local water resources (Member Agencies) | 21% | 20% | 20% | 19% | 19% |
| All-American Canal and Coachella Canal | | | | | |
| Lining Projects | 14% | 12% | 12% | 12% | 11% |
| Carlsbad Desalination Plant | 10% | 9% | 8% | 8% | 8% |

9.1.1 Regression models

Several regressions analyses have been run to determine the best forecast model to predict water demand seven days ahead. For the determining variables, the following environmental variables were identified:

- Temperature
- Rainfall
- Seasonal influence

Rainfall is expected to lower the water demand since residents are not allowed to irrigate their garden for up to 48 hours after a rainfall (sdcwa.org, 2016). Rainfall means that the determining variable 'Ri' should be negative for the regression models. If this is not the case, then the model is doubtful. Seasonable influence is defined in two different quantitative expressions. The two options have not been combined in a single model. The environmental variables are expressed as follow:

- Temperature.

- $T_i - \mu T(\Delta T_i)$ daily maximum temperature in °F – average maximum temperature over the years 2016 to 2018
- Rainfall
 - R_i expressed as the occurrence of rainfall (0 or 1): Previous data based on precipitation > 0.5 inches. Future weather forecast predicting the chance of rain above 50%.
- Seasonable influence
 - S_i , -1 for Jan to Mar; 0 for April to Nov and 1 for Dec.
 - $s^l i$, -1 for Jan to Mar; 2 for April to Nov and 0 for Dec.

S_i and $s^l i$ both identify Jan-Mar as the wet season, April-Nov as the dry season and December as the change between the wet and the dry season. However, by assigning different values to the latter two, the sensitivity of the forecast is tested.

Data on daily maximum temperatures and precipitation were collected from the National Oceanic and Atmospheric Administration (NOAA). Also, a combination is applied of the environmental variables with a moving average of previous demand and the client's monthly minimum committed demand. The demand seven days previously is defined per equation one below.

Previous weekly demand is further defined in two options. First, the previous weekly demand is defined in a moving average of the previous seven days. Further, the previous weekly demand is defined as the average demand of the previous calendar week. Both one or the other option and a combination of the two options were included in another model. The above variables are defined as follow:

- Previous demand
 - D_{i-7} , Demand 7 days previously (moving average of daily demand)

$$D_{i-7} = \frac{\sum_{i-7}^{-7} D_i}{7}$$
 - W_i , Moving average of the previous week's daily demand

$$W_i = \frac{\sum_{i-7}^{-14} D_i}{7}$$
 - $W^l i$, a fixed average of the demand of the previous calendar week
- Monthly minimum committed demand client
 - $MinD$, Minimum Daily demand commitment of the client for the calendar month

Data is used from 2016 until April 15th, 2019. February 29 in the leap year 2016 has been dropped to maintain 365 days in each year. The sampling rate was 1200. Initially, 75 regression analyses were run utilizing RegressIt⁷, where *Y* is demand and *X* is the determining variables, e.g., *Ti-μT*, *Ri*, *Si*, *s^li*, *Di-7*, *Wi*, *W^li*, and *MinD*. The regressions were based on a single variable to determine the variables' impact and multi regressions of a combination of variables. First, eight simple regressions were run on the independent variables to evaluate their effect on the dependent variable. After that, 26 multiple regressions were run with combinations of two variables and 25 regressions of triple variables. Four regressions of four variables, six of five, four of six and one of seven. Figure 9-1 shows the output of the regression analyses, utilizing RegressIt with the best results. Table 9-4 shows the corresponding coefficients.

| Linear Model For Di | Run 25 | Run 32 | Run 35 | Run 47 | Run 49 | Run 56 | Run 60 | Run 68 | Run 73 | Run 74 | Run 75 |
|------------------------------|---------------|---------------|---------------|---------------|---------------|---------------|---------------|---------------|---------------|---------------|---------------|
| # Fitted | 1200 | 1200 | 1200 | 1200 | 1200 | 1200 | 1200 | 1200 | 1200 | 1200 | 1200 |
| Mean | 46.195 | 46.195 | 46.195 | 46.195 | 46.195 | 46.195 | 46.195 | 46.195 | 46.195 | 46.195 | 46.195 |
| Standard Deviation | 13.041 | 13.041 | 13.041 | 13.041 | 13.041 | 13.041 | 13.041 | 13.041 | 13.041 | 13.041 | 13.041 |
| Number Of Variables | 2 | 2 | 2 | 3 | 3 | 3 | 3 | 5 | 6 | 5 | 5 |
| Standard Error of Regression | 9.995 | 9.957 | 9.749 | 9.970 | 9.942 | 9.967 | 9.726 | 9.458 | 9.421 | 9.698 | 9.731 |
| R-squared | 0.414 | 0.418 | 0.442 | 0.417 | 0.420 | 0.417 | 0.445 | 0.476 | 0.481 | 0.449 | 0.445 |
| Adjusted R-squared | 0.413 | 0.417 | 0.441 | 0.416 | 0.419 | 0.416 | 0.444 | 0.474 | 0.478 | 0.447 | 0.443 |
| Mean Absolute Error | 5.843 | 5.878 | 5.665 | 5.776 | 5.891 | 5.786 | 5.627 | 5.409 | 5.355 | 5.598 | 5.592 |
| Maximum VIF | 1.161 | 1.345 | 1.512 | 1.653 | 3.305 | 1.350 | 1.671 | 4.038 | 5.882 | 3.520 | 4.900 |
| Mean Absolute Scaled Error | 2.960 (lag 1) | 2.978 (lag 1) | 2.870 (lag 1) | 2.926 (lag 1) | 2.984 (lag 1) | 2.931 (lag 1) | 2.850 (lag 1) | 2.740 (lag 1) | 2.713 (lag 1) | 2.836 (lag 1) | 2.833 (lag 1) |
| Residual Autocorrelation | 0.82 (lag 1) | 0.81 (lag 1) | 0.80 (lag 1) | 0.82 (lag 1) | 0.80 (lag 1) | 0.82 (lag 1) | 0.80 (lag 1) | 0.77 (lag 1) | 0.78 (lag 1) | 0.79 (lag 1) | 0.80 (lag 1) |
| Coefficients: | Run 25 | Run 32 | Run 35 | Run 47 | Run 49 | Run 56 | Run 60 | Run 68 | Run 73 | Run 74 | Run 75 |
| Constant | 16.506 | 6.415 | 4.346 | 14.464 | 6.931 | 18.126 | 6.207 | 11.044 | 12.713 | 15.106 | 7.396 |
| Di_7 | | 0.254 | | | 0.317 | | | | 0.086 | 0.298 | -0.012 |
| MinD | 0.729 | 0.664 | 0.575 | 0.689 | 0.681 | 0.691 | 0.543 | 0.563 | 0.538 | 0.620 | 0.517 |
| Ri | | | | | | | | -0.352 | | | |
| Si | 5.314 | | | 4.662 | | 5.110 | | 3.882 | 3.783 | 4.325 | |
| Si1_ | | | | | | | | | | | 0.287 |
| Ti_μT | | | | | | 0.129 | 0.118 | | 0.108 | 0.097 | 0.110 |
| Wi | | | | 0.079 | -0.090 | | | -0.286 | -0.319 | -0.171 | |
| Wi1_ | | | 0.380 | | | | 0.370 | 0.547 | 0.483 | | 0.374 |

Figure 9-1. Regressions models with an R-squared > 0.4. Data from January 2016 to April 2019

Table 9-4. Coefficients regression models with an R-squared of above 0.4

| | Intercept a | ΔTi b | <i>Ri</i> c | <i>Si</i> d | <i>S^li</i> e | <i>D-7i</i> g | <i>Wi</i> h | <i>W^li</i> n | <i>MinDi</i> p |
|--------|----------------|------------------|----------------|----------------|----------------------------|------------------|----------------|----------------------------|-------------------|
| Run 25 | 16.506 | | | 5.314 | | | | | 0.729 |
| Run 32 | 6.415 | | | | | 0.254 | | | 0.664 |
| Run 35 | 4.346 | | | | | | | 0.380 | 0.575 |
| Run 47 | 14.464 | | | 4.662 | | | 0.079 | | 0.689 |
| Run 49 | 6.931 | | | | | 0.317 | -0.090 | | 0.681 |
| Run 56 | 18.126 | 0.129 | | 5.110 | | | | | 0.691 |
| Run 60 | 6.207 | 0.118 | | | | | | 0.370 | 0.543 |
| Run 68 | 11.044 | | -0.352 | 3.882 | | | -0.286 | 0.547 | 0.563 |
| Run 73 | 12.713 | 0.108 | | 3.783 | | 0.086 | -0.319 | 0.483 | 0.538 |
| Run 74 | 15.106 | 0.097 | | 4.325 | | 0.298 | -0.171 | | 0.620 |
| Run 75 | 7.396 | 0.110 | | | 0.287 | -0.012 | | 0.374 | 0.517 |

⁷ RegressIt™ is a free Excel add-in for multivariate descriptive data analysis and regression analysis from regressit.com and was developed at the Duke University for teaching regression and time series analysis in MBA courses. <https://regressit.com/>

From the simple regressions, the minimum daily demand commitment of the client for the calendar month (MinD) had the highest impact on the forecast with an R-Squared of 0.367. Rainfall had a neglectable impact with an R-squared of 0.004. Twelve results of the multiple regressions gave a positive coefficient for rainfall. This positive coefficient implies that rainfall would increase demand. The latter is contradictory to logic and therefore has been disregarded.

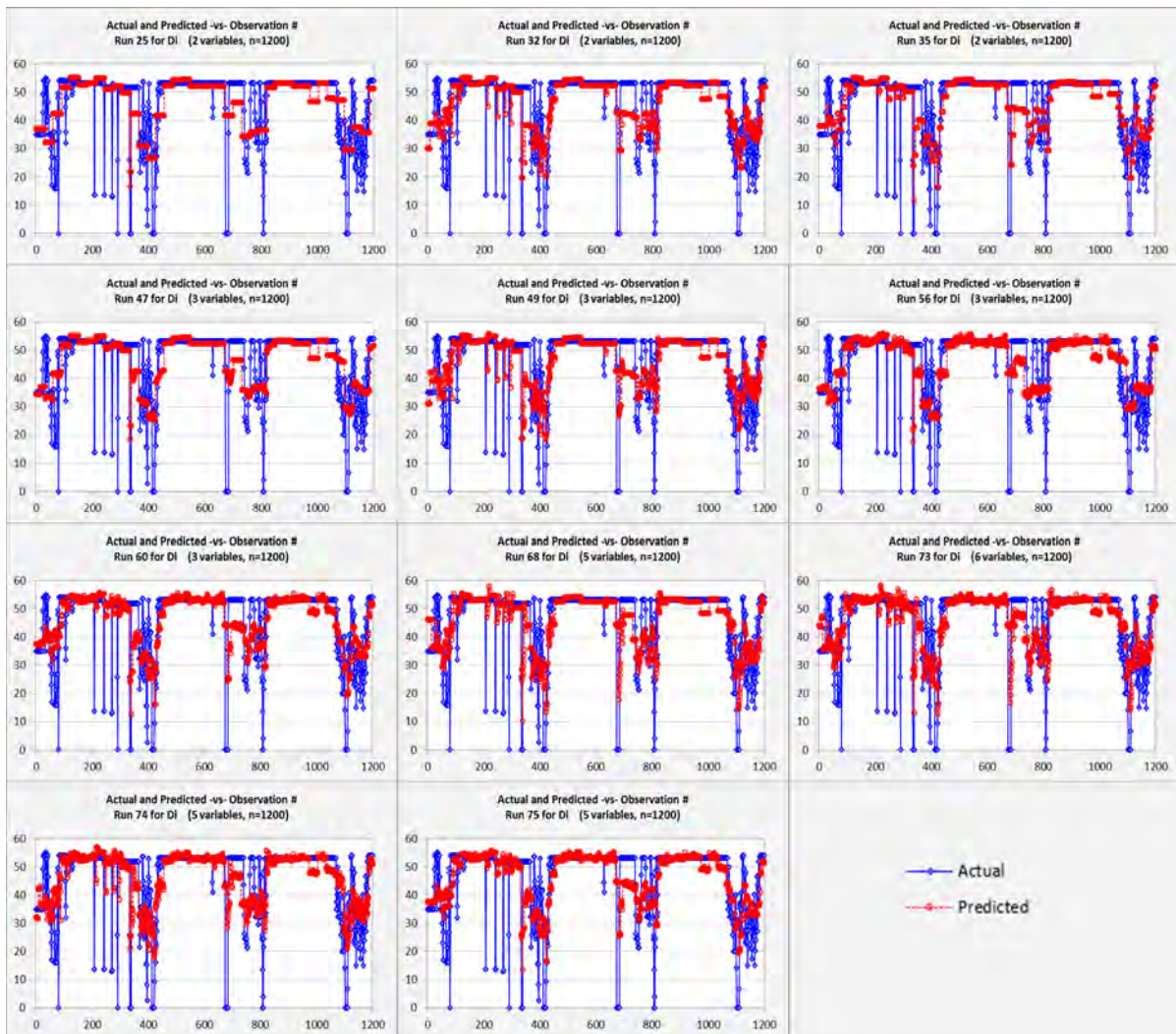


Figure 9-2. Trend charts of regression models with an R-squared of above 0.4. The Y-axes show the daily water demand in MGD, and the X-axes show the days.

From the remaining regressions, 11 models had an R-squared of above 0.4. These regression models include the moving average of the previous demand, i.e., D_{i-7} , W_i and W^1_i and the minimum monthly committed demand by the client. The regression model with only environmental variables, i.e., ΔT_i , R_i , and S_i or S^1_i , gave an R-squared of below 0.4 (0.239 with the combination of S_i and 0.323 with the combination of S^1_i).

The corresponding trend graphs of the regression models with an R-squared above 0.4 are shown in Figure 9-2 above. The 11 models were tested by running forecasts against the data from January to March 2019. Data from January 6 to January 16 was removed since the plant was shut down for scheduled major maintenance during that period. Unfortunately, the forecast did not correlate with the actual demand when a lower demand than 51.8 MGD was predicted. The model with the best fit scored a poor R-squared of 0.01. The latter might be influenced by the client’s commercial interest, i.e. the minimum demand commitment, as described earlier. Further, the initial regression analysis is affected by a demand of 51.8 MGD or above for 71% of the time between January 2016 and April 2019.

9.1.1.1 Concentrating forecasting during the ‘wet season.’

The concentration of rainfall between December and March is reflected in demand during the wet period (December to March) and the Dry season (April to November). On average, 32% of the days during the wet season, the demand was above 51 MGD. During December 2018 and March 2019, the days of demand over 51 MGD were just 9%. Throughout the dry season, 95% of the days, the demand is above 51 MGD (see table 9-5).

Table 9-5. Demand for days above 51 MGD per dry and wet season

| | Jan - Mar 2016 | Dec 2016 – Mar 2017 | Dec 2017 – Mar 2018 | Dec 2018 – Mar 2019 | Total | Apr - Nov 2016 | Apr - Nov 2017 | Apr - Nov 2018 | Total |
|---------------------|----------------------|---------------------------|---------------------------|---------------------------|-------|----------------------|----------------------|----------------------|-------|
| Count > 51 MGD | 22 | 50 | 60 | 11 | 143 | 226 | 230 | 243 | 699 |
| Total days period | 90 | 121 | 121 | 121 | 453 | 244 | 244 | 244 | 732 |
| Percentage > 51 MGD | 24% | 41% | 50% | 9% | 32% | 95% | 93% | 94% | 95% |

Figure 9-3 below shows the demand in the time series. From this data, we can conclude that demand between April and November is expected to be above 51 MGD with a forecast error of 5%. The demand between January and March seems to be somewhat random.

Observing highly probable events provides very little information (Miller and Childers, 2012, p. 155).

Following this observation, forecasting is limited for the period of December to March to investigate if a more precise prediction of demand can be made in this season. Regression models were rerun from December to March, from January 2016 until March 2019. The number of rows of the excel file was reduced from 1200 to 373. We can now neglect the seasonal influence. The number of regression models was reduced to 46. In four of the 46 models, the rainfall had a positive coefficient which is at odds with the logic. Demand 7 days

previously ($Di-7$) and the average of the demand of the previous calendar week (W^i) had the most significant impact on the single regression analyses.

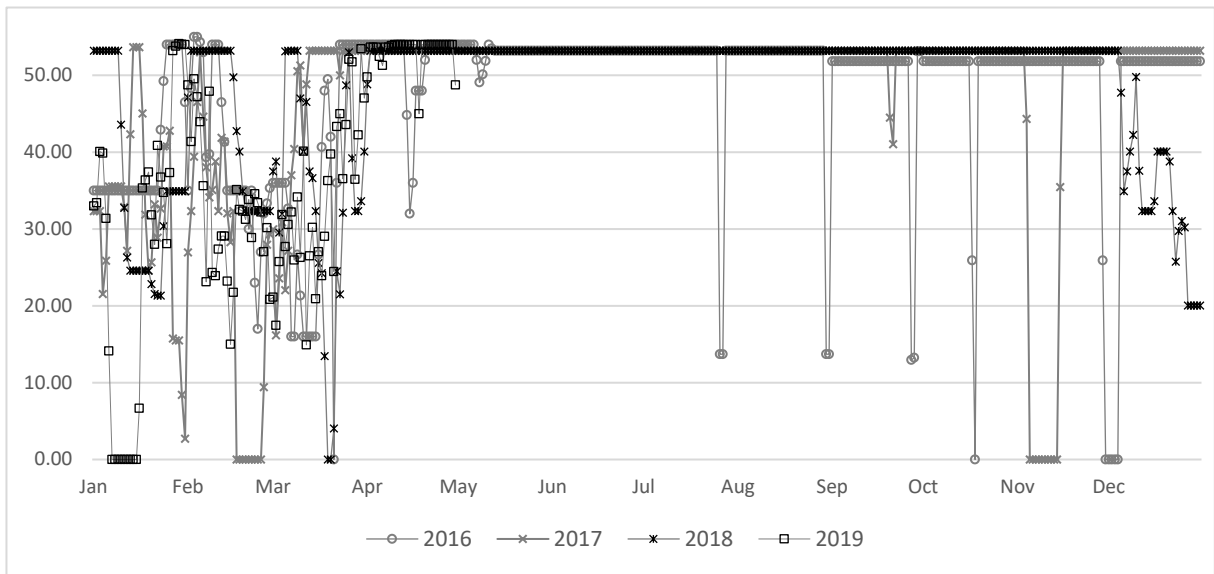


Figure 9-3. Daily demand requests from 2016 to 2019. The Y-axes show the daily water demand in MGD, and the X-axes show the days arranged per month.

All models had a poor fit, with only six models with an R-squared above 0.2. The model with the best fit had an R-squared of only 0.232. The six models were tested by running forecasts against the data from January to March 2019. Again, data from January 6 to January 16 was removed since the plant was shut down. The forecasts vary between 25 and 45 MGD, while the actual demand varies between 15 and 54 MGD (see figure 9-3). The forecasts are unable to predict the sudden increases to 50 MGD or above. The demand at points 16 to 20 went to 54 MGD, while all forecasts predicted a drop-in demand. A value of just 0.11 was the highest R-squared reached.

We can conclude from these demand forecasts that there is a high degree of randomness during the period of December to March. The forecast confirmed the high degree of randomness of the time-series trend graph shown in Figure 9-4. The literature review confirmed that forecasting the demand would be complicated due to the urban character of San Diego County. Further, as mentioned earlier, the division of the region’s daily demand between the 12 water treatment plants adds additional uncertainty to demand projections of CDP. Temporally supply limitations of any of those 12 water treatment plants can influence the water request to the desalination plant for that day.

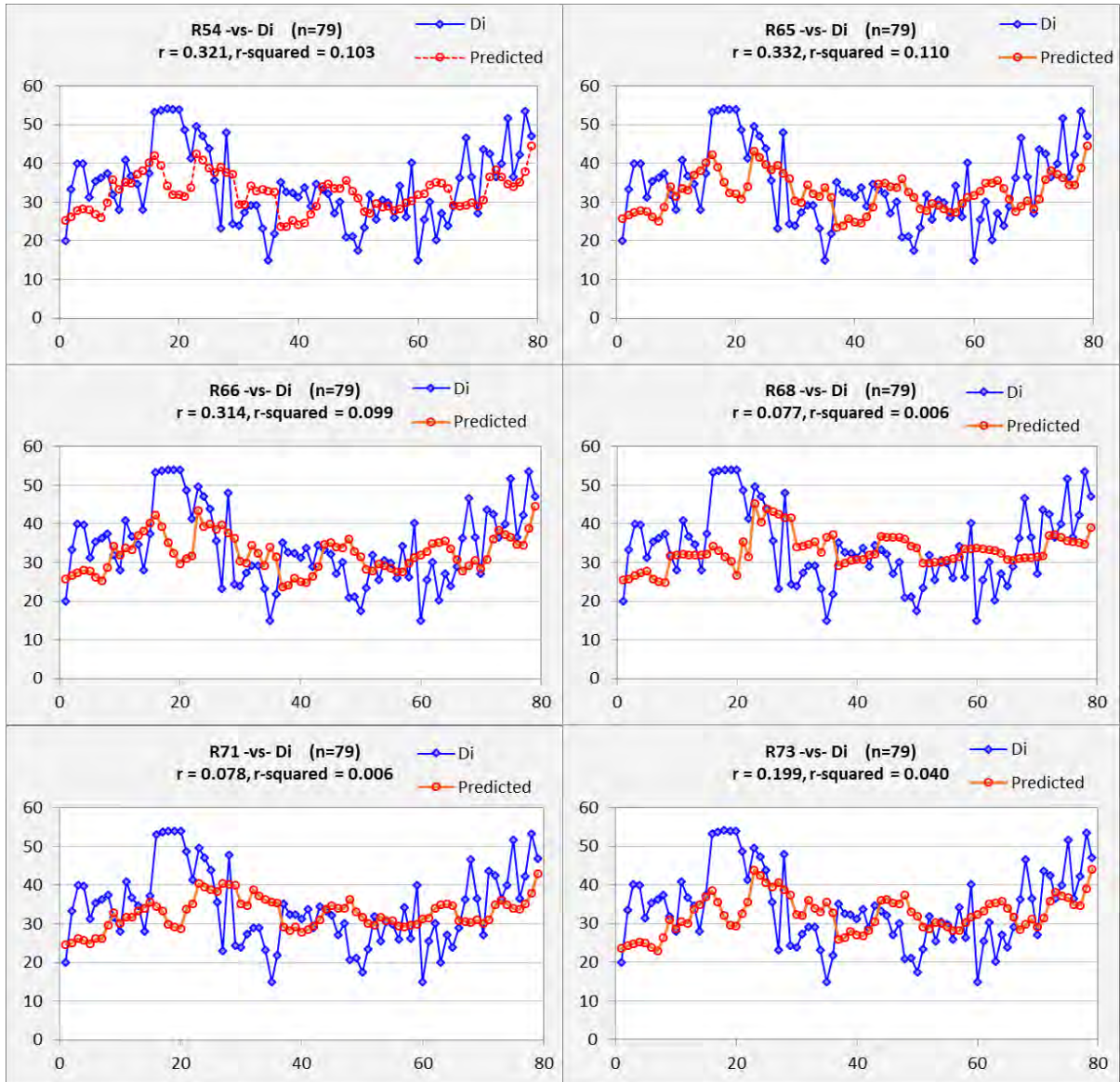


Figure 9-4. Trend charts of regression models applied to the data from January to March 2019. The Y-axes show the daily water demand in MGD, and the X-axes show the days. The blue pen is the actual, Red pen is the forecast.

9.1.2 Exponential smoothing and moving average

In addition to the regression models, forecasting models based on exponential smoothing ($Y_t = Y_{t-1} + coefficient(X_t - Y_{t-1})$) and moving averages ($Y_t = (X_{t-1} + X_t) / 2$) were investigated. Makridakis et al. (1982) stated that the more randomness of the data, the less important it is to use sophisticated statistical methods. Therefore, time-series forecasting based on exponential smoothing could perform better based on one or two periods ahead. This reasoning was also observed in this research. Forecasting the demand one day in advance gave an R-squared of 0.430 for the reduced dataset. A random exponential coefficient of 0.3 was used.

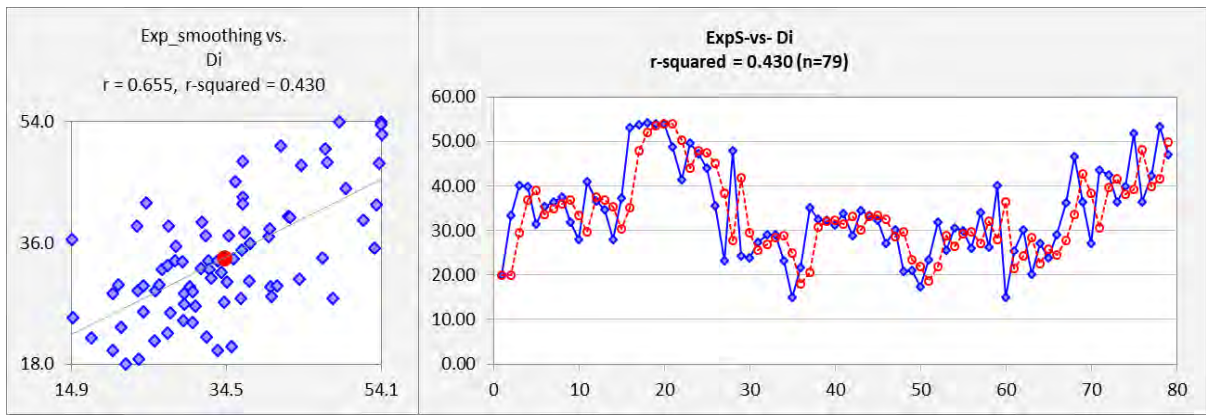


Figure 9-5. Left, a scatterplot of the predicted (*Y-axes*) vs the actual demand (*X-axes*) of exponential smoothing. Right, a trend chart of the time-series data. The blue pen is the actual, Red pen is the forecast. The Y-axes show the daily water demand in MGD, and the X-axes show the days.

Figure 9-5 gives the scatterplot and trend chart of the predicted vs the actual demand for the reduced dataset. Applying the method of moving average gives a similar result. A period of two days in the past has been applied. Forecasting the demand one day in advance gave an R-squared of 0.404 on the reduced dataset.

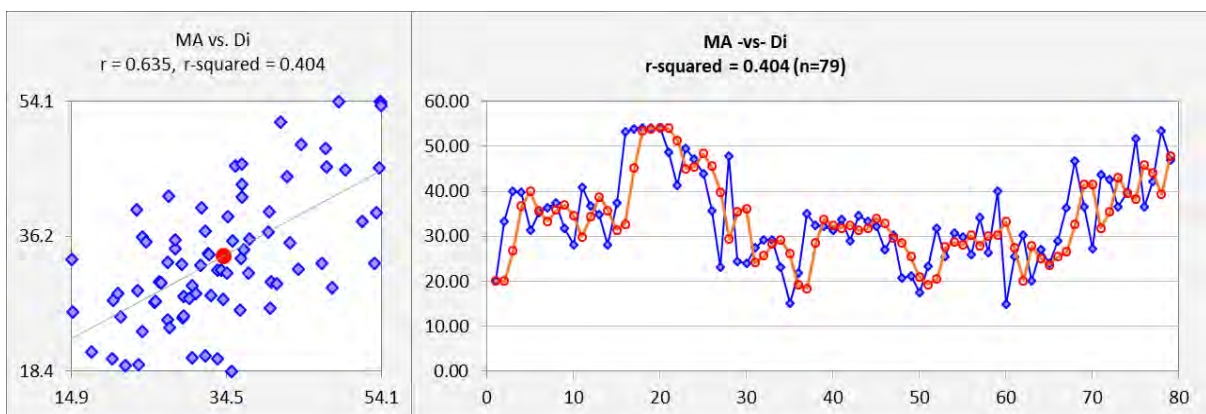


Figure 9-6. Left, a scatterplot of the predicted (*Y-axes*) vs the actual demand (*X-axes*) of by moving average. Right, a trend chart of the time-series data. The Y-axes show the daily water demand in MGD, and the X-axes show the days. The blue pen is the actual, Red pen is the forecast.

The exponential smoothing and moving average models, forecasting only one day ahead, performed better than the regression analysis. However, both exponential smoothing and moving averages lag with one to a few days. This lagging means that when the maximum demand is requested, this only shows up a few days later. The purpose of the forecast is to estimate when maximum demand will be required and when there is reduced demand. The forecasts failed on this task. Figure 9-6 gives the scatterplot and trend chart of the predicted vs the actual demand forecasting applying the moving average.

9.1.3 Autoregressive moving average

Several papers on short-term electrical load forecasting include AutoRegressive Moving Average (ARMA) (Papalexopoulos and Hesterberg, 1990) or AutoRegressive Integrated Moving Average (ARIMA) (Che and Wang, 2014; Dudek, 2016). The thesis author limited additional forecasting techniques only to ARMA forecasting. ARMA models use a polynomial for autoregression (p) and another for moving average (q). The equation for the

$$\text{ARMA}(p,q) \text{ model is } Y_t = c + \sum_{i=1}^p \varphi Y_{t-i} + \sum_{i=1}^q \theta_i \varepsilon_{t-i} \tag{21}$$

where φ is the autoregressive model's parameter;

θ is the moving average model's parameter;

ε the white noise process (a random process of uncorrelated random variables, with mean zero and a finite variance);

c is a constant.

An ARMA model has been applied to the reduced dataset from 2016 to 2018 for the first week of 2019. Afterwards, a daily forecast for a new week ahead was conducted.

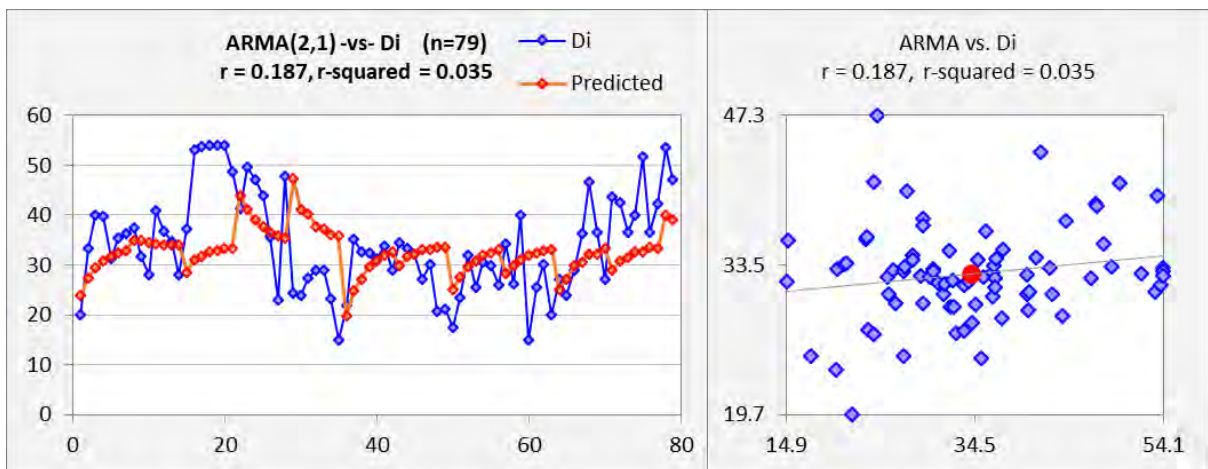


Figure 9-7. Left a trend chart of the time-series data by moving average. The blue pen is the actual, Red pen is the forecast. The Y-axes show the daily water demand in MGD, and the X-axes show the days. Right, a scatterplot of the predicted (Y-axes) vs the actual demand (X-axes).

The forecast based on ARMA gave a low fit like the multi-regression analyses when applied to the data of January to March 2019. The R-squared was 0.035. Figure 9-7 gives both the time-series comparison and the scatterplot of the ARMA applied to the data of 2019. Similar to the exponential smoothing and moving average models, the ARMA model failed to estimate if the demand will be reduced for the next day providing the opportunity to service

major equipment without affecting demand obligations. The model did not predict the demand of 50 MGD or higher during the seven days.

9.1.4 Summary forecasting.

This research could not establish a short-term demand forecast model for the case study. The pattern of the demand is too random. Forecasting models based on multi-regression gave no correlation. Environmental factors such as temperature, rainfall, and seasonal influence were neglectable in the multi-regression analysis. The forecasts could predict the demand for 54 MGD during the dry period between April and November. However, this gave a misleading fit for the remaining wet period of the year. When disregarding the data from April to November, there was no correlation anymore, and the requested demand seems to be highly random.

Forecast models based on exponential smoothing and simple moving average gave a poor fit with an R-squared of 0.43 for exponential smoothing and an R-squared of 0.404 for moving average. An autoregressive moving average (ARMA), successfully to short-term electrical load forecasting, had poor results in the water demand forecasting in this case study. Like the regression models, the correlation (R-squared 0.04) was poor. More importantly, all three models could not predict the cases when the demand was raised to the entire design capacity. The latter was the main objective.

There are two complicating factors in predicting the demand for the plant. First, the water authorities supply water to several small towns. Previous research has shown that demand is more random when dealing with small towns. Further, the plant supplies only approx. 10% of the overall water supply to the water authorities. Most of the supply comes from 12 other water treatment plants. Therefore, temporally supply limitations of those plants can influence the water request to the desalination plant for that day. In addition, commercial interests seem to motivate the client to request maximum demand when the plant capacity is reduced.

9.2 Condition-based maintenance of centrifugal pumps

The following section demonstrates a DT-based DSS concept for the plant's large centrifugal pumps based on initial research on vibrations anomaly detection and performance analysis. A virtual replica of the centrifugal pump can show the flow, power consumption, and vibrations according to feed and discharge pressure and pump speed. The virtual replica can then be compared to the physical pump to determine wear, and the wear source is bearings or the pump's internal components. The latter requires significantly higher fixed set-up costs.

Besides the RO trains, the main focus of this research, all other primary equipment of the plant consists of or includes centrifugal pumps. The electrical motors of the majority of these pumps, e.g., Intake Pumps (IP), Low-pressure booster (LPB) pumps, High-pressure Booster (HPB) pumps, Energy Recovery System (ERS) booster pumps, and Brackish Water RO (BWRO) feed pumps, are driven by Variable Frequency Drives (VFD). Most pumps are relatively large, from 250 kW up to 1.6 MW. Further, pumps with the same purpose are connected parallel to common headers.

9.2.1 Vibration monitoring and analysis of centrifugal pumps.

Bearing vibration and temperature monitoring has been dominant in the predictive maintenance of centrifugal pumps. Wear of bearings often results in increased vibration and rising bearing temperature. Several Predictive maintenance studies have concentrated on vibrations (Parrondo et al., 1998; Orhan et al., 2006; Ugechi et al., 2009; Babu and Das, 2013; Xue et al., 2014; Stan et al., 2018). Vibration monitoring is the most common method applied in predictive maintenance (Beebe, 2004) and a predictive maintenance system not including vibration monitoring would be significantly hampered. Vibration analysis is complex, especially for centrifugal pumps. Many practising engineers spend decades troubleshooting vibrations before developing an indebt understanding of the matter.

The source of the vibrations can be due to mechanical, hydraulic and peripheral courses, e.g., misalignment between pump and motor, bearing fatigue, unbalance of the impeller or shaft, cavitation, or vortices. The primary purpose of vibration analysis is to detect a developing vibration tendency on time. After all, increasing vibration levels are an early sign of failure (Birajdar et al., 2009). Thus, a maintenance activity can be planned instead of the need for unplanned corrective maintenance firefighting due to a critically advanced failure.

Vibrations are inherent to centrifugal pumps generated by both mechanical and hydrodynamic sources. Mechanical and fluid-dynamic borne vibrations can be further intensified in the bends, joints, pipe diameter changes, and pipe assembly's T-joints (Birajdar et al., 2009; Albraik et al., 2012; Barzdaitis et al., 2016). Additional vibration problems can occur when implementing VFDs. Harmonics from a VFD with six pulse output converters can cause torsional vibration. The primary VFDs in this case study have 18 pulse output converters. Besides harmonics, the motor can contribute vibrations due to electromagnetic and electromechanical forces. Electromagnetic forces are, e.g., the air gap dissymmetry between the motor rotor and stator and the magnetic pull force of the line frequency. Electromechanical forces are mechanical unbalances and motor slip (Costello, 1990).

Combined with the vibrations due to the mechanical and fluid dynamics of the pump, these sources of vibrations intensify the overall vibrations (Dickau and Perera, 2000).

9.2.1.1 Fluid dynamics-borne vibrations.

Fluid-dynamic-borne vibrations in centrifugal pumps are transferred to the outer casing due to the fluid's pressure fluctuations. These pressure fluctuations occur when the impeller vanes pass the diffuser vanes or cutwater in case of a volute. The speed of this occurrence is defined as the Blade Pass Frequency (Stickland et al., 2000; Guo and Maruta, 2005; Jiang et al., 2007; Gülich, 2010; Albraik et al., 2012; Zhao et al., 2013; Jun et al., 2014; Schofield et al., 2016; Zhang et al., 2018; Dhanasekaran and Kumaraswamy, 2019; Li et al., 2019).

Having an equal number of impeller vanes and a double volute, as is the case with the HPB pumps of this case study, results in two pressure pulses coinciding when the vanes pass the cutwater (Dickau and Perera, 2000). Zhang et al. (2018) studied the amplification of pressure pulsation under cavitation conditions, which can result in a considerable increase in vibrations. In the short term, these elevated vibrations disappear when cavitation conditions cease to exist.

Complications intend to increase when running pumps parallel with a common discharge header. Kogler et al. (2014) investigated the effects of a slight rotational speed difference due to the motor slip of two identical centrifugal pumps operating in parallel. The Pressure pulsations and pump performance were sensitive to the slightest deviations in speed between the pumps. The latter was reflected in the individual energy consumption of the pumps.

According to Schofield et al. (2016), the noise and vibration levels tend to be higher due to increased power density at higher rotational speeds. A study by Dhanasekaran and Kumaraswamy (2019) did not find a correlation between the amplitude of pressure fluctuations and operating frequency. However, the study was based on a multi-stage high-pressure pump, and the maximum pressure fluctuation amplitude per stage differed per operating frequency. On the other hand, studies by Stickland et al. (2000) and Albraik et al. (2012) have highlighted a correlation between the flow rate and vibration. An experimental study by Stickland et al. (2000), based on a single-stage pump, showed that the flow rate was the main reason for the amplitude of pressure fluctuations in the volute. A study by Albraik et al. (2012), also based on a single-stage pump, showed a positive correlation between pump flow and vibrations.

Studies so far have concentrated on design improvement to reduce hydrodynamic vibrations (Guo and Maruta, 2005; Jiang et al., 2007; Zhao et al., 2013; Jun et al., 2014;

Wang et al., 2018; Li et al., 2019). Studies further concentrated on fault detection on bearings (Dwyer-Joyce, 1999; Orhan et al., 2006; Azeez and Alex, 2014; Golbaghi et al., 2017; Amarnath and Krishna, 2019) or fault detection on impellers (Tobi and AL-Mahdi, 2016; Jami and Heyns, 2018).

9.2.1.2 A simplified method of filtering vibration data when pump flows are dynamic

Several predictive maintenance programs involving vibration analysis are based on measurements of vibrations with a portable accelerometer, involving expertise knowledge to analyze the test results (Parrondo et al., 1998; Orhan et al., 2006; Babu and Das, 2013) or are based on complex algorithms (Xue et al., 2014). In this study, all pumps with 250 kW or above power include velocity transducers (VT). VTs are used to monitor vibrations and are permanently installed on the bearing houses of the pumps and drives. Statistical methods were used on one of the pumps' data to investigate if a simple correlation could be established between pumps' speed and vibration levels.

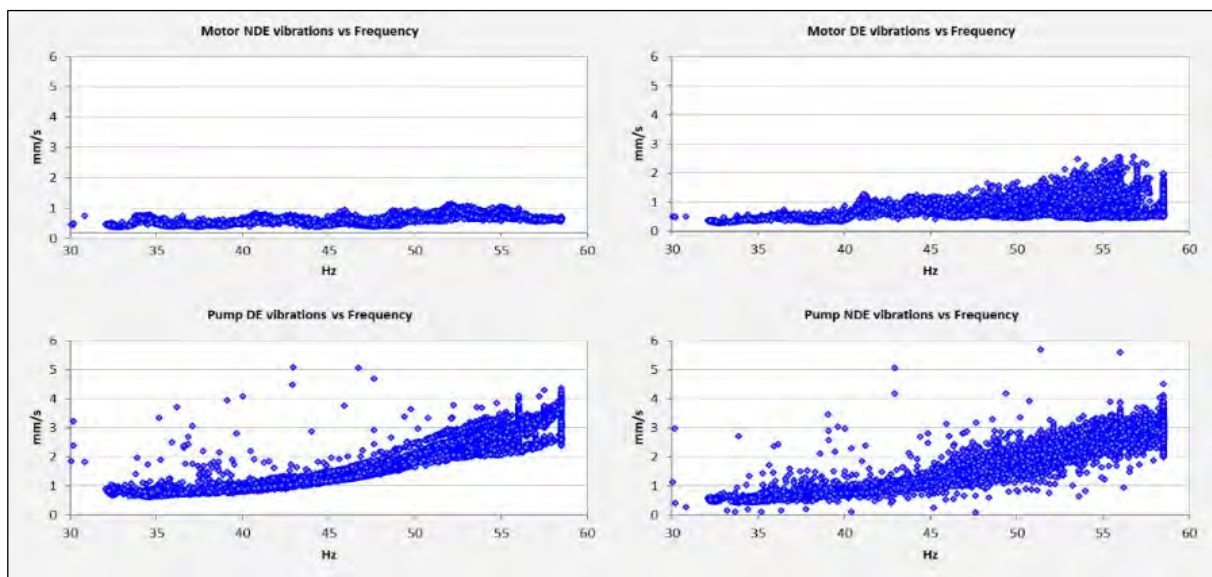


Figure 9-8: Scatterplot of vibrations vs frequency for DE and non-drive-end (NDE) of HPB pump 2 (Data 2016). Y-axis vibrations, X-axis motor frequency.

The data of HPB pump 2 over the first year of operation, 2016, is used as a baseline for this correlation. We can assume that at this time, the bearings were in normal/good/non-worn condition. In the case of the pump, we can observe a clear positive correlation of vibration vs frequency at the scatterplots. The vibrations of the pump drive-end (DE) are expected to impact that of the motor DE due to the transfer by the coupling. This impact can be observed in Figure 9-8.

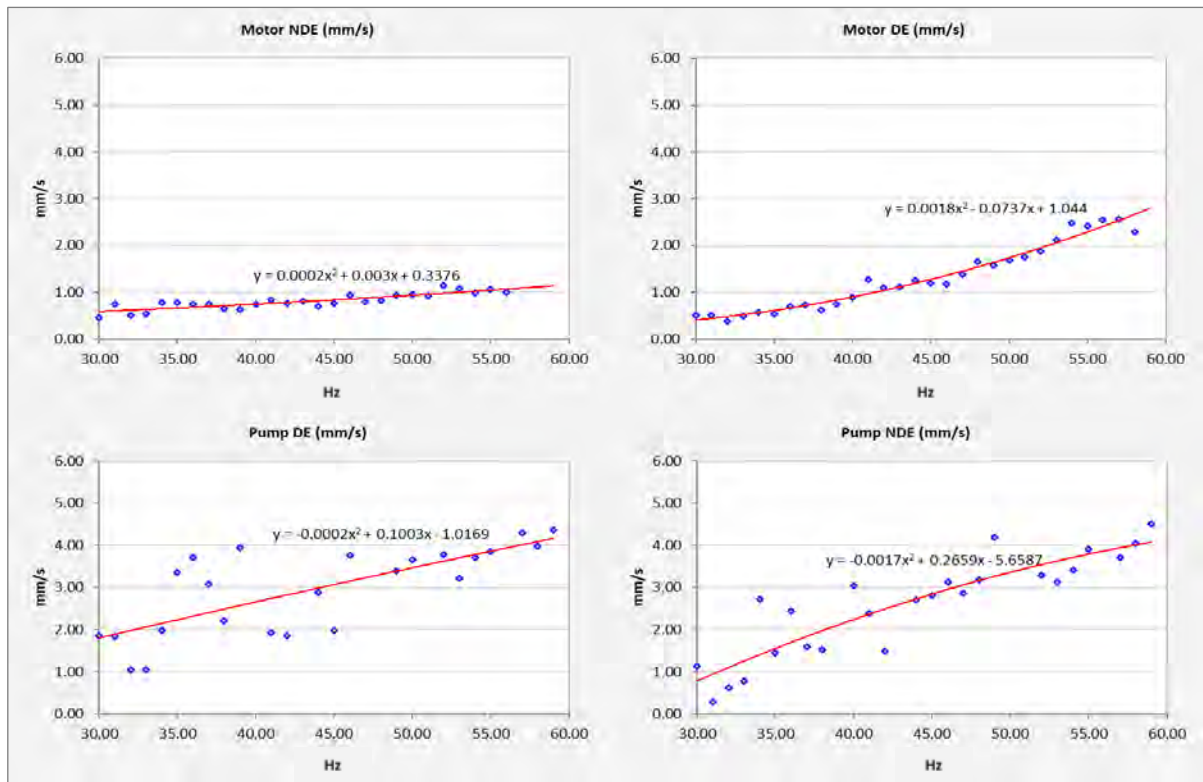


Figure 9-9. Scatter plot of the maximum vibration data vs the Frequency of HPB pump 2. Y-axes vibrations, X-axes motor frequency.

Following the upper limit of fluid-dynamic borne vibrations can be established by discretizing frequency to intervals of one Hz and selecting the maximum vibration values from the data accordingly. Figure 9-9 shows the scatter diagrams of the maximum vibration values for the frequencies from 30 Hz to 59 Hz with intervals of one Hz. A Polynomial trendline is added in the order 2.

The values analyzed per frequency interval were 0.5 Hz below up to 0.5 Hz above the frequency interval. Those values which were far out of the trend were omitted. The equation of the polygons (see Figure 9-9) is used as the baseline of the relation between vibrations and frequency of healthy bearing and no wear or damage on the impeller. Wear resulting in increased vibration can be revealed by subtracting the calculated maximum expected vibration according to the polygon equations from the observed vibrations. The thesis author defines the latter as *Normalized Vibration*. Figure 9-10 shows the applied vibration normalization for HPB pumps 2 and 3.

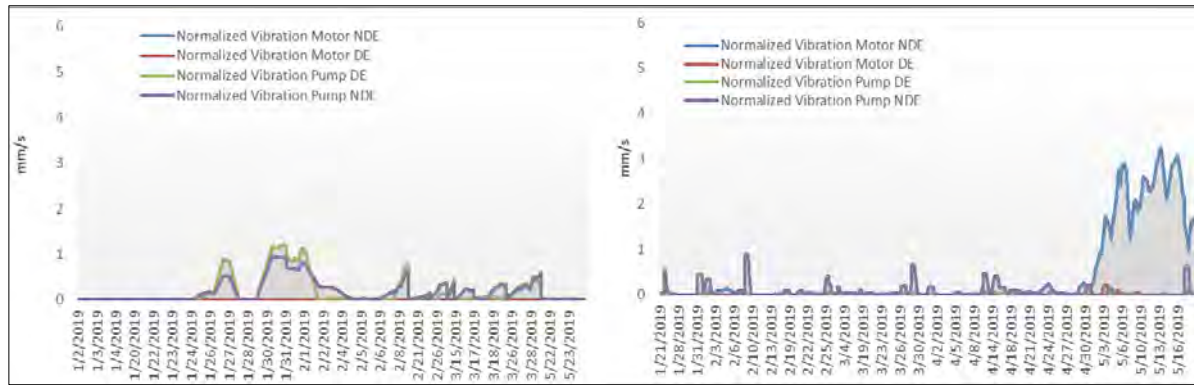


Figure 9-10: normalized vibration data HPB pump 2 (left) and for HPB pump 3 (right).

Y-axes vibrations, X-axes date.

HPB pump 3 showed the start of an increase in motor NDE vibrations at the end of April. The manufacturer recommends the replacement of the bearings after 25,000 hours of operation. The actual hours of operation were 23,961 hours for pump 1, 23,085 hours for pump 2, 19,068 hours for pump 3 and 13,506 hours for pump 4. Nevertheless, based on the normalized motor vibration data, the bearings of the motor of HPB pump 3 were removed and examined. Examination of the removed roller bearing showed grooving of the inner raceway surface and denting of the rollers (see Figure 9-11).

This grooving and denting are likely to be caused by small debris. Lubricant grease can contain some quantities of solid debris particles. Much of this debris is larger than the lubricant film between the roller elements and the raceway, which is typically less than a micron in thickness. This debris results in grooves and denting damage (Dwyer-Joyce, 1999).



Figure 9-11: Left, Grooves inner raceway ring NDE bearing; Middle: expanded detail Grooves; Right, Denting roller surface.

Further, if the grease is not replaced correctly, it can accumulate debris particles. Grease further gradually loses its lubricant properties (SKF, 2010). What could be observed after the old bearings were removed was that the new grease stayed at the outside of the bearings, and

the old grease was not replenished between the rollers and the raceway. The replacement of the motor bearings resolved the vibrations.

Besides bearings, the internal wear of the pump can cause increased vibration due to wear of the wear-rings of the impeller. The wear-rings limit the gap between the impeller and casing. The size of the gap between the rotating impeller and stationary casing defines the amount of leakage flow from the impeller outlet back to the inlet. An increased gap due to wear increases the leakage flow. Not only does this reduce efficiency (Shiels, 1997; Liu et al., 2015; Mou et al., 2016), but an increased gap between the impeller wear-ring and casing wear-ring decreases the damping of unsteady hydraulic forces and further decreases shaft stiffness. Thus, wear-rings' wear increases vibration (Aronen, 2011).

9.2.2 Pump performance monitoring

However, developing wear of the inner pump components does not necessarily result in increased vibrations. Wear of the inner pump elements can result in a hidden performance deterioration affecting the pumping efficiency. A deterioration of efficiency can manifest itself in increased power consumption, loss of pump Total Dynamic Head (TDH) and flow or a combination of this (Ilott and Griffiths, 1997; Beebe, 2004; Stoffel, 2015).

Azadeh et al. (2010) developed a rule-based fuzzy inference system for failure diagnosis of centrifugal pumps. Their system transferred human expertise logic in automated diagnostics, considering pump performance based on pump curves from the original equipment manufacturer (OEM), vibration and temperature. The rule-based fuzzy inference system identified the source of the problem after a fault had occurred. Therefore, this fuzzy inference system can be implemented as descriptive analytics to describe the problem. The method provides additional value on top of a condition-based maintenance system. Since it cannot detect early developing wear, the method alone cannot replace wear monitoring.

Keyvan (2001) presented an improved method to identify anomalies in pump performance based on the statistical method ARMA. To detect the progress of a detected anomaly, he introduced a new parameter named Contribution Ratio (CR). The CR parameter represents the fractional contribution of the unexplained residuals. Keyvan applied this on time-series data of a 0.01-second interval of pump power consumption, whereby the peaks in power due to the pull of the motor poles can be detected. An increase in power peaks would define abnormal performance. This method has the drawback that the rate of efficiency deviation can not be directly determined from this method. The high time-series sampling interval makes implementation as a continuous monitoring system impractical.

Beebe (2004) presented textbook examples of performance testing where flow, pump TDH and efficiency were tested against the pump curves of the OEM. The method requires adjusted operating conditions according to the design points at the pump curves of the OEM during the measuring periods. Soldevila et al. (2018) presented a pump performance monitoring method based on pump efficiency and hydraulic balance based on the equations of Beebe (2004). However, their method was independent of the initial pump curves of the OEM. The detection of deterioration is achieved after future extraction and change detection. Like in the method of Beebe (2004), the method requires constant operating conditions during the measuring periods, e.g., the same operational speed of the pump as during the previous tests.

This section presents a performance monitoring method like Beebe (2004) and Soldevila et al. (2018) based on pump efficiency and hydraulic balance. The method elaborates on the methodology presented by Stoffel (2015). The presented methodology compares the actual performance to the initial pump performance given by the pump curves of the OEM. The methodology further recalculates the hydraulic balance according to the variable speed of the pump drive based on the basic pump affinity laws (Walski et al., 2003; Simpson and Marchi, 2013). In contrast to Beebe (2004) and Soldevila et al. (2018), the presented methodology allows continuous performance monitoring without adjusting the plant operation to specific test conditions.

9.2.2.1 Experiment using textbook affinity laws for pump performance monitoring

The primary pumps in this case study are custom designed, and detailed specifications are available. The OEM provided Pump curves of flow vs pump Total Dynamic Head (TDH), power and efficiency. Based on these pump curves, the pumps have undergone Factory Acceptance Tests (FAT), and the performance is usually further verified at the commissioning stage of the plant.

The actual measured parameters against the expected parameters retrieved from the pump curves are compared to evaluate the performance. The first step is to digitalize the pump curves. A software application has been used to convert the curve from a bitmap picture to coordinates in a CSV file (see Figure 9-12). The pump flow vs the pump TDH and pump flow vs efficiency have been digitalized for both design points: 1 for a shaft speed of 859 rpm and 2 for a shaft speed of 1197 rpm. The power consumption will be retrieved from these two parameters.

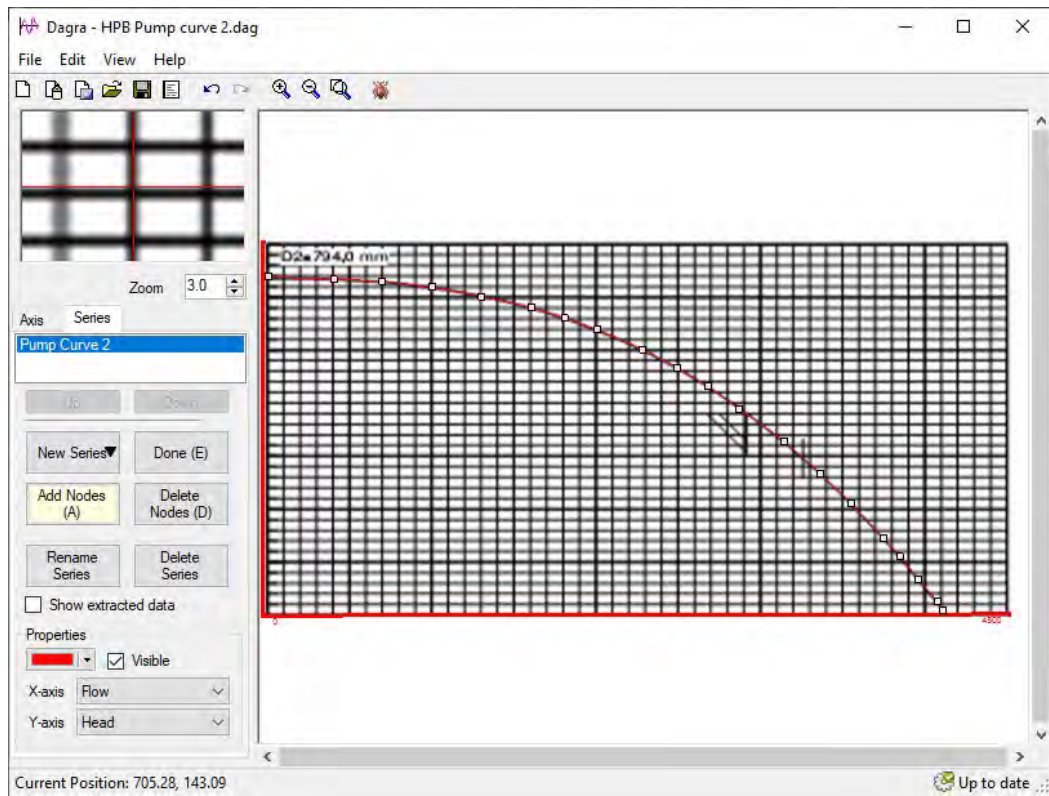


Figure 9-12. Digitalizing of pump curves.

Figure 9-13 gives the x-y diagram of pump TDH against pump flow for both operating points. Pump shaft efficiency is defined as the ratio of useful hydraulic power delivered to the fluid to the power input at the drive shaft. Figure 9-14 gives the x-y diagram of pump shaft efficiency against pump flow for both operating points.

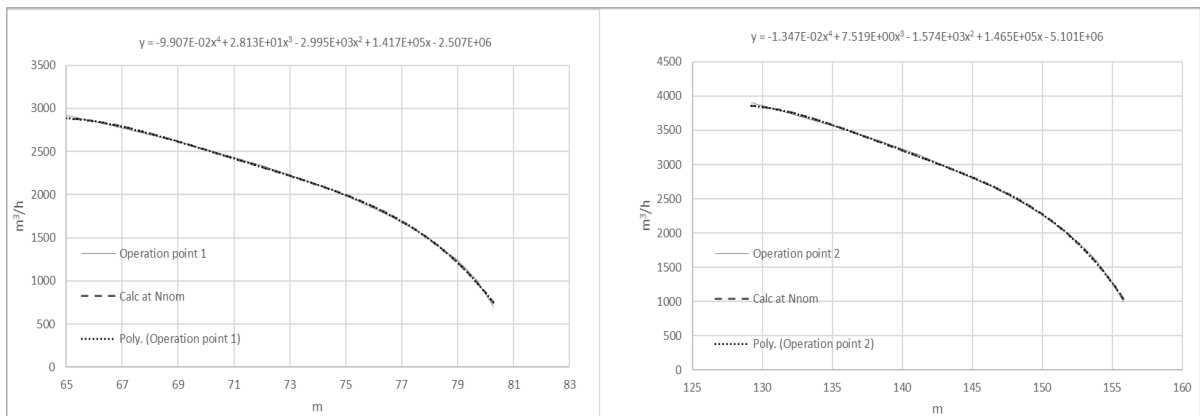


Figure 9-13: Pump TDH against pump flow for both operating points. Left shaft speed of 859 rpm, right shaft speed of 1197 rpm.

By fitting polynomial trendlines, pump curves can be translated to equations. An order of 4 fits the flow curve the best against the TDH. An order of 3 was enough for the curve of

flow against efficiency. Based on the polynomials' coefficients, the curve was recalculated to verify the fit with the digitalized pump curve (see Figure 9-13 and 9-14).

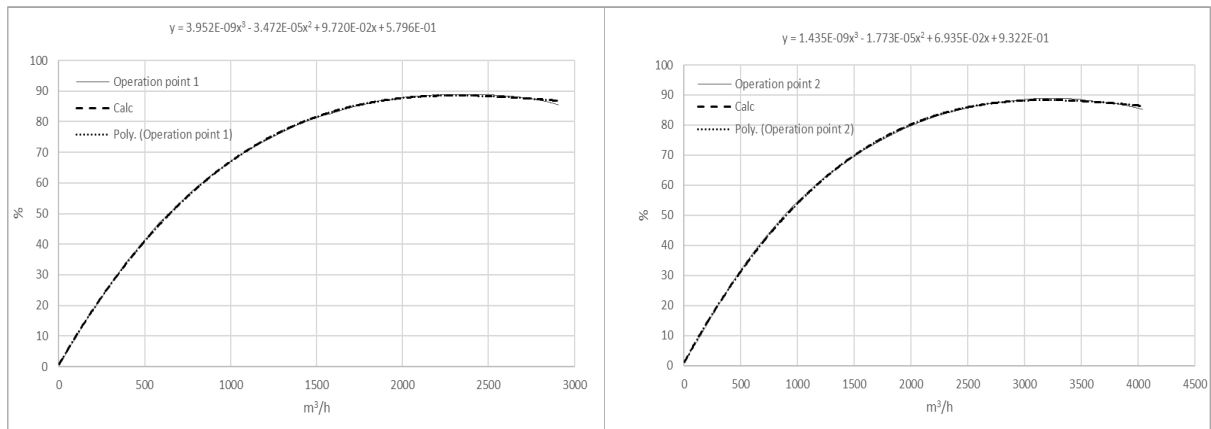


Figure 9-14: Pump shaft efficiency against pump flow for both operating points. Left shaft speed of 859 rpm, right shaft speed of 1197 rpm.

The pump TDH (H) is the pressure differential (ΔP) between the suction and the discharge of the pump, divided by the fluid density (ρ) and gravity (g). The equation is given below, where H is in meters, ρ in kg/m^3 and g in m/s^2 . The density, ρ for seawater, is $1,030 \text{ kg/m}^3$. The gravity, g is 9.80665 m/s^2 .

$$H = \frac{100,000 \times \Delta P}{\rho \times g} \tag{22}$$

The polynomial of the fourth-order for flow against the TDH is given here:

$$Q_o = \alpha + \beta_1 H_o + \beta_2 H_o^2 + \beta_3 H_o^3 + \beta_4 H_o^4 \tag{23}$$

where:

Q_o is the flow rate at the design point on the curve supplied by the OEM

H_o is the corresponding TDH on the curve supplied by the OEM

However, the pump speed varies. The calculation must be adjusted from the design point speed of the pump curve to the actual operating speed. The equation is derived from the pump affinity laws (Bachus & Custodio, 2003; Kayode Coker, 2007)):

$$\frac{Q_1}{Q_2} \approx \frac{N_1}{N_2} \tag{25}$$

where:

Q is the flow rate

N is the rotating speed [rpm or Hz]

$$\frac{H_1}{H_2} \simeq \left(\frac{N_1}{N_2} \right)^2 \tag{25}$$

where H is the pump TDH [in meter]

The provided pump curve is translated supplied by the Original Equipment Manufacturer (OEM) of Q_o vs H_o into a polynomial of the fourth order, giving the best fit:

From (Eq. 25) follows: $H_o = H_a \left(\frac{N_o}{N_a} \right)^2$ (26)

where:

H_a is the actual measured TDH

N_o is the pump speed at the OEM pump curve

N_a is the actual pump speed

$$y = \frac{N_a}{N_o} \tag{27}$$

From (Eq. 25) and (Eq. 27) follows: $H_o = \frac{H_a}{y^2}$ (28)

Putting (Eq. 28) into (Eq. 22) gives: $Q_o = \alpha + \beta_1 \frac{H_a}{y^2} + \beta_2 \frac{H_a^2}{y^4} + \beta_3 \frac{H_a^3}{y^6} + \beta_4 \frac{H_a^4}{y^8}$ (29)

From (Eq. 24) follows: $Q_o = Q_a \frac{N_o}{N_a} = Q_a \frac{1}{y}$ (30)

Putting (Eq. 30) into (Eq. 28) gives: $\frac{Q_a}{y} = \alpha + \beta_1 \frac{H_a}{y^2} + \beta_2 \frac{H_a^2}{y^4} + \beta_3 \frac{H_a^3}{y^6} + \beta_4 \frac{H_a^4}{y^8}$ (31)

The expected flow is then: $Q_a = \alpha y + \beta_1 \frac{H_a}{y} + \beta_2 \frac{H_a^2}{y^3} + \beta_3 \frac{H_a^3}{y^5} + \beta_4 \frac{H_a^4}{y^7}$ (32)

The polynomial of the pump curve from operation point 2 has been applied since two-thirds of the operating conditions fit in this range. Table 9-6 shows the coefficients of the polynomials of operating points 1 and 2 for the flow calculation.

Table 9-6: Coefficients of the polynomials for flow calculation

| | Operation point 1 | Operation point 2 |
|-----------|-------------------|-------------------|
| β_4 | -9.907E-02 | -1.347E-02 |
| β_3 | 2.813E+01 | 7.519E+00 |
| β_2 | -2.995E+03 | -1.574E+03 |
| β_1 | 1.417E+05 | 1.465E+05 |
| α | -2.507E+06 | -5.101E+06 |

The required hydraulic power (P_h) in kW is calculated as follows:

$$P_h = \frac{Q\rho gH}{3.6 \times 10^6} \tag{33}$$

where:

Q is the pump flow

ρ is the fluid density

g is the gravity

The pump shaft power (P_s) is the hydraulic power times the shaft efficiency (η_s):

$$P_s = \frac{P_h}{\eta_s} \tag{34}$$

The shaft efficiency (η_s) is calculated from the efficiency polynomial (Figure 9-14):

$$\eta_s = \gamma + \delta_1 Q + \delta_2 Q^2 + \delta_3 Q^3 \tag{35}$$

Table 9-7 shows the coefficients of the polynomials for pump shaft efficiency calculation.

Table 9-7: Coefficients of the polynomials for pump shaft efficiency calculation

| | Operation point 1 | Operation point 2 |
|------------|-------------------|-------------------|
| δ_3 | 3.952E-09 | 1.435E-09 |
| δ_2 | -3.472E-05 | -1.773E-05 |
| δ_1 | 9.720E-02 | 6.935E-02 |
| γ | 5.796E-01 | 9.322E-01 |

Finally, we must divide the pump power with the efficiency of the pump drive (η_d). The efficiency curve is empirically established since we do not have datasheets on the drive's specific efficiency. The power readings from HPB pump 1 throughout 2017 were taken for reference. The efficiency for HPB pump 1 looked very stable over 2017, and we can assume that wear was minimal or non-existing after one year of operation.

On the other hand, the power readings for the year 2016 were very erratic. Presumably, the pumps were not operated at the best efficiency point in the first year. After plotting the power data vs the frequency in a scatter diagram, we can superimpose correlation points over the scatter diagram. A third-order polynomial trend line was then added for the correlation points. Figure 9-15 shows the scatter diagram. The equation of the trendline gives the coefficients of the polynomial.

$$\eta_d = \iota + \kappa_1 N + \delta\kappa_2 N^2 + \kappa_3 N^3 \tag{36}$$

where N is the Drive Frequency in Hz.

Table 9-8: Coefficients of the polynomials for the efficiency calculation of the drive

| Operation point 1&2 | |
|---------------------|------------|
| κ_3 | 2.776E-06 |
| κ_2 | -5.150E-04 |
| κ_1 | 3.131E-02 |
| ι | 3.185E-01 |

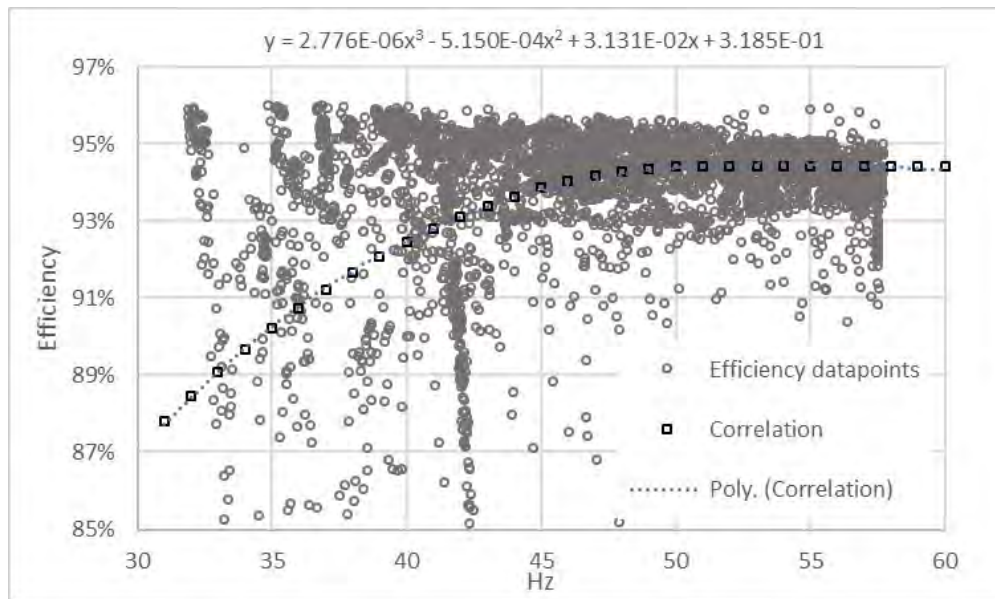


Figure 9-15: Scatterplot of empirically estimated drive efficiency and polynomial trendline

The total expected input power (P_t) is thereafter:

$$P_t = \frac{P_s}{\eta_d} \tag{37}$$

The overall expected efficiency (η_t) is:

$$\eta_t = \eta_s \times \eta_d \tag{38}$$

Since efficiency, power consumption and efficiency fluctuate at a time series trend due to fluctuations in speed, the deviations (σ) is calculated of expected values against the measured values at that moment in time.

The deviation of efficiency (σ_η) is

$$\frac{\frac{P_h}{P_m} - \eta_t}{\eta_t} \tag{39}$$

where:

P_h is the hydraulic power

P_m is the measured power

The deviation in power (σ_p) is

$$\sigma_p = \frac{P_m - P_t}{P_t} \tag{40}$$

The deviation in Flow (σ_Q) is

$$\sigma_Q = \frac{Q_m - Q}{Q} \tag{41}$$

where:

Q is the expected flow according to the calculations

Q_m is the measured flow by the flow meter

We can assume that if wear sets in, this will affect the pump's efficiency, whereby the flow will decrease or the energy consumption will increase. However, this might not always be obvious since the pumps operate parallel at a common discharge header, whereby the speed is controlled common for all operating pumps.

For example, if the impeller shrinks due to wear, both the flow and the power consumption will reduce. The flow loss will be compensated by increasing the speed of the pump. However, this is applied to all operating pumps in parallel. Therefore, a healthy pump will take a more significant share of the load, resulting in this pump requiring a higher power consumption. Therefore, we must look at each pump's deviation from the calculated efficiency and power consumption.

9.2.2.2 Testing calculated with measured power consumption

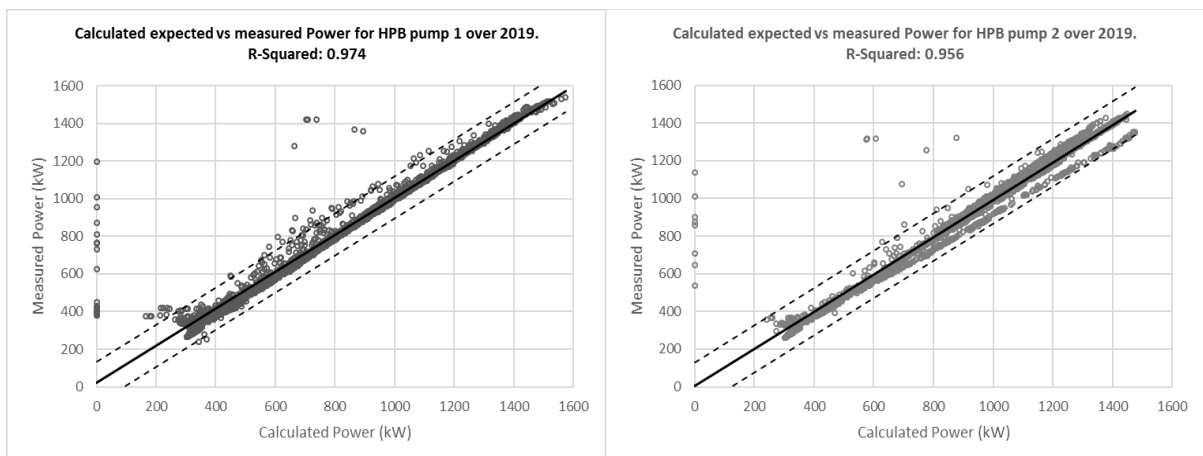


Figure 9-16: Scatterplots of measured power vs expected calculated power for HPB pumps 1 and 2 (Data 2019).

The scatterplots of measured power vs expected calculated power for HPB pumps 1 and 2 from the trend-series data of 2019 (see figure 9-15) shows that the fit between the calculated expected power consumption and the measured power consumption is high. The R-Squared for HPB pump 1 was 0.974, and HPB pump 2 was 0.956. The fit verifies that the method presented to calculate the expected performance is accurate. The close fit at the scatterplots also underlines that there is no neglectable wear after four years of operation.

9.2.3 Implementation.

The demonstrated initial research on vibrations anomaly detection and performance analysis for the plant's large centrifugal pumps can be applied to DT-based DSS. The virtual performance of the DT can then be compared to the physical pump, and decision support can determine wear, and the wear source is bearings or the pump's internal components. The latter is vital since there is a significant difference in fixed set-up costs between bearing replacement and the need to open the pump case. The concept of such a DT-based DSS for large centrifugal pumps is based on the same principles as the presented DT-based DSS for membrane maintenance.

The presented approach differs from commercial anomaly detection applications since the latter only provides early warning for an anomaly, not the cause. The thesis author has been approached by suppliers of commercial ANN-based predictive analytics programs for a pilot test. Unfortunately, this has not materialized. The investment, including licenses to run the pilot test, was considered excessive. The suppliers of the Management Information System (MIS) used for data storage, reporting and analysis of Operational data, marketed under the name iGreen, recently offered an alternative opportunity for implementing anomaly detection. Their anomaly detection module can be added as an additional module to the existing MIS, which will significantly reduce implementation time and resources. The anomalies detection module is marketed under the name iDetect.

The anomaly detection method is a rule-based engine utilizing the Hartley transform, closely related to the Fourier Transform, but the former works with real instead of complex numbers in the case of the Fourier Transform. The Fourier Transform is a statistical function that allows a signal to be treated in the complex frequency domain (Le-Ngoc and Vo, 1989; Bracewell, 1995). Fourier transform and Hartley transform are compatible, i.e., Hartley transform does the same as Fourier transform (Bracewell, 1995).

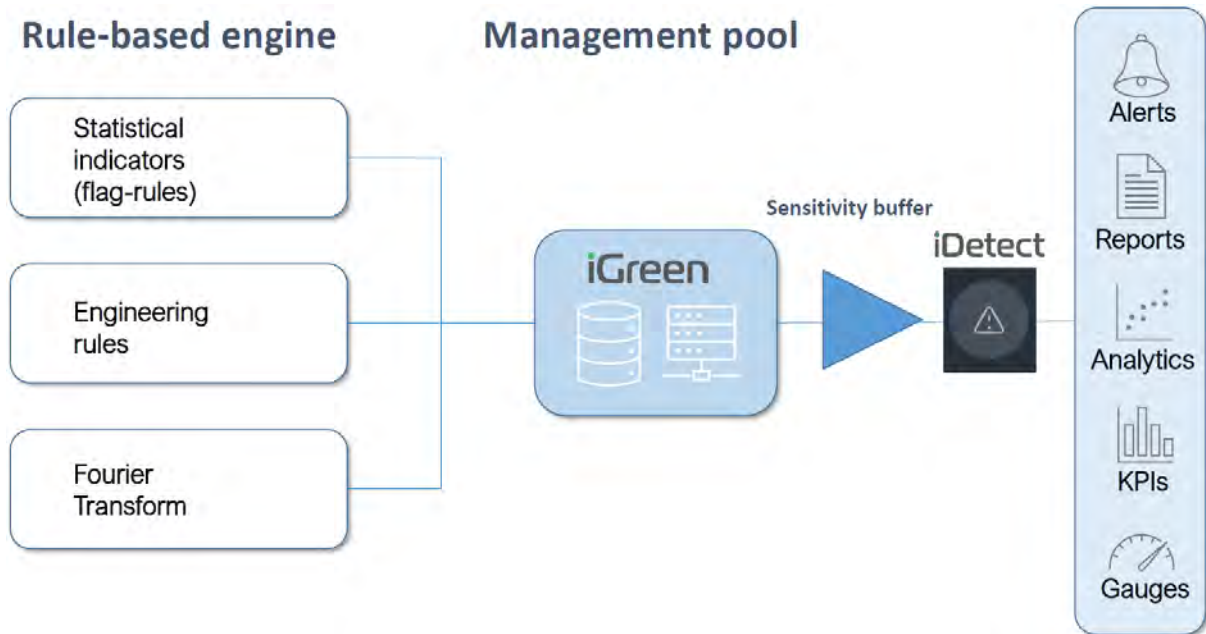


Figure 9-17. Incorporation of an anomalies detection module into the OT MIS.

An optimized algorithm of discrete Fourier transformation, called Fast Fourier Transformation (FFT), is often applied in signal processing. FFT converts a signal into the individual components of the frequency spectrum (Rapuano and Harris, 2007). Xue et al. (2014) and Lin and Ye (2019) presented a vibration anomalies detection of pumps and bearings utilizing FFT and enhanced FFT algorithms. Assaf et al. (2018) pointed out that since FFT is limited to the frequency domain, this method fails to show a progression of the fault over time. Assaf et al. (2018) proposed a short-time Fourier transform (STFT) that allows the analyses to be performed in both the frequency and time domain. A 3D surface plot can then visualize both the time domain (X-axis) and frequency domain (Y-Axis). The STFT was demonstrated with a gearbox-accelerated life testing platform.

Fourier transform vibration analyses utilize accelerometers, which provide a frequency signal similar to an acoustic sound. At CDP, mainly viscosity transducers are used, where the signal is random without a frequency component and the data logging frequency is low (60 seconds interval). So, the anomaly detection of this vendor does not apply a Fourier transform directly to the vibration signal but the frequency of statistical indicators based on engineering rules, as the frequency of anomalies, which then is fed to a Fourier Transform to flag for anomalies.

The precise method and benefits of the offered iDetect anomaly detection application are currently not fully understood. The O&M company is still evaluating if it is beneficial for the plant. Of interest is that the iDetect application offers the option to program custom-defined

equations. The latter would allow the implementation of the presented vibration normalization and theoretical pump performance analysis presented above.

9.3 Summary results compared to baseline

In this section, we look back at the improvements since the baseline set at the onset of this research. The data of baseline was taken from the year 2018. The plant was in commercial operation for three years and a year preceding this research. The early results of the impact of the research follow three years afterwards, by the end of 2021. The baseline is based on three performance indicators (PI). In short, these are, P1: The ratio of shortfall (volume of potable water) to designed capacity (volume of potable water per day); P2: Ratio of failure-based to all maintenance activity; P3: Annual percentage of membrane replacement. All three PIs are expressed in days of lost production to have a common measurement of the effect of the PI on the plant performance. For a detailed definition of the PIs and how they are calculated, see chapter 2.

Maintenance performance analysis based on multi-dimensional Pareto diagrams (see chapter 2.5) identified the shortcomings over the first three years of operation, especially in the second year, due to skill level upgrade (SLU) and design out maintenance (DOM). SLU and DOM indicate that the first three years of operation can be characterized as a ‘break-in’ or start-up period. This phenomenon is referred to as the initial stage of the bathtub curve. The bathtub curve is a characterization of the lifespan of an engineered object (EO) often referred to in reliability studies (see chapter 5.2).

The improvement of the first two PIs is, to an extent, due to the plant's lifespan having passed the ‘break-in’ period. The O&M team is now more experienced (SLU), and design changes have been implemented (DOM). Further, the computerized maintenance management system (CMMS) configuration and implementation continued during the first years of operation. The CMMS manages the time-based preventative maintenance and condition-based inspections.

We will now review the PIs three years after the baseline was set. The continued availability, demand and delivery have been analysed for approximately three years, i.e., January 2019 to November 2021. Over the period 2016 to 2018, the total shortfall was 4,235 MG. Since 2019, this shortfall has been reduced to zero liability. Figure 9-18 shows the daily trend-series chart of availability, demand and delivery since January 2019.

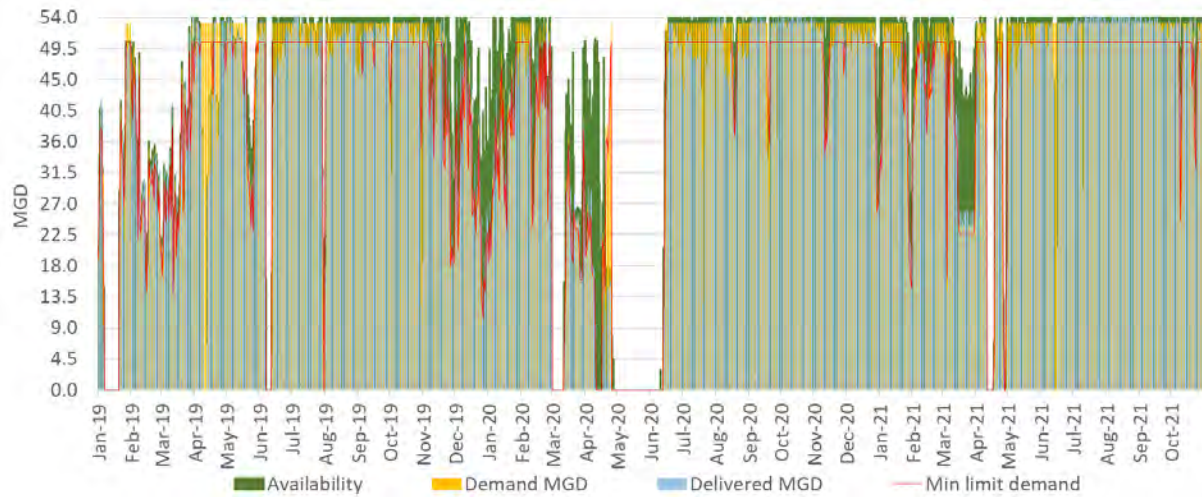


Figure 9-18. Availability, demand, and delivery from Jan 2019 to November 2021

The hours spent on failure-based maintenance for the year 2021 is 20%. The target is 25% or less. Previously in the performance analysis, the performance indicators were expressed in days of lost production. Figure 9-19 shows the current performance indicators P1, for shortfall and P2, ratio failure-based to all maintenance activities, against the baseline.

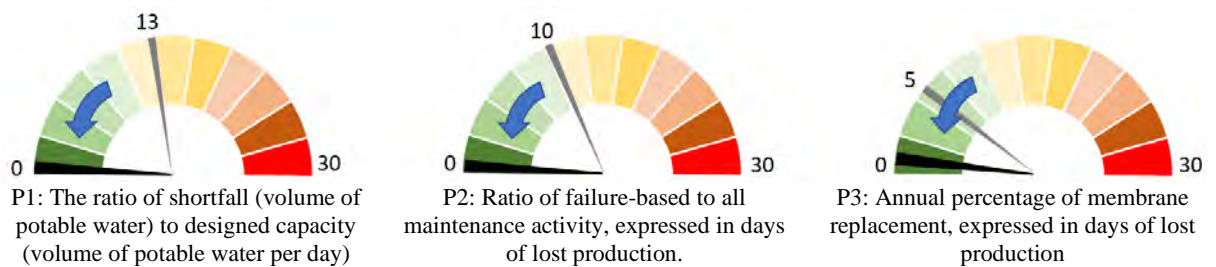


Figure 9-19. Performance indicators for water shortfall, ratio failure-based to all maintenance activities, and annual percentage of membrane changes. All expressed in days of lost production. Grey needle is the performance at the baseline of the year 2018, black needle is the performance in 2021.

This research concentrates on the third performance indicator (P3), annual membrane replacement. In contrast to the other two performance indicators, the unforeseen rate of membrane degradation was not due to a break-in period, but biofouling accelerated through seasonal algae blooms. Although biofouling is difficult to combat, this research has shown that the consequences can be mitigated to an acceptable level. The annual average Reverse Osmosis (RO) membrane replacement target was 11.5%. Tested alternative policies 11 and 12 showed that an annual average replacement rate of 10.6 to 11.8% is achievable. One percent of replacement is equal to the penalty cost of 5.4 days of lost production (see chapter 2.2). Converted to days of lost production, policy 11 results in zero and policy 12 to one day of lost production.

Following a better understanding of the effects of biofouling, the O&M company came up in 2019 with a long-term membrane maintenance plan that will result in an average annual membrane replacement rate of 16% for the following six years. The current membrane replacement rate would bring the total replacement rate over ten years to 139.25%. The O&M company policies 1 and 10 reflect these replacement rates. Thus, P3 would have deteriorated from 5 to 9 days of lost production. Continuing this maintenance strategy, the following long-term plan beyond the current 10-year plan will result in a total replacement rate of 160% over the next ten years. P3 will then further deteriorate to 24 days of lost production.

This research shows that the maintenance policy can be improved by modelling the deterioration and restoration of the membrane elements in a vessel. A membrane replacement rate equal to the estimated level at the beginning of the O&M plan is viable. For the coming five years, a cost-saving can be reached from a conservative number of \$0.7 million to a more defiant number of \$1.7 million. The current inflation rate of the membrane element cost ranges between \$0.9 million and \$2.1 million.

Projections show that the improved CIP method that first soaks the RO membranes in sodium-bisulphate before performing a high and low pH cleaning, referred to as the C2 method, significantly reduces risk compared to the standard high and low pH cleaning.

Nonetheless, policies 11 and 12 require an increase in clean-in-place (CIP). The CIP frequency utilizing the C2 method must increase beyond the current capacity of the CIP system to enable a significant reduction in membrane replacement rate. However, the bottleneck of the current system is the discharge of the used solution. An upgrade of the CIP system would modify the neutralization system so that the latter can be used to discharge the cleaning solution. This modification can be performed in-house. Following this research, the O&M company and the asset owners have agreed to upgrade the CIP system.

10 Discussion

This research is about maintenance planning for the long-term reliability of an engineered object (EO) subject to stochastic wear conditions and imperfect repair. A Decision Support System (DSS) is developed for maintenance planning. A general framework for the design of a DSS for maintenance planning is proposed. This framework of maintenance principles is demonstrated using a real-life industry example.

The DSS is designed using the principles in the proposed framework. The purpose of the DSS is to support the management of restoration of reverse osmosis (RO) membrane elements. These elements degrade due to biofouling caused by seasonal algae blooms, a global problem in the desalination industry. A digital twin (DT) is the engine of the DSS. The DT virtualises the degradation and restoration of reverse osmosis (RO) membrane elements (components) in an RO pressure vessel. This virtualisation is novel because individual membrane elements are modelled. This allows the effect of membrane swapping and replacement to be quantified. In this way, the RO vessel and its membranes are considered a novel multi-component system. A further novelty in the thesis is the framework of the maintenance principle.

The DT itself is a simulator. The DT estimates the hidden states of the individual components over time, and allows the operator to evaluate the effectiveness of different restoration policies. The wear of the individual elements (components) is quantified using a mathematical model that describes extrinsic and intrinsic degradation, with dependencies between individual elements (components). Statistical methods are used to estimate the parameters of the model.

The principles in the proposed framework provide a basis for further developing the general understanding of maintenance planning. So far, the discussion in the literature on the design of DTs for maintenance planning has been application-oriented. General principles have not been articulated so far. The principles proposed in this thesis can be considered a work in progress, and discussion by others about limitations and adaptations will be most welcome. At a higher level, the principles are relevant to broader maintenance management issues, and the thesis author hopes it will spark discussion in the broader engineering services community. The principles of the lower layers of the framework guide the development of custom DTs for high-performance EOs. The DSS and the DT for managing the restoration of RO membranes not only give a practical example of the application of the principles but have

also shown that significant cost savings can be made using a DSS that enables the exploration of alternative maintenance policies. The DSS provides well-informed decision support on membrane maintenance planning instead of the ad-hoc approach currently used in the industry.

More details follow in Section 10.1, which describes how the principles for the design of a DSS for maintenance planning were implemented for the specific EO. Section 10.2 concentrates on the research contributions. Section 10.3 concludes the research, with Section 10.4 reflecting on the limitations and Section 10.5 outlining further research plans and proposals.

10.1 A DT-driven DSS for maintenance planning

This research aims to establish a maintenance planning methodology for an EO with stochastic wear and imperfect repairs. The practitioner will not be able to determine the long-term reliability of the EO due to uncertainties about future wear and the effects of repair without examining various maintenance scenarios. The practitioner can physically experiment on the EO, but this is time-consuming and potentially undesirably sacrificing the EO. A DT is the only practical way to study the effectiveness of various competing policies without undergoing physical tests.

This research proposes a DSS for maintenance planning that allows policy testing with predictions showing effectiveness before implementation. Such a DSS must be thoughtfully designed and must contain an in-depth understanding of the process of degradation and restoration. The presented framework of maintenance principles supports the practitioner in designing such a DT-driven DSS for maintenance planning. The DSS is thereby dedicated to a specific EO. The framework consists of different layers of maintenance principles and sub-principles (chapter 1.2). The framework first defines the principles of maintenance and maintenance planning, as these are the foundations from which the principles for managing planned maintenance are derived. After this, the principles of a DT-driven DSS can be derived. The latter, level four, is the last group of sub-principles. Level four of the framework of maintenance principles addresses the first research question. It specifies the general requirements of a DSS for restoration so that the DSS is fit for purpose.

- A DSS should monitor degradation or the indicators of degradation.
- Competing maintenance policies should be testable in the DSS.
- Known unknowns should be represented in the DSS.
- The costs of developing a DSS is bearable for only some units of the EO.

The research then demonstrates the design and implementation of a DSS for maintenance planning with a practical example, a DSS for planning the restoration of RO membranes. The second research question raises how the restoration of membrane components in RO desalination in the presence of seasonal algal blooms should be managed.

The specific DT-based DSS for planning follows the framework of maintenance principles. All four principles of level four apply. The research first identified the unique drivers of the degradation and restoration of this particular EO. The latter meets level two of the framework: maintenance should use knowledge of both degradation and the effect of the restoration.

The following sub-section describes how process engineering knowledge is used to identify the root cause of the degeneration of the specific EO, in this case, process engineering in RO desalination.

10.1.1 Understanding the drivers of degradation of the specific EO

Degradation or degradation indicators were studied from the perspective of process engineering in desalination (chapter 4). The latter provides an understanding of the physical-biochemical processes of membrane component degradation due to biofouling, i.e., biofilm-producing microorganisms' obstruction of the saline water feed-concentrate channels. This obstruction results in a pressure loss or pressure differential (PD) over the feed-concentrate channels of the components. Note that operational and seasonal effects can change the PD of a new element having no wear. Therefore this research filters out these effects and the term normalised pressure differential (NPD) is used.

The rate of biofilm growth, i.e., the rate of blocking, is positively related to the amount of nutrients. Algae, when it dies and decomposes, becomes a nutrient. Thus, an algae bloom provides excessive nutrients, resulting in a sharp increase in component degradation.

The physical-biochemical processes explain why fouling first starts at the lead component and unequally spreads to the tail over time. The latter is a process of attachment of microorganisms at the beginning of the surface, growth of the colony, maturing of the biofilm, and then dispersion of a group of microbes to colonise the next component area. Further, process engineering also identifies faster fouling when a new component is placed before fouled components due to excessive permeation flux. Higher flux results in a higher fouling rate.

Restoration involves two types of interventions. The first is a clean-in-place (CIP), a combined chemical and mechanical cleaning without opening the vessels and removing the

components. Cleaning solutions are pumped through the vessels, whereby the biofilm is partially removed. Thus, the degradation is reduced but not entirely undone. The effect of restoration differs stochastically. The other type of restoration is to open the vessels, identify the most severe fouled components and replace them with new ones. As described previously, new components are preferably positioned at the tail by pushing the older retained components forward to the lead side of the vessel.

10.1.2 The EO, from a maintenance engineering perspective

After gaining insight into the degradation and restoration processes of the specific EO, the research approaches the EO from a maintenance engineering perspective (chapter 5). From the perspective of maintenance theory, the RO pressure vessel is classified as a unique multi-component system. This specific multi-component system is then evaluated against the characteristics of other multi-component systems in the literature. Approaching the RO vessel in this way distinguishes this research from other RO degradation studies in the literature.

Degradation or the degradation indicators described earlier from an RO process engineering perspective are now classified as extrinsic or intrinsic dependencies, where the supply of nutrients is extrinsic, and biomass distribution over the elements is intrinsic. Furthermore, placing less degraded components in front of more highly degraded components is intrinsic rate-state wear dependence. These classifications matter for the modelling of degradation. In short, the specific EO engineering know-how identifies the root cause of degradation. Maintenance engineering know-how, then translate these dependencies in a manner so they can be expressed in mathematical equations for modelling.

Multi-component systems have structural and economic dependencies that affect how restoration is executed. Structural dependence influences decision-making on maintenance interventions. Since the components are in series, other components need to be removed before reaching the component to be swapped or relocated. The need to remove other components is in the maintenance literature defined as structural dependence from a technical point. Based on hydraulic laws, a fouled membrane component has a higher NPD when positioned at the lead than at the tail. In the maintenance literature, this change in performance is defined as structural dependence from a performance point.

A typical economic dependence is the fixed set-up cost before the actual intervention occurs. Typical fixed set-up costs are spare part procurement, hiring a temporal workforce, training the workforce and vessel opening. When undertaking RO permutations, all trains are scheduled to undergo this intervention in a continuous sequence, train after train. The latter

reduces the fixed set-up costs. This research considers economic dependence mostly fixed and adds the spare part procurement costs to the component. Hiring the temporal workforce, training the workforce, and vessel opening are added to the labour costs. However, labour costs are half when permutations only involve the first four components. This difference in labour costs is captured in the DT.

The thesis further adds the classification of economic dependence from a performance point when wear affects energy consumption. The latter was reported in the literature in the case of brackish water RO systems. The feed pressure in brackish water RO systems is significantly lower than in seawater RO systems. Therefore increase in feed pressure to compensate for the NPD losses is proportionally much higher in brackish water than in seawater RO systems. For seawater RO, the proportional increase is insignificant.

10.1.3 Degradation model

This research chose a degradation model based on mathematical equations derived from a physics-based model and statistical methods. A physics-based model requires expert engineering knowledge to identify the EO's specific process of degradation and restoration. The thesis author acquired this knowledge through a long professional career in RO desalination.

Furthermore, statistical methods require numerical data. The plant in this case study is relatively new. It contains a considerable amount of in-field sensors continuously read by the plant's Industrial Control System (ICS). The data is stored in time-series databases in cycles of a minute. The availability of operational data allows the model to be data-driven. The number of nutrients in the RO feed water, the extrinsic degradation dependency (κ) that is stochastic and the primary driver of wear, can be derived from the time-series dataset. This data provides a distribution where the value of κ for future projected degradation can be sampled.

Not only are the degradation or the degradation indicators monitored (the first principle of level four of the framework of maintenance principles), but the maintenance effects can also be measured. The component's modelled NPD is computed according to the wear and socket position. When swapping components to a different location, the wear follows the component to the new socket. Similarly, replacing a component with a new one, the latter has no wear. Previous interventions have been recorded in the computerised maintenance management system (CMMS), and the model computes the restoration effects.

The CMMS also record when a CIP takes place. Since CIP is an imperfect restoration with stochastic results, the latter can be computed from the time-series dataset, which provides a distribution where the amount of restoration can be sampled in projections.

10.1.4 Evaluating the performance of different policies

Testing of competing maintenance policies is the second principle of level 4 of the framework of maintenance principles. This research opted for a DT-driven DSS where practitioners can test maintenance policies they designed before physically implementing them. This method contrasts with a DT that would generate an optimum maintenance policy. The thesis author believes that a DSS where practitioners can test their maintenance policies would be less likely to be met with scepticism. Besides that, a practitioner probably wants to compare their policies against the 'machine'. Therefore the DSS for maintenance planning must, in any case, have the capability to test various policies on their long-term restoration effectiveness, independent of who generates them. Nevertheless, the latter does not exclude an additional function of the DT that can generate an optimum maintenance policy. However, this would complicate the scope of the current research and can be addressed in future research.

The stochastic degradation and imperfect restoration imply a spread of probability, i.e., the uncertainties. This spread of probability is the known unknowns that, according to level four of the framework of maintenance principles, should be presented in the DSS. This research resolved this by sampling the model's stochastic parameters from a data distribution derived from the time-series dataset. Projections generate a hundred probabilities per day from random samples of the κ distribution, the extrinsic wear dependency. When an imperfect restoration is conducted, a hundred probabilities for that day are taken from the distribution of δ , the restoration rate. These hundred projections provide a spread of probability as the ensembled forecast envelope. The number of hundred samples compromises the probability accuracy against the computational costs.

10.1.5 Sensitivity analysis

Initial sensitivity analysis concentrates on the modelled NPD fit, comparing the modelled against the observed NPD over the time-series dataset. Sensitivity analysis is further conducted on other fronts. The sensitivity analysis utilises a data analysis module, part of the DSS. The fit of observed biomass distribution over the vessel's components is compared to the modelled wear distribution for each train. The same data analysis module was utilised to

test the sensitivity of the intrinsic rate-state effect parameter γ compared to α , the wear distribution parameter.

Further, the robustness of the projections is tested by applying different sampling methods and smoothing regimes and comparing the results. Two different sampling methods were utilised to determine the stochastic extrinsic dependence parameter and the restoration effect of imperfect restoration by CIP. These parameters were sampled from a Weibull distribution or by bootstrap sampling. Further, the projections using bootstrap sampling were repeated three times. Each time different smoothing strengths were applied to the data set of κ , the extrinsic wear dependency. Projections of the tested policies were therefore repeated four times for all the trains.

Different strengths of smoothing do not change the risk ranking of the tested policies, nor when Weibull distribution sampling is applied instead of bootstrap sampling. Bootstrap sampling with a longer smoothing window of the distribution of extrinsic parameter κ provides a more apparent differentiation between algae and non-algae bloom periods.

Weibull distribution might be more practicable if limited data is available. However, results with Weibull distribution tend to differ when re-running the projection and are, therefore, less accurate. The Weibull distribution projections also result in complete restoration at the lower range of the ensemble forecast envelope over time, which is unrealistic. Therefore, bootstrap sampling is preferable if enough data is available.

Although this research tested three smoothing ranges for bootstrap sampling, the purpose of the different smoothing ranges was only for sensitivity analysis. The thesis author recommends using a single longer smoothing range since this accentuates better periods of algae and non-algae bloom periods.

10.2 Research contributions

This research contributes on two fronts, desalination engineering and, on the other hand, maintenance modelling and simulation literature. A scientific approach to membrane maintenance has been presented to the current ad-hoc approach in the industry. The presented novel model of degradation of a multi-component system and its DT provides a unique simulation application that further contributes to multivariate degradation processes and imperfect repair models within the body of maintenance theory, modelling and simulation literature.

10.2.1 The novelty of this research

This research presents a DT based on a mathematical model that describes an RO vessel as a novel multi-component system in which the wear-states of individual components are quantified, and components can be swapped or replaced. The demonstrated approach contrasts with the contemporary presentation of a RO membrane system as a single system in the literature. The work has been appreciated as an interesting and novel approach to RO maintenance. The presented DT of a seawater RO train in terms of simulation of their fouling process is significant, interesting and innovative. These appraisals are from the editor of the journal *Desalination* and its peer reviewers (van Rooij et al., 2021).

The presented framework of maintenance principles and sub-principles further fills a gap in the maintenance theory literature. Currently, a general framework for designing maintenance decision support driven by a DT does not exist in the literature. In presenting the framework (chapter 1.2), the thesis author intends to encourage a debate on the principles of where a good DSS for maintenance planning should be founded.

Such an opportunity has recently been opened. The representatives of Rockwell Automation have approached the thesis author to participate as a panel member in a forum on digital transformation in the water and wastewater sector at their annual fair in Chicago.

The publication in the journal *Desalination* has further resulted in an invitation to contribute to a handbook on DTs. Collaborating with Philip Scarf, Professor of Management Mathematics at Cardiff Business School, a chapter on the design of a digital twin for maintenance planning has been submitted.

10.2.2 Research contribution to the current discussion on Industry 4.0

The first level of the framework of maintenance principles states that maintenance is necessary. Otherwise, an engineered (EO) object will fail. The recognition of maintenance being part of business strategy is relatively recent. The scientific approach toward maintenance management started in the 1950s and 1960s, with time-based preventative maintenance to reduce failures and unplanned downtime. The next level of maintenance optimisation was the introduction of condition-based maintenance, developed in the 1970s as a cost-effective alternative to the expanding large time-based preventative maintenance programs, followed by predictive maintenance involving degradation simulation and prediction of remaining-useful-life (RUL). The latter was possible due to the introduction of the PC in the 1980s. The PC also led to the CMMS as a popular application for maintenance administration and analysis.

Maintenance planning is one of the components that underpins the smooth operation of an ever more global interconnected manufacturing environment, together with the growing complexity of the supply chain, i.e., the interactions between different manufacturing segments. The recent semiconductor shortage (Voas et al., 2021) shows how devastating a bottleneck of one production segment can have on the extended manufacturing environment. The increasing interdependence and competitive market drive the recent orientation towards the digital transformation of the industry also referred to as Industry 4.0.

The philosophy behind Industry 4.0 is that predictive decisions can be made from information involving big data. The wide availability of data is made possible due to technological innovation, e.g., computing power, network communication and intelligent field sensors that can autonomously communicate over high-speed data networks. The recent development of such intelligent field sensors is the internet of things (IoT) and its industrial variant, the industrial internet of things (IIoT).

Digitalisation from both a technological and a management perspective is also evolving towards Maintenance 4.0 or Smart Maintenance. Computerised maintenance analysis and the CMMS go back to the 1980s. Thus, the digitalisation of maintenance is not an entirely new concept but is now elevated to new dimensions. The virtualisation of physical objects, also known as Digital Twins (DT) or Cyber-Physical Systems (CPS), has recently gained immense attention, including regarding maintenance.

Less attention is given to the recent discussions on DT for maintenance about what action should be undertaken. Currently, the implementation of DTs in maintenance is predominantly based on anomaly detection and, therefore, predicting short-term when to undertake maintenance. This research contributes to long-term maintenance planning by providing a DT-based DSS where practitioners can evaluate competing policies.

A vital contribution of this thesis to the discussion on DT is regarding the concept of a DT. Starting with Kritzinger et al. (2018), a narrowed concept of DT dominated the discussions. According to these authors, a DT could only be called so if the physical unit and virtual model were fully interconnected. The physical unit would continuously update the virtual model, and the latter would directly control the physical unit. This concept unnecessarily limits the deployment of a DT as a practical tool. Looking back to the first practical implementation of a DT in the aerospace industry and NASA, those DTs were used to study different phenomena and test solutions before applying them to the physical unit. The latter is what this research intends to achieve in maintenance planning. Thus, a DT should be kept to its core, a digital entity that reflects the behaviour of the physical entity and keeps updating

through the whole lifecycle limited to the specifics being investigated, using only relevant data and models. The concept of a DT presented in this thesis is that of a virtual replica that can be studied and tested, involving various projections, without interfering with the physical object.

10.2.3 Achievement of this research

Coming back to the practical implementation of this research, the implementation of a DT-driven DSS for RO membrane maintenance planning has resulted in concrete achievements. The DT's exploration of alternative maintenance policies has shown that significant cost savings can be achieved over the next five years. At the same time, these alternative policies improve recovery performance compared to the O&M company's current policies. Adjustments must be made to the current CIP system to make this possible. The benefits far outweigh the required investments. Both the O&M company and the owners have agreed on this upgrade following the outcome of this research.

Furthermore, the O&M company has embraced the DSS for future membrane maintenance planning. The DSS is now being used for a possible extension of the RO trains with an additional 16 vessels. The DT evaluates different options for membrane component permutations to balance the wear between the existing and new vessels.

Finally, contributing to the community of researchers and practitioners in the industry, little attention has been given so far to the literature on RO maintenance planning. A scientific approach is currently absent. Even with available human expertise, decision-making is currently, to a degree, ad hoc. This research fulfilled the gap in the literature on RO maintenance planning and set a new gold standard for membrane maintenance management.

This research aims to establish a maintenance planning methodology for an EO. The objective is for a DSS to forecast the effectiveness before implementing the policies. The aim and objectives have been achieved. The research has demonstrated the design and implementation of a particular EO using a real-life industry example. The research shows how significant cost savings can be made, while the same projections show that the risk involving the long-term reliability of the EO is reduced. The O&M company and the owners have recognised the research contribution. The Desalination journal editor and reviewers recognised the unique contributions of this research to the research community.

Two research questions (RQ) were put forward. RQ1: What are the general requirements of a DSS for restoration so that the DSS is fit for purpose? The research answered RQ1 by proposing a framework of maintenance principles and sub-principles. Rather than an answer,

the framework of maintenance principles and sub-principles is more of an opening of a discussion in the broader engineering services community on the principles of maintenance planning. The lower-level principles were used to guide the design of the practical DSS implemented. Therefore, although in development, the framework of maintenance principles and sub-principles has already shown its usefulness. RQ2 stated: How should the restoration of membrane elements in RO desalination in the presence of seasonal algal blooms be managed? RQ2 has been answered in-depth in this research. In parallel to this thesis, the research has been published in a high-impact academic journal and conference papers. The positive results of the exploration of policies using the DSS confirm this.

10.3 Conclusions

This research emphasises the need for a DSS to assist in the long-term maintenance planning of an EO. A DSS should be driven by a DT that can model degradation and restoration for the time-series data and forecast long-term projections. A mathematical model and its implementation as a DT have been presented as an example. However, alternatives, like Artificial Intelligence (AI) based models, should not be excluded. Nevertheless, a mathematical model based on engineering know-how can significantly shorten the development time compared to AI training, requiring extensive training data. The drawbacks of AI may change in the near future when AI's technical and cognitive capabilities improve. Nonetheless, even when applying an AI-driven DT, a successful DSS for maintenance requirements should still be based on the principles in the presented framework of maintenance principles and sub-principles. The latter could also become the domain of AI in the future.

Although most facilities now have some kind of maintenance management system, often involving a CMMS, DSS are mostly absent. Therefore a DSS has to be added on. Incorporating a DSS inside a commercial CMMS platform is impractical and results in high integration costs. Further, EOs can be so diverse that a one-fits-for-all approach probably will not work. This research, therefore, proposes that the DSS should be located beside the CMMS but data-driven from both the CMMS and the plant's Operational Technology (OT) time-series database. A preliminary analysis of maintenance performed at the plant (see chapter 2) justified the investment necessary to develop the DT (Principle four, level four of the framework of maintenance principles).

This research has provided a practical example of the maintenance management of RO membrane elements. The DT-driven DSS used in this research is not limited to RO

membrane maintenance planning and can be implemented for other EOs. In chapter 9.2, the thesis author presented initial research on vibrations anomaly detection and performance analysis for the High-Pressure Booster pumps, one group of the plant's large centrifugal pumps. The latter can be used as a model for developing a DT-based DSS for this specific EO. A virtual replica of the centrifugal pump can show the flow, power consumption, and vibrations according to feed, discharge pressure and pump speed. The virtual replica can then be compared to the physical pump to determine whether the wear involves bearings or the pump's internal components. The latter requires significantly higher fixed set-up costs.

Each EO category has to be approached individually. However, the presented principles set out in the framework of maintenance principles apply in general, thus also in the case of centrifugal pumps. The framework can be considered a guide for the design of a DSS for a specific unit.

This research emphasises modelling degradation and restoration. Availability of operational and maintenance data is thereby essential. Engineering know-how of the EO is required to develop a mathematical model of degradation and restoration. Finally, the author recommends establishing a baseline so tangible metrics can measure the impact of the planned improvements, as has been done in this study.

10.4 Limitations

Essential factors of the success of a digital twin for managing the restoration of membranes in reverse osmosis desalination are the ability to identify the degradation dependencies and the effects of partial restoration, the ability to trend this and the available supporting data. These factors are not always available. In some cases, wear and repair clues are limited to failure data. Such cases support the principle that failure data are useful for identifying critical systems and where to deploy a DSS. However, restriction to failure data can have the additional limitation that the system might evolve or that there are too many random failure modes to draw patterns. The available data are then insufficient for designing a DT.

This study concentrated on the degradation or, in other words, the wear aspect of increased differential pressure over seawater RO trains due to biofouling. RO membrane wear resulting in increased differential pressure was the primary concern in this case study. The model is therefore limited to one aspect of fouling. In the case of brackish water RO systems, a combination of biofouling and mineral scaling can occur. In this case, wear at the lead elements is combined with the tail elements' wear due to different circumstances. The latter

requires an extension of the current model. The model further does not consider other factors of long-term wear, e.g., a decrease in salt rejection due to the ageing of the elements. The DT uses a fixed recovery for the projection, whereas the actual recovery varies slightly seasonally and with demand.

Specific to this case study, although five years of systematic data were available, data on annual occurrence and length of algae blooms was limited. This limited data is one of the reasons that a normal distribution of occurrences and duration of algae blooms gave inaccurate results.

The study was applied to an existing installation that was put into operation several years earlier. As a result, some initial data was missing. In this case, specifically, the original weight of the membrane components when they were new. Since the weight of a new wet component varies significantly, this cannot be replaced by measuring the weight of a random new element. As a result, there is some tolerance in the accuracy of the biomass weight measurement used to define the biomass distribution parameter in the model.

The research applied particle filtering for other model parameters, specifically the rate-state severity constant γ and the extrinsic wear dependency κ . The estimation of multiple parameters simultaneously is more complex since the exact fit of the modelled NPD with the observed NPD can be achieved with different pairs of γ and κ . The difference of γ , in this case, was of minor influence. However, further research on parameter estimation, whether or not involving particle filtering, is of interest. Although the model's parameters have been tuned to fit the case study, further study is required to finetune the parameters beyond.

Finally, despite introducing randomness for the stochastic extrinsic wear dependency and the imperfect restoration, the presented model is still highly deterministic. In practice, the degeneration of membrane components is probably more stochastic.

10.5 Further research

This research has concentrated on a decision support system (DSS) for maintenance planning for RO membranes that uses a Digital Twin (DT). The presented DT-based DSS allows an operator to compare competing restoration (maintenance) policies. Future research could investigate an optimisation module that seeks an optimum maintenance policy. Of course, optimisation is a mathematical concept. Nonetheless, finding the best policy from among all possible policies would be expected to have a practical benefit. In the context of membrane restoration, the number of possible policies is very large, and it would be interesting to use automation to seek the best policy. As such, this context would lend itself to

the investigation of the use of AI for decision support in maintenance planning. In this way, rather than a DSS with a human interface, as proposed in this thesis, an AI module might “front-end” the DT.

The RO trains are only one section of the plant. The design of a DSS and its DT for other plant equipment will be of interest. Initial work has already been conducted regarding the plant's large high-pressure booster pumps (see chapter 9.2). The initial research on vibrations anomaly detection and performance analysis for the plant's large centrifugal pumps can be the basis of a DT that provide the parallel data of flow, power consumption, and vibrations of a healthy unit. The virtual replica can then be compared to the physical pump to determine the wear of the specific component or group of components. Specific DTs can be further developed for the intake pumps, dilution pumps, Low-pressure booster pumps, high-pressure pumps, and product pumps. Of interest is to compare the above outlined DT for the centrifugal pumps against an anomaly detection method, iDetect, based on the Fourier transform for vibration analyses recently offered by the management information systems (MIS) supplier.

In addition, the Digital Twin for an RO train has been limited to a single case study, a seawater desalination plant in California. Testing the DT and DSS at other seawater RO plants worldwide will be valuable in extending the model and increasing its robustness. The O&M company operates several facilities worldwide. One of these facilities is nearby located in Santa Barbara, California, which is also affected by algae blooms.

As a first step, the thesis author intends to develop a specific DT for the RO trains at Santa Barbara. The Carlsbad plant uses only one type of element for the SWRO vessels. In contrast, the Santa Barbara plant has a hybrid configuration, i.e., a combination of different element types in a vessel. Further, the Santa Barbara plant is based on a single RO pass, which means that the rear product of the vessel, having reduced quality, is not undergoing further treatment of an additional RO pass. Controlling the degradation of salt rejection is, in this case, crucial. Thus, besides biofouling, the DT of the RO vessel can also include the degradation of salt rejection.

Finally, the literature review states that several desalination plants worldwide suffer from algae blooms. Although the specifics of algae blooms can differ per region, combining this data and its effects on other plants would be interesting. The thesis author encourages researchers to take on this vital research.

References

1. Adams, E. W. & Levine, H. P., 1975. On the Uncertainties Transmitted from Premises to Conclusions in Deductive Inferences. *Synthese*, 30(3/4), pp. 429-460.
2. Adumene, S., Adedigba, S., Khan, F. & Zendehboudi, S., 2020. An integrated dynamic failure assessment model for offshore components under microbiologically influenced corrosion. *Ocean Engineering*, Volume 218.
3. Agawin, N., Duarte, C. & Agustí, S., 2000. Nutrient and temperature control of the contribution of picoplankton to phytoplankton biomass and production. *Limnology and Oceanography*, 45(3), pp. 591-600.
4. Åhrén, T. & Aditya, A., 2009. Maintenance performance indicators (MPIs) for benchmarking the railway infrastructure: A case study. *Benchmarking: An International Journal*, 16(2), pp. 247-258.
5. Albraik, A., Althobiani, F., Gu, F. & A., B., 2012. Diagnosis of Centrifugal Pump Faults Using Vibration Methods. *Journal of Physics*, Volume Conference Series 364.
6. Alcácer, V. & Cruz-Machado, V., 2019. Scanning the Industry 4.0: A Literature Review on Technologies for Manufacturing Systems. *Engineering Science and Technology*, Volume 22, p. 899-919.
7. Altunkaynak, A., Özger, M. & Çakmakci, M., 2005. Water Consumption Prediction of Istanbul City by Using Fuzzy Logic Approach. *Water Resources Management*, Volume 19, p. 641-654.
8. Amarnath, M. & Krishna, R. P., 2019. Experimental Investigations to Assess Surface Contact Fatigue Faults in the Rolling Contact Bearings by Enhancement of Sound and Vibration Signals. *Journal of Nondestructive Evaluation*, 38(34).
9. Anderson, C., 2010. Central limit theorem. *The Corsini Encyclopedia of Psychology*, pp. 1-2.
10. Anderson, C. & Hepner-Medina, M., 2020. *Red Tide Bulletin: Spring 2020*, San Diego, California: Southern California Coastal Ocean Observing System (SCCOOS).
11. Aronen, R., 2011. The Power of Wear Rings, Part 1. *Pumps & Systems*, March, Volume March 2011.
12. Arts, R., Knapp, G. M. & Mann, L. J., 1998. Some aspects of measuring maintenance performance in the process industry. *Journal of Quality in Maintenance Engineering*, 4(1), pp. 6-11.
13. Ascher, H. & Feingold, H., 1984. *Repairable systems reliability: modeling, inference, misconceptions and their causes*. New York: Marcel Dekker.
14. Assaf, R., Do, P., Nefti-Meziani, S. & Scarf, P., 2018. Wear rate-state interactions within a multi-component system: a study of a gearbox-accelerated life testing platform. *Journal of Risk and Reliability*, 232(4), p. 425-434.
15. Attaway, S., 2018. *MATLAB*. Fifth ed. s.l.:Elsevier Science.
16. Azadeh, A., Ebrahimipour, V. & Bavar, P., 2010. A fuzzy inference system for pump failure diagnosis to improve maintenance process: The case of a petrochemical industry. *Expert Systems with Applications*, Volume 37, p. 627-639.
17. Azeez, N. I. & Alex, A. C., 2014. *Detection of Rolling Element Bearing Defects by Vibration Signature Analysis: A review*. Kottayam, India, International Conference on Magnetics, Machines & Drives (AICERA-2014 iCMMD).

18. Babu, G. S. & Das, V. C., 2013. Condition Monitoring and Vibration Analysis of Boiler Feed Pump. *International Journal of Scientific and Research Publications*, 3(6).
19. Bachus, L. & Custodio, A., 2003. *Know and understand centrifugal pumps*. 1 ed. s.l.:Elsevier.
20. Badruzzaman, M., Voutchkov, N., Weinrich, L. & Jacangelo, J. G., 2019. Selection of pretreatment technologies for seawater reverse osmosis plants: A review. *Desalination*, Volume 449, pp. 78-91.
21. Baier, R., Shafrin, E. & Zisman, W., 1968. Adhesion: Mechanisms that Assist or Impede It. *Science*, 162(3860), pp. 1360-1368.
22. Bakri, A. & Januddi, M., 2020. Computerized-Based Maintenance. In: *Systematic Industrial Maintenance to Boost the Quality Management Programs*. Cham: Springer, pp. 69-78.
23. Balali, F., Seifoddini, H. & Nasiri, A., 2020. Data-driven predictive model of reliability estimation using degradation models: a review. *Life Cycle Reliability and Safety Engineering*, 9(9), pp. 113-125.
24. Bartman, A. R. et al., 2011. Mineral scale monitoring for reverse osmosis desalination via real-time membrane surface image analysis. *Desalination*, Volume 273, p. 64–71.
25. Barzdaitis, V. et al., 2016. 2012. Investigation of pressure pulsations in centrifugal pump system. *Journal of Vibroengineering*, 18(3), pp. 1849-1860.
26. Bashitialshaaer, R., 2020. Solar-Energy Innovative and Sustainable Solution for Freshwater and Food Production for Lake Titicaca Islands. *EJERS, European Journal of Engineering Research and Science*, 5(4), pp. 436-442.
27. Battin, T. J., Kaplan, L. A., Newbold, J. D. & Hansen, C. M. E., 2003. Contributions of microbial biofilms to ecosystem processes in stream mesocosms. *Nature*, Volume 426, pp. 439-441.
28. Beebe, R. S., 2004. *Predictive Maintenance of Pumps Using Condition Monitoring*. New York: Elsevier Science & Technology Books.
29. Beirlaen, M., 2017. Qualitative Inductive Generalization and Confirmation. In: T. B. Lorenzo Magnani, ed. *Springer Handbook of Model-Based Science*. Pavia, Italy: Springer International Publishing, pp. 231-248.
30. Ben-Daya, M. & Duffuaa, S., 2000. Overview of maintenance modeling areas. In: M. Ben-Daya, S. Duffuaa & A. Raouf, eds. *Maintenance, modeling and optimization*. s.l.:Kluwer Academic Publisher, pp. 3-35.
31. Ben-Daya, M., Duffuaa, S. & Raouf, A., 2000. *Maintenance, modeling and optimization*. s.l.:Kluwer Academic Publisher.
32. Ben-Daya, M., Kumar, U. & Murthy, D. N. P., 2016. *Introduction to Maintenance Engineering: Modelling, Optimization and Management*. Dhahran, Saudi Arabia; Lulea, Sweden; Brisbane, Australia: Wiley.
33. Benecke, J., Haas, M., Baur, F. & Ernst, M., 2018. Investigating the development and reproducibility of heterogeneous gypsum scaling on reverse osmosis membranes using real-time membrane surface imaging. *Desalination*, Volume 428, p. 161–171.
34. Bengtsson, T., Bickel, P. & Li, B., 2008. Curse-of-dimensionality revisited: Collapse of the particle filter in very large scale systems. In: *Probability and statistics: Essays in honor of David A. Freedman*. s.l.:Institute of Mathematical Statistics, pp. 316-334.

35. Bereschenko, L. A., Stams, A. J. M., Euverink, J. W. & van Loosdrecht, M. C. M., 2010. Biofilm Formation on Reverse Osmosis Membranes Is Initiated and Dominated by *Sphingomonas* spp. *Applied and Environmental Microbiology*, 76(8), p. 2623–2632.
36. Bhattacharya, S. & Hwang, S., 1997. Concentration polarization, separation factor, and Peclet number in membrane processes. *Journal of membrane science*, 132(1), pp. 73-90.
37. Bian, L. & Gebraeel, N., 2014. Stochastic framework for partially degradation systems with continuous component degradation-rate-interactions. *Naval Research Logistics*, Volume 61, pp. 286-303.
38. Birajdar, R., Patil, R. & Khanzode, K., 2009. *Vibration and noise in centrifugal pumps - sources and diagnosis methods*. Porto/Portugal, 3rd International Conference on Integrity, Reliability and Failure.
39. Birnbaum, Z. W., Esary, J. & Saunders, S., 1961. Multicomponent systems and structures and their reliabilities. *Technometrics*, Volume 3, pp. 95-77.
40. Blatter, P. D. J. & Haverland, D. M., 2012. *Designing Case Studies Explanatory Approaches in Small-N Research*. Kindle Edition ed. Basingstoke, Hampshire: Palgrave Macmillan UK.
41. Bracewell, R., 1995. Computing with the Hartley transform. *Computers in Physics*, 9(4), pp. 373-379.
42. Bravo, I. & Figueroa, R. I., 2014. Towards an Ecological Understanding of Dinoflagellate Cyst Functions. *Microorganisms*, 2014(2), pp. 11-32.
43. Brenna, A., Ormellese, M. & Lazzari, L., 2014. *Markov chain model to predict localised corrosion of stainless steels*. Milan, Italy, Proceedings of the EUROCORR.
44. Bristow, N. W. et al., 2020. Flow field in fouling spiral wound reverse osmosis membrane modules using MRI velocimetry. *Desalination*, Volume 491.
45. Brkić, D., 2012. Discussion of “Jacobian Matrix for Solving Water Distribution System Equations with the Darcy-Weisbach Head-Loss Model” by Angus Simpson and Sylvan Elhay. *Journal of hydraulic engineering*, 128(11), pp. 1000-1001.
46. Brover, S., Lester, Y., Brenner, A. & Sahar-Hadar, E., 2022. Optimization of ultrafiltration as pre-treatment for seawater RO desalination. *Desalination*, Volume 524.
47. Brundage, M. P. et al., 2019. Where do we start? Guidance for technology implementation in maintenance management for manufacturing. *Journal of Manufacturing Science and Engineering*, 141(9).
48. Bucs, S. S. et al., 2018. Review on strategies for biofouling mitigation in spiral wound membrane systems. *Desalination*, Volume 434, pp. 189-197.
49. Burhanuddin, M. A., Halawani, S. M. & Ahmad, a. A., 2011. An Efficient Failure-Based Maintenance Decision Support System for Small and Medium Industries. In: C. Jao, ed. *Efficient decision support systems: Practice and challenges from current to future*. s.l.:BoD–Books on Demand, pp. 195-210.
50. Caiado, J., 2010. Performance of Combined Double Seasonal Univariate Time Series Models for Forecasting Water Demand. *Journal of Hydrologic Engineering*, 15(3), pp. 215-222.
51. Camci, F., 2009. System Maintenance Scheduling With Prognostics Information Using Genetic Algorithm. *IEEE Transactions on Reliability*, 58(3), pp. 539-552.
52. Candy, J., 2007. Bootstrap particle filtering. *IEEE Signal Processing Magazine*, 24(4), pp. 73-85.

53. Carfagno, S. & Gibson, R., 1980. *A Review of Equipment Aging Theory and Technology*, Philadelphia, Pennsylvania: Electric Power Research Institute.
54. Carnero Moya, M. C., 2004. The control of the setting up of a predictive maintenance programme using a system of indicators. *Omega, The International Journal of Management Science*, Volume 32, p. 57–75.
55. Carter, M., 2020. [SIO-Pier-HAB-List-L] 20200427-20200504 La Jolla, Scripps Pier Reports, La Jolla, California: University of California, San Diego. Scripps Institution of Oceanography.
56. Catt, P. J., 2020. A tailorable framework of practices for maintenance delivery. *Journal of Quality in Maintenance Engineering*.
57. Che, J. & Wang, J., 2014. Short-term load forecasting using a kernel-based support vector regression combination model. *Applied Energy*, Volume 132, p. 602–609.
58. Chernick, M. R. & LaBudde, R. A., 2011. *An Introduction to Bootstrap Methods with Applications to R*. New Jersey: Wiley.
59. Chiou, Y.-T., Hsieh, M.-L. & Yeh, H.-H., 2010. Effect of algal extracellular polymer substances on UF membrane fouling. *Desalination*, Volume 250, p. 648–652.
60. Cho, D. & Parlar, M., 1991. A survey of maintenance models for multi-unit systems. *European journal of operational research*, 51(1), pp. 1-23.
61. Costello, M. J., 1990. *Understanding the vibration forces in induction motors*. Dallas (Texas), The Nineteenth Turbomachinery Symposium.
62. Crowther, D. & Lancaster, G., 2005. *Research Methods*. 2nd ed. Oxford: Elsevier Butterworth-Heinemann.
63. Crump, B. C., Hopkinson, C. S., Sogin, M. L. & Hobbie, J. E., 2004. Microbial Biogeography along an Estuarine Salinity Gradient: Combined Influences of Bacterial Growth and Residence Time. *Applied and environmental microbiology*, 70(3), p. 1494–1505.
64. Cui, Y., Kara, S. & Chan, K. C., 2020. Manufacturing big data ecosystem: A systematic literature review. *Robotics and Computer Integrated Manufacturing*, Volume 62.
65. Dalton, T., Annunziata, U., del Vigo Pisano, F. & Gallego, S., 2004. Membrane autopsy helps to provide solutions to operational problems. *Desalination*, Volume 167, pp. 239–245.
66. Dao, C. D. & Zuo, M. J., 2017. Selective maintenance of multi-state systems with structural dependence. *Reliability Engineering and System Safety*, Volume 159, pp. 184–195.
67. Dawkins, R., 2008. *The God Delusion*. Kindle Edition ed. s.l.:HMH Books.
68. Day, J. et al., 2021. Deltas in Arid Environments. *Water*, 13(12).
69. de Almeida, A. T., Ferreira, R. J. P. & Cavalcante, C. A. V., 2015. A review of the use of multicriteria and multi-objective models in maintenance and reliability. *IMA Journal of Management Mathematics*, 26(3), p. 249–271.
70. De Finetti, B., 2017. *Theory of probability: A critical introductory treatment*. 6 ed. s.l.:John Wiley & Sons.
71. de Jonge, B. & Scarf, P. A., 2020. A review on maintenance optimization. *European Journal of Operational Research*, pp. 805-824.
72. Dekker, R., 1996. Applications of maintenance optimization models: a review and analysis. *Reliability engineering & system safety*, 51(3), pp. 229-240.

73. Dekker, R. & Smeitink, E., 1991. Opportunity-based block replacement. *European Journal of Operational Research*, 53(1), pp. 46-63.
74. Dekker, R., Wildeman, R. & van der Duyn Schouten, F., 1997. A review of multi-component maintenance models with economic dependence. *Mathematical Methods of Operations*, 45(3), p. 411–435.
75. Dhanasekaran, A. & Kumaraswamy, S., 2019. Study of Stage-wise Pressure Pulsation in an Electric Submersible Pump under Variable Frequency Operation at Shut-off Condition. *Journal of The Institution of Engineers (India)*, 100(1), pp. 213-220.
76. Di Lorenzo, E. et al., 2008. North Pacific Gyre Oscillation links ocean climate and ecosystem change. *Geophysical research letters*, Volume 35.
77. Diallo, C., Aït-Kadi, D. & Chelbi, A., 2009. Integrated Spare Parts Management. In: M. Ben-Daya et al. eds. *Handbook of Maintenance Management and Engineering*. s.l.:Springer, pp. 191-222.
78. Dickau, R. & Perera, L., 2000. *Mechanical vibration problems with variable frequency drives*. Calgary (Canada), American Society of Mechanical Engineers (ASME).
79. Dinh, D.-H., Do, P. & Iung, B., 2020. Degradation modeling and reliability assessment for a multi-component system with structural dependence. *Computers & Industrial Engineering*, Volume 144.
80. Dodge, J., 1989. *Marine Species Identification Portal*. [Online] Available at: http://species-identification.org/species.php?species_group=dinoflagellates&id=68 [Accessed 10 May 2020].
81. Dohi, T., Kaio, N. & Osaki, S., 2000. Basix preventive maintenance policies and their variations. In: M. Ben-Daya, S. Duffuaa & A. Raouf, eds. *Maintenance, modeling and optimization*. s.l.:Kluwer Academic Publisher, pp. 155-183.
82. Donkor, E. A., Mazzuchi, T. A., Soyer, R. & Roberson, J. A., 2014. Urban Water Demand Forecasting: Review of Methods and Models. *Journal of Water Resources Planning and Management*, 140(2), pp. 146-159.
83. Do, P., Assaf, R., Scarf, P. & Iung, B., 2019. Modelling and application of condition-based maintenance for a two-component system with stochastic and economic dependencies. *Reliability Engineering & System Safety*, Volume 182, pp. 86-97.
84. Doucet, A., Freitas, N. d. & Gordon, N., 2001. An Introduction to Sequential Monte Carlo Methods. In: A. Doucet, N. d. Freitas & N. Gordon, eds. *Sequential Monte Carlo Methods in Practice. Statistics for Engineering and Information Science*. New York, NY: Springer, pp. 3-14.
85. Doucet, A. & Johansen, A., 2009. A tutorial on particle filtering and smoothing: Fifteen years later. *Handbook of nonlinear filtering*, 12(656-704).
86. Dudek, G., 2016. Pattern-based local linear regression models for short-term load forecasting. *Electric Power Systems Research*, Volume 130, p. 139–147.
87. Duffuaa, S. & Ben-Daya, M., 2009. Turnaround Maintenance. In: M. Ben-Daya et al. eds. *Handbook of Maintenance Management and Engineering*. s.l.:Springer, pp. 223-235.
88. Duffuaa, S. O. & Haroun, A. E., 2009. Maintenance Control. In: M. Ben-Daya et al. eds. *Handbook of Maintenance Management and Engineering*. s.l.:Springer, pp. 93-113.
89. Duffuaa, S. O. & Raouf, A., 2015. *Planning and Control of Maintenance Systems. Modelling and Analysis*. Second ed. Dhahran, Saudi Arabia; Lahore Pakistan: Springer.

90. Dunleavy, P., 2003. *Authoring a PhD*. Kindle Edition ed. London: Macmillan Education UK.
91. Duranceau, S. J., 2000. Membrane replacement in desalting facilities. *Desalination*, Volume 132, pp. 243-248.
92. Dwight, R., Scarf, P. & Gordon, P., 2012. Dynamic maintenance requirements analysis in asset management. In: C. Berenguer, A. Grall & C. G. Soares, eds. *Advances in Safety, Reliability, and Risk Management*. London: Taylor and Francis, pp. 847-852.
93. Dwyer-Joyce, R., 1999. Predicting the abrasive wear of ball bearings by lubricant debris. *Wear*, Volume 233, pp. 692-701.
94. El-Akruti, K., Kiridena, S. & Dwight, R., 2018. Contextualist-retroductive case study design for strategic asset management research. *Production Planning & Control*, 29(16), pp. 1332-1342.
95. Elfring, J., Torta, E. & van de Molengraft, R., 2021. Particle Filters: A Hands-On Tutorial. *Sensors*, 21(2), p. 438.
96. Ellis, G. & Silk, J., 2014. Defend the integrity of physics. *Nature*, 516(18/25 December 2014), pp. 321-323.
97. Elsayed, E., 2003. Accelerated Life Testing. In: *Handbook of Reliability Engineering*. London: Springer, pp. 415-428.
98. Emamjome, A., Zahedi, M. M. & Ziyaadini, M., 2019. Economic analysis for process optimization of Chabahar Maritime University reverse osmosis desalination plant: a case study. *Applied Water Science*, 9(114), pp. 1-8.
99. Errandonea, I., Beltrán, S. & Arrizabalaga, S., 2020. Digital Twin for maintenance: A literature review. *Computers in Industry*, Volume 123.
100. Farooque, A. M., Al-Amoudi, A. S. & Hassan, A. M., 2002. *Chemical cleaning experiments for performance restoration of NF membranes operated on seawater feed*. Manama, Bahrain, International Desalination Association (IDA).
101. Fortunato, L. et al., 2020. Fouling investigation of a full-scale seawater reverse osmosis desalination (SWRO) plant on the Red Sea: Membrane autopsy and pretreatment efficiency. *Desalination*, Volume 496.
102. Franks, R. et al., 2006. *A pilot study using seawater reverse osmosis membranes in combination with various pretreatments to meet the challenges of pacific seawater desalination*, Oceanside, California: Hydranautics.
103. Fu, Y., Yuan, T. & Zhu, X., 2019. Optimum Periodic Component Reallocation and System Replacement Maintenance. *IEEE Transactions on Reliability*, Volume 68, pp. 753-763.
104. Gallimore, K. F. & Penlesky, R. J., 1988. A framework for developing maintenance strategies. *Production and Inventory Management Journal*, 29(1), pp. 16-22.
105. Gaskin-Reyes, C., 2016. *Water Planet: The Culture, Politics, Economics, and Sustainability of Water on Earth: The Culture, Politics, Economics and Sustainability of Water on Earth*. Santa Barbara, California: ABC-CLIO.
106. Gauch Jr, H. G., 2003. *Scientific Method in Practice*. Kindle Edition ed. Cambridge: Cambridge University Press.
107. Gelman, A., 2011. Induction and Deduction in Bayesian Data Analysis. *RMM Journal*, Volume 2, p. 67-78.

108. Geng, J. u., Azarian, M. & Pecht, M., 2015. Opportunistic maintenance for multi-component systems considering structural dependence and economic dependence. *Journal of Systems Engineering and Electronics*, 26(3), pp. 493 - 501.
109. Ginter, A., 2012. *Unidirectional Security Gateways: NOT your grandma's data diodes*, Ashburn, Virginia, US: Waterfall Security Solutions.
110. Gits, C., 1992. Design of maintenance concepts. *International Journal of Production Economics*, Issue 24, pp. 217-226.
111. Gobler, C. J. et al., 2017. Ocean warming since 1982 has expanded the niche of toxic algal blooms in the North Atlantic and NorthPacific oceans. *PNAS*, 114(19), pp. 4975-4980.
112. Gómez, C. B. & Fontaine, M., 2017. Argumentation and Abduction in Dialogical Logic. In: T. B. Lorenzo Magnani, ed. *Springer Handbook of Model-Based Science*. Pavia, Italy: Springer International Publishing, pp. 295-314.
113. Gorjian, N. et al., 2010. A review on degradation models in reliability analysis. In: D. Kiritsis, C. Emmanouilidis, A. Koronios & J. Mathew, eds. *Engineering Asset Lifecycle Management*. London: Springer, pp. 369-384.
114. Grieves, M. & Vickers, J., 2017. Digital Twin: Mitigating Unpredictable, Undesirable Emergent Behavior in Complex Systems. In: F. Kahlen, S. Flumerfelt & A. Alves, eds. *Transdisciplinary Perspectives on Complex Systems*. s.l.: Springer International Publishing, pp. 85-113.
115. Gutiérrez Ruiz, S. et al., 2020. Study of reverse osmosis membranes fouling by inorganic salts and colloidal particles during seawater desalination. *Chinese Journal of Chemical Engineering*, Volume 28, p. 733–742.
116. Haag, S. & Anderl, R., 2018. Digital twin – Proof of concept. *Manufacturing Letters*, Volume 15, p. 64–66.
117. Haile, G. G. et al., 2020. Drought: Progress in broadening its understanding. *Wiley Interdisciplinary Reviews: Water*, 7(2).
118. Hallegraeff, G. M., 2010. Ocean climate change, phytoplankton community responses, and harmful algal blooms: A formidable predictive challenge. *Phycol*, Volume 46, p. 220–235.
119. Hamming, R., 1973. *Numerical Methods for Scientists and Engineers*. Kindle, 2 Edition ed. s.l.:Dover Publications.
120. Hansson, S. O., 2013. ALARA: What is Reasonably Achievable? In: D. Oughton & S. O. Hansson, eds. *Social and Ethical Aspects of Radiation Risk Management*. Oxford, UK: Elsevier, pp. 143-155.
121. Hawking, S., 2001. *The Universe in a Nutshell*. Cambridge: Bantam Press.
122. Hawking, S. & Penrose, R., 1996. *The Nature of Space and Time (Issac Newton Institute Series of Lectures)*. 13th, 2010 ed. Cambridge: Princeton University Press.
123. Hinrichsen, R. & Holmes, E., 2009. Using multivariate state-space models to study spatial structure and dynamics. In: S. Cantrell, C. Cosner & S. Ruan, eds. *Spatial ecology*. s.l.:Taylor and Francis, pp. 145-166.
124. Hoang, T. A., Ang, H. M. & Rohl, A. L., 2007. Effects of temperature on the scaling of calcium sulphate in pipes. *Powder Technology*, Volume 179, p. 31–37.
125. Hoek, E. & Elimelech, M., 2003. Cake-enhanced concentration polarization: a new fouling mechanism for salt-rejecting membranes. *Environmental science & technology*, 37(24), pp. 5581-5588.

126. Hollyman, R., Petropoulos, F. & Tipping, M. E., 2021. Understanding forecast reconciliation. *European Journal of Operational Research*, 294(1), p. 149–160.
127. Hubbard, R., Bayarri, M. J., Berk, K. N. & Carlton, M. A., 2003. Confusion Over Measures of Evidence (p's) Versus Errors (a's) in Classical Statistical Testing. *The American Statistician*, 57(3), pp. 171-182.
128. Ibe, O., 2014. *Fundamentals of applied probability and random processes*. s.l.:Academic Press.
129. Ilott, P. W. & Griffiths, A. J., 1997. Fault diagnosis of pumping machinery using artificial neural networks. *Proceedings of the Institution of Mechanical Engineers*, 211(3), pp. 185-194.
130. Ip, J., Qiu, J. & Chan, B., 2021. Genomic insights into the sessile life and biofouling of barnacles (Crustacea: Cirripedia). *Heliyon*, Volume 7.
131. Iung, B., Do, P., Levrat, E. & Voisin, A., 2016. Opportunistic maintenance based on multi-dependent components of manufacturing system. *CIRP Annals - Manufacturing Technology*, Volume 65, p. 401–404.
132. Jafari, M. et al., 2021. Cost of fouling in full-scale reverse osmosis and nanofiltration installations in the Netherlands. *Desalination*, Volume 500.
133. Jahangirian, M. et al., 2010. Simulation in manufacturing and business: A review. *European Journal of Operational Research*, Volume 203, pp. 1-13.
134. Jaidka, H., Sharma, N. & Singh, R., 2020. *Evolution of IoT to IIoT: Applications & challenges*. New Delhi, India, Proceedings of the International Conference on Innovative Computing & Communications (ICICC).
135. Jain, A. & Ormsbee, L. E., 2002. Short-term water demand forecast modeling techniques - conventional methods versus AI. *American Water Works Association Journal*, 94(7), pp. 64-72.
136. Jamieson, T. et al., 2021. Survival of the fittest: Prokaryotic communities within a SWRO desalination plant. *Desalination*, Volume 514.
137. Jasiulewicz-Kaczmarek, M. & Gola, A., 2019. Maintenance 4.0 Technologies for Sustainable Manufacturing – an Overview. *IFAC (International Federation of Automatic Control) Hosting by Elsevier Ltd.*, 52(10), p. 91–96.
138. Jiang, A. et al., 2015. Operational cost optimization of a full-scale SWRO system under multi-parameter variable conditions. *Desalination*, Volume 355, p. 124–140.
139. Jiang, S., Li, Y. & Ladewig, B. P., 2017. A review of reverse osmosis membrane fouling and control strategies. *Science of the Total Environment*, Volume 595, p. 567–583.
140. Jonker, J. & Pennink, B., 2010. *The Essence of Research Methodology*. Nijmegen, Groeningen: Springer.
141. Julien, N. & Martin, E., 2021. *A Usage-driven Approach to Characterize and Implement Industrial Digital Twins*. Angers, France, ESREL 2021. Published by Research Publishing, Singapore, pp. 1721-1728.
142. Kadouri, D. & O'Toole, G. A., 2005. Susceptibility of Biofilms to Bdellovibrio bacteriovorus Attack. *Applied and Environmental Microbiology*, 71(7), pp. 4044-4051.
143. Kantas, N. et al., 2015. On Particle Methods for Parameter Estimation in State-Space Models. *Statistical Science*, 30(3), pp. 328-351.
144. Karanasiou, A., Karabelas, A. & Mitrouli, S., 2021. Incipient membrane scaling in the presence of polysaccharides during reverse osmosis desalination in spacer-filled channels. *Desalination*, Volume 500.

145. Kayode Coker, A., 2007. *Ludwig's Applied Process Design for Chemical and Petrochemical Plants*. 1 ed. s.l.:Elsevier.
146. Kerdi, S. et al., 2020. Membrane filtration performance enhancement and biofouling mitigation using symmetric spacers with helical filaments. *Desalination*, Volume 484.
147. Keyvan, S., 2001. Traditional signal Pattern Recognition versus Artificial Neural Networks for Nuclear Plant Diagnostics. *Progress in Nuclear Energy*, 39(1), pp. 1-29.
148. Killick, R., Fearnhead, P. & Eckley, I. A., 2012. Optimal Detection of Changepoints With a Linear Computational Cost. *Journal of the American Statistical Association*.
149. Kim, K., Jung, M., Tsang, Y. & Kwon, H., 2020. Stochastic modelling of chlorophyll-a for probabilistic assessment and monitoring of algae blooms in the Lower Nakdong River, South Korea. *Journal of Hazardous Materials*, Volume 400, p. 123066.
150. Kim, S. K., Lim, J. H. & Kim, Y. S., 2017. Evaluation of the Existing Maintenance Policy for Seawater Reverse-Osmosis Plant at Kuwait Bay Based on the Degradation Characteristics of Membranes. *International Journal of Applied Engineering Research*, 12(12), pp. 3197-3202.
151. King, G., Keohane, R. O. & Verba, S., 1994. *Designing Social Inquiry*. Cambridge, Massachusetts: Princeton university press.
152. Koutsakos, E. & Moxey, D., 2007. Membrane Management System. *Desalination*, Volume 203, p. 307–311.
153. Kranendonk, R., 2016. *The Convergence and Integration of Operational Technology and Information Technology Systems*, Delft: repository.tudelft.nl.
154. Kritzinger, W. et al., 2018. *Digital Twin in manufacturing: A categorical literature review and classification*. Seville, Spain, Elsevier B.V., p. 1016–1022.
155. Kucera, J., 2019. Biofouling of Polyamide Membranes: Fouling Mechanisms, Current Mitigation and Cleaning Strategies, and Future Prospects. *Membranes*, 9(9), pp. 1-81.
156. Kuhn, T. S., 1996. *The structure of scientific revolutions*. 3rd ed. Berkeley, California: University of Chicago Press.
157. Labib, A., 2004. A decision analysis model for maintenance policy selection using a CMMS. *Journal of Quality in Maintenance Engineering*, 10(3), p. 191–202.
158. Labib, A., 2008. Computerised Maintenance Management Systems. In: K. A. Kobbacy & D. P. Murthy, eds. *Complex System Maintenance Handbook*. s.l.:Springer Series in Reliability Engineering, pp. 416-435.
159. Laggoune, R., Chateaneuf, A. & Aissani, D., 2010. Impact of few failure data on the opportunistic replacement policy for multi-component systems. *Reliability Engineering and System Safety*, Volume 95, p. 108–119.
160. Lai, C., Jiang, W. & Jackson, P., 2019. Internet of Things enabling condition-based maintenance in elevator service. *Journal of Quality in Maintenance Engineering*, 25(4), pp. 563-588.
161. Lakritz, T., 2019. *Global Agenda*. [Online] Available at: <https://www.weforum.org/agenda/2019/09/11-sinking-cities-that-could-soon-be-underwater/>
162. Landaburu-Aguirre, J. et al., 2016. Fouling prevention, preparing for re-use and membrane recycling. Towards circular economy in RO desalination. *Desalination*, Volume 393, p. 16–30.
163. Lavielle, M., 2005. Using penalized contrasts for the change-point problem. *Signal Processing*, Volume 85, p. 1501–1510.

164. Lawson, B. & Leemis, L., 2008. *Monte Carlo and discrete-event simulations in C and R*. s.l., IEEE, pp. 11-16.
165. Lehmann, E., 1993. The Fisher, Neyman-Pearson theories of testing hypotheses: one theory or two? *Journal of the American Statistical Association*, 88(424), pp. 1242-1249.
166. Le-Ngoc, T. & Vo, M., 1989. Implementation and performance of the fast Hartley transform. *IEEE Micro*, 9(5), pp. 20-27.
167. Letelier, R. M., Karl, D. M., Abbott, M. R. & Bidigare, R. R., 2004. Light-driven seasonal patterns of chlorophyll and nitrate in the lower euphotic zone of the North Pacific Subtropical Gyre. *Limnol. Oceanogr.*, Volume 49(2), p. 508–519.
168. Lewis, J. T. J. N. K. a. L. S., 2018. Expanding known dinoflagellate distributions: Investigations of slurry cultures from Caspian Sea sediment. *Botanica Marina*, 61(1), p. 21–31.
169. Lin, H. & Ye, Y., 2019. Reviews of bearing vibration measurement using fast Fourier transform and enhanced fast Fourier transform algorithms. *Advances in Mechanical Engineering*, 11(1), pp. 1-12.
170. Li, S. et al., 2015. Compositional similarities and differences between transparent exopolymer particles (TEPs) from two marine bacteria and two marine algae: Significance to surface biofouling. *Marine Chemistry*, Volume 174, p. 131–140.
171. Liu, M., Fang, S., Dong, H. & Xu, C., 2021. Review of digital twin about concepts, technologies, and industrial applications. *Journal of Manufacturing Systems*, Volume 58, pp. 346-361.
172. Liu, Q., Xu, G.-R. & Das, R., 2019. Inorganic scaling in reverse osmosis (RO) desalination: Mechanisms, monitoring, and inhibition strategies. *Desalination*, Volume 468.
173. Liu, Y. et al., 2019. Wireless network design for emerging IIoT applications: Reference framework and use cases. *Proceedings of the IEEE*, 107(6), pp. 1166-1192.
174. Liyanage, J. P., Lee, J., Emmanouilidis, C. & Ni, J., 2009. Integrated E-maintenance and Intelligent Maintenance Systems. In: M. Ben-Daya et al. eds. *Handbook of Maintenance Management and Engineering*. s.l.:Springer, pp. 499-544.
175. Machado, C. G., Winroth, M. P. & da Silva, E. H. D. R., 2020. Sustainable manufacturing in Industry 4.0: an emerging research agenda. *International Journal of Production Research*, 58(5), pp. 1462-1484.
176. Makridakis, S. et al., 1982. The accuracy of extrapolation (time series) methods: Results of a forecasting competition. *Journal of Forecasting*, 1(2), pp. 111-153.
177. Mansoori, G., 2001. *Deposition and fouling of heavy organic oils and other compounds*. Kurashiki, Okayama, Japan, s.n.
178. Martin, R., 2015. Plausibility Functions and Exact Frequentist Inference. *Journal of the American Statistical Association*, 110(512), pp. 1552-1561.
179. Matin, A., Khan, Z., Zaidi, S. & Boyce, M., 2011. Biofouling in reverse osmosis membranes for seawater desalination: Phenomena and prevention. *Desalination*, Volume 281, p. 1–16.
180. Matin, A., Laoui, T., Falath, W. & Farooque, M., 2020. Fouling control in reverse osmosis for water desalination & reuse: Current practices & emerging environment-friendly technologies. *Science of the Total Environment*, pp. 1-20.

181. Mazur, D. C., Stewart, B. G., Clark, H. E. & Paes, R., 2021. Industrial Petrochemical Applications - Analysis of Programmable Logic Controllers and Distributed Control Systems. *IEEE Industry Applications Magazine*, July/August, pp. 36-44.
182. McCall, J., 1965. Maintenance policies for stochastically failing equipment: a survey. *Management Science*, 11(5), pp. 493-524.
183. McKibben, S. M. et al., 2017. Climatic regulation of the neurotoxin domoic acid. *PNAS*, 114(2), p. 239–244.
184. McMullin, E., 2013. The inference that makes science. *Zygon®*, 48(1), pp. 143-191.
185. Miller, J. E., 2003. *Review of Water Resources and Desalination Technologies*, Albuquerque, New Mexico and Livermore, California: Sandia National Laboratories.
186. Miller, O. L. et al., 2021. Changing climate drives future streamflow declines and challenges in meeting water demand across the southwestern United States. *Journal of Hydrology X*, Volume 11.
187. Miller, S. L. & Childers, D., 2012. *Probability and Random Processes*. Second ed. s.l.:Academic Press.
188. Mishra, S. & Datta-Gupta, A., 2017. *Applied statistical modeling and data analytics: A practical guide for the petroleum geosciences*. s.l.:Elsevier.
189. Mitra, S. S. et al., 2009. Fujairah SWRO — management of membrane replacement. *Desalination and Water Treatment*, 10(1-3), pp. 255-264.
190. Mobley, R. K., 2002. *An introduction to predictive maintenance*. Second ed. Knoxville, Tennessee: Butterworth-Heinemann (Elsevier Science USA).
191. Mourtzis, D., 2020. Simulation in the design and operation of manufacturing systems: state of the art and new trends. *International Journal of Production Research*, 58(7), pp. 1927-1949.
192. Mourtzis, D., Doukas, M. & Bernidaki, D., 2014. Simulation in Manufacturing: Review and Challenges. *Procedia CIRP*, Volume 25, p. 213 – 229.
193. Murthy, D. & Jack, N., 2008. Maintenance Outsourcing. In: K. A. Kobbacy & D. P. Murthy, eds. *Complex System Maintenance Handbook*. s.l.:Springer Series in Reliability Engineering, pp. 373-393.
194. Murthy, D. N. P., 2000. Maintenance service contracts. In: M. Ben-Daya, S. Duffuaa & A. Raouf, eds. *Maintenance, modeling and optimization*. s.l.:Kluwer Academic Publisher, pp. 112-132.
195. Myung, I., 2003. Tutorial on maximum likelihood estimation. *Journal of Mathematical Psychology*, 47(1), pp. 90-100.
196. Najem, A. & Coolen, F., 2018. *Cost-effective component swapping to increase system reliability*. Manchester, UK, 10th IMA International Conference on Modelling in Industrial Maintenance and Reliability.
197. Nakagawa, T., 2000. Imperfect preventive maintenance models. In: M. Ben-Daya, S. Duffuaa & A. Raouf, eds. *Maintenance, modeling and optimization*. s.l.:Kluwer Academic Publisher, pp. 201-214.
198. Nakaya, S. et al., 2021. Detection of dynamic biofouling from adenosine triphosphate measurements in water concentrated from reverse osmosis desalination of seawater. *Desalination*, Volume 518.
199. NEAC, 2013. *Role of Modeling and Simulation in Scientific Discovery*. [Online] Available at: <https://www.energy.gov/ne/nuclear-energy-advisory-committee> [Accessed 21 10 2021].

200. Nebot, E., Casanueva, J., Casanueva, T. & Sales, D., 2007. Model for fouling deposition on power plant steam condensers cooled with seawater: Effect of water velocity and tube material. *International Journal of Heat and Mass Transfer*, 50(17-18), pp. 3351-3358.
201. Negahban, A. & Smith, J. S., 2014. Simulation for manufacturing system design and operation: Literature review and analysis. *Journal of Manufacturing Systems*, Volume 33, p. 241–261.
202. Negri, E., Fumagalli, L. & Macchi, M., 2017. A review of the roles of Digital Twin in CPS-based production systems. *Procedia Manufacturing*, Volume 11, p. 939–948.
203. Nekrašas, E., 2001. Pragmatism and positivism. *Problemos*, Volume 59, pp. 41-52.
204. Neto, A. et al., 2021. *Digital twin-driven decision support system for opportunistic preventive maintenance scheduling in manufacturing*. Athens, Greece, 30th International Conference on Flexible Automation and Intelligent Manufacturing (FAIM2021).
205. Nguyen, K.-A., Do, P. & Grall, A., 2015. Multi-level predictive maintenance for multi-component systems. *Reliability Engineering and System Safety*, Volume 144, p. 83–94.
206. Nicolai, R. & Dekker, R., 2008. Optimal Maintenance of Multi-component Systems: A Review. In: K. A. H. Kobbacy & D. N. P. Murthy, eds. *Complex System Maintenance Handbook*. London: Springer Series in Reliability Engineering, pp. 263-286.
207. Noor, H. M., Mazlan, S. A. & Amrin, A., 2021. Computerized Maintenance Management System in IR4.0 Adaptation - A State of Implementation Review and Perspective. *IOP Conf. Series: Materials Science and Engineering*, Volume 1051.
208. Oh, J., 2012. Understanding scientific inference in the natural sciences based on abductive inference strategies. In: L. Magnani & P. Li, eds. *Philosophy and Cognitive Science*. Berlin, Heidelberg: Springer, pp. 221-237.
209. Olde Keizer, M. C. A., Flapper, S. D. P. & Teunter, R. H., 2017. Condition-based maintenance policies for systems with multiple dependent components: A review. *European Journal of Operational Research*, Volume 261, pp. 405-420.
210. ÖNEL, Đ. Y., ÇAĞLAR, E. & DUYAR, A., 2009. *New Horizons on Predictive Maintenance*. Istanbul, Elsevier, pp. 120-125.
211. Paltridge, B. & Starfield, S., 2007. *Thesis and Dissertation Writing in a Secondary Language*. New York: Taylor & Francis.
212. Panetto, H. et al., 2019. Challenges for the cyber-physical manufacturing enterprises of the future. *Annual Reviews in Control*, Volume 47, p. 200–213.
213. Pan, Y. et al., 2022. Probability forecast of storm surge levels in the Changjiang Estuary induced by tropical cyclones based on the Error-Estimation Ensemble method. *Ocean Engineering*, 245(110524).
214. Papalexopoulos, A. D. & Hesterberg, T. C., 1990. A regression-based approach to short-term system load forecasting. *IEEE Transactions on Power Systems*, 5(4), pp. 1535-1550.
215. Parida, A., 2007. Study and analysis of maintenance performance indicators (MPIs) for LKAB: A case study. *Journal of Quality in Maintenance Engineering*, 13(4), pp. 325-337.
216. Parida, A. & Kumar, U., 2006. Maintenance performance measurement (MPM): issues and challenges. *Journal of Quality in Maintenance Engineering*, 12(3), pp. 239-251.
217. Park, S., Serpedin, E. & Qaraqe, K., 2013. Gaussian assumption: The least favorable but the most useful [lecture notes]. *IEEE Signal Processing Magazine*, 30(3), pp. 183-186.

218. Patrone, C., Lattuada, M., Galli, G. & Revetria, R., 2018. *The role of internet of things and digital twin in healthcare digitalization process*. London, United Kingdom, The World Congress on Engineering and Computer Science (pp. 30-37). Springer, Singapore.
219. Pham, H. & Wang, H., 1996. Imperfect maintenance. *European Journal of Operational Research*, Volume 94, pp. 425-438.
220. Picard, F. et al., 2005. A statistical approach for array CGH data analysis. *BMC Bioinformatics*, 6(1), pp. 1-14.
221. Pidd, M., 2004. *Computer Simulation in Management Science*. 5th ed. Lancaster, UK: Wiley.
222. Pintelon, L. & Muchiri, P. N., 2009. Safety and Maintenance. In: M. Ben-Daya et al. eds. *Handbook of Maintenance Management and Engineering*. s.l.:Springer, pp. 612-648.
223. Pintelon, L. & Parodi-Herz, A., 2008. Maintenance: An Evolutionary Perspective. In: K. A. H. Kobkacy & D. N. P. Murthy, eds. *Complex System Maintenance Handbook*. London: Springer, pp. 21-48.
224. Podar, M. et al., 2021. Microbial diversity analysis of two full-scale seawater desalination treatment trains provides insights into detrimental biofilm formation. *Journal of Membrane Science Letters*, Volume 100001.
225. Popper, K., 1959. *The Logic of Scientific Discovery*. Kindle Edition ed. s.l.:(Routledge Classics) Taylor and Francis.
226. Poullikkas, A., 2001. algorithm for reverse osmosis desalination economics. *Desalination*, Volume 133, pp. 75-81.
227. Pruzan, P., 2016. *Research Methodology*. Kindle Edition ed. Copenhagen: Springer International Publishing.
228. Qasim, M. et al., 2019. Reverse osmosis desalination: A state-of-the-art review. *Desalination*, Volume 459, p. 59–104.
229. Rabah, S. et al., 2018. *Towards improving the future of manufacturing through digital twin and augmented reality technologies*. Columbus, OH, USA, Procedia Manufacturing.
230. Raouf, A., 2009. Maintenance Quality and Environmental Performance Improvement: An Integrated Approach. In: M. Ben-Daya et al. eds. *Handbook of Maintenance Management and Engineering*. s.l.:Springer, pp. 649-664.
231. Rapuano, S. & Harris, F., 2007. An introduction to FFT and time domain windows. *IEEE instrumentation & measurement magazine*, 10(6), pp. 32-44.
232. Rebs, T., Brandenburg, M. & Seuring, S., 2019. System dynamics modeling for sustainable supply chain management: A literature review and systems thinking approach. *Journal of Cleaner Production*, Volume 208, pp. 1265-1280.
233. Rengefors, K., Karlsson, I. & Hansson, L.-A., 1998. Algal cyst dormancy: a temporal escape from herbivory. *Proceedings of the Royal Society B: Biological Sciences*, Volume 265, pp. 1353-1358.
234. Research, A. D., 2017. *Academic Ethics Policy*, Salford, Greater Manchester: Research and Enterprise Division University of Salford.
235. Riane, F., Roux, O., Basile, O. & Dehombreux, P., 2009. Simulation Based Approaches for Maintenance Strategies Optimization. In: M. Ben-Daya et al. eds. *Handbook of Maintenance Management and Engineering*. s.l.:Springer, pp. 133-153.
236. Robinson, G., Grooms, I. & Kleiber, W., 2018. Improving particle filter performance by smoothing observations. *Monthly Weather Review*, 146(8), pp. 2433-2446.

237. Rockaway, T. D., Coomes, P. A., Rivard, J. & Kornstein, B., 2011. Residential water use trends in North America. *American Water Works Association*, 103(2), pp. 76-89.
238. Ruiz-García, A., Melián-Martel, N. & Nuez, I., 2017. Short Review on Predicting Fouling in RO Desalination. *Membranes*, 7(62), pp. 1-17.
239. Ruiz, P. P., Foguem, B. K. & Grabot, B., 2014. Generating knowledge in maintenance from Experience Feedback. *Knowledge-Based Systems*, Volume 68, p. 4–20.
240. Salmon, W. C., 2017. *The Foundations of Scientific Inference*. 50th Anniversary edition ed. s.l.:University of Pittsburgh Press.
241. Sandin, R. et al., 2012. *Reverse osmosis membranes oxidation by hypochlorite and chlorine dioxide: Spectroscopic techniques vs Fujiwara test*. Barcelona, Spain, European Desalination Society (EDS).
242. Saunders, M., Lewis, P. & Adrian, T., 2009. *Research methods for business students*. 5th ed. Essex: Pearson Education.
243. Saunders, M. N. K. & Lewis, P., 2017. *Doing Research in Business and Management*. 2nd ed. s.l.:Pearson Education.
244. Scarf, P. A., 1997. On the application of mathematical models in maintenance. *European Journal of Operational Research*, Volume 99, pp. 493-506.
245. Scarf, P. A., 1997. On the application of mathematical models in maintenance. *European Journal of Operational Research*, Volume 99, pp. 493-506.
246. Scarf, P. A. & Cavalcante, C. A., 2010. Hybrid block replacement and inspection policies for a multi-component system with heterogeneous component lives. *European Journal of Operational Research*, Volume 206, p. 384–394.
247. Scarf, P. A. & Deara, M., 2003. Block Replacement Policies for a Two-Component System with Failure Dependence. *Naval Research Logistics*, Volume 50, pp. 70-87.
248. Schafer, R. W., 2011. What Is a Savitzky-Golay Filter?. *IEEE Signal processing magazine*, pp. 111-117.
249. sdcwa.org, 2016. *2015 Urban Water Management Plan*. San Diego: San Diego County Water Authority Water Resources Department.
250. Shahriari, S., Ghasri, M., Sisson, S. A. & Rashidia, T., 2020. Ensemble of ARIMA: combining parametric and bootstrapping technique for traffic flow prediction. *TRANSPORTMETRICA A: TRANSPORT SCIENCE*, 16(3), p. 1552–1573.
251. Sharma, R. & Govindaraju, N., 2020. Maintenance Planning Activity using Intelligent Support System. *International Journal of Mechanical Engineering*, 5(2), pp. 83-88.
252. Sherif, Y. S., 1982. Optimal maintenance schedules of systems subject to stochastic failure. *Microelectronics Reliability*, 22(1), pp. 15-29.
253. Shi, H. & Zeng, J., 2016. Real-time prediction of remaining useful life and preventive opportunistic maintenance strategy for multi-component systems considering stochastic dependence. *Computers & Industrial Engineering*, Volume 93, p. 192–204.
254. Sigman, D. M. & Hain, M. P., 2012. The Biological Productivity of the Ocean. *Nature Education*, Volume 3(10):21.
255. Silvestri, L. et al., 2020. Maintenance transformation through Industry 4.0 technologies: A systematic literature review. *Computers in Industry*, Volume 123.
256. Simpson, A. R. & Marchi, A., 2013. Evaluating the Approximation of the Affinity Laws and Improving the Efficiency Estimate for Variable Speed Pumps. *Journal of Hydraulic Engineering*, 139(12), pp. 1314-1317.

257. Singh, R., 2014. *Membrane technology and engineering for water purification: application, systems design and operation*. s.l.:Butterworth-Heinemann.
258. SKF, 2010. *SKF bearing maintenance handbook*, Gothenburg, Sweden: SKF Group.
259. Smith, J. et al., 2018. A decade and a half of Pseudo-nitzschia spp. and domoic acid along the coast of southern California. *Harmful Algae*, Volume 79, pp. 87-104.
260. Stoodley, P., Sauer, K., Davies, D. & Costerton, J., 2002. Biofilm as Complex Differentiated Communities. *Annual Review of Microbiology*, 56(1), pp. 187-209.
261. Stover, R. et al., 2017. *Creative Solutions and Innovative Strategies for Today's Water Challenges: Blue Paper*. Miami, Florida, International Desalination Association.
262. Sun, Y. et al., 2022. UAV and IoT-Based Systems for the Monitoring of Industrial Facilities Using Digital Twins: Methodology, Reliability Models, and Application. *Sensors*, 22(17), pp. 1-31.
263. Takabatake, H., Taniguchi, M. & Kurihara, a. M., 2021. Advanced Technologies for Stabilization and High Performance of Seawater RO Membrane Desalination Plants. *Membranes*, 11(2), pp. 138-158.
264. Tao, F., Qi, Q., Wang, L. & Nee, A., 2019. Digital Twins and Cyber-Physical Systems toward Smart Manufacturing and Industry 4.0: Correlation and Comparison. *Engineering*, Volume 5, p. 653–661.
265. Thomas, A. G., 1986. Specific conductance as an indicator of total dissolved solids in cold, dilute waters. *Hydrological Sciences Journal*, 31(1), pp. 81-92.
266. Thornton, S., 2015. *Stephen Thornton*, Stanford, California: Stanford Encyclopedia of Philosophy Archive.
267. Trulear, M. G. & Characklis, W. G., 1982. Dynamics of Biofilm Processes. *Journal WPCF (Water Pollution Control Federation)*, 54(9), pp. 1288-1301.
268. Tuegel, E. J., Ingraffea, A. R., Eason, T. G. & Spottswood, S. M., 2011. *International Journal of Aerospace Engineering*, Volume 2011.
269. UpSkill, 2016. *Programming with MATLAB for Beginners - A Practical Introduction to Programming and Problem Solving*. Kindle Edition ed. s.l.:MathWorks.
270. Utomo, D. S., Onggo, B. S. & Eldridge, S., 2018. Applications of agent-based modelling and simulation in the agri-food supply chains. *European Journal of Operational Research*, Volume 269, p. 794–805.
271. van der Zee, D.-J., 2019. Model simplification in manufacturing simulation – Review and framework. *Computers & Industrial Engineering*, Volume 127, p. 1056–1067.
272. van Noortwijk, J., 2009. A survey of the application of gamma processes in maintenance. *Reliability Engineering and System Safety*, Volume 94, p. 2–21.
273. van Rijn, C., 2007. *Maintenance modeling and applications; lessons learned*. Alghero, Italy, Proceedings of the 32nd ESReDA seminar and 1st ESReDA-ESRA seminar.
274. van Rooij, F. & Scarf, P., 2019. *Towards a maintenance requirements analysis for maximizing production*. Hannover, Germany, European Safety and Reliability Association.
275. van Rooij, F., Scarf, P. & Do, P., 2021. Planning the restoration of membranes in RO desalination using a digital twin. *Desalination*, Volume 519.
276. VanHorenbeek, A. & Pintelon, L., 2013. Development of a maintenance performance measurement framework—using the analytic network process (ANP) for maintenance performance indicator selection. *Omega*, Issue 42, pp. 33-46.

277. Verhulst, E., 2014. Applying systems and safety engineering principles for antifragility. *Procedia Computer Science*, Volume 32, p. 842–849.
278. Villacorte, L. O. et al., 2017. Biofouling in capillary and spiral wound membranes facilitated by marine algal bloom. *Desalination*, Volume 424, p. 74–84.
279. Villacorte, L. O. et al., 2015b. MF/UF rejection and fouling potential of algal organic matter from bloom-forming marine and freshwater algae. *Desalination*, Volume 367, p. 1–10.
280. Villacorte, L. O. et al., 2015a. Seawater reverse osmosis desalination and (harmful) algal blooms. *Desalination*, Volume 360, p. 61–80.
281. Voas, J., Kshetri, N. & DeFranco, J., 2021. Scarcity and Global Insecurity: The Semiconductor Shortage. *IT Professional*, 23(5), pp. 78-82.
282. Voutchkov, N., 2016. *Desalination – Past, Present and Future*. [Online] Available at: <https://iwa-network.org/desalination-past-present-future/>
283. Voutchkov, N., 2017. *Pretreatment for Reverse Osmosis Desalination*. Winter Springs, Florida, United States: Elsevier.
284. Vrouwenvelder, J., Bakker, S., Wessels, L. & van Paassen, J., 2007. The Membrane Fouling Simulator as a new tool for biofouling control of spiral-wound membranes. *Desalination*, Volume 204, p. 170–174.
285. Vu, H. C., Do, P., Barros, A. & Bérenguer, C., 2015. Maintenance planning and dynamic grouping for multi-component systems with positive and negative economic dependencies. *IMA Journal of Management Mathematics*, Volume 26, p. 145–170.
286. Waeyenbergh, G. & Pintelon, L., 2002. A framework for maintenance concept development. *International Journal of Production Economics*, Volume 77, p. 299–313.
287. Waeyenbergh, G. & Pintelon, L., 2009. CIBOCOF: A framework for industrial maintenance concept development. *International Journal of Production Economics*, Volume 121, p. 633–640.
288. Walski, T., Zimmerman, K., Dudinyak, M. & Dileepkumar, P., 2003. *Some Surprises in Estimating the Efficiency Of Variable-Speed Pumps with the Pump Affinity Laws*. Philadelphia, Pennsylvania, US, American Society of Civil Engineers.
289. Wang, L., Chu, J. & Wu, J., 2007. Selection of optimum maintenance strategies based on a fuzzy analytic hierarchy process. *International Journal of Production Economics*, Volume 107, p. 151–163.
290. Wang, R. & Chen, N., 2016. *A survey of condition-based maintenance modeling of multi-component systems*. Bali, Indonesia, IEEE International Conference on Industrial Engineering and Engineering Management (IEEM), pp. 1664-1668.
291. Wenger, M. & Zoitl, A., 2012. *Re-use of IEC 61131-3 Structured Text for IEC 61499*. Athens, Greece, IEEE International Conference on Industrial Technology.
292. Wiles, L. & Peirtsegaale, E., 2018. *Reverse Osmosis: A History and Explanation of the Technology and How It Became So Important for Desalination*. Scottsdale, Arizona, 79th International Water Conference.
293. Wilf, M., 2015. Membrane-Based Desalination Processes: Challenges and Solutions. In: Z. Amjad & K. D. Demadis, eds. *Mineral Scales and Deposits. Scientific and Technological Approaches*. s.l.:Elsevier B.V., pp. 477-497.
294. Wilks, D. & Vannitsem, S., 2018. Uncertain forecasts from deterministic dynamics. In: S. Vannitsem, D. Wilks & J. Messne, eds. *Statistical Postprocessing of Ensemble Forecasts*. s.l.:Elsevier, pp. 1-13.

295. Wolfe, T. D., 2003. *Membrane Process Optimization Technology*, Grass Valley, California: United States Department of the Interior Bureau of Reclamation.
296. Xue, H., Li, Z., Wang, H. & Chen, P., 2014. Intelligent diagnosis method for centrifugal pump system using vibration signal and support vector machine. *Shock and Vibration*, Volume 2014.
297. Xu, J., Huang, E., Chen, C.-H. & Lee, L. H., 2015. Simulation Optimization: A Review and Exploration in the New Era of Cloud Computing and Big Data. *Asia-Pacific Journal of Operational Research*, 32(3).
298. Younos, T., 2005. The Economics of Desalination. *Journal of contemporary water research & education*, Issue 132, pp. 39-45.
299. Zamanillo, M. et al., 2019. Main drivers of transparent exopolymer particle distribution across the surface Atlantic Ocean. *Biogeosciences*, Volume 16, p. 733–749.
300. Zapata-Sierra, A., Cascajares, M., Alcayde, A. & Manzano-Agugliaro, F., 2022. Worldwide research trends on desalination. *Desalination*, Volume 519.
301. Zhang, L., Zhou, L., Ren, L. & Laili, Y., 2019. Modeling and simulation in intelligent manufacturing. *Computers in Industry*, Volume 112.
302. Zhang, W., Zhu, J. & Gao, T., 2016. Integrated Layout and Topology Optimization. In: W. Zhang, J. Zhu & T. Gao, eds. *Topology Optimization in Engineering Structure Design*. s.l.:Elsevier, pp. 159-215.
303. Zhang, X. & Zeng, J., 2017. Joint optimization of condition-based opportunistic maintenance and spare parts provisioning policy in multiunit systems. *European Journal of Operational Research*, Volume 262, p. 479–498.
304. Zhong, R. Y., Xu, X., Klotz, E. & Newman, S. T., 2017. Intelligent Manufacturing in the Context of Industry 4.0: A Review. *Engineering*, Volume 3, p. 616–630.
305. Zhou, C. et al., 2021. Analytics with digital-twinning: A decision support system for maintaining a resilient port. *Decision Support Systems*, 143(113496).
306. Zhou, K., Liu, T. & Zhou, L., 2015. *Industry 4.0: Towards future industrial opportunities and challenges*. Zhangjiajie, China, IEEE, pp. 2147-2152.
307. Zhou, S., McMahon, T., Walton, A. & Lewis, J., 2000. Forecasting daily urban water demand: A case study of Melbourne. *Journal of Hydrology*, Volume 236, p. 153–164.
308. Zhou, T., Droguett, E. L. & Modarres, M., 2020. A common cause failure model for components under age-related degradation. *Reliability Engineering and System Safety*, Volume 195.
309. Zhou, X., Huang, K., Xi, L. & Lee, J., 2015. Preventive maintenance modeling for multi-component systems with considering stochastic failures and disassembly sequence. *Reliability Engineering and System Safety*, Volume 142, p. 231–237.
310. Zhu, Y., 2005. Ensemble Forecast: A New Approach to Uncertainty and Predictability. *Advances in atmospheric sciences*, 22(6), p. 781–788.
311. Žitković, G., 2010. *Introduction to stochastic processes-lecture notes*. Austin, Texas: s.n.
312. Zonta, T. et al., 2020. Predictive maintenance in Industry 4.0: A systematic literature review. *Computers & Industrial Engineering*, 150(106889).

Appendix A Instructions for MATLAB application of the RO train digital twin

The DT of an RO Train is available on request and includes all required data files. The DT is built as an app in MATLAB, and both the shared application running in MATLAB and a stand-alone application are available for researchers who do not have a MATLAB license. The application can be accessed at the link given earlier. Here again is the link:

https://drive.google.com/drive/folders/1eUCKvJkl2rn7Qu_J6kfx-1ikpaW19z-u?usp=sharing.

As mentioned earlier in this thesis, there are two methods to install the RO train DT, running as an app in MATLAB or, if you do not have MATLAB version R2020b, as a stand-alone application.

1. If you have MATLAB R2020b installed on your computer, go to the 'App in MATLAB installation' folder and download the file 'RO_DT_V3.0mlappinstall' in your MATLAB Current Folder. After completing the download, double click on the file that will install the application and the supporting excel files. After installation, you will find the app in your MATLAB Toolstrip (see figure A-1).

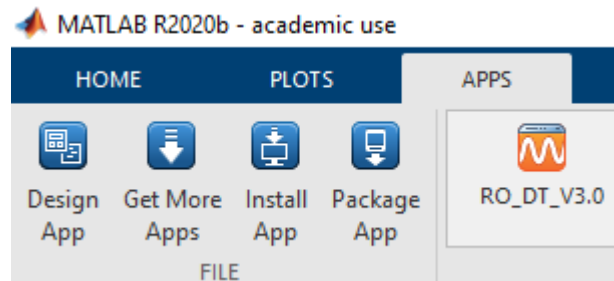


Figure A-1: MATLAB Toolstrip showing the installed RO train DT application

2. If you do not have MATLAB R2020b installed on your computer, you can download the standalone version. Only a standalone version is available for Windows OS. In case you require MAC or Linux, please send an email at f.vanrooij@edu.salford.ac.uk. This standalone MATLAB application requires the runtime module to be downloaded during the installation. You do not need to have the full version of MATLAB. Open the folder 'StandAlone' and copy the file 'MyAppInstaller_web.exe' to your computer. After completing the download, double click on the file 'MyAppInstaller_web.exe' and follow the installation instructions.

The supporting files of the DT are stored at the directory C:\Users\[user name]\AppData\Roaming\MathWorks\MATLAB Add-Ons\Apps\RO_DT_V30. These files

can be separately opened in excel but are required for running the DT application.

After the opening of the application, the dashboard of the Decision Support System (DSS) is loaded. No trains are retrieved yet (see figure A-7). The DSS comprises of a ‘Data Analysis Module’ (see the top left section of the dashboard at figure A-7), the ‘Planning Module’ (see the bottom-left section of the dashboard in figure A-2) and the output of the DT module (see the right section of the dashboard at figure A-2. No trains are retrieved yet.).

At the analysis module α , β and γ are the parameters of the model. $\alpha < 1$ quantifies the variation in biofouling along a vessel due to preferential attachment of biomass to leading elements. K_t is the extrinsic (common cause) wear effect due to the feed water quality on day t . β is the factor determining the decay of the extrinsic wear component. γ adjusts the rate-state of wear interaction due to wear of the trailing elements. Default values are loaded during the startup of the application. Further, tables are shown with records of maintenance history, preservation, and inspection record of the last inspection of biomass at the elements.

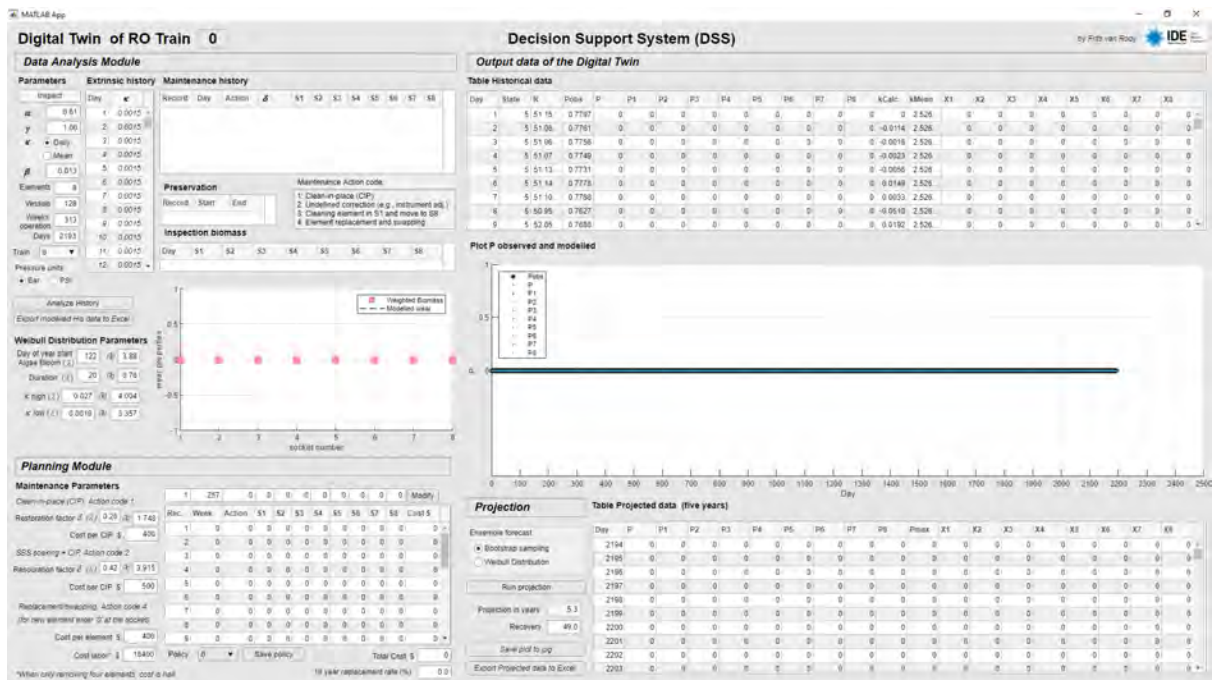


Figure A-2: Decision Support System (DSS) dashboard after the start-up of the application.

The user can select the preference of pressure units, see figure A-3. The default pressure unit is Bar.

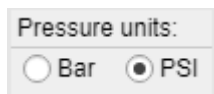


Figure A-3: Selection of preferable pressure units, Bar or PSI.

There are two ways to determine the extrinsic wear component κ over the historical period. Default is the daily calculation that the DT calculates based on the discrete difference of the observed **NPD** over time and the model parameters. The other method is based on the mean κ through change point analysis. This changepoint analysis is performed separately in MATLAB Live Editor and retrieved by the DSS from an excel file. The mean values are given in the table 'Extrinsic History.' The daily method provides a better fit than the mean option. The latter's purpose is mainly to investigate the dependencies, so recommended is using daily κ (see figure A-4).



Figure A-4: Method of determining historical κ .

By selecting a train from the drop-down menu (see figure A-5), the historical data of the train is pulled up from the incorporated excel sheet in discrete daily intervals.



Figure A-5: the selection of train

The provided data consists of five years of operation. This data includes the normalized DP defined as P observed, the train's operational state, and the recovery. After the data has been loaded, the dashboard should look like figure A-6 below.

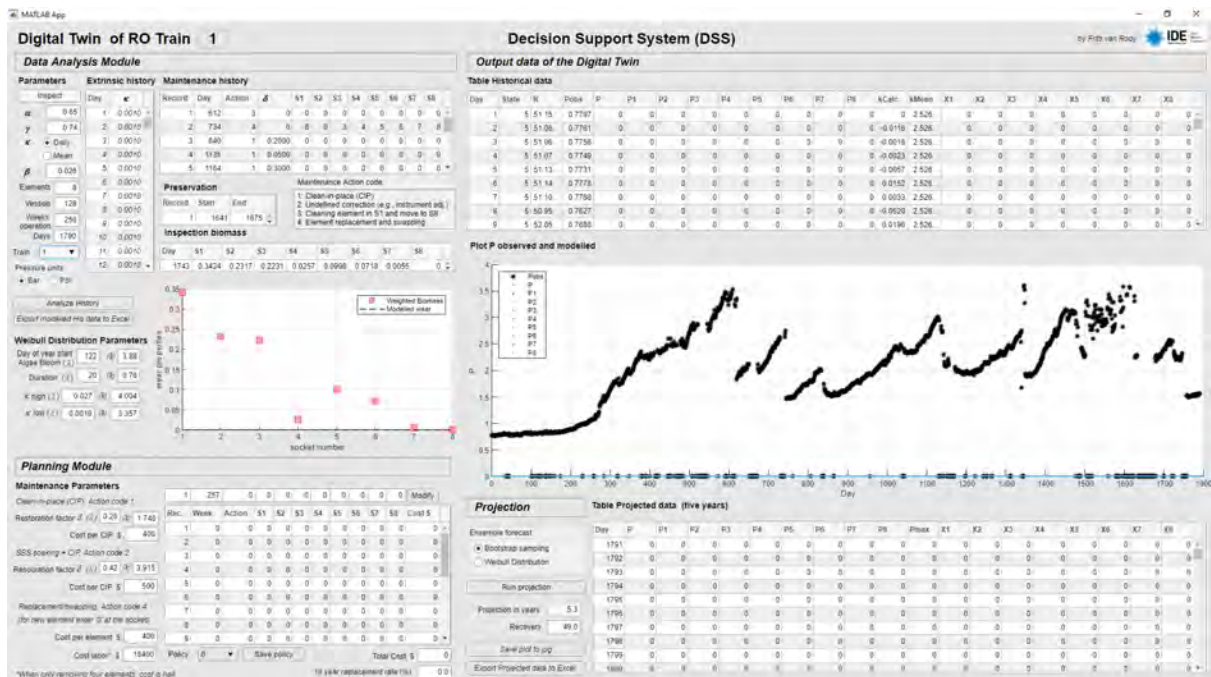


Figure A-6: retrieval of historical data of train 1 over a period of five years.

After pressing the ‘Analyze History’ button, the modelled wear and pressures are computed and shown on the dashboard (see figure A-7).

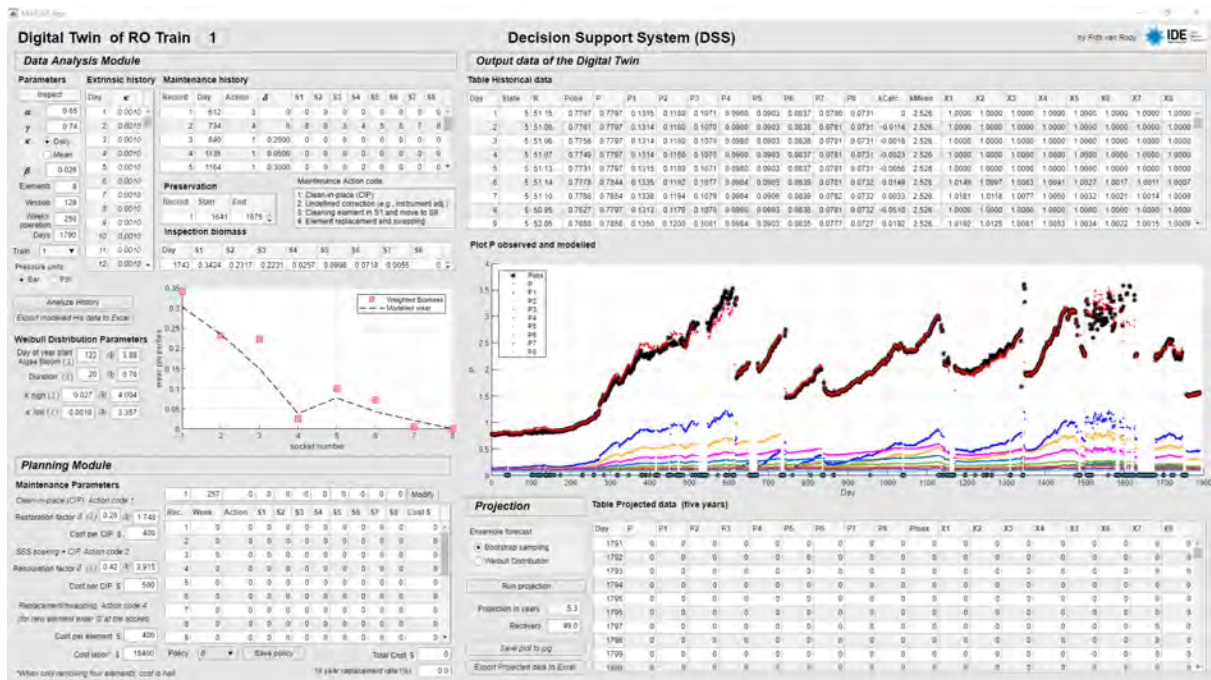


Figure A-7: DT of modelled wear (X), P and daily κ .

The plot at the left shows the distribution of weighted biomass over the elements (red boxes) and the modelled wear distribution at the time of inspection (--- line). The plot at the right gives the observed NPD and the modelled NPD over the historical period. Besides the overall modelled NPD, the modelled NPD of the individual elements is shown. The modelled data over the historical period can be exported by clicking the ‘Export modelled His data to Excel.’ The excel file will be located in the working folder of MATLAB.

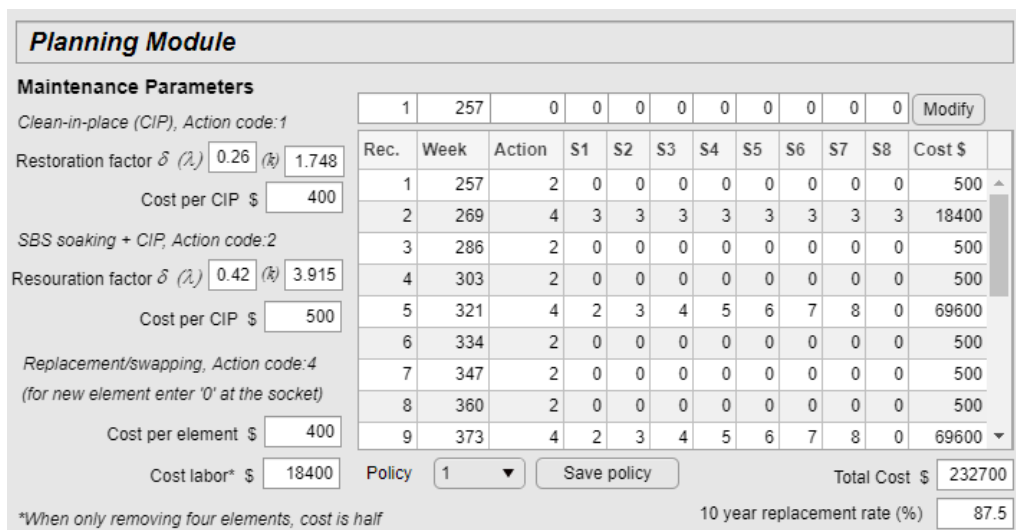


Figure A-8: Maintenance planning module

After the historical data has been analyzed, various maintenance policies can be simulated to determine the most desirable medium-term efficiency. At the planning module on the left side (see figure A-8), the different maintenance actions are listed, where the user can define the cost factor and, in the case of clean-in-place (CIP), the reduction of wear (δ). The restoration factor displayed and accessible for modification applies only for the Weibull distribution sampling. For a detailed explanation, see chapter 7 of the thesis.

There are 12 predefined policies. The policies can be selected from the Policy dropdown menu. The DSS calculates the costs of each maintenance action. Further, the five-year maintenance cost is given below the table, followed by the ten-year element replacement rate.

The table inputs can be modified from the row above the table. One row at a time, each row must be written down to the table by clicking on the ‘Modify’ button. In case of permutations, the previous position of the element must be entered. Whereby 1 is the front element, and 8 is the tail element. In case a new element is loaded into a slot (S), then a zero is entered. After modifying the table, the policy can be saved from the ‘Save policy’ button.

Finally, the policy projection can be generated for the following five years. Factors that determine the projection are the current state of wear of the RO train, the model parameters, and the maintenance policy. The extrinsic (common cause) wear effect κ is unknown and must be forecasted by the DT. There are two methods available to generate the projection, bootstrap sampling or by a Weibull distribution (see figure A-9)

Figure A-9: Projection setup

In the case of projection by bootstrap sampling, κ (feed quality) for each day of the projection is selected at random with replacement from its respective bootstrap sample. That

is, κ for Jan 1st in year 1 of the projection is sampled from the Jan 1st bootstrap sample, and so on throughout year 1, repeating the same for year 2, and so on. Then, clean-in-place is scheduled, and the individual cleaning effects are bootstrapped from the estimated cleaning effects samples for each cleaning method (see section 7.2). Further, element swaps and replacements are scheduled. Their effects are known and deterministic. Finally, the model is executed, obtaining the projected states of each element. The corresponding NPD for the train and at each socket is forecasted for each day of the projection. Besides the degradation parameters and the imperfect restoration parameter, the projection further requires system recovery R , which in turn implies the hydraulic effect of the socket position ω_i to calculate the modelled P. For details on the socket pressure distribution parameter ω_i , see chapter 6. Projections are repeated 100 times to obtain the ensemble forecast (grey ribbon in figure A-13) and the ensemble mean (red pen).

In the case of projection involving a Weibull distribution, κ (feed quality) for each day of the projection is randomly selected by a Weibull distribution. From the Weibull distribution parameters defined at the DSS (see figure A-8), the start day of the year and the duration of days of the algae bloom are forecasted using a random Weibull distribution. This defines the period where $\kappa_t = \kappa_2$ or $\kappa_t = (\kappa_2 - \kappa_1)e^{-\beta\tau}$ is utilized for κ . After this, A Weibull Distribution is applied to generate the daily random severity of the extrinsic wear dependency κ_t , based on the Weibull parameters for κ_1 and κ_2 . We model the daily wear over the projected period applying the selected maintenance policy (see chapter 8). In the case of a CIP, a random Weibull distribution is applied of δ per intervention, with $\delta \sim N(\delta_1, \lambda_1)$ for C1 and $\delta \sim N(\delta_2, \lambda_2)$ for C2. Finally, the daily NPD per socket is calculated and the vessel NPD.

The ensemble forecast method is widely utilized in weather forecasting. To generate the projection, click on the ‘Projection’ button. Due to the number of computations, running the ensemble forecast has some delay depending on the power of the user PC. It takes about 1½ minutes on an i7-3770 CPU @ 3.40GHz (16 GB RAM) Desktop and nearly 3½ minutes on a Celeron N4100 CPU @ 1.10 GHz (8 GB RAM) PC. During the projection computation, a progress indicator is shown to inform the user of the status (see figure A-12).

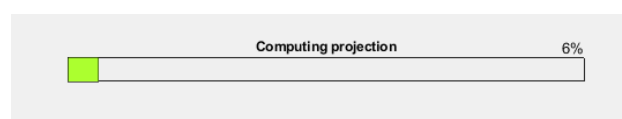


Figure A-10. Progress indicator during computation of the projection.

After finalizing the computation, the dashboard looks like that of figure A-13.

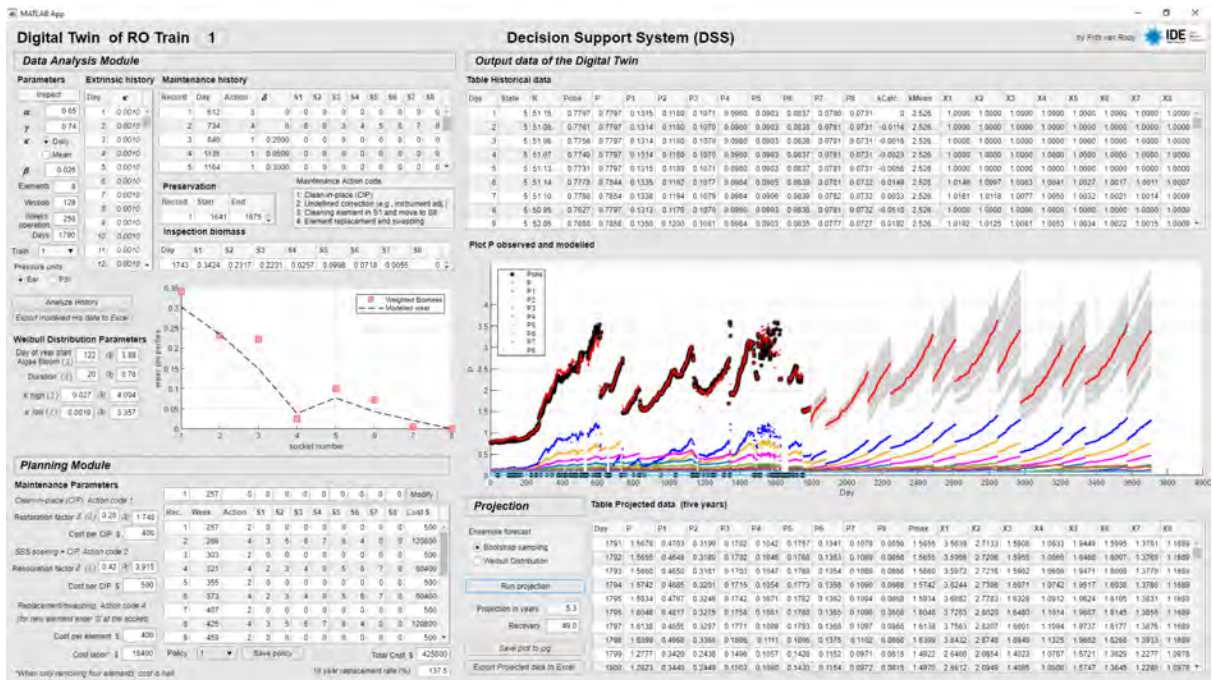



Figure A-11. Decision Support System (DSS) dashboard after finalizing a projection.

Appendix B CMMS work order examples

B.1 membrane replacement




IDE
Americas, Inc.

Your
Water
Partners

Work Order 44308
 Carlsbad Desalination Plant
 Closed
 Printed 11/3/2021 - 9:36 AM (Duplicate Copy)

Maintenance Details

| | | |
|--|---|-----------------------------|
| Requested By: Hernandez, Joe on 4/22/2021 10:36:00 AM | Target: 4/26/2021 | Carlsbad Desalination Plant |
| Phone: | Priority/Type: 2 - Normal / Preventive | RO Building |
| Email: | Supervisor: Papachristoforou, Dimitris | Area 500 RO Trains |
| Taken By: Hernandez, Joe | Shop: CDP-ME | RO Train 14 (RO 14) |
| Problem: No Problem (NO PROBLEM) | | Model: |
| Last PM: 5/14/2021 | | Serial: |
| Reason: Membrane exchange/rotation on RO Train 14 (RO 14) | | Manufacturer: |
| | | Vicinity: |



Special Instructions:

If unable to physically accomplish Assigned Tasks, notify your Supervisor immediately

Reference LOTO Procedure steps attached (if required/needed)

Shutdown
 Lockout
 Attach

Tasks

| # | Description | Rating | Meas. | Initials | Failed | N/A | Complete |
|------------------------------|--|--------|-------|----------|--------------------------|--------------------------|-------------------------------------|
| Before starting work | | | | | | | |
| 20 | Inform Operations of work being conducted | | | | <input type="checkbox"/> | <input type="checkbox"/> | <input checked="" type="checkbox"/> |
| 30 | Ensure appropriate PPE is being used for assigned Tasks | | | | <input type="checkbox"/> | <input type="checkbox"/> | <input checked="" type="checkbox"/> |
| 40 | Complete JHA if required | | | | <input type="checkbox"/> | <input type="checkbox"/> | <input checked="" type="checkbox"/> |
| 50 | Complete LOTO if required | | | | <input type="checkbox"/> | <input type="checkbox"/> | <input checked="" type="checkbox"/> |
| After completing work | | | | | | | |
| 70 | Remove all tools used when complete | | | | <input type="checkbox"/> | <input type="checkbox"/> | <input checked="" type="checkbox"/> |
| 80 | Clean Up the Area | | | | <input type="checkbox"/> | <input type="checkbox"/> | <input checked="" type="checkbox"/> |
| 90 | Run Systems check for work conducted, before returning to operations | | | | <input type="checkbox"/> | <input type="checkbox"/> | <input checked="" type="checkbox"/> |
| 100 | Return all equipment to Operations | | | | <input type="checkbox"/> | <input type="checkbox"/> | <input checked="" type="checkbox"/> |
| 110 | Return all tools used to Maintenance | | | | <input type="checkbox"/> | <input type="checkbox"/> | <input checked="" type="checkbox"/> |
| | | | | | <input type="checkbox"/> | <input type="checkbox"/> | <input type="checkbox"/> |

Labor

| Labor | Assigned | Work Date | Start | End | Reg Hrs | OT Hrs | Other Hrs |
|---------------|----------------|-----------|-------|-----|---------|--------|-----------|
| Rivera, David | 4/26/2021 / 10 | | | | | | |

Parts/Tools

| Item | Location | Est Qty | Actual Qty |
|------|----------|---------|------------|
| | | | |
| | | | |
| | | | |

Documents

| ID | Document Name | Type | Location |
|-------|--------------------------------------|------------------------|----------------------|
| 203 | S-05119.docx | Informational Document | View |
| 204 | S-05119.pdf | Informational Document | View |
| 21264 | Train 14 LOTO.pdf | Informational Document | View |
| 22089 | Job Hazards Assessment.pdf | Informational Document | View |
| 22090 | LOTO Train_Membrane_Replacement.docx | Informational Document | View |
| 22091 | LOTO Train_Membrane_Replacement.xlsx | Informational Document | View |
| 22092 | Train 14 (4_26_21).xlsx | Informational Document | View |
| 22866 | JHA_44308.pdf | Informational Document | View |
| 22867 | LOTO_44308.pdf | Informational Document | View |

Labor Report

Completed: _____ Failure: _____

Report:

| | | | |
|------------------|------|------------------|------|
| Signature / Name | Date | Signature / Name | Date |
|------------------|------|------------------|------|

B.1.1 Attachment 1: Standard Operating Procedure (SOP)



Carlsbad Desalination Plant



| | | | |
|-----------------|----------------------|-----------------------|--|
| Section: | MAINTANACE PROCEDURE | Procedure No.: | CDP-03-500-04 |
| Area: | 500 – RO | Title: | Membranes rotation and replacement procedure |
| Rev | Approval Date | Effective Date | Page |
| 00 | 11/01/2017 | 11/01/2017 | Page 1 of 8 |

1. Purpose

This procedure is intended to describe step-by-step actions that must be taken when the RO membranes going through replacement and/or rotation.

2. Procedure

1. Clean the work area around the RO train which will receive rotation and/or replacement of membranes.
2. Prepare wood pallets covered with nylon above to be utilized for membranes temporary storage while R&R is programmed. Spray alcohol over the nylon.



Figure 1: Wood pallets covered with nylon

| | | |
|----------------|----------------|-----------------|
| Revised | Checked | Approved |
| Y. Pinhas | Dean Rauscher | D. Moxey |

t: +1-619-487-0760 | f: +1-619-487-0759 | www.ide-tech.com |
5050 Avenida Encinas, Suite 250, Carlsbad, CA 92008





Carlsbad Desalination Plant



| | | | |
|-----------------|-----------------------------|-----------------------|---|
| Section: | MAINTANACE PROCEDURE | Procedure No.: | CDP-03-500-04 |
| Area: | 500 – RO | Title: | Membranes rotation and replacement procedure |
| Rev | Approval Date | Effective Date | Page |
| 00 | 11/01/2017 | 11/01/2017 | Page 2 of 8 |

3. All worker need to cover their hands with gloves and disinfect them with alcohol solution. The disinfection with alcohol must be done periodically or every time new set of gloves are worn.
4. Open all end cups from both sides (front and rear).
5. Start cleaning the end cups with permeate water. During the cleaning checking the seals and O-rings. Lubricate the seals with Molykote.



Figure 2: Cleaning and storage od the end cups

6. Check end adaptor and replace the two O- rings and lubricate them with Molykote.
7. If new membrane expected to installed, prepare the new membrane prior to further steps
 - a. Take membranes out of the box without opening the nylon bag
 - b. Place the membranes in vertical position.

| | | |
|----------------|----------------|-----------------|
| Revised | Checked | Approved |
| Y. Pinhas | Dean Rauscher | D. Moxey |

T: +1-619-487-0760 | F: +1-619-487-0759 | www.ide-tech.com |
 5050 Avenida Encinas, Suite 250, Carlsbad, CA 92008





Carlsbad Desalination Plant



| | | | |
|-----------------|-----------------------------|-----------------------|---|
| Section: | MAINTANACE PROCEDURE | Procedure No.: | CDP-03-500-04 |
| Area: | 500 – RO | Title: | Membranes rotation and replacement procedure |
| Rev | Approval Date | Effective Date | Page |
| 00 | 11/01/2017 | 11/01/2017 | Page 3 of 8 |



Figure 3: New element prepared in advance in vertical position in their original plastic bags

8. Receive instructions from Supervisor/Process Engineer what is the rotation configuration or replacement required.

9. Prepare for rotation the utilized membranes.
 Example:
 For rotation of element at last position (position 8): Take out from the rear side the membranes no.8 and remove them manually towards the prepared cleaned and covered pallets.

| | | |
|----------------|----------------|-----------------|
| Revised | Checked | Approved |
| Y. Pinhas | Dean Rauscher | D. Moxey |

t: +1-619-487-0760 | f: +1-619-487-0759 | www.ide-tech.com |
 5050 Avenida Encinas, Suite 250, Carlsbad, CA 92008





Carlsbad Desalination Plant



| | | | |
|-----------------|-----------------------------|-----------------------|---|
| Section: | MAINTANACE PROCEDURE | Procedure No.: | CDP-03-500-04 |
| Area: | 500 – RO | Title: | Membranes rotation and replacement procedure |
| Rev | Approval Date | Effective Date | Page |
| 00 | 11/01/2017 | 11/01/2017 | Page 4 of 8 |



Figure 4: Wood pallet covered with nylon with membranes

10. Never step on the pallet with membranes

| | | |
|----------------|----------------|-----------------|
| Revised | Checked | Approved |
| Y. Pinhas | Dean Rauscher | D. Moxey |

t: +1-619-487-0760 | f: +1-619-487-0759 | www.ide-tech.com |
 5050 Avenida Encinas, Suite 250, Carlsbad, CA 92008





Carlsbad Desalination Plant



| | | | |
|-----------------|-----------------------------|-----------------------|---|
| Section: | MAINTANACE PROCEDURE | Procedure No.: | CDP-03-500-04 |
| Area: | 500 – RO | Title: | Membranes rotation and replacement procedure |
| Rev | Approval Date | Effective Date | Page |
| 00 | 11/01/2017 | 11/01/2017 | Page 5 of 8 |

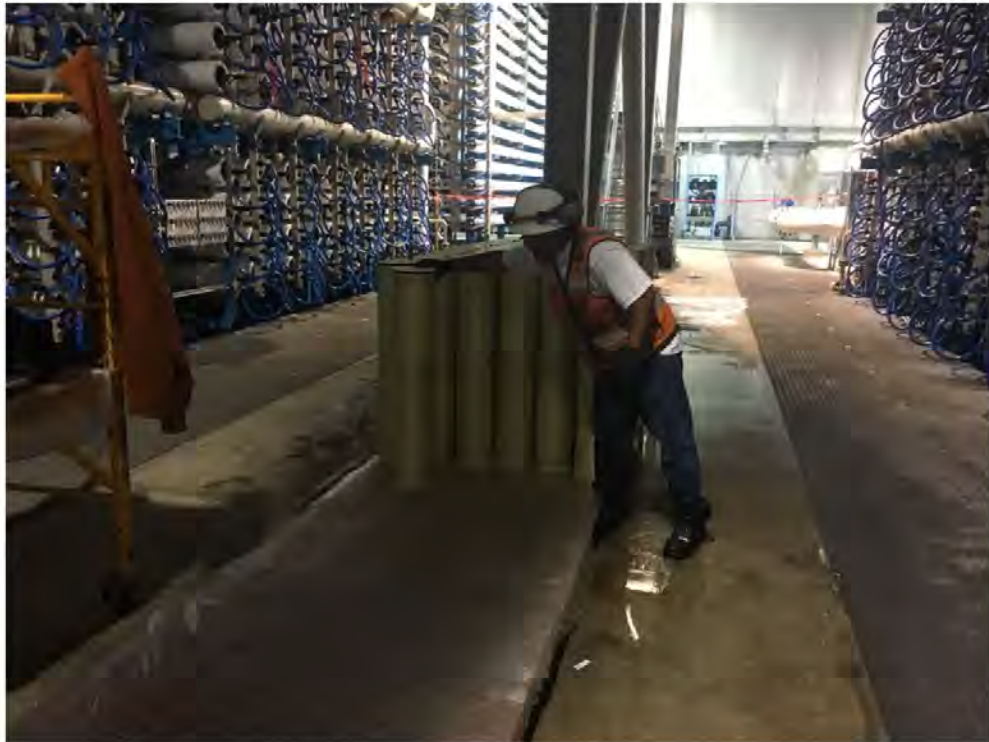


Figure 5: Storing the membranes on wood pallet without stepping on the pallet

11. If new elements are installed on the rear/front side of the train (according to the instructions of Supervisor/Process Engineer), the installation must be done without touching the membrane, only by pushing through the nylon bag, after cutting the end of the nylon bag.

| | | |
|----------------|----------------|-----------------|
| Revised | Checked | Approved |
| Y. Pinhas | Dean Rauscher | D. Moxey |

t: +1-619-487-0760 | f: +1-619-487-0759 | www.ide-tech.com |
 5050 Avenida Encinas, Suite 250, Carlsbad, CA 92008





Carlsbad Desalination Plant



| | | | |
|-----------------|-----------------------------|-----------------------|---|
| Section: | MAINTANACE PROCEDURE | Procedure No.: | CDP-03-500-04 |
| Area: | 500 – RO | Title: | Membranes rotation and replacement procedure |
| Rev | Approval Date | Effective Date | Page |
| 00 | 11/01/2017 | 11/01/2017 | Page 6 of 8 |



Figure 6: Loading new element without touching membrane itself

12. Close the end cups on the rear side.
13. Remove membrane no. 1+2 at front side (if required)
14. Separate them on 2 different pallets.
15. Prepare those membranes as per Supervisor/ Process Engineer instructions either for rotation or disposal.

| | | |
|----------------|----------------|-----------------|
| Revised | Checked | Approved |
| Y. Pinhas | Dean Rauscher | D. Moxey |

t: +1-619-487-0760 | f: +1-619-487-0759 | www.ide-tech.com |
 5050 Avenida Encinas, Suite 250, Carlsbad, CA 92008





Carlsbad Desalination Plant



| | | | |
|-----------------|-----------------------------|-----------------------|---|
| Section: | MAINTANACE PROCEDURE | Procedure No.: | CDP-03-500-04 |
| Area: | 500 – RO | Title: | Membranes rotation and replacement procedure |
| Rev | Approval Date | Effective Date | Page |
| 00 | 11/01/2017 | 11/01/2017 | Page 7 of 8 |

Example:

1st position element – disposed of site.

2nd position element –visual check and weighting all the membranes for further Process Engineer decision.



Figure 7: Pallet with membrane which need to be disposed.

16. Continue as per provided configuration.

Example:

Install a new membrane instead of membrane on second position

Install 8th element instead of 1st element

| | | |
|----------------|----------------|-----------------|
| Revised | Checked | Approved |
| Y. Pinhas | Dean Rauscher | D. Moxey |

t: +1-619-487-0760 | f: +1-619-487-0759 | www.ide-tech.com |
5050 Avenida Encinas, Suite 250, Carlsbad, CA 92008





Carlsbad Desalination Plant



| | | | |
|-----------------|-----------------------------|-----------------------|---|
| Section: | MAINTANACE PROCEDURE | Procedure No.: | CDP-03-500-04 |
| Area: | 500 – RO | Title: | Membranes rotation and replacement procedure |
| Rev | Approval Date | Effective Date | Page |
| 00 | 11/01/2017 | 11/01/2017 | Page 8 of 8 |

17. Continue with proper shimming (as per pressure vessel manufacturer instructions according to Operation Manual) and close the end cups on the front side (after visual inspection and changing the 2 O-rings and lubrication with Molikote.)

3. Responsibilities

- Process Engineer to provide membranes rotation and replacement plan.
- Process Engineer to decide the order of trains which will go for replacement.
- Maintenance Manager/Supervisor responsible to verify that the R&R done according to the plan and the pressure vessels are sealed according to manufacturer requirement after membranes R&R.

4. Records

- Each new membrane which will be loaded to the train must be scanned
- Excel file with the scanned membranes need to be provided to Maintenance manager
- If any element changed position in the train, this element need to be scanned and membrane position need to be updated in excel file.

5. Appendix

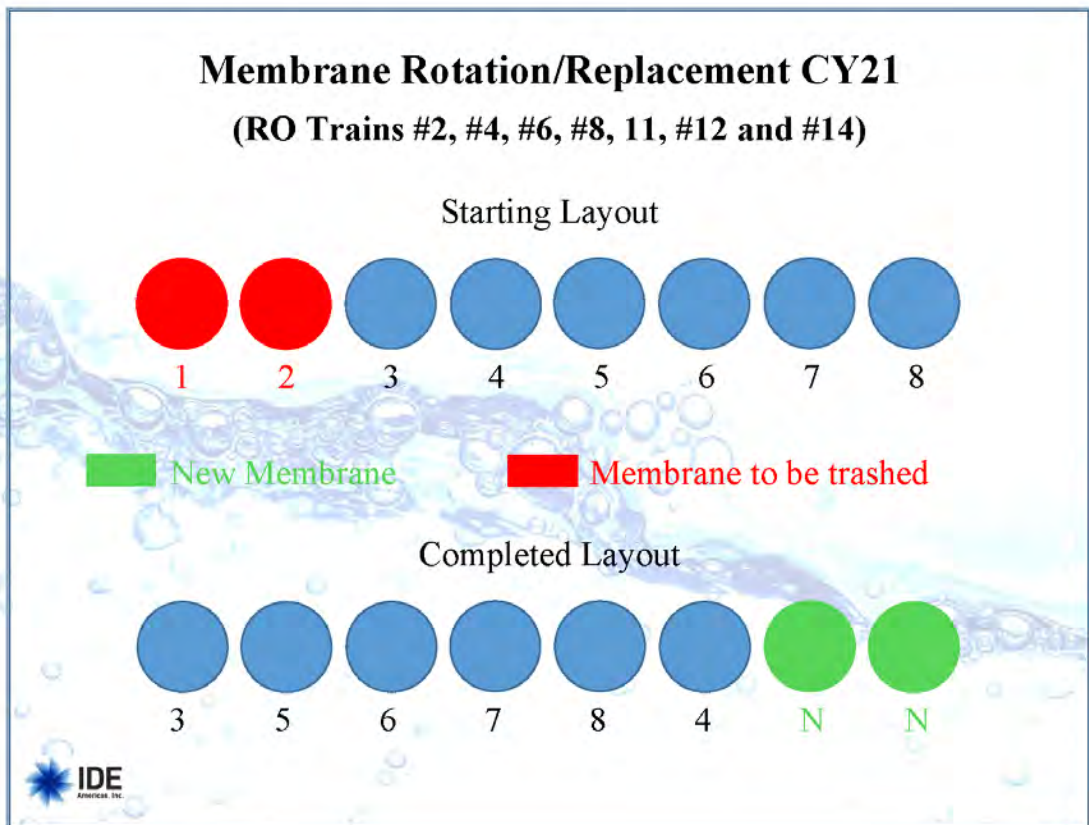
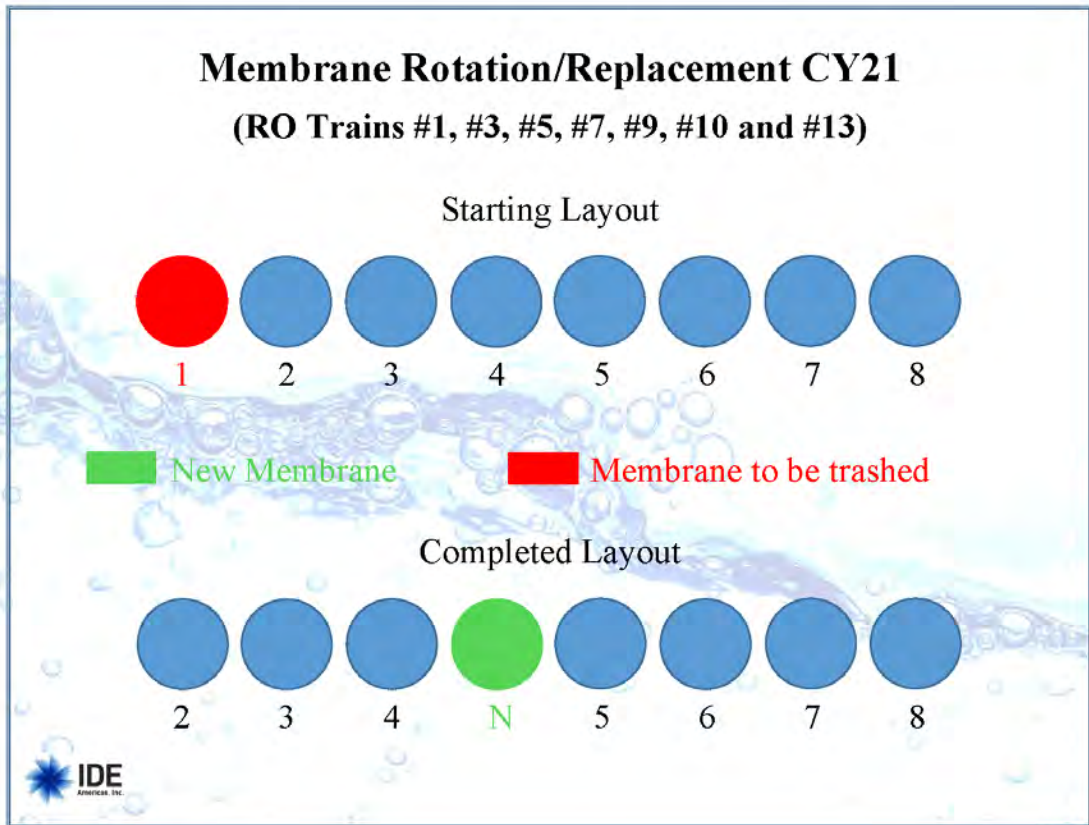
Not applicable.

| | | |
|----------------|----------------|-----------------|
| Revised | Checked | Approved |
| Y. Pinhas | Dean Rauscher | D. Moxey |


t: +1-619-487-0760 | f: +1-619-487-0759 | www.ide-tech.com |
5050 Avenida Encinas, Suite 250, Carlsbad, CA 92008



B.1.2 Attachment 2: Plan of elements permutations



B.2 CMMS work order example CIP SBS socking







IDE
Americas, Inc.

Your
Water
Partners

Work Order 23599
Carlsbad Desalination Plant
Closed
Printed 11/3/2021 - 9:58 AM (Duplicate Copy)

Maintenance Details


| | | |
|--|--|--|
| <p>Requested By: Hernandez, Joe on 4/29/2019 10:52:00 AM</p> <p>Phone: (434) 228-9103</p> <p>Email:</p> <p>Taken By:</p> <p>Problem: No Problem (NO PROBLEM)</p> <p>Last PM: 2/1/2019</p> <p>Project: CIP ON TRAINS (P-CDP-3)</p> | <p>Target: 5/6/2019</p> <p>Priority/Type: 2 - Normal / Preventive</p> <p>Supervisor: Beck, Ian</p> <p>Shop: CDP-OP</p> | <p> Carlsbad Desalination Plant</p> <p> RO Building</p> <p> Area 500 RO Trains</p> <p> RO Train 4 (RO 4)</p> |
|--|--|--|

Model:

Serial:

Manufacturer:

Vicinity:



Reason: Conduct CIP (SBS) on RO Train 4 (RO 4)

Special Instructions:

If unable to physically accomplish Assigned Tasks, notify your Supervisor Immediately

Reference LOTO Procedure steps attached (if required/needed)

Shutdown Attach

Tasks

| # | Description | Rating | Meas. | Initials | Failed | N/A | Complete |
|------------------------------|---|--------|-------|----------|--------------------------|--------------------------|-------------------------------------|
| 0 | RO Train 4 [RO 4] Asset | | | NL | <input type="checkbox"/> | <input type="checkbox"/> | <input checked="" type="checkbox"/> |
| Before starting work | | | | | | | |
| 20 | Inform Operations of work being conducted | | | NL | <input type="checkbox"/> | <input type="checkbox"/> | <input checked="" type="checkbox"/> |
| 30 | Ensure appropriate PPE is being used for assigned Tasks | | | NL | <input type="checkbox"/> | <input type="checkbox"/> | <input checked="" type="checkbox"/> |
| 40 | Complete JHA if required | | | NL | <input type="checkbox"/> | <input type="checkbox"/> | <input checked="" type="checkbox"/> |
| 50 | Complete LOTO if required | | | NL | <input type="checkbox"/> | <input type="checkbox"/> | <input checked="" type="checkbox"/> |
| After completing work | | | | | | | |
| 70 | Remove all tools used when complete | | | NL | <input type="checkbox"/> | <input type="checkbox"/> | <input checked="" type="checkbox"/> |
| 80 | Clean Up the Area | | | NL | <input type="checkbox"/> | <input type="checkbox"/> | <input checked="" type="checkbox"/> |
| 90 | Return all equipment to Operations | | | NL | <input type="checkbox"/> | <input type="checkbox"/> | <input checked="" type="checkbox"/> |
| 100 | Return all tools used to Maintenance | | | NL | <input type="checkbox"/> | <input type="checkbox"/> | <input checked="" type="checkbox"/> |

Labor

| Labor | Work Date | Start | End | Reg Hrs | OT Hrs | Other Hrs |
|----------------|-----------|-------|-----|---------|--------|-----------|
| Leso, Nicholas | 5/10/2019 | | | 2 | 0 | 0 |

Labor Report

Completed: 5/10/2019 1:31:00 PM Failure: N/A / N/A

Report: 5/5/2019 PS DM JR / JA SH DB
5/6/2019 PS DM JR NL / JM PH NV
5/7/2019 AL NL DBM / JM PH NV
5/8/2019 AL NL DBM
Work Order completed as requested.


Signature / Name

Date

Signature / Name

Date

B.3 CMMS work order example High and Low CIP







IDE
Americas, Inc.

Your
Water
Partners

Work Order 23601
Carlsbad Desalination Plant
Closed
Printed 11/3/2021 - 9:57 AM (Duplicate Copy)

Maintenance Details


| | | |
|---|--|--|
| <p>Requested By: Hernandez, Joe on 4/29/2019 12:50:00 PM</p> <p>Phone: (434) 228-9103</p> <p>Email:</p> <p>Taken By:</p> <p>Problem: No Problem (NO PROBLEM)</p> <p>Last PM: 5/10/2019</p> <p>Project: CIP ON TRAINS (P-CDP-3)</p> | <p>Target: 5/6/2019</p> <p>Priority/Type: 2 - Normal / Preventive</p> <p>Supervisor: Beck, Ian</p> <p>Shop: CDP-OP</p> | <p> Carlsbad Desalination Plant</p> <p> RO Building</p> <p> Area 500 RO Trains</p> <p> RO Train 4 (RO 4)</p> |
|---|--|--|

Model:

Serial:

Manufacturer:

Vicinity:



Reason: Conduct CIP (High/Low) on RO Train-4 (RO 4)

Special Instructions:

If unable to physically accomplish Assigned Tasks, notify your Supervisor immediately.

Reference LOTO Procedure steps attached (if required/needed)

Shutdown Attach

Tasks

| # | Description | Rating | Meas. | Initials | Failed | N/A | Complete |
|------------------------------|---|--------|-------|----------|--------------------------|--------------------------|-------------------------------------|
| 0 | RO Train 4 [RO 4] Asset | | | NL | <input type="checkbox"/> | <input type="checkbox"/> | <input checked="" type="checkbox"/> |
| Before starting work | | | | | | | |
| 20 | Inform Operations of work being conducted | | | NL | <input type="checkbox"/> | <input type="checkbox"/> | <input checked="" type="checkbox"/> |
| 30 | Ensure appropriate PPE is being used for assigned Tasks | | | NL | <input type="checkbox"/> | <input type="checkbox"/> | <input checked="" type="checkbox"/> |
| 40 | Complete JHA if required | | | NL | <input type="checkbox"/> | <input type="checkbox"/> | <input checked="" type="checkbox"/> |
| 50 | Complete LOTO if required | | | NL | <input type="checkbox"/> | <input type="checkbox"/> | <input checked="" type="checkbox"/> |
| After completing work | | | | | | | |
| 70 | Remove all tools used when complete | | | NL | <input type="checkbox"/> | <input type="checkbox"/> | <input checked="" type="checkbox"/> |
| 80 | Clean Up the Area | | | NL | <input type="checkbox"/> | <input type="checkbox"/> | <input checked="" type="checkbox"/> |
| 90 | Return all equipment to Operations | | | NL | <input type="checkbox"/> | <input type="checkbox"/> | <input checked="" type="checkbox"/> |
| 100 | Return all tools used to Maintenance | | | NL | <input type="checkbox"/> | <input type="checkbox"/> | <input checked="" type="checkbox"/> |

Labor

| Labor | Work Date | Start | End | Reg Hrs | OT Hrs | Other Hrs |
|-------------------|-----------|-------|-----|---------|--------|-----------|
| Anderson, Joseph | 5/9/2019 | | | 8 | 0 | 0 |
| Bowler, David | 5/9/2019 | | | 8 | 0 | 0 |
| Hernandez, Sergio | 5/9/2019 | | | 8 | 0 | 0 |
| Anderson, Joseph | 5/10/2019 | | | 8 | 0 | 0 |
| Bowler, David | 5/10/2019 | | | 8 | 0 | 0 |
| Hernandez, Sergio | 5/10/2019 | | | 8 | 0 | 0 |
| Leso, Nicholas | 5/10/2019 | | | 8 | 0 | 0 |
| Lewis, Awni | 5/10/2019 | | | 8 | 0 | 0 |
| Mercado, Daniel | 5/10/2019 | | | 8 | 0 | 0 |

| | | | | |
|------------------|-----------|----|---|---|
| Leso, Nicholas | 5/11/2019 | 8 | 0 | 0 |
| Marler, Dan | 5/11/2019 | 8 | 0 | 0 |
| Rebolledo, Julio | 5/11/2019 | 81 | 0 | 0 |
| Sabadin, Paul | 5/11/2019 | 8 | 0 | 0 |
| Marler, Dan | 5/12/2019 | 8 | 0 | 0 |
| Rebolledo, Julio | 5/12/2019 | 8 | 0 | 0 |
| Sabadin, Paul | 5/12/2019 | 8 | 0 | 0 |
| Leso, Nicholas | 5/16/2019 | 2 | 0 | 0 |

Labor Report

5/16/2019
Completed: 2:34:00 PM **Failure:** N/A / N/A

Report: 5/9 JA SH DB
5/10 AL NL DBM / JA SH DB
5/11 PS DM JR NL
5/12 PS DM JR
Work Order completed as requested. (Released/Received by Operations during all tasks)

Signature / Name Date Signature / Name Date

Appendix C Additional projections with Bootstrapping

Additional Digital Twin (DT) output projections are given for train 11, covering the 12 policies with first Bootstrap sampling with smoothening -1,+4, followed by smoothening -2,+8. Due to the amount of data, the trends of the projections of only train 11 are given. However, the rends of the other trains are available on request.

C.1 Projection with bootstrap sampling with smoothening -1,+4

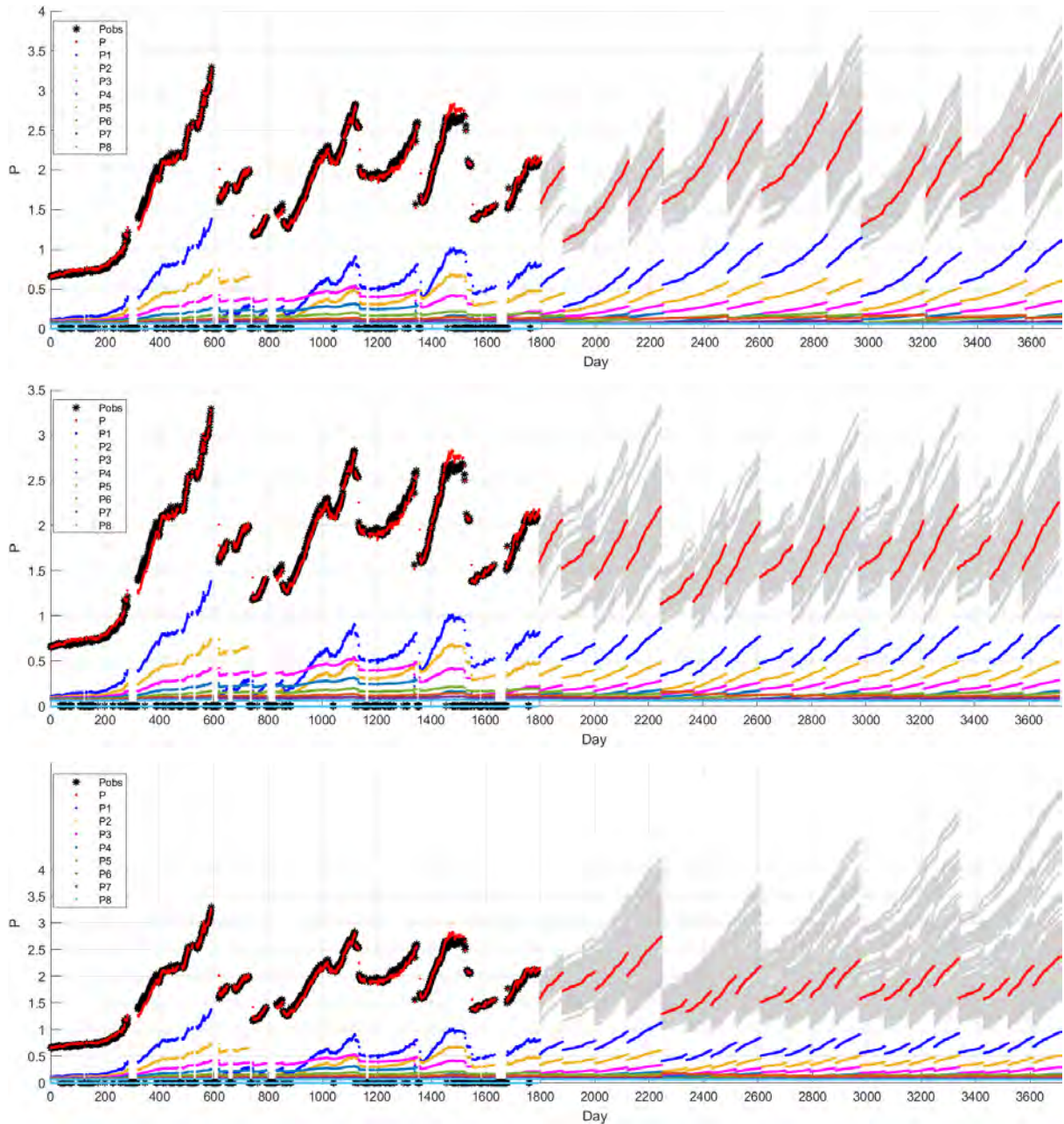


Figure C-1: Bootstrap with smoothening -1,+4, Train 11 for policy 1, (top) to policy 3 (bottom).

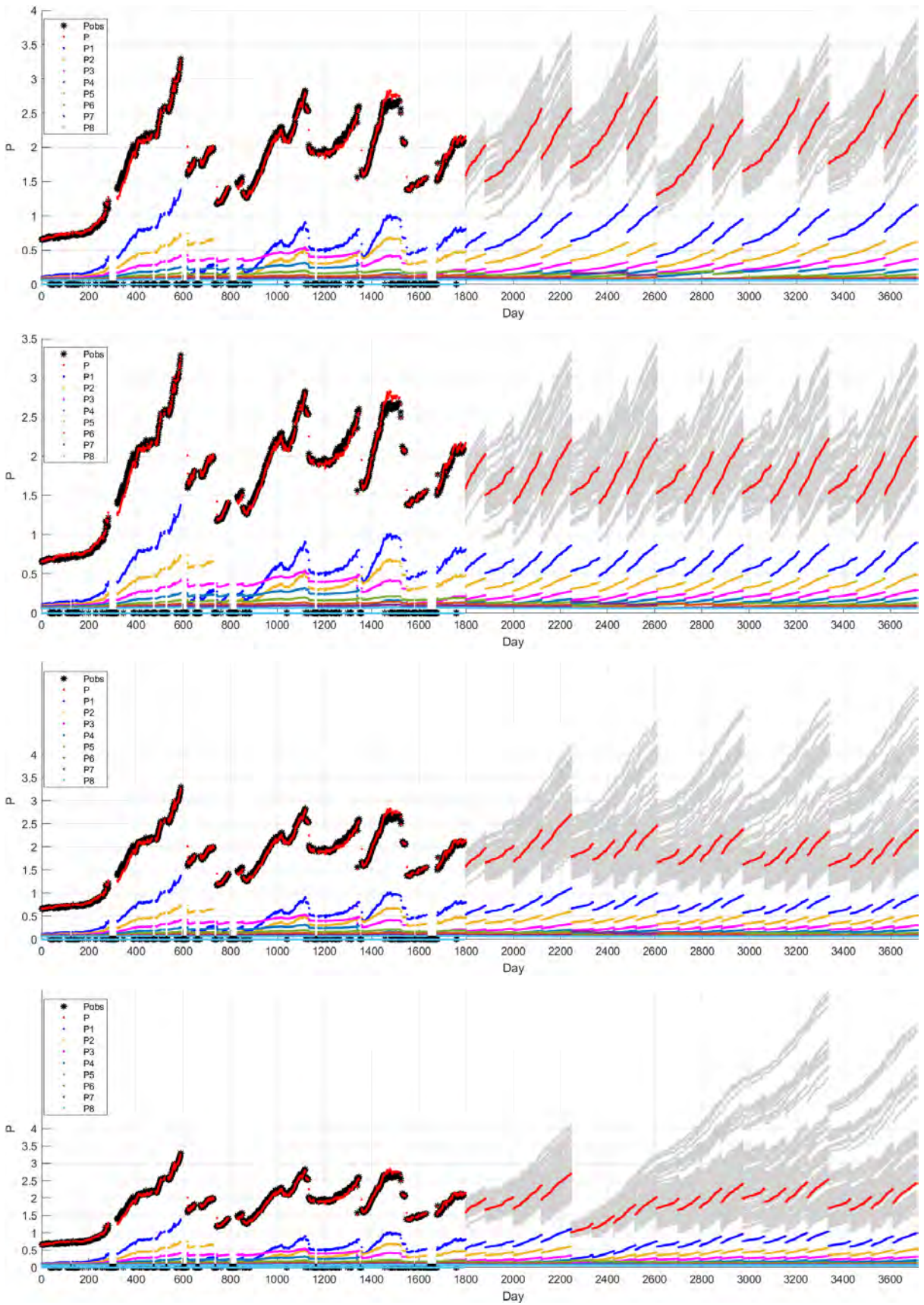


Figure C-2: Bootstrap with smoothening -1,+4, Train 11 for policy 4, (top) to policy 7 (bottom).

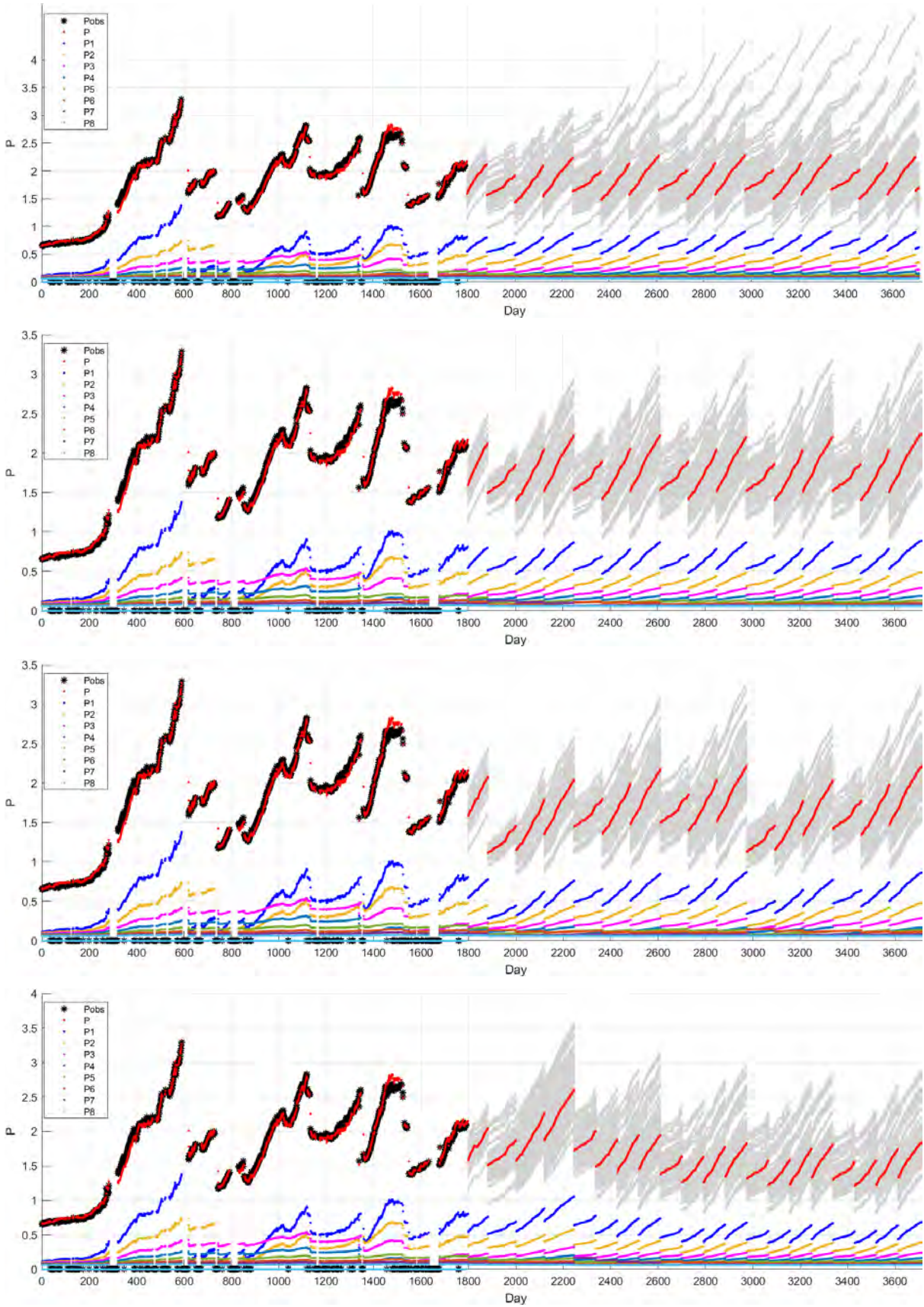


Figure C-3: Bootstrap with smoothing -1,+4, Train 11 for policy 8, (top) to policy 11 (bottom).

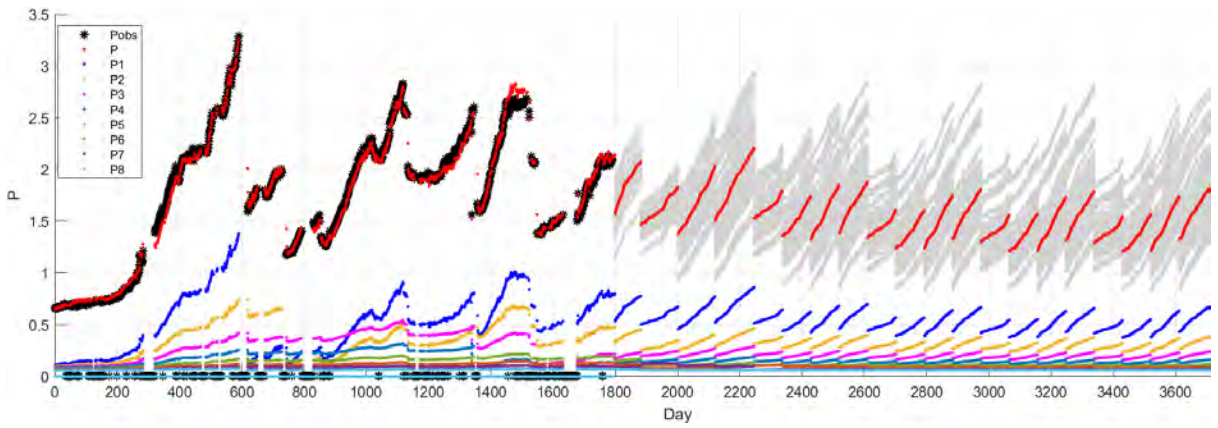


Figure C-4: Bootstrap with smoothing -1,+4, Train 11 for policy 12.

C.2 Projection with bootstrap sampling with smoothing -2,+8

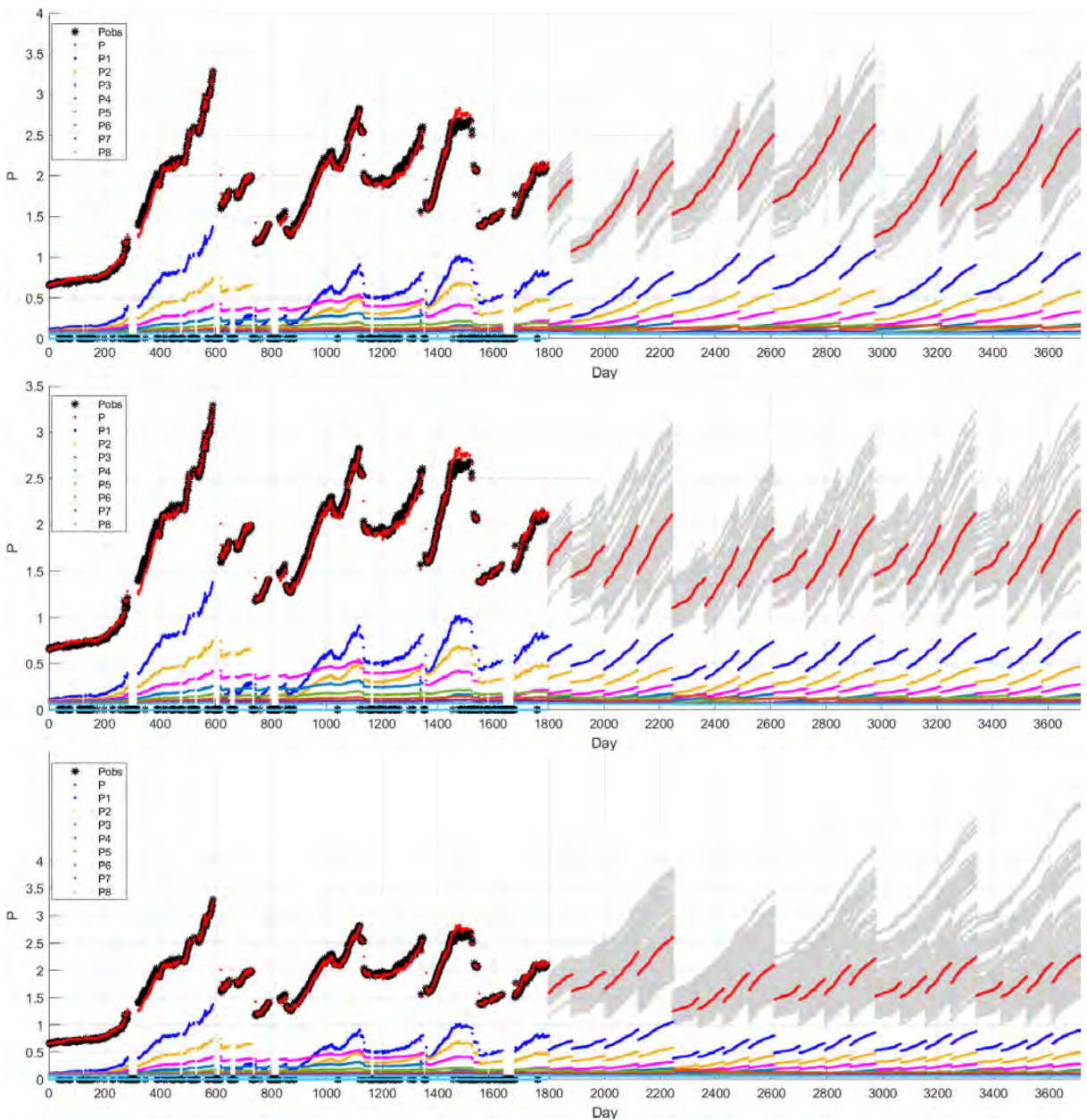


Figure C-5: Bootstrap with smoothing -2,+8, Train 11 for policy 1, (top) to policy 3 (bottom).

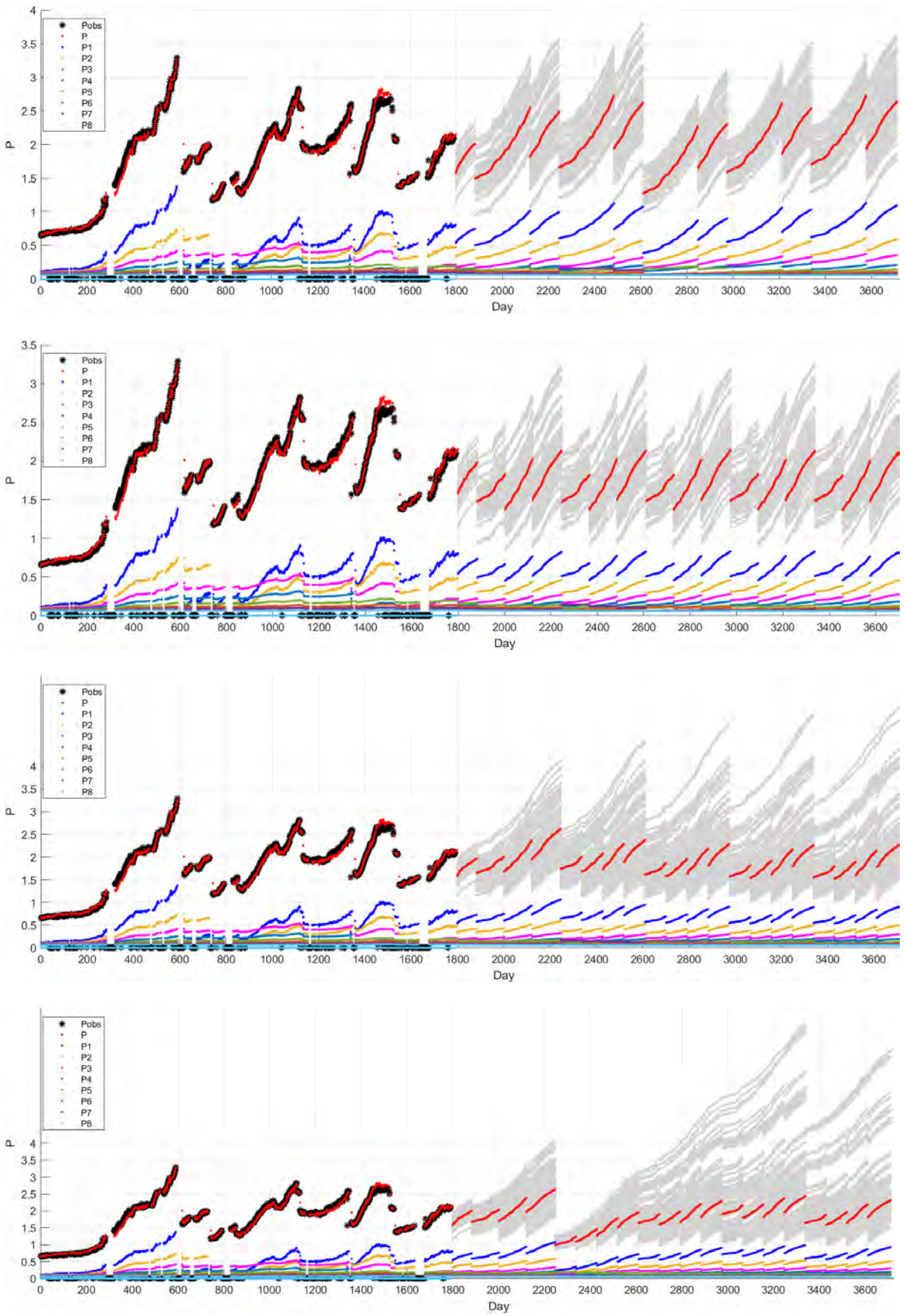


Figure C-6: Bootstrap with smoothening -2,+8, Train 11 for policy 4, (top) to policy 7 (bottom).

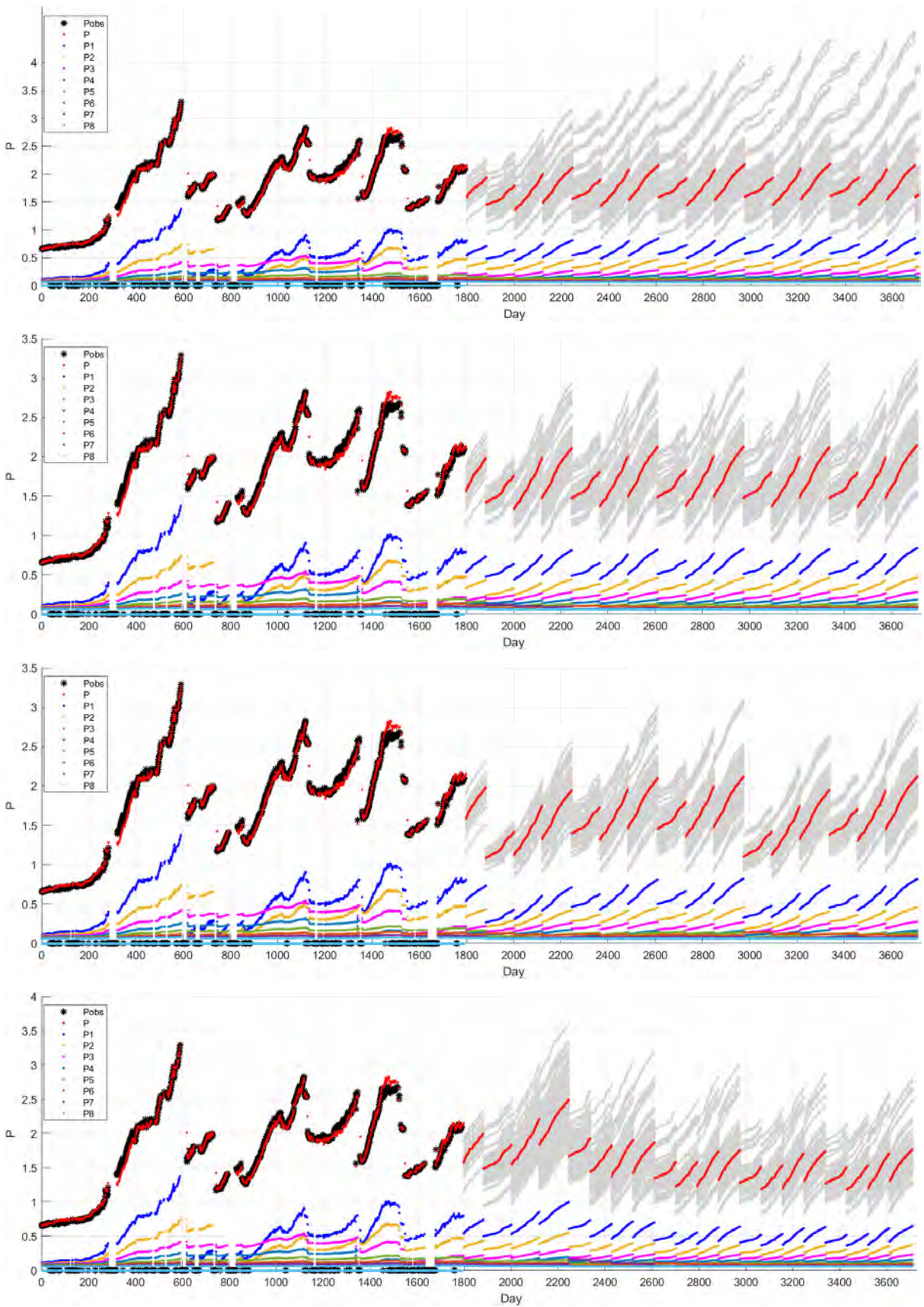


Figure C-7: Bootstrap with smoothing $-2,+8$, Train 11 for policy 8, (top) to policy 11 (bottom).

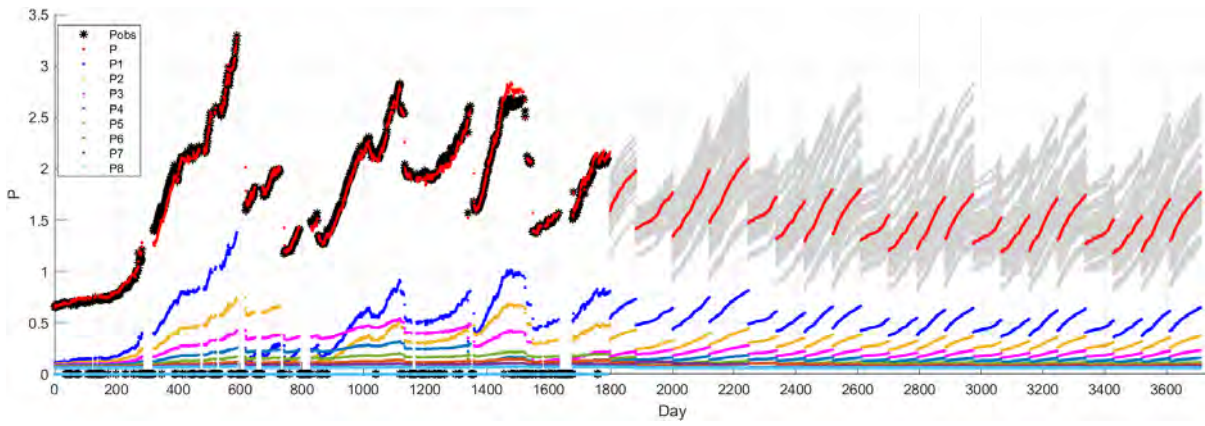


Figure C-8: Bootstrap with smoothing -2,+8, Train 11 for policy 12.

Appendix D MATLAB source code for Functions Model historical state-space and Projections

D.1 Function: Model historical state-space

```

001 % Button pushed function: RunHis
002 function RunHisButtonPushed(app, event)
003     if app.Daily.Value == true
004         app.cntnr = 0;
005         %Ratestate
006         app.Pmodelled(1) = app.Pobs(1);
007         for j=1:app.Elements.Value
008             app.Psocket(1,j) = app.Omega(1,j) * app.Pobs(1);
009         end
010         for i=2:app.Hisdata
011             x = sum(app.Xhis(i-1,:));
012             for j=1:app.Elements.Value - 1
013                 x = x - app.Xhis(i-1,j);
014                 app.RShis(i,j) = (x / (app.Elements.Value - ...
015                     j))^(app.Rec(i)/100*app.Gamma.Value);
016             end
017             %Kappa
018             if app.State(i) == 5
019                 if app.State(i-1) == 5
020                     x = 0.0;
021                     for j=1:app.Elements.Value
022                         x = x + app.Alpha.Value^(j-1) * app.RShis(i,j) * ...
023                             app.Omega(i,j);
024                     end
025                     y=app.Pobs(1) * x;
026                     %Perfect fit is to use app.Pmodelled(i-1) instead of
027                     %app.Pobs(i-1)
028                     if app.cntnr > 0
029                         app.kHis(i) = (app.Pobs(i)-app.Pmodelled(i-1)) / y;
030                         app.cntnr = app.cntnr - 1;
031                     else
032                         app.kHis(i) = (app.Pobs(i)-app.Pobs(i-1)) / y;
033                     end
034                 else
035                     app.kHis(i) = 0.0;
036                 end
037             else
038                 app.kHis(i) = 0.0;
039             end
040             %DX
041             for j=1:app.Elements.Value
042                 app.DXhis(i,j) = app.Alpha.Value^(j-1) * app.kHis(i) * app.RShis(i,j);
043             end
044             %check for maintenance actions
045             app.Maint = zeros(1,app.nMaintHis.Value);
046             for j=1:app.nMaintHis.Value
047                 if app.MaintHis.Day(j) == i
048                     app.Maint = table2array(app.MaintHis(j,:));
049                 end
050             end
051             %Calculate Wear X
052             if app.Maint(3) > 0
053                 app.cntnr = 7;
054             end
055             switch app.Maint(3)
056                 case 0
057                     for j=1:app.Elements.Value
058                         app.Xhis(i,j) = app.Xhis(i-1,j) + app.DXhis(i,j);
059                         if app.Xhis(i,j) < 1
060                             app.Xhis(i,j) = 1;
061                         end
062                     end
063                 case 1
064                     for j=1:app.Elements.Value
065                         app.Xhis(i,j) = (1 - app.Maint(1,4)) * app.Xhis(i-1,j) + ...
066                             app.Maint(4);
067                         if app.Xhis(i,j) < 1

```

```

065         app.Xhis(i,j) = 1;
066     end
067 end
068 case 2
069     for j=1:app.Elements.Value
070         app.Xhis(i,j) = (1 - app.Maint(1,4)) * app.Xhis(i-1,j) + ...
071             app.Maint(4);
072         if app.Xhis(i,j) < 1
073             app.Xhis(i,j) = 1;
074         end
075     end
076 case 3
077     app.Xhis(i,1) = app.Xhis(i-1,8);
078     app.Xhis(i,8) = 1.1;
079     for j=2:app.Elements.Value-1
080         app.Xhis(i,j) = app.Xhis(i-1,j);
081     end
082 case 4
083     for j=1:app.Elements.Value
084         m = app.Maint(j+4);
085         if m == 0
086             app.Xhis(i,j) = 1;
087         else
088             app.Xhis(i,j) = app.Xhis(i-1,m);
089         end
090     end
091 end
092 %Calculating P modelled
093 if app.State(i) == 5
094     app.Pmodelled(i) = 0;
095     for j=1:app.Elements.Value
096         app.Psocket(i,j) = app.Xhis(i,j) * app.Omega(i,j) * app.Pobs(1);
097         app.Pmodelled(i) = app.Pmodelled(i) + app.Psocket(i,j);
098     end
099 else
100     app.Pmodelled(i) = 0;
101     for j=1:app.Elements.Value
102         app.Psocket(i,j) = 0;
103     end
104 end
105 else
106     %Ratestate
107     app.Pmodelled(1) = app.Pobs(1);
108     for j=1:app.Elements.Value
109         app.Psocket(1,j) = app.Omega(1,j) * app.Pobs(1);
110     end
111     app.kHis(1) = app.Kfltr.Kappa(1);
112     app.KappaHigh = 0.0;
113     for i=2:app.Hisdata
114         x = sum(app.Xhis(i-1,:));
115         for j=1:app.Elements.Value - 1
116             x = x - app.Xhis(i-1,j);
117             app.RShis(i,j) = (x / (app.Elements.Value - ...
118                 j))^(app.Rec(i)/100*app.Gamma.Value);
119         end
120     end
121     %Kappa
122     if app.cnter > 0
123         if app.State(i) == 5
124             if app.State(i-1) == 5
125                 x = 0.0;
126                 for j=1:app.Elements.Value
127                     x = x + app.Alpha.Value^(j-1) * app.RShis(i,j) * ...
128                         app.Omega(i,j);
129                 end
130                 y=app.Pobs(1) * x;
131                 app.kHis(i) = (app.Pobs(i)-app.Pmodelled(i-1)) / y;
132                 app.cnter = app.cnter - 1;
133             else
134                 app.kHis(i) = 0.0;
135             end
136         end
137     else
138         app.kHis(i) = 0.0;
139     end
140 end
141 if app.Kfltr.Kappa(i) > app.Kfltr.Kappa(i-1)
142     app.tau = 0;

```

```

139         app.KappaHigh = app.Kfltr.Kappa(i);
140     elseif app.Kfltr.Kappa(i) < app.Kfltr.Kappa(i-1)
141         app.tau = 1;
142     else
143         if app.tau > 0
144             app.tau = app.tau + 1;
145         end
146     end
147     if app.KappaHigh == 0
148         app.kHis(i) = app.Kfltr.Kappa(i);
149     else
150         x = (app.KappaHigh - app.Kfltr.Kappa(i)) * ...
151             exp(-app.Beta.Value*app.tau) + app.Kfltr.Kappa(i);
152         if x < app.Kfltr.Kappa(i)
153             app.kHis(i) = app.Kfltr.Kappa(i);
154         else
155             app.kHis(i) = x;
156         end
157     end
158     %DX
159     for j=1:app.Elements.Value
160         app.DXhis(i,j) = app.Alpha.Value^(j-1) * app.kHis(i) * app.RShis(i,j);
161     end
162     %check for maintenance actions
163     app.Maint = zeros(1,12);
164     for j=1:25
165         if app.MaintHis.Day(j) == i
166             app.Maint = table2array(app.MaintHis(j,:));
167         end
168     end
169     %Calculate Wear X
170     if app.Maint(3) > 0
171         app.cntr = 7;
172     end
173     switch app.Maint(3)
174     case 0
175         for j=1:app.Elements.Value
176             app.Xhis(i,j) = app.Xhis(i-1,j) + app.DXhis(i,j);
177             if app.Xhis(i,j) < 1
178                 app.Xhis(i,j) = 1;
179             end
180         end
181     case 1
182         for j=1:app.Elements.Value
183             app.Xhis(i,j) = (1 - app.Maint(1,4)) * app.Xhis(i-1,j) + ...
184                 app.Maint(4);
185             if app.Xhis(i,j) < 1
186                 app.Xhis(i,j) = 1;
187             end
188         end
189     case 2
190         for j=1:app.Elements.Value
191             app.Xhis(i,j) = (1 - app.Maint(1,4)) * app.Xhis(i-1,j) + ...
192                 app.Maint(4);
193             if app.Xhis(i,j) < 1
194                 app.Xhis(i,j) = 1;
195             end
196         end
197     case 3
198         app.Xhis(i,1) = app.Xhis(i-1,8);
199         app.Xhis(i,8) = 1.1;
200         for j=2:app.Elements.Value-1
201             app.Xhis(i,j) = app.Xhis(i-1,j);
202         end
203     case 4
204         for j=1:app.Elements.Value
205             m = app.Maint(j+4);
206             if m == 0
207                 app.Xhis(i,j) = 1;
208             else
209                 app.Xhis(i,j) = app.Xhis(i-1,m);
210             end
211         end
212     end
213     %Calculating P modelled
214     if app.State(i) == 5

```

```

213         app.Pmodelled(i) = 0;
214         for j=1:app.Elements.Value
215             app.Psocket(i,j) = app.Xhis(i,j) * app.Omega(i,j) * app.Pobs(1);
216             app.Pmodelled(i) = app.Pmodelled(i) + app.Psocket(i,j);
217         end
218     else
219         app.Pmodelled(i) = 0;
220         for j=1:app.Elements.Value
221             app.Psocket(i,j) = 0;
222         end
223     end
224 end
225 end
226 app.train.P(:) = app.Pmodelled(:);
227 app.train.P1(:) = app.Psocket(:,1);
228 app.train.P2(:) = app.Psocket(:,2);
229 app.train.P3(:) = app.Psocket(:,3);
230 app.train.P4(:) = app.Psocket(:,4);
231 app.train.P5(:) = app.Psocket(:,5);
232 app.train.P6(:) = app.Psocket(:,6);
233 app.train.P7(:) = app.Psocket(:,7);
234 app.train.P8(:) = app.Psocket(:,8);
235 app.train.kCalc(:) = app.kHis(:);
236 app.train.X1(:) = app.Xhis(:,1);
237 app.train.X2(:) = app.Xhis(:,2);
238 app.train.X3(:) = app.Xhis(:,3);
239 app.train.X4(:) = app.Xhis(:,4);
240 app.train.X5(:) = app.Xhis(:,5);
241 app.train.X6(:) = app.Xhis(:,6);
242 app.train.X7(:) = app.Xhis(:,7);
243 app.train.X8(:) = app.Xhis(:,8);
244 app.LargeChart=false;
245 updatePlot(app);
246 end

```

D.2 Function: Projections

```

001 % Button pushed function: RunProjection
002 function RunProjectionButtonPushed(app, event)
003     if app.Forecastvector.Value == false % Bootstrap method
004         % retrieving data-sets
005         CIPHIS=readtable("CIPHIS.xlsx");
006         nc1=sum( ~isnan(CIPHIS.C1));
007         nc2=sum( ~isnan(CIPHIS.C2));
008         C1His=table2array(CIPHIS(1:nc1,1));
009         C2His=table2array(CIPHIS(1:nc2,2));
010         Turned=table2array(readtable("KappaMatris.xlsx"));
011         kDataSet=Turned';
012         %Calculating projected wear
013         %Calculating socket recovery and socket ratio
014         % Set up the progress bar axis
015         fh = clf();
016         ax = axes(fh,'Position',[.1 .4 .8 .05],'box','on','xtick',[],'ytick',[],...
017             'Color',[0.9375 0.9375 0.9375],'xlim',[0,1],'ylim',[0,1]); %gray94
018         title(ax,'Computing extrinsic projection ')
019         % Create empty patch that will be updated
020         ph = patch(ax,[0 0 0 0],[0 0 1 1],[0.67578 1 0.18359]); %greenyellow
021         % Create the percent-complete text that will be updated
022         th = text(ax,1,1,'0%','VerticalAlignment','bottom',...
023             'HorizontalAlignment','right');
024         %End initiating progress bar
025         app.Rsocket(1) = 0.006098 .* app.Rprojected.Value.^2 - 0.216765 .* ...
026         app.Rprojected.Value + 6.663636;
027         k = 0;
028         for j=2:app.Elements.Value
029             k = k + 1;
030             app.Rsocket(j) = app.Rsocket(1) / (1+k*0.99 * app.Rsocket(1)/100);
031         end
032         x = sum(app.Rsocket(:));
033         for j=1:8
034             app.Osocket(j) = app.Rsocket(j) / x;
035         end
036         %We transfer last day His to first day projected
037         app.Pprj(1,1)=0;
038         for j=1:8
039             app.Xprj(1,j) = app.Xhis(app.Hisdata,j);

```

```

037         app.Pprj(1,j+1)=app.Psocket(app.Hisdata,j);
038         app.Pprj(1,1)=app.Pprj(1,1)+app.Pprj(1,j+1);
039     end
040     %Ensemble fore cast of Kappa
041     kEnsemble =zeros(1920,100);
042     kData=zeros(365,100);
043     for l=1:365
044         kData(l,:)=datasample(kDataSet(l,:),100);
045     end
046     Day = 0;
047     CaldDay=365-app.StartYear(1);
048     for j=1:app.StartYear(1)-1 % j is the day of projection
049         % update patch size and percentage text
050         ph.XData = [0 j/2281 j/2281 0];
051         th.String = sprintf('%.0f%%',round(j/2281*100));
052         drawnow %update graphics
053         Day = Day + 1;
054         CaldDay = CaldDay + 1;
055         for i=1:100 % i is the envelop
056             kEnsemble(j,i)=kData(CaldDay,i);
057         end
058     end
059     CaldDay = 0;
060     for l=1:365
061         kData(l,:)=datasample(kDataSet(l,:),100);
062     end
063     for j=app.StartYear(1):app.StartYear(2)-1 % j is the day of projection
064         % update patch size and percentage text
065         ph.XData = [0 j/2281 j/2281 0];
066         th.String = sprintf('%.0f%%',round(j/2281*100));
067         drawnow %update graphics
068         CaldDay = CaldDay + 1;
069         Day = Day + 1;
070         if Day <= 1920 % This is the max span of the application
071             for i=1:100 % i is the envelop
072                 kEnsemble(j,i)=kData(CaldDay,i);
073             end
074         end
075     end
076     for m=2:6
077         CaldDay = 0;
078         for l=1:365
079             kData(l,:)=datasample(kDataSet(l,:),100);
080         end
081         for j=app.StartYear(m):app.StartYear(m+1)-1 %app.StartYear(6) % j is ...
082             the day of projection [(m+1)-1]
083             % update patch size and percentage text
084             ph.XData = [0 j/2281 j/2281 0];
085             th.String = sprintf('%.0f%%',round(j/2281*100));
086             drawnow %update graphics
087             CaldDay = CaldDay + 1;
088             if CaldDay > 365
089                 for l=1:365
090                     kData(l,:)=datasample(kDataSet(l,:),100);
091                 end
092                 CaldDay = 1;
093             end
094             Day = Day + 1;
095             if Day <= 1920 % This is the max span of the application
096                 for i=1:100 % i is the envelop
097                     kEnsemble(j,i)=kData(CaldDay,i);
098                 end
099             end
100         end
101     end
102     app.kMatrix = kEnsemble;
103     for l =1:1920
104         app.kF(l)=mean(kEnsemble(l,:));
105     end
106     close(fh);
107     % Set up the progress bar axis
108     fh = clf();
109     ax = axes(fh,'Position',[.1 .4 .8 .05],'box','on','xtick',[],'ytick',[],...
110         'Color',[0.9375 0.9375 0.9375],'xlim',[0,1],'ylim',[0,1]); %gray94
111     title(ax,'Computing wear projection')
112     % Create empty patch that will be updated
113     ph = patch(ax,[0 0 0 0],[0 0 1 1],[0.67578 1 0.18359]); %greenyellow

```

```

112 % Create the percent-complete text that will be updated
113 th = text(ax,1,1,'0%', 'VerticalAlignment', 'bottom', 'HorizontalAlignment', ...
      'right');
114 %End initiating progress bar
115 C1=datasample(C1His,100);
116 C2=datasample(C2His,100);
117 for m =1:100
118     % update patch size and percentage text
119     th.String = sprintf('%.0f%%',round(m/100*100));
120     ph.XData = [0 m/100 m/100 0];
121     drawnow %update graphics
122     %Projection time series
123     for i=2:1920
124         %Ratestate
125         x = sum(app.Xprj(i-1,:));
126         for j=1:app.Elements.Value - 1
127             x = x - app.Xprj(i-1,j);
128             app.RSprj(i,j) = (x / (app.Elements.Value - j))^ ...
                (app.Rprojected.Value/100*app.Gamma.Value);
129         end
130         %DX
131         for j=1:app.Elements.Value
132             app.DXprj(i,j) = app.Alpha.Value^(j-1) * app.kMatrix(i,m) * ...
                app.RSprj(i,j);
133         end
134         %check for maintenance actions
135         app.Maint = zeros(1,app.nWO.Value);
136         action=table2array(app.MA);
137         for j=1:app.nWO.Value
138             if action(j,2)*7 == app.Hisdata + i
139                 app.Maint = action(j,:);
140             end
141         end
142         %Calculate Wear X
143         switch app.Maint(3)
144             case 0
145                 for j=1:app.Elements.Value
146                     app.Xprj(i,j) = app.Xprj(i-1,j) + app.DXprj(i,j);
147                     if app.Xprj(i,j) < 1
148                         app.Xprj(i,j) = 1;
149                     end
150                 end
151             case 1
152                 for j=1:app.Elements.Value
153                     app.Xprj(i,j) = (1 - C1(m)) * app.Xprj(i-1,j) + C1(m);
154                     if app.Xprj(i,j) < 1
155                         app.Xprj(i,j) = 1;
156                     end
157                 end
158             case 2
159                 for j=1:app.Elements.Value
160                     app.Xprj(i,j) = (1 - C2(m)) * app.Xprj(i-1,j) + C2(m);
161                     if app.Xprj(i,j) < 1
162                         app.Xprj(i,j) = 1;
163                     end
164                 end
165             case 3
166                 app.Xprj(i,1) = app.Xprj(i-1,8);
167                 app.Xprj(i,8) = 1.1;
168                 for j=2:app.Elements.Value-1
169                     app.Xprj(i,j) = app.Xprj(i-1,j);
170                 end
171             case 4
172                 for j=1:app.Elements.Value
173                     l = app.Maint(j+3);
174                     if l == 0
175                         app.Xprj(i,j) = 1;
176                     else
177                         app.Xprj(i,j) = app.Xprj(i-1,l);
178                     end
179                 end
180         end
181         %Calculating P modelled
182         app.Pmatrix(i+app.Hisdata,m) = 0;
183         for j=1:app.Elements.Value
184             app.Pprj(i,j+1) = app.Xprj(i,j) * app.Osocket(j) * app.Pobs(1);

```



```

185             app.Pmatrix(i+app.Hisdata,m) = app.Pmatrix(i+app.Hisdata,m) ...
186                 + app.Pprj(i,j+1);
187         end
188     end
189     for l =1:1920
190         app.Pmax(l) = max(app.Pmatrix(l+app.Hisdata,:));
191     end
192     %repeat wear calculation for kEnsemble
193     %Projection time series
194     for i=2:1920
195         %Ratestate
196         x = sum(app.Xprj(i-1,:));
197         for j=1:app.Elements.Value - 1
198             x = x - app.Xprj(i-1,j);
199             app.RSprj(i,j) = (x / (app.Elements.Value - ...
200                 j))^(app.Rprojected.Value/100*app.Gamma.Value);
201         end
202         %DX
203         for j=1:app.Elements.Value
204             app.DXprj(i,j) = app.Alpha.Value^(j-1) * app.kF(i) * app.RSprj(i,j);
205         end
206         %check for maintenance actions
207         app.Maint = zeros(1,app.nWO.Value);
208         action=table2array(app.MA);
209         for j=1:app.nWO.Value
210             if action(j,2)*7 == app.Hisdata + i
211                 app.Maint = action(j,:);
212             end
213         end
214         %Calculate Wear X
215         switch app.Maint(3)
216             case 0
217                 for j=1:app.Elements.Value
218                     app.Xprj(i,j) = app.Xprj(i-1,j) + app.DXprj(i,j);
219                     if app.Xprj(i,j) < 1
220                         app.Xprj(i,j) = 1;
221                     end
222                 end
223             case 1
224                 for j=1:app.Elements.Value
225                     app.Xprj(i,j) = (1 - app.deltaC1.Value) * app.Xprj(i-1,j) ...
226                         + app.deltaC1.Value;
227                     if app.Xprj(i,j) < 1
228                         app.Xprj(i,j) = 1;
229                     end
230                 end
231             case 2
232                 for j=1:app.Elements.Value
233                     app.Xprj(i,j) = (1 - app.deltaC2.Value) * app.Xprj(i-1,j) ...
234                         + app.deltaC2.Value;
235                     if app.Xprj(i,j) < 1
236                         app.Xprj(i,j) = 1;
237                     end
238                 end
239             case 3
240                 app.Xprj(i,1) = app.Xprj(i-1,8);
241                 app.Xprj(i,8) = 1.1;
242                 for j=2:app.Elements.Value-1
243                     app.Xprj(i,j) = app.Xprj(i-1,j);
244                 end
245             case 4
246                 for j=1:app.Elements.Value
247                     m = app.Maint(j+3);
248                     if m == 0
249                         app.Xprj(i,j) = 1;
250                     else
251                         app.Xprj(i,j) = app.Xprj(i-1,m);
252                     end
253                 end
254             end
255         %Calculating P modelled
256         app.Pprj(i,1) = 0;
257         for j=1:app.Elements.Value
258             app.Pprj(i,j+1) = app.Xprj(i,j) * app.Osocket(j) * app.Pobs(1);
259             app.Pprj(i,1) = app.Pprj(i,1) + app.Pprj(i,j+1);
260         end

```

```

258     end
259 else % Weibull Distribution method
260     %Calculating projected wear
261     %Calculating socket recovery and socket ratio
262     % Set up the progress bar axis
263     fh = clf();
264     ax = axes(fh,'Position',[.1 .4 .8 .05],'box','on','xtick',[],'ytick',[],...
265         'Color',[0.9375 0.9375 0.9375],'xlim',[0,1],'ylim',[0,1]); %gray94
266     title(ax,'Computing extrinsic projection ')
267     % Create empty patch that will be updated
268     ph = patch(ax,[0 0 0 0],[0 0 1 1],[0.67578 1 0.18359]); %greenyellow
269     % Create the percent-complete text that will be updated
270     th = text(ax,1,1,'0%','VerticalAlignment','bottom','HorizontalAlignment', ...
271         'right');
272     %End initiating progress bar
273     app.Rsocket(1) = 0.006098 .* app.Rprojected.Value.^2 - 0.216765 .* ...
274     app.Rprojected.Value + 6.663636;
275     k = 0;
276     for j=2:app.Elements.Value
277         k = k + 1;
278         app.Rsocket(j) = app.Rsocket(1) / (1+k*0.99 * app.Rsocket(1)/100);
279     end
280     x = sum(app.Rsocket(:));
281     for j=1:8
282         app.Osocket(j) = app.Rsocket(j) / x;
283     end
284     %We transfer last day His to first day projected
285     app.Pprj(1,1)=0;
286     for j=1:8
287         app.Xprj(1,j) = app.Xhis(app.Hisdata,j);
288         app.Pprj(1,j+1)=app.Psocket(app.Hisdata,j);
289         app.Pprj(1,1)=app.Pprj(1,1)+app.Pprj(1,j+1);
290     end
291     %Ensemble forecast of Kappa
292     kEnsemble =zeros(1920,100);
293     k2Last = zeros(100,1);
294     Bloom=random('Weibull',app.WeekStartAlgae.Value, ...
295         app.StartAlgae_std.Value,100,1);
296     Duration=random('Weibull',app.WeeksAlgae.Value,app.Duration_std.Value,100,1);
297     klow=random('Weibull',app.Kmin.Value,app.kLow_std.Value,100,1);
298     kHigh=random('Weibull',app.Kmax.Value,app.kHigh_std.Value,100,1);
299     Day = 0;
300     for j=1:app.StartYear(1)-1 % j is the day of projection
301         % update patch size and percentage text
302         ph.XData = [0 j/2281 j/2281 0];
303         th.String = sprintf('%.0f%%',round(j/2281*100));
304         drawnow %update graphics
305         Day = Day + 1;
306         for i=1:100 % i is the envelop
307             k1=klow(i);
308             kEnsemble(j,i)=k1;
309         end
310     end
311     CaldDay = 0;
312     for j=app.StartYear(1):app.StartYear(2)-1 % j is the day of projection
313         % update patch size and percentage text
314         ph.XData = [0 j/2281 j/2281 0];
315         th.String = sprintf('%.0f%%',round(j/2281*100));
316         drawnow %update graphics
317         CaldDay = CaldDay + 1;
318         Day = Day + 1;
319         if Day <= 1920 % This is the max span of the application
320             for i=1:100 % i is the envelop
321                 k1=klow(i);
322                 k2=kHigh(i);
323                 if CaldDay < round(Bloom(i))
324                     kEnsemble(j,i)=k1;
325                 end
326                 if CaldDay >= round(Bloom(i))
327                     if CaldDay < round(Bloom(i)) + round(Duration(i))
328                         kEnsemble(j,i)=k2;
329                         app.tau = 0;
330                         k2Last(i)=kEnsemble(j,i);
331                     else
332                         app.tau = app.tau + 1;
333                         x = (k2Last(i) - k1) * exp(-app.Beta.Value*app.tau) + k1;
334                         kEnsemble(j,i)=x;

```

```

331                                     end
332                                 end
333                             end
334                         end
335                     end
336                 for m=2:6
337                     CaldDay = 0;
338                     for j=app.StartYear(m):app.StartYear(m+1)-1 %app.StartYear(6) % j is ...
339                         the day of projection [(m+1)-1]
340                         % update patch size and percentage text
341                         ph.XData = [0 j/2281 j/2281 0];
342                         th.String = sprintf('%.0f%%',round(j/2281*100));
343                         drawnow %update graphics
344                         CaldDay = CaldDay + 1;
345                         Day = Day + 1;
346                         if Day <= 1920 % This is the max span of the application
347                             for i=1:100 % i is the envelop
348                                 k1=klow(i);
349                                 k2=kHigh(i);
350                                 if CaldDay < round(Bloom(i))
351                                     app.tau = app.tau + 1;
352                                     kEnsemble(j,i)=(k2Last(i) - k1) * ...
353                                     exp(-app.Beta.Value*app.tau) + k1;
354                                 end
355                                 if CaldDay >= round(Bloom(i))
356                                     if CaldDay < round(Bloom(i)) + round(Duration(i))
357                                         kEnsemble(j,i)=k2;
358                                         app.tau = 0;
359                                         k2Last(i)=kEnsemble(j,i);
360                                     else
361                                         app.tau = app.tau + 1;
362                                         kEnsemble(j,i)=(k2Last(i) - k1) * ...
363                                         exp(-app.Beta.Value*app.tau) + k1;
364                                     end
365                                 end
366                             end
367                         end
368                     end
369                 end
370             end
371             app.kMatrix = kEnsemble;
372             for l =1:1920
373                 app.kF(l)=mean(kEnsemble(l,:));
374             end
375             close(fh);
376             % Set up the progress bar axis
377             fh = clf();
378             ax = axes(fh,'Position',[.1 .4 .8 .05],'box','on','xtick',[],'ytick',[],...
379             'Color',[0.9375 0.9375 0.9375],'xlim',[0,1],'ylim',[0,1]); %gray94
380             title(ax,'Computing wear projection')
381             % Create empty patch that will be updated
382             ph = patch(ax,[0 0 0 0],[0 0 1 1],[0.67578 1 0.18359]); %greenyellow
383             % Create the percent-complete text that will be updated
384             th = text(ax,1,1,'0%','VerticalAlignment','bottom', ...
385             'HorizontalAlignment','right');
386             %End initiating progress bar
387             C1=random('Weibull',app.deltaC1.Value,app.dC1_std.Value,100,1);
388             C2=random('Weibull',app.deltaC2.Value,app.dC2_std.Value,100,1);
389             for m =1:100
390                 % update patch size and percentage text
391                 ph.XData = [0 m/100 m/100 0];
392                 th.String = sprintf('%.0f%%',round(m/100*100));
393                 drawnow %update graphics
394                 %Projection time series
395                 for i=2:1920
396                     %Ratestate
397                     x = sum(app.Xprj(i-1,:));
398                     for j=1:app.Elements.Value - 1
399                         x = x - app.Xprj(i-1,j);
400                         app.RSprj(i,j) = (x / (app.Elements.Value - ...
401                         j))^(app.Rprojected.Value/100*app.Gamma.Value);
402                     end
403                     %DX
404                     for j=1:app.Elements.Value
405                         app.DXprj(i,j) = app.Alpha.Value^(j-1) * app.kMatrix(i,m) * ...
406                         app.RSprj(i,j);
407                     end
408                 end
409             end
410             %check for maintenance actions

```

```

401         app.Maint = zeros(1,app.nWO.Value);
402         action=table2array(app.MA);
403         for j=1:app.nWO.Value
404             if action(j,2)*7 == app.Hisdata + i
405                 app.Maint = action(j,:);
406             end
407         end
408         %Calculate Wear X
409         switch app.Maint(3)
410             case 0
411                 for j=1:app.Elements.Value
412                     app.Xprj(i,j) = app.Xprj(i-1,j) + app.DXprj(i,j);
413                     if app.Xprj(i,j) < 1
414                         app.Xprj(i,j) = 1;
415                     end
416                 end
417             case 1
418                 for j=1:app.Elements.Value
419                     app.Xprj(i,j) = (1 - C1(m)) * app.Xprj(i-1,j) + C1(m);
420                     if app.Xprj(i,j) < 1
421                         app.Xprj(i,j) = 1;
422                     end
423                 end
424             case 2
425                 for j=1:app.Elements.Value
426                     app.Xprj(i,j) = (1 - C2(m)) * app.Xprj(i-1,j) + C2(m);
427                     if app.Xprj(i,j) < 1
428                         app.Xprj(i,j) = 1;
429                     end
430                 end
431             case 3
432                 app.Xprj(i,1) = app.Xprj(i-1,8);
433                 app.Xprj(i,8) = 1.1;
434                 for j=2:app.Elements.Value-1
435                     app.Xprj(i,j) = app.Xprj(i-1,j);
436                 end
437             case 4
438                 for j=1:app.Elements.Value
439                     l = app.Maint(j+3);
440                     if l == 0
441                         app.Xprj(i,j) = 1;
442                     else
443                         app.Xprj(i,j) = app.Xprj(i-1,l);
444                     end
445                 end
446             end
447             %Calculating P modelled
448             app.Pmatrix(i+app.Hisdata,m) = 0;
449             for j=1:app.Elements.Value
450                 app.Pprj(i,j+1) = app.Xprj(i,j) * app.Osocket(j) * app.Pobs(1);
451                 app.Pmatrix(i+app.Hisdata,m) = app.Pmatrix(i+app.Hisdata,m) + ...
452                     app.Pprj(i,j+1);
453             end
454         end
455     for l =1:1920
456         app.Pmax(l) = max(app.Pmatrix(l+app.Hisdata,:));
457     end
458     %repeat wear calculation for kEnsemble
459     %Projection time series
460     for i=2:1920
461         %Ratestate
462         x = sum(app.Xprj(i-1,:));
463         for j=1:app.Elements.Value - 1
464             x = x - app.Xprj(i-1,j);
465             app.RSprj(i,j) = (x / (app.Elements.Value - ...
466                 j))^(app.Rprojected.Value/100*app.Gamma.Value);
467         end
468         %DX
469         for j=1:app.Elements.Value
470             app.DXprj(i,j) = app.Alpha.Value^(j-1) * app.kF(i) * app.RSprj(i,j);
471         end
472         %check for maintenance actions
473         app.Maint = zeros(1,app.nWO.Value);
474         action=table2array(app.MA);
475         for j=1:app.nWO.Value
476             if action(j,2)*7 == app.Hisdata + i

```

```

477         app.Maint = action(j,:);
478     end
479 end
480 %Calculate Wear X
481 switch app.Maint(3)
482     case 0
483         for j=1:app.Elements.Value
484             app.Xprj(i,j) = app.Xprj(i-1,j) + app.DXprj(i,j);
485             if app.Xprj(i,j) < 1
486                 app.Xprj(i,j) = 1;
487             end
488         end
489     case 1
490         for j=1:app.Elements.Value
491             app.Xprj(i,j) = (1 - app.deltaC1.Value) * app.Xprj(i-1,j) ...
492                 + app.deltaC1.Value;
493             if app.Xprj(i,j) < 1
494                 app.Xprj(i,j) = 1;
495             end
496         end
497     case 2
498         for j=1:app.Elements.Value
499             app.Xprj(i,j) = (1 - app.deltaC2.Value) * app.Xprj(i-1,j) ...
500                 + app.deltaC2.Value;
501             if app.Xprj(i,j) < 1
502                 app.Xprj(i,j) = 1;
503             end
504         end
505     case 3
506         app.Xprj(i,1) = app.Xprj(i-1,8);
507         app.Xprj(i,8) = 1.1;
508         for j=2:app.Elements.Value-1
509             app.Xprj(i,j) = app.Xprj(i-1,j);
510         end
511     case 4
512         for j=1:app.Elements.Value
513             m = app.Maint(j+3);
514             if m == 0
515                 app.Xprj(i,j) = 1;
516             else
517                 app.Xprj(i,j) = app.Xprj(i-1,m);
518             end
519         end
520     end
521 %Calculating P modelled
522 app.Pprj(i,1) = 0;
523 for j=1:app.Elements.Value
524     app.Pprj(i,j+1) = app.Xprj(i,j) * app.Osocket(j) * app.Pobs(1);
525     app.Pprj(i,1) = app.Pprj(i,1) + app.Pprj(i,j+1);
526 end
527 end
528 app.Pmax(1) = app.Pmax(2);
529 for i=app.Hisdata+1:app.ProjectionSize
530     for j=1:9
531         app.Pchart(i,j)=app.Pprj(i-app.Hisdata,j);
532     end
533 end
534 app.Projection(:,2) = app.Pprj(:,1);
535 app.Projection(:,3) = app.Pprj(:,2);
536 app.Projection(:,4) = app.Pprj(:,3);
537 app.Projection(:,5) = app.Pprj(:,4);
538 app.Projection(:,6) = app.Pprj(:,5);
539 app.Projection(:,7) = app.Pprj(:,6);
540 app.Projection(:,8) = app.Pprj(:,7);
541 app.Projection(:,9) = app.Pprj(:,8);
542 app.Projection(:,10) = app.Pprj(:,9);
543 app.Projection(:,11) = app.Pmax(:);
544 app.Projection(:,12) = app.Xprj(:,1);
545 app.Projection(:,13) = app.Xprj(:,2);
546 app.Projection(:,14) = app.Xprj(:,3);
547 app.Projection(:,15) = app.Xprj(:,4);
548 app.Projection(:,16) = app.Xprj(:,5);
549 app.Projection(:,17) = app.Xprj(:,6);
550 app.Projection(:,18) = app.Xprj(:,7);
551 app.Projection(:,19) = app.Xprj(:,8);
552 app.UITableProjected.Data=app.Projection;

```

@00419918

Fredericus I. M. (Frits) van Rooij

```
553         app.LargeChart=true;  
554         close(fh);  
555         updatePlot(app);  
556     end
```

About the author

Frits was born more than 60 years ago in a small rural village northeast in the province of Brabant in the Netherlands. The village had academically not more to offer than elementary education. Further education had to be pursued in nearby towns. Like the average boys of the village, Frits went to the technical school in the nearby town, Oss, after finishing elementary school. Inspired by his uncle, a self-taught electrician, he decided to pursue his career in electrical engineering. After the technical school, technical college followed, which can be compared to the associate degree in the US and the technical university after that, which prepares for a bachelor's degree.

The small Brabant village became soon too narrow in opportunities, and at the age of 21, he moved to the capital, Amsterdam. In Amsterdam, hoping to add some human dimensions to the years of technical education, Frits shortly studied on the social academy, but the latter was not a fit. He worked as an electrician and a technical draftsman in the years after. During this period, Frits married for the first time to a Greek-Cypriot. Their first son was born in Amsterdam, and during the pregnancy of their second son, she got homesick and returned to Cyprus, so he followed.

Cyprus, at the time, offered all kinds of opportunities, provided the right time and the proper interest. The first job was at a small electro-mechanical services firm that, besides contracting, also built low-voltage switchgear and control panels. The firm was getting offers for control systems involving programmable logic controllers (PLC) but had no programming resources in-house. So, like his uncle once became a self-taught electrician, Frits became a self-taught control systems integrator. Later onwards, he followed several courses to strengthen his skills.

Most projects involving PLC systems integration were by the Cyprus Water Development Department, which appreciated his work and recommended Frits to the company IDE Technologies, which won the contract for the second seawater desalination plant of the island end 1990s. Following the successful completion of the Larnaca desalination plant, IDE offered Frits a dual position as Operational Technology manager at the Larnaca plant and at the same time that of control system integrator at future projects. The job resulted in writing industrial control system (ICS) code and the production of the functional design of the unique plant configurations, involving the common pressure centre, which was developed during this period and the trademark of the company. In this position, Frits has contributed to

approximate 20 desalination projects worldwide. He developed, commissioned and managed the ICS of the most advanced and complex desalination facilities, including award-winning plants.

In the meantime, his marriage broke up, and he remarried a Javanese from the Indonesian capital Jakarta. His next three sons were born in Nicosia, Cyprus. On a note, for those interested in the history of former western colonial powers, the first act Frits undertook when meeting his wife from Indonesia was to offer his excuse for the Dutch's role during that epoch.

In 2014, Frits was relocated with his family to California to commission the ICS he developed for the Carlsbad Desalination Plant (CDP). His youngest son was only three months old at the time. Southern California felt like home, and he pursued a permanent residence in the US.

Career planning seemed sensible, having a young family with small kids. So, in 2015, Frits conducted a remote, online Master's degree in project management. The Robert Kennedy College offered the course, and the certificate was provided by the SBS of the University of Salford.

Frits enjoyed the academic study and challenges, so he started to look around for the opportunity to conduct a PhD research. He came in contact with Prof. Phil Scarf, who led the recruitment of candidates who pursued an online study. After some orientational conversations, a research topic on maintenance optimisation based on a case study of CDP seemed the right choice. Frits had already developed some pump performance models in the ICS for CDP, and maintenance optimisation seemed to be a good connection point. Phil offered to supervise, and IDE Technologies offered to sponsor it. The rest can be read in this thesis.